Università Campus Bio-Medico di Roma

Corso di Dottorato di Ricerca in Scienze Biochimiche e Tecnologie Applicate agli Alimenti ed alla Nutrizione

XXV ciclo anno 2010

Titolo tesi

Redox and fructan metabolism - implication for productivity and nutritional value of crops

Sara Cimini

Coordinatore

Prof.ssa Laura De Gara

Tutore

Prof.ssa Laura De Gara

26 Marzo 2013

Sara Cimini

Chapter 1

General Introduction

1.1 LITERATURE OVERVIEW

1.1.1 Human Nutrition and Cereals

Food is the primary source of nutrients required to stay in good health, promote normal growth and guarantee the perpetuation of human species. Although significant improvements in food production have been done in recent decades, food security still remains a problem in many parts of the world (FAOSTAT, 2011; Foley *et al.*, 2011). According to the 1996 World Food Summit *"food security exists when all people, at all times, have physical and economic access to sufficient, safe and nutritious food to meet their dietary needs and food preferences for an active and healthy life"* (FAO, 1996; Burchi *et al.*, 2011). Consequently, food security is strictly dependent on food availability, food accessibility, stability of food supply and nutritional quality of food. Food availability is, in turn, influenced by different kind of bio-physical forces among which food production level, percentage of land covered by crops and available food production technologies (FAO, 2005). Even though the undernourished population has gradually declined over the last 50 years, according to the Food and Agriculture Organization (FAO) of the United Nations, more than 1 billion people in the world are chronically undernourished due to the perpetuation of poverty conditions and rising of food prices (FAO, 2009; McMichael, 2001). An overwhelming majority of these people is to be found in developing countries (approximately 95% of total undernourished people) while, in developed countries, only 5% are caloric deficient (McMichael, 2001; FAO, 2005).

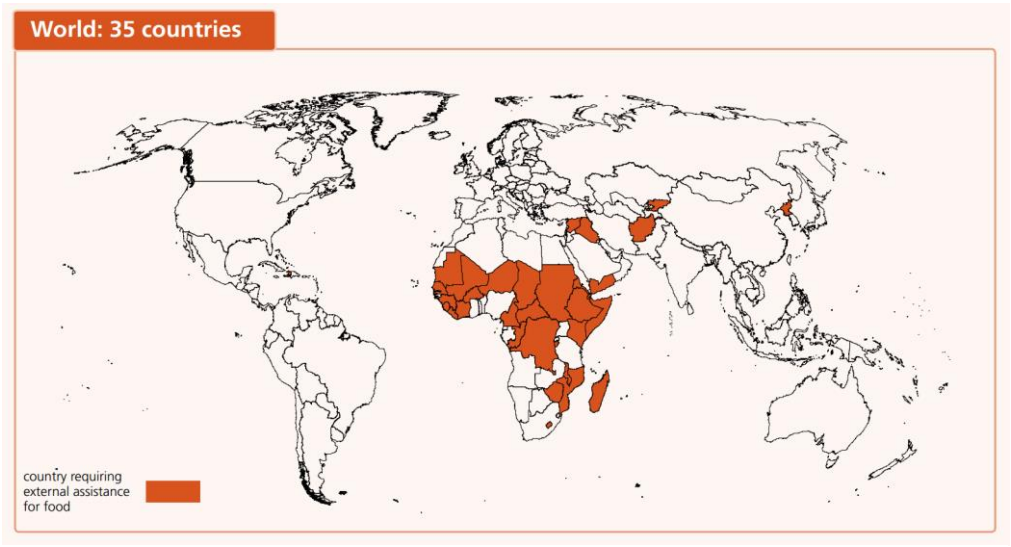

Fig. 1.1. Countries requiring external assistance for food. From FAO, 2012

Undernourishment has severe effect on human health. It is the cause of about 16% of the global burden of diseases leading to health problems and long-term disability, as well as poor educational and developmental outcomes (McMichael, 2001).

As a matter of fact undernourishment strongly increases the vulnerability to serious illness and premature death, particularly in early age (Murray and Lopez, 1996). To now, 35 different countries require external assistance for food supply due to lack of food availability or limited access to food (Fig. 1.1; FAO, 2012). At present, forty thousands of people die of undernourishment every day and half of them are children (Chrispeels, 2000).

Supporting this already critical picture, in the coming years we will see a further increase of the population. By 2050 it is predicted that there will be 9 billion people on Earth after which world population size may reach a plateau not further increasable. In order to adequately feed all these people, total food consumption will have to rise by nearly 50-70% (Smil, 2005; FAO, 2009; Jaggard *et al.*, 2010; McMichael, 2001). Thus, it is becoming crucial find a way to roughly duplicate total food production with the final aim of reducing worldwide undernourishment, as well as health, social and economic problems. In this context, the improvement of productivity and nutritional value of edible plants is a pivotal point due to the relevance of plant-derived foods for humans as well as for food web.

To date, more than 250000 plants have been described. About 75000 are edible and about 7000 are cultivated and used as food. Twenty plant species are broadly used, and in the future only six species, namely wheat, rice, soybean, maize, sorghum and rape, will be more that 80% of our food (Kern, 2002). Accordingly, gains in the production of the main 4 cereal crops (wheat, maize, rice and sorghum) will have a heavy impact on human nutrition as they currently occupy 83% of the world cereal production area and 56% of the world arable land (Jaggard *et al.*, 2010).

Global crop production has significantly increased in recent decades. Studies of common crop groups (including cereals, oilseeds, fruits and vegetables) suggest that crop production has increased by 47% between 1985 and 2005 (Foley *et al.*, 2011). This net gain is due to two main factors: the expansion of agriculture and the increase of crop yields. Regarding the expansion of agriculture, the world's croplands have been greatly enlarged in recent decades and now about 1.5 billion hectares (about 12% of Earth's ice-free land) are croplands. This net increase includes significant expansion in certain areas, mainly tropical areas, and little changes in temperate regions, thus resulting in a redistribution of cultivated lands toward the tropics where about 80% of new croplands are replacing tropical forests (Foley *et al.*, 2011).

This redistribution causes concerns in the scientific worldwide community, since tropical forests are the main biodiversity resource and key source of ecosystem services. Another aspect that has contributed to the observed increase in crop production in the developed and developing Countries is due to technological and bio-technological development that has enormously changed the agronomic practices in the last century giving an increased crop yield. As an example, world average yield of wheat has risen from 1.08 to 2.7 t ha^{-1} (Jaggard *et al.*, 2010). A large study conducted by Hafner (2003) pointed out that national average yields of wheat, rice and maize in 188 countries were mostly increasing. The growth in yields detected by Hafner exhibits a predominantly linear trend over the past 40 years and approximately 20% of the nation-crop data sets considered in this study show a growth increase greater than 33.1 Kg ha^{-1} yr^{-1} (Hafner, 2003).

In the developed and developing Countries this increase has been mostly due to nitrogen fertilization, the use of phyto-chemicals and selected varieties that were more productive or more resistant to environmental conditions (Jaggard *et al.*, 2010).

The impact of the so-called Green Revolution in stimulating cereal productivity and ensuring near-global food security is well recognized. Unfortunately, Green Revolution's technologies were not adequately spread in all underdeveloped areas (Tolmay, 2001). There are regions in the world where food production is still inadequate and environmentally unsustainable (Chrispeels, 2000). Moreover, recent studies show that the increase in food production shown in relation to human population growth is now at the end: around 2003, net per cent increase in cereals yields and population size were roughly equivalent (Ziska *et al.*, 2012). Therefore, new strategies are required to guarantee food security and therefore to decrease undernourishment.

To date, undernourishment has been dealt with approaches focused on providing sufficient calories to people in developing Countries (Blasbag *et al.*, 2011). Since over the last 50 years we have witnessed to a significant increase of the global food production, that is induced by the Green Revolution, the caloric intake has increased from 2280 kcal/person/day in 1960 to 2800 kcal/person/day in 2003 (United Nations Standing Committee on Nutrition, 2004; Blasbag *et al.*, 2011). Therefore, according to FAO estimates, based on calories-criterion, the overall undernourishment level has decreased. However undernourishment comprises different forms of malnutrition, including not only an insufficient amount of calories, but also lack of essential nutrients, poor absorption and excessive loss of nutrients due to pathological

conditions, often caused by non-adequate hygienic conditions (DeClerck *et al.*, 2011). In many areas of the world, poor dietary quality and micronutrient deficiencies are more common troubles than low energy intake (Stewart *et al.*, 2010) with shattering consequences: 11% of all death before the age of 5 years can be attributed to deficiencies in vitamin A, zinc, iron and iodine (Murgia *et al.*, 2012; Prentice *et al.*, 2008; Bhutta, 2008). Consequently, a qualitative approach has been now taken into account for all the people who have access to a sufficient amount of calories but do not take micronutrients in adequate amounts (Kennedy *et al.*, 2007). This phenomenon has been defined as "hidden hunger" since its symptoms are not always obvious and people may not be aware of it. Its negative, sometimes lifelong, consequences on health, productivity and mental impairment are devastating (Burchi *et al.*, 2011).

Micronutrients are nutrients required by living organisms in order to carry out a lot of different kind of physiological functions. It is accepted that humans required at least 49 different nutrients in adequate amounts to meet their metabolic needs (Graham *et al.*, 2007), and 19 essential micronutrients are needed for physical and mental development, immune system functioning and various metabolic processes (Kennedy *et al.*, 2007; Branca and Ferrari, 2002; Golden, 1991; Grantham-McGregor and Ani, 1999; Ramakrishnan *et al.*, 1999). At present, over 2 billion people suffer from one or more micronutrient deficiencies (Graham *et al.*, 2007).

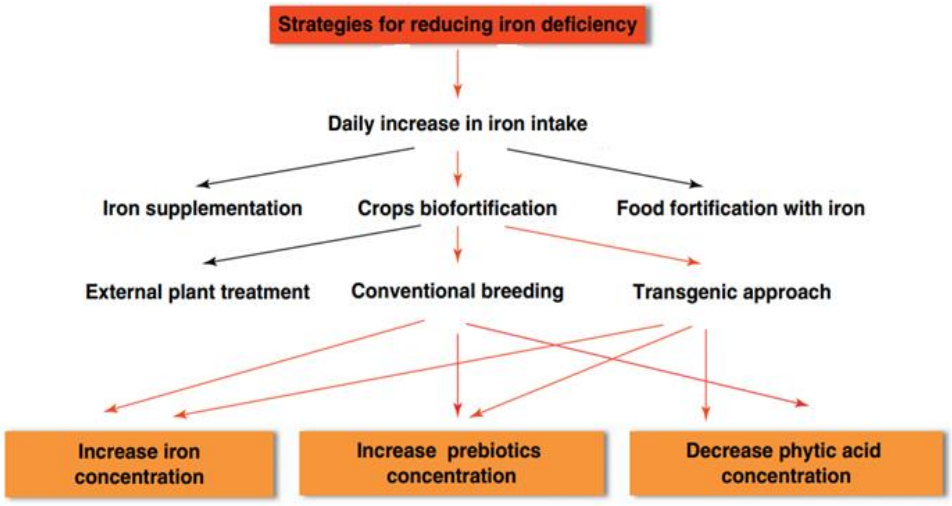

Fig. 1.2. With minor modification from Murgia *et al.*, 2012. Flow chart showing different strategies for reducing iron deficiency.

Most development programs have focused on three important micronutrients: vitamin A, iron and iodine. Particularly iron deficiency (ID) is one of the most common and widespread nutritional disorder (Murgia *et al.*, 2012). Recent analyses indicate that ID within the first year of life is responsible for irreversible effects on brain development, structure and function (Beard, 2008). Pharmacological iron supplementation, food fortification and biofortification are three different approaches aimed to increase iron intake (Fig. 1.2; Murgia *et al.*, 2012).
In relation to biofortification, three main strategies can be applied to crops in order to favor dietary iron absorption in humans: 1) reduce the concentration in the so-called "antinutrients", compounds able to reduce iron absorption (such as phytic acid and polyphenols); 2) increase the concentration in compounds favoring iron absorption (such as inulins); 3) direct increase of the iron concentration within food matrixes (Murgia *et al.*, 2012). These biofortification strategies, which can be implemented by breeding or genetic modification, offer a sustainable and low-cost way to make micronutrients available to consumers.

Factors that strongly influence food production, both in qualitative and quantitative terms, are climate conditions. There are strong scientific evidences about climate changes occurring over time. The increase in the concentration of CO_2 and other gasses released in the atmosphere by human activities is contributing to the global warming occurring in the last century. By 2050, global warming is expected to increase the average annual temperature of 1.8°C (Gornall, *et al.*, 2010; Jaggard *et al.*, 2010). Hence, growing concerns about the potential impact of climate change on crops production, population health and social well-being are emerging (Leakey, 2009; FAO, 2005). The global warming will have different effects on food production especially in relation to the geographical location of crops. In order to quantify local impacts on crop yields, geographical shift in cultivated land and general implications on food security, FAO, in collaboration with the International Institute of Applied Systems Analysis (IIASA), has developed a new methodology, called Agro-Ecological Zones (AEZ). The FAO/IIASA studies point out that in already hard-pressed developing countries, the impact of climate changes on food production will be devastating. In Asia, Africa and Latin America the effects on wheat potential production are expected to be the worst in the world. Conversely, developed countries would experience a potential expansion of arable land and a potential increase in the production of many crops but only considering lands at high latitudes such as in North America, Northern Europe, The Russian Federation and East Asia. Accordingly, climate change will impact food security particularly in those countries having

Sara Cimini

low economic growth potential that already have highest malnourishment levels (FAO, 2005; McMichael, 2001).

In order to counteract environmental changes able to affect agriculture causing yield and quality losses, the development of preventive strategies and the selection of crops that are better adapted to future growing conditions are becoming to be a crucial issue (Ainsworth *et al.*, 2008). Extreme climate events like changing rainfall regime, high salinity, drought, extreme cold and frost are among the abiotic stresses more closely related to environmental changes. Thus, a decisive aim is find a way to improve crop tolerance against several abiotic stresses in order to maintain productivity and improve the nutritional value of foods despite climate changes (Kern, 2002; Tolmay, 2001).

Crop productivity is not only affected by abiotic stresses. Biotic stresses also strongly influence crop production. Many types of plant pathogenic organisms, including bacteria, insects, fungi and nematodes are spread all over the world. Each Country has its own defined set of phytopathogenic organisms specialized to use a host plant adapted to a particular environment. These organisms and the diseases caused by them are spread both in developing and in industrialized Countries. Moreover, globalization and the easier exchanges of goods and people have already caused the spread of new phytopathogens with devastating effects on crop productivity.

The use of crops resistant to biotic and abiotic stresses could be strongly relevant for stabilizing crop yield and minimizing diseases and pest damages (Tolmay, 2001). However this solution is easy only in theory because it requires great effort in basic research for understanding the mechanisms of infection by phytopathogenic organisms, the mode of action of phytopathogenic toxins as well as the mechanisms conferring resistance to abiotic stresses.

1.2 AIMS AND EXPERIMENTAL SYSTEMS

The experimental analyses that will be described in this thesis have been mainly focused on nutritional qualities of cereal crops, especially of wheat kernels. Wheat is always considered a

leading source of fiber and energy in the human diet with higher protein content than almost all other cereals. Recently it has received attention also as source of other compounds that have positive effects on the human health. These compounds include fructans and antioxidant molecules such as ascorbate (ASC), glutathione (GSH) and polyphenols. Fructans are water-soluble sugars naturally occurring in plants. They are the most widely used prebiotics and they have quickly gained a great importance as beneficial food ingredients. Recently a novel propriety has been attributed to fructans, since they have been reported to have antioxidant properties (Stoyanova *et al.*, 2011). Wheat fructans are mainly "graminan type" containing both β-(2,1) and β-(2,6) linkages. It is known that fructan level is high in the kernels during the first period of maturation (15-20% of kernel dry weight in the milky phase) while it only reaches 2% of kernel dry weight at the end of the process (De Gara *et al.*, 2003a). Here we report a study on metabolic changes during the maturation of *Triticum durum* kernels. Kernels from durum wheat cv Neolatino were collected at different phases of maturation (from 7 to 52 DAA). Changes in activities of the enzymes involved in fructan metabolism, antioxidant metabolites as well as antioxidant total power were analyzed.

To date, fructan metabolism in wheat is not completely known although grass-type fructans probably contribute to more efficient gut disease prevention (Van den Ende *et al.*, 2011b). In this thesis we present also a study aimed to deepen the knowledge about the enzymes involved in fructan biosynthesis and breakdown. The final goal of that increases of knowledge would be to obtain durum wheat flour with higher fructan content due to a stronger expression of biosynthetic enzymes or a weaker expression of fructan breakdown enzymes.

Moreover a study on resistance mechanisms against biotic stresses has been performed in order to reduce losses in crop yields from both a quantitative and qualitative point of view. It is known that the productivity of plants and the nutritional value of their edible parts strongly depend on plant capability to avoid phytopathogen attack. Phytopathogenic fungi and bacteria affect plant growth and produce toxins that are accumulated in colonized tissues (Gayed, 1962). In this thesis we investigated on secondary metabolites produced by some pathogenic fungi (*Bipolaris* and *Aspergillus* spp) that attack rice, maize and sorghum (Evidente *et al.*, 2006). These secondary metabolites, called ophiobolins, are reported to produce different effects in plants but their mode of action is still unclear. The study of the biochemical alterations on plant metabolism induced by ophiobolins can enlarge our knowledge on plant-

Sara Cimini

pathogen interaction. This could highlight how to reinforce specific plant defense mechanisms in order to reduce the loss in crops caused by biotic stress in monocots. The current work is aimed to characterize ophiobolin A-mediated effects on cell proliferation versus death features in plant cells. All these experiments have been performed using Tobacco Bright Yellow – 2 (TBY-2) cell suspension culture as model system.

Chapter 2

Antioxidant profile and fructan metabolism during durum wheat kernels maturation

2.1 INTRODUCTION

2.1.1 Wheat: origin and evolution

Wheat was one of the first crops to be domesticated more than 10000 years ago in the Middle East during the Neolithic Revolution, which saw a transition from hunting and gathering food to settled agriculture (Charmet, 2011). The domestication of cereals, specifically of wheat, was one of the most significant changes for humanity. It was significant in particular from the cultural and socio-economic point of view, since it influenced not only human evolution but also the development of civilization. Now wheat is counted among the 'big three' cereal crops in the world, with over 600 million tons being harvested annually. In 2010 world wheat production was 651 million tons, making it the third most-produced cereal after maize (844 million tons) and rice (672 million tons) (http://faostat.fao.org/site/339/default.aspx). However, wheat is unique for environmental and ecological diversity of the areas where it is cultivated, from 67° N in Scandinavia and Russia to 45°S in Argentina, including elevated regions in tropic and sub-tropic regions (Feldman, 1995). It is also unmatched in its range of morphological and genetic diversity.

Triticum genus comprises several species with different ploidy levels. All species belonging to *Triticum* genus present a genome based on a set of seven chromosomes and include diploid species (2n = 14), tetraploid species (4n = 28) and hexaploid species (6n = 42). In tetraploid and hexaploid species most of the genes are present in four or six copies. As a consequence, gene variability, which occurs through mutations and crossings, is more tolerated in these species than in diploid ones. Moreover, the genes present in multiple copies can acquire new functions, thus promoting higher genetic flexibility and, therefore, greater adaptation to environmental changes. The polyploid species of the *Triticum* genus are classical examples of evolution through amphydiploidy. The species of this group are originated as a result of an interspecific crossing between two parental species followed by spontaneous chromosome doubling (Zohary and Feldman, 1962). Each tetraploid species arise as the hybridization product of two diploid species followed by spontaneous chromosome doubling, while each hexaploid species is the hybridization product of a tetraploid species with a diploid species followed by spontaneous chromosome doubling.

Triticum genus includes three polyploid species: two tetraploid species (*Triticum turgidum* and *Triticum timopheevii*) and one hexaploid species (*Triticum aestivum*). *T. turgidum ssp.*

Sara Cimini

dicoccoides (AABB genome) has been originated as a result of a cross between *Triticum urartu* (AA genome) and *Aegilops speltoides* (BB genome). This species was then domesticated and it is considered the progenitor of durum wheat (*T. turgidum ssp. durum*) (Fig. 2.1). *T. timopheevii* (AAGG genome) come from a cross between *Triticum monococcum ssp. aegilopoides* (AA genome) and *A. speltoides* (BB genome). The cultivation of *T. timopheevii* is restricted to certain regions of Russia where it is mainly used as fodder for animals. *T. aestivum* (AABBDD genome) has most probably been derived from a relatively small number of independent crosses between domesticated tetraploid wheat (probably *T. turgidum ssp. dicoccum* – AABB genome) and *Aegilops squarrosa* or *Triticum taushii* (DD genome), followed by spontaneous chromosome doubling (Shewry, 2009) (Fig. 2.1).

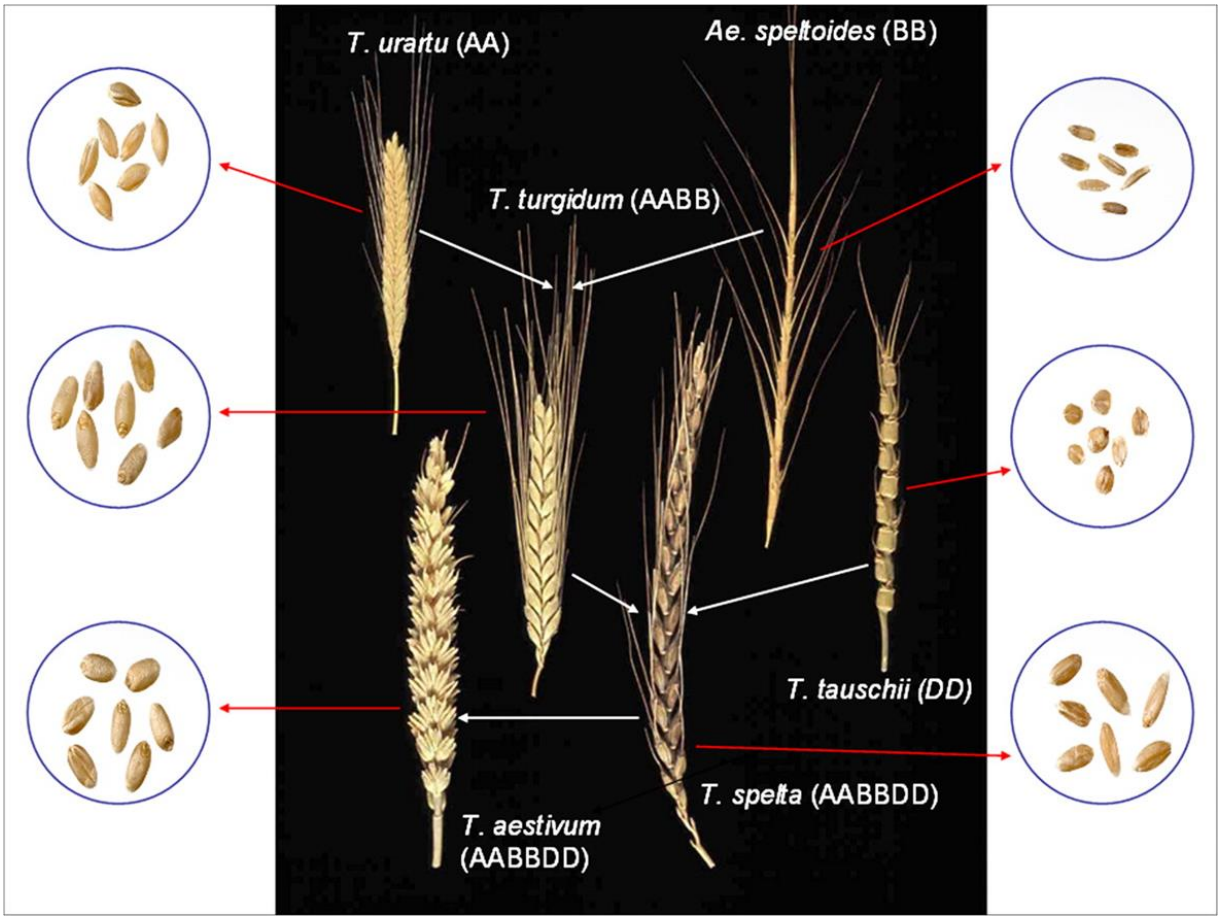

Fig. 2.1. The evolutionary and genome relationships between cultivated bread and durum wheats and related wild diploid grasses, showing examples of spikes and grain. From Shewry, 2009.

The earliest wheat cultivated forms were diploid (genome AA) and tetraploid (genome AABB) and they originated from the south-eastern part of Turkey, the socalled Fertile

Crescent (Heun *et al.*, 1997; Nesbitt, 1998; Dubcovsky and Dvorak, 2007). The cultivation of wheat was spread during the VI and V millennium B.C. from the Fertile Crescent to Europe, Africa and Asia. This is largely demonstrated by archaeological and genetic studies on genes distribution in several wheat varieties in different regions of the Old World (Feldman, 2001). Bread wheat made its first appearance about 9000 years ago (Feldman, 2001).
Wheat has later arrived into Western China (~ 4500 years ago) and during the second millennium B.C. into Eastern China. Only 2300 years ago it has also reached Japan. More recently, bread wheat has been introduced in America in 1529 and in 1788 in Australia. Currently, about 95% of the wheat grown worldwide is *T. aestivum*, and the tetraploid *T. durum* represents the remaining 5% (Shewry, 2009).

At present, the main wheat producing Countries, by order of importance, are: China, India, Russian Federation, United States of America and European Union. Within European Union, France is the largest wheat producer followed by Germany. However, considering only durum wheat production, Italy still is the main producer in the world, together with Canada (World Grain Statistics, 2008).

The wheat intake enriches human diet with essential amino acids, minerals, vitamins, beneficial phytochemicals and dietary fiber compounds, and this is particularly true for products derived from whole-grain. However, the growing importance and use of wheat is due not only to its employment as a major renewable resource for food, but also for feed and industrial raw materials.

2.1.2 Seed maturation

The independent existence of plant is ensured by seed production. Monocot species, like wheat and other cereals, form caryopses (cereal kernels) as propagation units. Caryopses are dry fruits containing only one seed the external tissue of which is fused with fruit tissues forming caryopsis as an indivisible unit. Caryopses have an ovoid shape, more or less elongated depending on the species, with a dorsal and ventral region. A longitudinal section through wheat caryopsis points out an outer tegument, called pericarp which surrounds the aleurone layer and the endosperm (dead storage tissue). The embryo is also enclosed in the pericarp. Embryo and nutritive tissues are produced by fertilization of egg cell by spermatic

Sara Cimini

nuclei, whereas the seed coat cells derive only from maternal tissues. Organs of the cereal embryo are coleoptile, scutellum, radicula and coleorrhiza. Seed endosperm contains very high levels of starch though it also contains oils and proteins. During germination, scutellum absorbs nutrients from starchy endosperm and delivers them to the growing seedling.

Phenological stages and seed growth

Wheat can be sown from autumn to spring depending on the Country. In Italy, sowing-season generally takes place in autumn while, in Northern Europe, where the climate is more rigid, it is almost always springy. After sowing, wheat grains absorb humidity and swell up (up to 45% of its dry weight). The reserve substances present in the endosperm are mobilized and reach the embryo that has already started to grow by elongating its cells as a consequence of water uptake. The availability of molecules produced by reserve mobilization further stimulates embryonic axes, hypocotyl and epicotile growth. The embryonic root, the radicle, breaks the coleorhiza and stretches out into a primary root which in turn develops 4 secondary roots. The plumule, pushed by epicotyl, begins to stretch out and, protected by the coleoptile, it reaches ground surface. After about 10 days from sowing, the emergence of the first leaf occurs. The young seedling, in good humidity and temperature conditions, comes into full autotrophy after the emergence of 2-3 leaves. Up to this stage, the young seedling drew nourishment from the endosperm. The tillering stage starts with the emergence of lateral shoots (tillers) from the axils of the true leaves at the base of the main stem of the new plant. Primary tillers form in the axils of the true leaves of the main stem. Secondary tillers may develop from the base of primary tillers. Tillering usually begins when the seedling plant has three or more fully developed leaves. Tillers depend on the main stem for nutrition during their development. Once a tiller has developed three or more leaves, it becomes nutritionally independent from the main stem and forms its own root system. The tillering stage goes on for the whole winter and gradually stops during spring when temperatures rise. Stem elongation is the next phase of growth. It occurs as a result of internode elongation. During this phase, the stem nodes and internodes emerge above the soil surface and become visible. Winter wheat cultivars, which may have a prostrate growth habit during the development and vegetative life, begin to grow erect. After the flag leaf emergence the booting stage occurs. This phase is rather short and indicates that the ear is ready to emerge. The boot stage ends when the awns is visible at the flag leaf sheath and the leaf sheath is forced to open by the ear. Once ear is completely developed, flowering (anthesis) occurs. Generally, flowering begins in

Sara Cimini

wheat within three or four days after ear emergence. During flowering, the anther opening takes place from each floret on the ear and the pollen moves from anthers to stigmas. After fertilization, the embryo starts to develop and photosynthates and other compounds previously produced, are transferred in the endosperm of developing grains. During embryo development, a first increase in fresh weight and seed size occurs. During the first stage of grain filling, called watery ripe stage, kernels rapidly increases in size but does not accumulate much dry matter. Later, in the milk stage, the kernels are filled with a white, milky fluid. An appreciable increase in nutrients, especially sugars, takes place in the endosperm of developing kernels. By the end of the milk stage (at about 14 days after fertilization), cell division, expansion and differentiation are completed (Evers and Millar, 2002). After the milk stage, the sugar content decreases and the starch content increases.

The last stage of grain filling can be divided into two different phases:

- the soft dough phase in which water concentration decreases remarkably and kernel rapidly accumulates starch and nutrients. Most of the kernel dry weight is accumulated by the end of this phase;
- the hard dough phase in which kernel moisture content decreases from a level of 40 percent to 30 percent. At the end of the hard dough stage, the kernel reaches its maximum dry weight.

During the ending ripening stage the kernels reach a moisture level suitable with their conservation that is usually less than 20%. The dehydration process and acquisition of desiccation tolerance are characterized by water loss, decrease in size and weight of the kernels (De Gara *et al.*, 2003a) as well as synthesis of LEA (Late Embryogenesis Abundant) proteins (Vicente-Carbajosa *et al.*, 2005). Starting from the middle ripening period, wheat endosperm cells also undergoes to programmed cell death (Paradiso *et al.*, 2012), and, at the end of kernel maturation, the aleuronic cells are the only endospematic cells still alive. The dehydration state allows the seeds to delay the germination process until better environmental conditions are reached (Bewley, 1997). Germination of the seeds starts when the dormancy is broken, if water is available.

All the processes characterizing seed development and germination, such as embryo growth, storage products accumulation, protective tegument differentiation, development of tolerance to desiccation and dormancy broken, are regulated by the concerted action of several

Sara Cimini

hormonal and metabolic signaling pathways. Some hormones like abscisic acid, auxins, cytokinins and gibberellins are involved in the process of seed development. Particularly abscissic acid (ABA) has been suggested to be the key hormone required throughout the process of seed maturation, even if gibberellins (GA) also play an important role. For example, dormancy induction is reliant on a high ABA to GA ratio (Seo *et al.*, 2006; Feurtado and Kermode, 2007). Dormancy in cereals can be broken by changes in environmental conditions, including temperature, light, oxygen, and nutrients (Jacobsen *et al.*, 2002; Benech-Arnold *et al.*, 2006). Evidence so far indicate that dormancy release is due, at least in part, to changes in ABA metabolism and probably ABA signaling (Benech-Arnold *et al.*, 2006; Chono *et al.*, 2006; Millar *et al.*, 2006; Barrero *et al.*, 2010).

Seed development is guaranteed by the photoassimilates produced by leaves and vegetative parts of inflorescences. In wheat, as the photosynthetic rate of the flag leaf steeply falls during the period of kernel maturation, kernel loading depends on remobilization of stem reserves, apart a certain photosynthetic activity occurring in the inflorescence (Richards, 2000).

As generally occurs in other species, the principal imported sugar in developing kernel is sucrose (Suc). In seed development, the regulation of the expression of enzymes that hydrolyze Suc to glucose and fructose, called invertases (INVs), has been reported to be particularly important during prestorage phase. Indeed, alterations in the level of soluble sugars, such as glucose, fructose and Suc, have been shown to affect different developmental programs in seed: for example a high glucose/Suc ratio is suggested to be associated with cell division, whereas a high Suc/hexose ratio seems to be crucial for the storage product pathways (Morley-Smith *et al.*, 2008). As a matter of fact, during seed maturation, Suc signals control storage and differentiation processes through the regulation of cell metabolism by altering gene expression and enzyme activities, even if the mechanisms by which sugars influence seed development and gene expression are still far from being deciphered (Gibson, 2005).

Sugar-signaling is complicated by the fact that plants have multiple sugar-response pathways that may actually be regulated by alteration in sugar fluxes rather than by absolute sugar or sugar-metabolite levels. Sugar-response pathways also exhibit "cross-talk" with numerous other pathways, including those regulated involving phytohormones (Borisjuk *et al.*, 2004; Léon and Sheen, 2002) and light responses (Paul and Pellny, 2003; Ellis *et al.*, 2002). Moreover, sugars can act by affecting osmotic potential.

Sara Cimini

As previously mentioned, kernel starchy endosperm undergoes to programmed cell death as last event of its development (Paradiso *et al.*, 2012). Both cell division and programmed cell death require a strict control of reactive oxygen species (ROS) production (Potter *et al.*, 2002; Foyer and Noctor, 2011; de Pinto *et al.*, 2012). Therefore, molecules and enzymes involved in ROS metabolism take part in kernel development as well as they control the entire life cycle of the plant and plant adaptation to environmental changes.

2.1.3 Redox balance: reactive oxygen species and antioxidant systems

Reactive oxygen species

The sessile nature of higher plants precludes escaping from unfavorable environmental conditions. The exposure to changing conditions has led to the evolution of a highly flexible metabolism able to adapt to external changes in a proper manner (Chinnusamy *et al.*, 2004; Pitzschke *et al.*, 2006). The metabolism of higher plants, is not only extremely flexible, but is also strongly regulated in order to control a wide range of metabolic pathways.

Plants use molecular oxygen O_2 in many oxidative processes in which O_2 works as final electron acceptor. Although in the main reactions, such as mitochondrial respiration, the O_2 is subjected to tetravalent reduction with H_2O formation, ROS are continuously produced as products of various metabolic pathways in different cellular compartments such as chloroplast, mitochondria, peroxisomes and cell wall (Halliwell, 2006; Gill and Tuteja, 2010). The term ROS is related to highly reactive molecules which derive from the molecular oxygen ground state. O_2 itself is a reactive molecule since it has two unpaired electrons in its outmost π orbital. This makes O_2 a strong oxidant even if it slowly reacts with non-radical species due to the spin restriction for the putative electron donor (Halliwell, 2006).
ROS can be produced either by energy transfer or by electron transfer reactions (Apel and Hirt, 2004) (Fig. 2.2). It has been estimated that 2% of O_2 consumption leads to the formation of ROS in plant tissues.

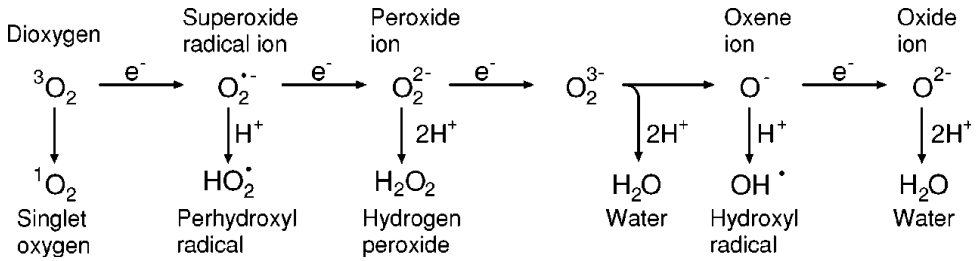

Fig. 2.2. Generation of different ROS by energy transfer or sequential univalent reduction of ground state triplet oxygen (from Apel and Hirt, 2004).

Singlet oxygen ($^1O_2$) can be produced by energy transfer inducing an electron rearrangement (Apel and Hirt, 2004; Asada, 2006). In $^1O_2$, spin restriction is removed and its oxidizing ability greatly increased. $^1O_2$ is a highly unstable free radical characterized by a half-life of 4

μs in aqueous solution and unable to cross the biological membranes (Foyer and Harbinson, 1994).

On the other hand, when O_2 is subjected to electron transfer reactions it forms other ROS, such as superoxide anion ($O_2^{\bullet -}$), hydrogen peroxide (H_2O_2) and hydroxyl radical ($OH^{\bullet}$) (Apel and Hirt, 2004; Scheibe *et al.*, 2005). The $O_2^{\bullet -}$ is a highly reactive molecule characterized by a half-life very short, ranging between 2 and 4 μs at physiological pH. Because of its high instability this molecule rapidly disproportionates to O_2 and H_2O_2 either spontaneously or by the action of superoxide dismutase (SOD). $OH^{\bullet}$, as $O_2^{\bullet -}$, is a very unstable molecule and is among the most highly reactive ROS known (half-life 1 ns). $OH^{\bullet}$, is thought to be largely responsible for mediating oxygen toxicity *in vivo*. Contrary to $OH^{\bullet}$ and $O_2^{\bullet -}$, H_2O_2 has relatively long half-life (1 ms). It can migrate at relative long distance from the production site, up to neighboring cells or compartments, crossing biological membranes.

$^1O_2$ and $OH^{\bullet}$ are considered the most toxic ROS for living organisms. These molecules are in fact extremely reactive and do not require specificity in their interaction with other molecules. Conversely, $O_2^{\bullet -}$ and H_2O_2 are less reactive and more selective.

Production and removal of ROS must be strictly controlled in order to avoid high intracellular ROS levels which can cause irreversible damage and lead to cell death by reacting with a large variety of biomolecules such as proteins, lipids, carbohydrates and DNA (Girotti, 2001; Blokhina *et al.*, 2003; Gill and Tuteja, 2010).

Furthermore, in recent years, much attention has been focused on defining the role of ROS as signaling molecules to control various biological processes in plants (Mittler *et al.*, 2004). Sure enough, lower levels of ROS are able to affect the expression of different genes and signal transduction pathways, proposing that cells have evolved mechanisms to use ROS as transducing signals (Fig. 2.3; Dalton *et al.*, 1999; Mittler *et al.*, 2004). For example, the production of $^1O_2$ during illumination in *Arabidopsis thaliana* conditional *flu* mutants induces a rapid change in nuclear gene

ROS	Half Life	Migration capacity
Superoxide ($O_2^{\bullet -}$)	2-4 μs	30 nm
Hydrogen peroxide (H_2O_2)	1 ms	1 μm
Hydroxil radical ($OH^{\bullet}$)	1 ns	1 nm
Singlet Oxygen ($^1O_2$)	4 μs	30 nm

expression that affects 5% of total genome (op den Camp, 2003). As a consequence of this $^1O_2$-dependent regulation of gene expression the growth rate of mature plants decreases whereas seedlings bleach and die (op Den Camp *et al.*, 2003). Much attention has been focus also on gene expression modulation by H_2O_2 in response to several stress stimuli. Specific induction of defense responses has been achieved with direct H_2O_2 treatment or by stressors able to induce its production (Desikan *et al.*, 2001; Vanderauwera *et al.*, 2005).

It has been shown that ROS are able to modulate gene expression directly by affecting the activity of specific transcription factor and indirectly by changing the cellular redox state. Moreover, non-enzymatically generated ROS oxidation products may act as second messengers capable of inducing biological responses (Pitzschke *et al.*, 2006).

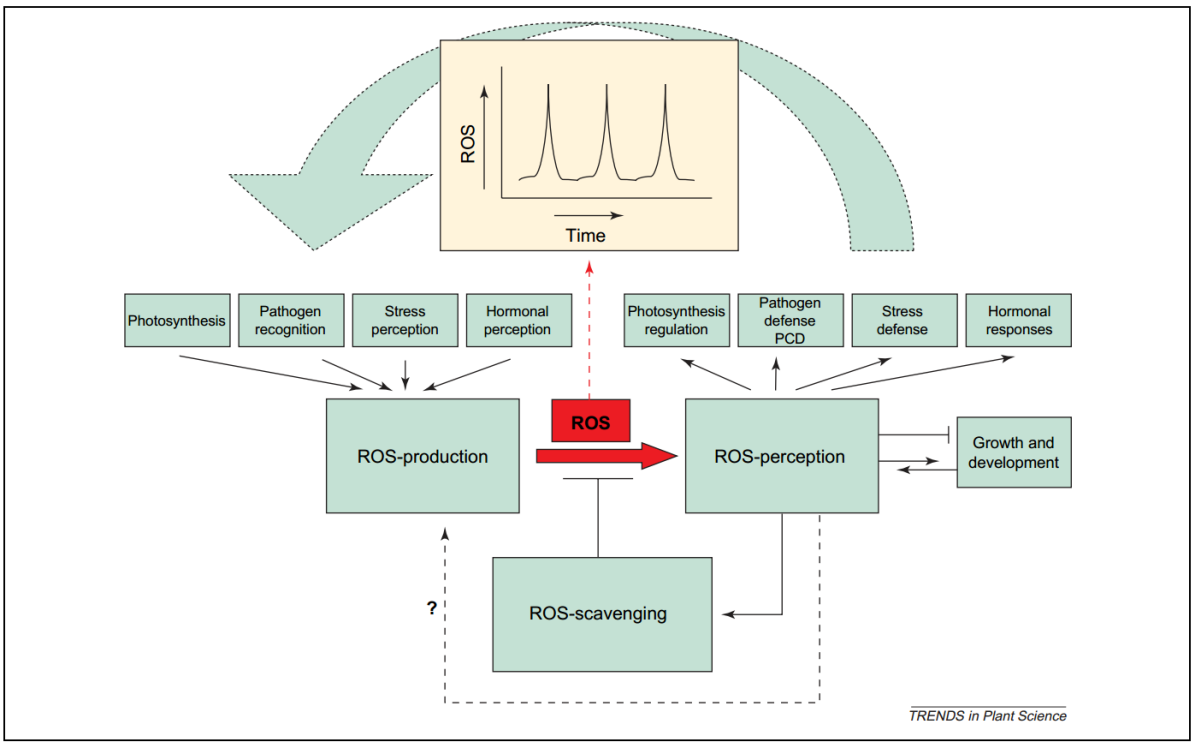

Fig. 2.3. The ROS scavenging pathways present in plant cells are responsible for maintaining a low steady-state level of ROS. However an enhanced production of ROS in plant cells can be a result of several cellular signals (e.g. pathogen recognition or stress perception). The intensity, duration and localization of the ROS signals are determined by interplay between the ROS producing and the ROS scavenging pathways. Moreover ROS perception can also affect growth and development: inhibition during stress or regulation during normal growth (from Mittler *et al.*, 2004).

Antioxidant systems

Under physiological steady-state conditions, ROS have been scavenged by different antioxidative defense components (Foyer and Noctor, 2005).

The balance between the production and the scavenging of ROS may be influenced by various biotic and abiotic stresses such as UV radiation, drought, temperature extremes, nutrient deficiency, herbicides and pathogen attacks. The development of cellular antioxidant systems is therefore of crucial importance in order to control ROS levels in different cellular compartments. Moreover, it has been demonstrated their activity as sensors of environmental conditions with the purpose to activate different signaling pathways on the basis of alterations in the cellular redox state (Fig. 2.3).

The antioxidant system is a network consisting of several mechanisms such as the enzymes SOD, ascorbate peroxidase (APX), catalase (CAT), glutathione peroxidase and peroxiredoxins. Also non-enzymatic compounds contributing to the antioxidant network, like ASC, GSH and polyphenols, are receiving increasing attention (Chen and Arora, 2011).

SOD catalyzes the dismutation of $O_2^{\bullet -}$ to H_2O_2. Three classes of SOD activity have been identified in plant cells that differ by using specific metal cofactor: manganese in mitochondrial isoenzyme, iron in one of the plastidic isoenzyme and copper and zinc in the other plastidic isoenzyme and in the cytosolic one (Kliebenstein *et al.*, 1998; Bowler *et al.*, 1992). Moreover, peroxisomal and extracellular SODs have been described (Streller and Wingsle, 1994; Bueno *et al.*, 1995).

CAT dismutates H_2O_2 to O_2 and H_2O. In plant cells three different CAT isoenzymatic forms have been characterized each of which specific for a particular cellular compartments: CAT1, presents in peroxisomes, CAT2, expressed in vascular tissues and CAT3 presents in the glyoxysomes (Willekens *et al.*, 1994).

In plant cells, another enzyme responsible of H_2O_2 detoxification is APX. APX reduces H_2O_2 to H_2O by utilizing ASC as specific electron donor. APX activities are located in chloroplasts, cytosol, mitochondria and peroxisomes, each cellular compartment possessing one or several APX isoforms (D'Arcy-Lameta *et al.*, 2006).

These are considered the main enzymatic systems for protecting cells against oxidative damage. However, also glutathione peroxidase, peroxideroxin and class III peroxidases are receiving increasing attention in the last decades. Glutathione peroxidases (GPX) are located

Sara Cimini

in several subcellular compartments and involved in the response to both biotic and abiotic stress conditions. These enzymes can reduce peroxides like H_2O_2, much more efficiently or sometimes only, by using the thioredoxin (Trx) rather than GSH as electron donor (Herbette *et al.*, 2002; Jung *et al.*, 2002; Tanaka *et al.*, 2005; Navrot *et al.*, 2006).

Peroxiredoxin (Prx) are a family of thiol-based peroxidases widely distributed in all living organisms, from archaebacteria to mammals (Baier and Dietz, 1996; Stacy *et al.*, 1996; Dietz, 2011). These enzymes catalyze the detoxification of H_2O_2 and other peroxides and in relation to their subunit composition, the position and number of the conserved cysteine residues they can be organized into four distinct subclasses: 1-Cys Prx, 2-Cys Prx, Prx II and PrxQ (Bhatt and Tripathi, 2011; Dietz *et al.*, 2002; Rouhier and Jacquot, 2002).

Class III peroxidases, also called secretory peroxidases (PODs), have many physiological functions in plant metabolism depending on their reducing substrates. APXs and PODs usually use H_2O_2 as electron acceptor. On the other hand, PODs do not generally use ASC as electron donor, but preferentially oxidize phenolic compounds (De Gara, 2004). However, two PODs with remarkably high APX activity have been described (Kvaratskhelia *et al.*, 1997). These enzymes could be involved in H_2O_2 scavenging.

Developmental and environmental stimuli are crucial factors in regulating the expression of all these genes constituting the cellular network for protecting the cells against ROS-induced damage (De Gara *et al.*, 2003b).

In addition to these enzymatic systems, also redox metabolites, like ASC, GSH and polyphenols, are involved in the protection of cells against oxidative stress.

The metabolism of ASC and GSH, small metabolites present in all cell compartments that have been analyzed until now, is involved both in plant developmental processes and in the cell protection against ROS (De Gara *et al.*, 2003b). In the ASC-GSH cycle APX fulfills a crucial role in ROS scavenging catalyzing the reduction of H_2O_2 to H_2O, using ASC as specific electron donor (Fig. 2.4). In this reaction ASC is converted to monodehydroascorbate (MDHA), intermediate radical intermediate that can spontaneously dismutate giving ASC and dehydroascorbate (DHA). Alternatively MDHA can be reduced back by NAD(P)H dependent reductase (MDHA-Reductase, MDHAR) (de Pinto *et al.*, 2000). DHA is also reconverted to ASC by DHA-reductase (DHAR) that uses the reducing power of GSH. GSH is the recycled

Sara Cimini

by the reduction of glutathione disulphide (GSSG) by GSSG reductase (GR) (Fig. 2.4; De Gara *et al.*, 2003b).

Because ASC and GSH are the main soluble redox metabolite in plant cells, regulation of this cycle hold a critical role in controlling the cellular redox balance.

Changes in the ASC-GSH cycle occur under the influence of different kind of stresses or developmental processes such as seed germination (Tommasi *et al.*, 2001; De Gara *et al.*, 2003b) or leaf senescence (Borraccino *et al.*, 1994).

Genetically modified plants over-expressing one of the genes involved in this cycle, are characterized by a higher resistance to abiotic stresses (Foyer *et al.*, 1995; Lee *et al.*, 2007; Prashanth *et al.*, 2008). For instance, a poplar hybrid containing enhanced foliar GSH pools and also overexpressing GR in the chloroplasts had increased tolerance against low temperature-induced photoinhibition (Foyer *et al.*, 1995).

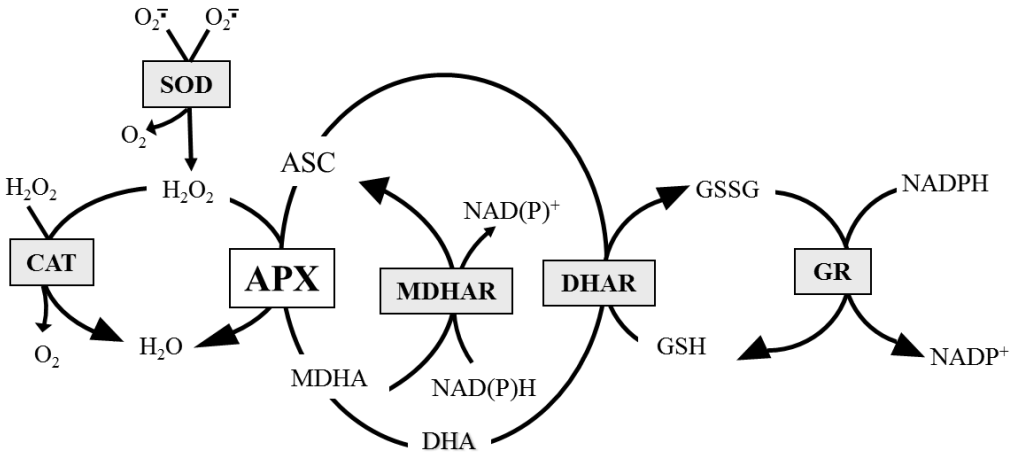

Fig. 2.4. The central role of APX in ROS detoxification. ASC–GSH cycle and connected ROS scavenging systems. From De Gara *et al.*, 2010.

GSH fulfill a central role not only in defense mechanism, but it also has functions in biosynthetic pathways, detoxification, cell cycle regulation, redox homeostasis and antioxidant biochemistry that cannot be performed by other thiols or antioxidants (Noctor *et al.*, 2012). In particular, in the last years, the involvement of GSH in the control of cell cycle proliferation is coming to light with growing evidences (Vernoux *et al.*, 2000; Potters *et al.*, 2002, 2004; Markovic *et al.*, 2009). The redox regulation of the mitotic cell cycle has not been intensively investigated in plant cells as in animals. Nonetheless, it has been established that there is a strong relationship between cellular redox state and the progression through the

cell cycle (Jiang and Feldman, 2005; Jiang *et al.*, 2006; Dinneny *et al.*, 2008; Markovic *et al.*, 2007). At the G1 phase of the plant cell cycle the recruitment of GSH into the nucleus is crucial for the redox state of the cytoplasm and the expression of redox-related genes (Pellny *et al.*, 2009; Diaz Vivancos *et al.*, 2010). An increase in total cellular GSH pool is required to cell cycle progression from the G1 to S phase (Diaz Vivancos *et al.*, 2010). Further experimental evidences show that in the absence of GSH, plant cells arrest at the G1 phase as well as in case of GSSG accumulation (Potters *et al.*, 2002, 2004).

Most (up to 80%) of the cellular GSH pool is recruited into the nucleus of plant and mammalian cells early in the proliferation. In particular GSH seems to be localized largely in the cytosol at the G0/G1 phase and in the nucleus when the cells are in the S and G2/M phase (Markovic *et al.*, 2007; Pallardó *et al.*, 2009; Pellny *et al.*, 2009; Diaz Vivancos *et al.*, 2010). The mechanisms that control GSH partitioning between the nucleus and cytoplasm are still unknown as well as the factors needed for GSH sequestration in the nucleus (Pellny *et al.*, 2009; Maughan *et al.*, 2010; Noctor *et al.*, 2012). However they have to be rapidly activated and de-activated in response to cell cycle checkpoints in order to ensure cell cycle proliferation (Pallardó *et al.*, 2009). Candidate GSH-recruiting proteins in the nucleus include Bcl-2, an anti-apoptotic protein involved in the maintaining of cell survival (Voehringer *et al.*, 1998). Moreover, similarly to the transport of GSH between the nucleus and the cytoplasm also the transport between cytosol and chloroplasts is very important in plant cell redox homeostasis and signaling (Foyer *et al.*, 2001; Maughan *et al.*, 2010; Diaz Vivancos *et al.*, 2010).

Finally, also polyphenolic compounds are known to contribute to ROS homeostasis by scavenging free radicals and acting as protectors against stresses triggered by ultraviolet radiation, unfavorable environmental conditions or aggression by pathogens. Polyphenols comprise a wide area of secondary metabolites naturally occurring in plant cells. Almost all of them exhibit a marked antioxidant activity.

In cereals, they are distributed as free, soluble-conjugated and insoluble-bound forms either esterified or etherified to the cell wall constituents. Polyphenols are principally present in the outer parts of the cereal grains (Manach *et al.*, 2004). Phenolic acids are the most abundant polyphenols in wheat and, among these, ferulic acid is the most abundant and principally present in insoluble-bound form (Adom and Liu, 2002; Zuchowski *et al.*, 2011). The aleurone layer and the pericarp of wheat grain contain 98% of the total ferulic acid (Manach *et al.*,

Sara Cimini

2004). Other phenolic acids identified in wheat are sinapic acid, p-coumaric acid, vanillic acid, caffeic acid, and diferulic acids, syringic acid, o-coumaric acid, gentisic acid and 2-hydroxybenzoic acid (Zuchowski *et al.*, 2011; Gawlik-Dziki *et al.*, 2012). According to Mpofu, total phenolic content, antioxidant activity, and phenolic acid composition are the results of the genotype and environment conditions in which plants are grown and of the genotype-environment interactions (Mpofu *et al.*, 2006).

Given the contribution of phenolic compounds to the cellular antioxidant system, it is clear the increasing interest about these compounds as bioactive food components (Van den Ende *et al.*, 2011b).

Reactive oxygen species during abiotic stress

In plants, ROS are constantly produced as inevitable consequence of aerobic metabolism. The main production sites in plant cells are chloroplasts, mitochondria and peroxisomes and, among these, chloroplasts provide the highest contribution to ROS production in green tissues. Plants are continuously exposed a lot of different kind of external stimuli that can cause alterations in the equilibrium between ROS production and removal as many ROS are generated as one of the earliest responses to biotic and abiotic stresses (Arora *et al.*, 2002). The onset of stressful conditions can give rise to oxidative stress in plant cell as a consequence of metabolic perturbation in the organelles that are sensitive to changes in environmental conditions (Elstner, 1991; Prasad *et al.*, 1994; Suzuki *et al.*, 2012; Miller *et al.*, 2008).

Abiotic stresses are defined as adverse environmental conditions able to disturb cellular functions and produce an imbalance that alters cellular redox state with the consequent reduction of the growth, survival and/or fecundity of plants (Jasper and Kangasjärvi, 2010). Most commonly mentioned abiotic stresses are high light, low or high temperatures, drought, salinity, humidity, UV-radiation, air-pollution and herbicides (Apel and Hirt, 2004). These stresses can cause several changes on plant metabolism and led to increased production of ROS. Depending on the nature of ROS, different plant signaling pathways can be activated (Jasper and Kangasjärvi, 2010) to handle the oxidative stress condition. The survival of plants to these adverse stresses depends on their ability to perceive the stimulus, generate and transmit a signal capable of activate defense responses. Redox and ROS signaling networks from organelles to the nucleus (retrograde signaling; Suzuki *et al.*, 2012) are central to

Sara Cimini

coordinate gene expression and modulate anterograde control (Woodson and Chory, 2008) and so are important in plant adaptation to stress conditions. Even mild abiotic stress can affect cereal yields and, in particular, grain production that is the most vulnerable yield component in grain crops (Dolferus *et al.*, 2011). Among the abiotic stresses, water deficit is starting to be an increasingly severe problem for cereal production and it occurs not only during drought but also as a consequence of high salinity or low temperature (Al Ghamdi, 2009). Plant water deficit tolerance requires a complex mechanism that responds differently to changes in external condition depending on plant species and genotypes (Jaleel *et al.*, 2009; Pastori and Trippi, 1993; Varga *et al.*, 2012).

The intervention of antioxidant defense systems plays a crucial role in protecting against oxidative damage (Gill and Tuteja, 2010). It was proposed that improving resistance to oxidative damage may increase stress tolerance. By way of example, it has been reported that SOD activity was higher in cold-tolerant *Zea diploperennis* than in cold-sensitive *Zea mays* (Jahnke *et al.*, 1991). Moreover, *Z. diploperennis* has a higher concentration of ASC and was able to remove H_2O_2 much better than *Z. mays* (Hull *et al.*, 1997).
The salt stress also increases the activity of SOD and CAT in both salt-tolerant and salt-sensitive wheat cultivars and POD activity increase in response to salt-treatment in salt-tolerant wheat cultivars (Mutlu *et al.*, 2009).

In addition to antioxidant defense mechanisms aforementioned, also other adaptive mechanisms are involved in plant protection against water deficit. Another mechanism is represented by the recovery of cellular osmotic potential (Langridge *et al.*, 2006). This can be achieved because the cells can sequester ions into cellular compartments or because they can synthetize specialized osmolytes, such as proline, glycine betaine, mannitol, fructans, able to adjust cellular osmotic potential. Many evidences correlate beneficial effect on abiotic stress tolerance with the storage of metabolites, such as fructans (Pilon-Smits *et al.*, 1995), proline (Kishor *et al.*, 1995), glicine betaine (Nomura *et al.*, 1995), trehalose (Romero *et al.*, 1997), and mannitol (Tarczynski *et al.*, 1993). Besides this most expectable function it has been proposed that these metabolites can be also active against ROS (Shen *et al.*, 1997; Stoyanova *et al.*, 2011) and stabilize the structure of some proteins under stress (Galinski, 1993; Jovanović *et al.*, 2006; Jain and Roy, 2010). It has also been hypothesized that they could act as low-molecular-weight chaperones (Bohnert and Jensen, 1996).

2.1.4 Fructans as part of carbohydrate metabolism during kernel maturation

Definition

Fructans are water soluble polymers based on fructose (Fru) that occur in plants, micro-organisms like bacteria, fungi (including yeast) and in some green algae (Hendry and Wallace, 1993; Lewis, 1984).

Fructans in plants

About 15% of flowering species produce fructans (Hendry, 1993), among which the Asteraceae (e.g. chicory, Jerusalem artichoke, and dahlia) are the most known, but other economically important families accumulates fructans in their tissues such as Poaceae (e.g. wheat and barley) and Liliaceae (e.g. onion and garlic). These sugars are synthetized starting from Suc, the primary end product of photosynthesis, and are accumulated in vacuoles of both photosynthetic and storage cells (Cairns, 2003) although it has been reported their presence also in the apoplast and within vascular bundles (Livingston and Henson, 1998; Van den Ende *et al.*, 2000). Fructans are mainly stored in roots and tubers of plants belonging to Asteraceae, in leaves and stems of plants belonging to Poaceae and in bulbs of Liliaceae (Hendry, 1993; Van den Ende *et al.*, 2000). Their presence has also been reported in seeds and inflorescences (Livingston *et al.*, 2009).

Fructan structure

Fructans are linear or branched oligo- or polysaccharides, consisting of at least two adjacent Fru moieties and, generally, one glucose (Glc) residue per molecule (Lewis, 1993). The first step of fructan biosynthesis consists of the addition of a fructosyl unit from Suc to one of the three primary hydroxyl groups of another Suc molecule, and results in the production of three trisaccharides, termed 1-kestose (1-K), 6-kestose (6-K) and 6G-kestose (neokestose, n-K) (Lewis, 1993; Chalmers *et al.*, 2005; Fig. 2.5). These trisaccharides are the starting molecule for the production of different types of fructans.

In higher plants, fructans are classified into five structurally distinct major categories, depending on the position of the glucosyl unit and on the type of glycosidic linkage between the fructosyl residues (Ritsema and Smeekens, 2003). The type of fructan and the degree of polymerization (DP) is species- and tissue-specific.

Sara Cimini

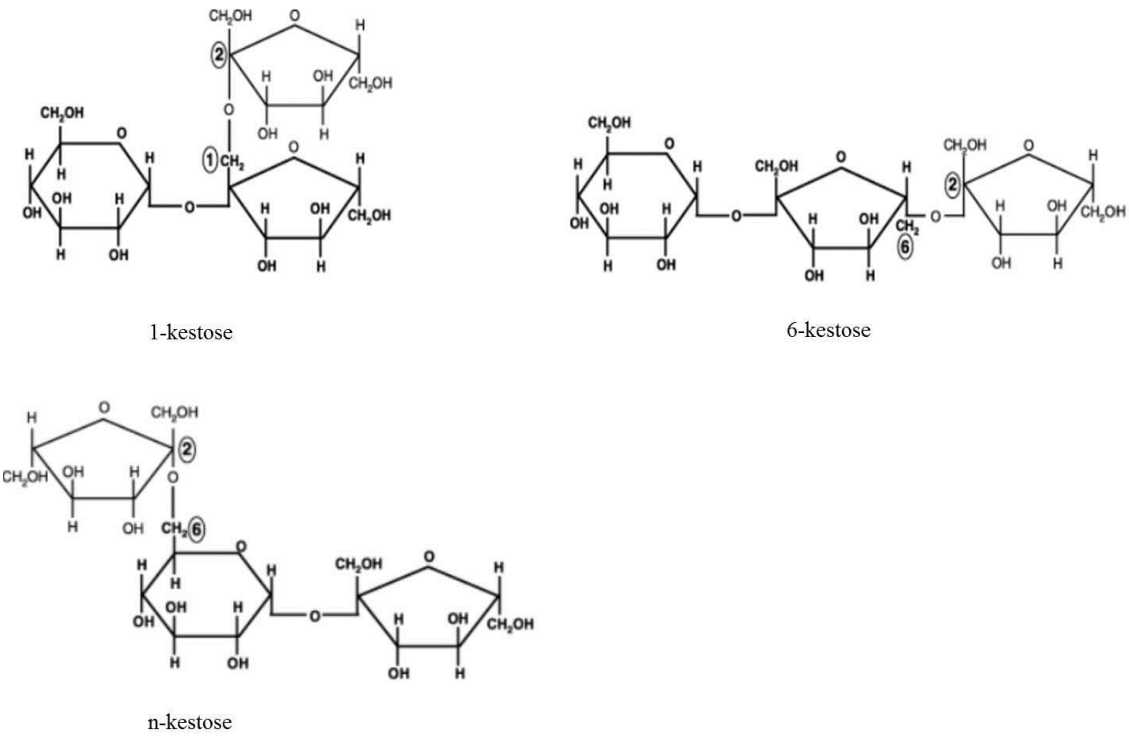

Fig. 2.5. Structure of fructan trisaccharides. (Chalmers *et al.*, 2005)

Inulins

Inulins are linear fructans characterized by a terminal glucosyl unit and β(2,1) glycosidic linkages between its fructosyl residues. They derived from 1-K and are generally presents in species belonging to Asterales (Boraginaceae, Asteraceae, Campanulaceae) such as chicory (*Cichorium intybus*) and artichoke (Koops and Jonker, 1996).

Levans

Levans are linear fructans characterized by β(2,6) glycosidic linkages between its fructosyl residues. The shortest levan is 6-K. They are very common in bacteria but they have also been found in some grasses such as *Dactylis glomerata* and in other monocots (Waterhouse and Chatterton, 1993; Chatterton *et al.*, 1993; Chatterton and Harrison 1997).

The term phlein has substantially the same meaning as levan but it has generally used to describe plant (and not bacterial) fructans with a low DP (4-12).

Differently from inulins, that are arranged in a random coil structure, levans are characterized by a helix structure what makes the molecules less flexible than that of inulin-type fructans (Vereyken *et al.*, 2003; Van den Ende and Valluru, 2009).

Graminans

Graminans are branched fructans, having both β(2-1) and β(2-6) linkages between the fructosyl residues. They are based on the trisaccharides 1&6-kestotetraose (bifurcose, Bif; Fig. 2.6). Graminans are typical of most plants belonging to the Poaceae family (such as wheat and barley) and Liliaceae family. These fructans were also found in some temperate grasses such as *Pachysandra terminalis* (Van den Ende *et al.*, 2011a).

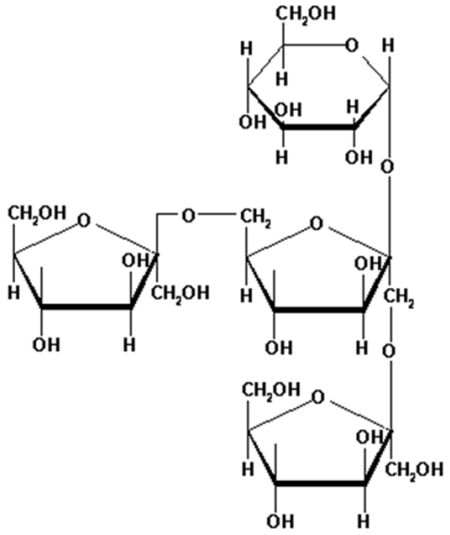

1&6-kestotetraose
(Bifurcose, Bif)

Fig. 2.6. Structure of the tetrasaccharide 1&6-kestotetraose (Bifurcose, Bif), the shortest graminan type.

Neoseries

Inulin and levan neoseries are linear molecules characterized by the presence of the glucosyl unit not in a terminal position, as usually happens in fructans, but between two fructosyl residues. The smallest neoseries-type fructan is n-K. Neoseries fructans occur in *Allium cepa* (onion) and *Asparagus officinalis* (asparagus) (Shiomi 1989, 1993) as well as in plants belonging to Poacea family such as *Avena sativa* (oat) and *Lolium perenne* (Livingston *et al.*, 1993).

The reason of the existence of several fructan types in plants is unknown. This difference could be necessary in order to supply to diverse physiological needs or it could be the result of a different evolutionary origin of fructan biosynthesis enzymes in different plant families.

In Poaceae family the presence of fructans is limited to the subfamily of Pooideae. In this subfamily, a wide range of fructan sizes and structures have been found (Chatterton *et al.*,

1993), including fructans having the Glc residue in internal (e.g. many fructans from *Avena sativa*, Livingston *et al.*, 1993) or in terminal position (e.g. fructans from *Triticum aestivum*, Bancal *et al.*, 1992). Moreover in some species fructans are branched (e.g. fructans from *Triticum aestivum*, Bancal *et al.*, 1992) while in others they are linear (e.g. *Phalaris aquatica*, Bonnett *et al.*, 1997).

Despite the wide range of fructans detected in the Poaceae, graminans and phlein are the fructan series predominantly present (Bonnett *et al.*, 1997). In the particular case of wheat, mixed-type fructans (graminans, DP 3-40) are the main water-soluble polysaccharides accumulated (Bancal *et al.*, 1992; Bonnett *et al.*, 1997) and their content can reach 10% or more of the fresh weight at the end of the cold hardening period (Kawakami and Yoshida, 2005; Yoshida *et al.*, 1998). Wheat is able to store fructans in all parts of the plant including stems, leaves and seeds even if in different amounts, depending on the growing stage, climate and genotype. Analysis of fructans content has been recently determined in different wheat species, together with quantitative trait loci (Huynh *et al.*, 2008; Paradiso *et al.* 2008; Brandolini *et al.*, 2011). As regards the fructans concentration in wheat grains, this has been estimated at 0.9–1.8 g/100 g in five cultivars from five growth places (Fardet, 2010). Moreover, depending on the part of the plants considered fructan content can change: it has been found higher in bran (2.0 g/100 g) and middlings (2.3 g/100 g) than in flour (1.6 g/100 g) and grain (1.5 g/100 g) (Knudsen, 1997). Finally, plant developmental stage and external conditions can influence not only fructan amounts but also the length of fructan molecules synthetized.

Fructan Metabolism

Fructan metabolism has been deeply investigated particularly in dicotyledonous species. The recent cloning of the enzymes involved in fructans biosynthesis and catabolism has substantially confirmed the model proposed by Edelman and Jefford in 1968 even if the existence of additional biosynthetic enzymes (e.g. sucrose:sucrose 6-fructosyltransferase (6-SST) or fructan:fructan 6-fructosyltransferase (6-FFT)) cannot be excluded. In this section an overview of the enzymes involved in fructan metabolism is given. Particular attention has been given to the enzymes studied in the Poaceae family and especially in wheat.

Sara Cimini

Biosynthesis

In plants, fructans are synthetized from Suc by the activity of several fructosyltransferases (FTs) that catalyze the addition of fructofuranosyl units to the fructan growing molecule (Fig. 2.7).

Within the Poaceae, the presence of a wide range of fructan structures suggests a complexity of the biosynthetic fructan pathways that is higher than those of dicotyledonous plants.

Inulin biosynthesis

According to the Edelman and Jefford model, the enzymes termed sucrose:sucrose 1-fructosyltransferase (1-SST; EC 2.4.1.99) and fructan:fructan 1-fructosyltransferase (1-FFT; EC 2.4.1.100) are responsible of the inulin biosynthesis. 1-SST catalyzes the transfer of fructofuranosyl units from a Suc donor to a Suc acceptor molecule, generating the trisaccharide 1-K and Glc as product. This is the most favorably reaction catalyzed by 1-SST.

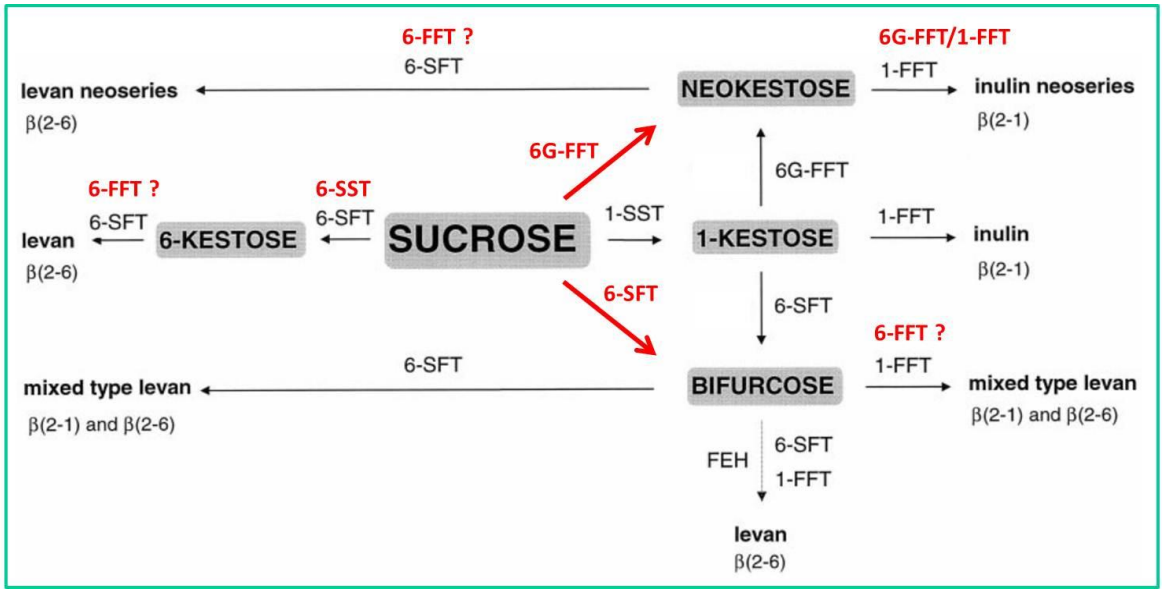

Fig. 2.7. Model of fructan biosynthesis in plants (adapted from Vijn and Smeekens, 1999).

However, futile cycle of carbon may occur, since 1-SST has also a β-fructosidase side activity and it can catalyze the removal of a terminal fructosyl unit from 1-K, which results in Suc and one molecule of Fru (Koops and Jonker, 1996). Afterwards the enzyme 1-FFT is responsible of the elongation of fructan molecule by the transfer of fructosyl residues from a fructan molecule with DP ≥ 3 to another fructan molecule (Vijn and Smeekens, 1999). This catalytic reaction produces inulin-type fructan molecules with different chain lengths. Suc can be used as acceptor substrate as well, but not as donor substrate. Moreover 1-FFT enzyme can use Fru

as acceptor substrate in *Cichorium intybus* generating reducing F_n-type fructan (Van den Ende *et al.*, 1996).

An interesting characteristic of these two enzymes is that they do not show simple Michaelis-Menten kinetics but their activity, reliant on both the substrate and the enzyme concentration, is essentially non-saturable (Koops and Jonker, 1996; Van Laere and Van den Ende, 2002). This is in severe contrast to the kinetic properties of vacuolar invertases (VIs) that are saturable enzymes reported to have K_m values ranging 2.0-6.6 mM using Suc as substrate (Isla *et al.*, 1995; Goosen *et al.*, 2007; Bhatti *et al.*, 2006; Konno *et al.*, 1993).

Graminan biosynthesis

The synthesis of graminans required the activity of both 1-SST and sucrose:fructan 6-fructosyltransferase (6-SFT; EC 2.4.1.10). The shortest graminan-type fructan is Bif a tetrasaccharides characterized by both β(2-1) and β(2-6) linkages (Fig. 2.6). 6-SFT catalyzes the production of Bif from Suc and 1-K. 1-K is produced by 1-SST, and it is subsequently used as acceptor by 6-SFT that forms β(2-6) linkage generating Bif (Kawakami and Yoshida, 2002). Like 1-SST, 6-SFT also show a β-fructosidase side activity when Suc is present as substrates (Duchateau *et al.*, 1995). For the elongation of Bif, the enzymes 6-SFT and 1-FFT are involved although the participation of 6-FFT activity cannot be excluded. 6-SFT uses only Suc as donor substrate and 1-K as preferred fructosyl acceptor. As a consequence, 1-SST activity is important during graminan synthesis as well as during inulin biosynthesis (Sprenger *et al.*, 1995).

Levan biosynthesis

6-SFT is also responsible of levan biosynthesis starting with the production of 6-K from two Suc molecules. It is still not clear if the synthesis of levans occurs only by the enzyme 6-SFT or if other enzymes, such as 6-SST or 6-FFT, are involved (Van den Ende *et al.*, 2002).

Neoseries fructans biosynthesis

Neoseries fructans are synthetized starting from the trisaccharide n-K. The main responsible for n-K biosynthesis is the enzyme fructan:fructan 6G-fructosyltransferase (6G-FFT) which catalyzes the fructosyl transfer from the donor fructan substrate, generally 1-K, to the C6 of the Glc residue of Suc acceptor substrate.

Sara Cimini

Further elongations of n-K require the activity of 6-SFT and 1-FFT that are responsible for levan and inulin neoseries fructans, respectively (Chalmers *et al.*, 2005). Moreover in some plants, such as *Lolium perenne* and *Allium cepa*, inulin neoseries fructan can be produced by a dual 6G-FFT/1-FFT activity (Lasseur *et al.*, 2006; Fujishima *et al.*, 2005).

It is important to take into account that the model of fructan biosynthesis might be more complex than that discussed above. It has been found that environmental factors and substrates availability can affect FTs activities. In particular FTs can catalyze the formation of fructans with structures, degree of branching and DP that mainly depend on substrate availability and incubation conditions (Chalmers *et al.*, 2005; Livingston *et al.*, 2009).

Catabolism

In plants fructans are degraded by fructan exohydrolases (FEHs). The activity of different types of FEHs has been recently described. These enzymes catalyze the hydrolysis of the fructan molecules releasing the terminal fructose molecule of the fructosyl chain. These enzymes essentially transfer a Fru moiety to a water molecule as acceptor and have no invertase activity although plant cell wall invertases (CWIs) and FEHs are very closely related enzymes at the molecular and structural level (Le Roy *et al.*, 2007a). Depending on their ability to hydrolyze β(2-1) or β(2-6) linkages they can be classified in two groups:

Fructan 1-exohydrolases (1-FEH)

1-FEH (EC 3.2.1.153) preferentially breaks β(2-1) linkages. In wheat stems the cDNA of three different isoforms of 1-FEH have been cloned (1-FEHw1, 1-FEHw2, 1-FEHw3; Van den Ende *et al.*, 2003a; Van Riet *et al.*, 2008) and the corresponding recombinant enzymes have been characterized. While some environmental conditions, like freezing temperatures, increase 1-FEH activity, the addition of Suc generally inhibits it (Van den Ende *et al.*, 2003a; Simpson *et al.*, 1991; Marx *et al.*, 1997; Bonnett and Simpson, 1995).

Fructan 6-exohydrolases (6-FEH)

6-FEH (EC 3.2.1.154) preferentially hydrolyzes β(2-6) linkages. In wheat several kinds of 6-FEH have been described. A 6-FEH enzyme that specifically hydrolyzes β(2-6) linkages has been detected in the spikes of wheat. This enzyme has been purified and the corresponding

cDNA has been cloned (Van Riet *et al.*, 2006). Another type of enzyme, able to hydrolyze both β(2-1) and β(2-6) linkages, has been purified from the crown tissues of wheat and the corresponding cDNA has been cloned (Kawakami *et al.*, 2005). This enzyme, termed 6&1-FEH, uses, as optimal substrates, low DP graminans and low DP inulins. Besides 6-FEH and 6&1-FEH, also 6-kestose exohydrolases (6-KEHs) are found in wheat. These enzymes have been purified from the crown tissues of wheat and are able to degrade specifically 6-K (Van den Ende *et al.*, 2005).

While in dicots the expression of FTs and FEHs genes are temporally separated (Van Laere and Van den Ende, 2002), FEHs are co-expressed with FTs in monocots (Van den Ende *et al.*, 2003a). For this reason Bancal *et al.* (1992) proposed that in wheat the graminan-type fructans are 'trimmed' by 1-FEH activity, namely the combined activity of FTs and FEHs may be crucial for the determination of the fructan pool patterns and their final DP. As a matter of fact, Van den Ende *et al.* (2003) show that at least 1-FEH w2 might be involved as a β-(2,1)-trimmer during graminan biosynthesis. Although 1-FEHs shows a very low activity against Bif or other small graminans, Van den Ende *et al.* (2003) suggested that 1-FEH could play a role in reducing the β-(2,1) linkages in favor of short branches or β-(2,6) linkages. Also Suc can intervene in the determination of the fructan pattern due to its function as substrate for FTs and inhibitor for FEHs (1-FEH) in some plant species (Verhaest *et al.*, 2007).

Interestingly, FEH occur not only in fructans accumulating plants, but also in other species like *Beta vulgaris* and *Arabidopsis thaliana* (Van den Ende *et al.*, 2004; Van den Ende *et al.*, 2003b; De Coninck *et al.*, 2005). It has been hypothesized that these FEHs might be considered as "catalytically defective invertases" that might be involved in signaling and defense responses or may fulfill a regulatory function in plants (Le Roy *et al.*, 2008; Valluru and Van den Ende, 2008). However the exact role of defective invertases in plants is still unknown.

Invertases - FTs - FEHs: molecular and evolutionary features

It is believed that FTs and FEHs are evolutionarily correlated to the group of INVs having acidic pH optima (acid INVs). These INVs are ionically bound to the cell wall (CWIs) or can be accumulated as soluble proteins in the vacuole (VIs). Moreover, in plant cells, non-glycosylated INVs having neutral or slightly alkaline pH optima are located in cytosol (Chen

Sara Cimini

and Black, 1992; Van den Ende and Van Laere, 1995; Lee and Sturm, 1996; Walker *et al.*, 1997; Roitsch and González, 2004; Ross *et al.*, 2006). It has been suggested that FTs have evolved from VIs, while FEHs are more closely related to CWIs and that these evolutionary processes took place after the separation between monocots and dicots (Ritsema and Smeekens, 2003; Valluru and Van den Ende, 2008).

FTs, FEHs, VIs and CWIs are grouped together with microbial β -fructosidases in the glycoside hydrolase family 32 (GH32) (Van den Ende *et al.*, 2009). GH32, together with the family GH68, constitute the clan GH-J, depending on protein folding similarities, despite their low sequence identity (<15% identity). The 3D protein structures resolved up to now reveal that proteins belonging to GH32 are characterized by an N-terminal β-propeller domain, also called large subunit, and by a C-terminal domain, formed by two antiparallel six-stranded β-sheets. The latter domain, characterized by a sandwich-like fold, is present only in GH32 members while the β-propeller domain is present in both GH32 and GH68 members. The β-propeller domain consists of a fivefold repeat of blades (I-V) each of which containing four antiparallel β strands (A-D) around a deep central cavity. The active site is localized within the β-propeller domain (Van den Ende *et al.*, 2009).

Multiple sequence alignments of the GH-J clan members point out 3 conserved motifs in the β-propeller domain: N**D**PNG, R**D**P and **E**C motifs, containing the three crucial acidic residues in the active site of all these enzymes (Pons *et al.*, 2004). These acidic residues, also termed "the catalytic triad", are localized at an equivalent position in all GH-J clan members and are needed for substrate binding and for catalysis (Reddy and Maley, 1996; Pons *et al.*, 2004; Lammens *et al.*, 2009). The aspartate of the first motif, also called Suc binding box, operates as nucleophile, the glutamate of the EC motif acts as the acid/base catalyst and, finally, the aspartate of the RDP motif seems to operate as transition state stabilizer (Van den Ende *et al.*, 2009).

It has been proposed that glycoside hydrolases retaining enzymes, such as GH32 and GH68 members, work via a double displacement mechanism (Reddy and Maley, 1996; Lammens *et al.*, 2009). In the first step of the reaction, the substrate (Suc/fructooligosaccharide) binds to the active site in a ground state and the glycosidic oxygen is protonated by the glutamate of the EC motif. Subsequently, a nucleophilic attack is performed by the carboxylic group of the nucleophile, giving a covalent fructosyl-enzyme intermediate. Once the fructosyl-enzyme

Sara Cimini

intermediate is formed, the glutamate of the EC motif, now acts as a general base to activate the incoming acceptor substrate (water, Suc or fructans). This results with the hydrolysis of the fructosyl-enzyme intermediate and with the release of the products (Lammens *et al.*, 2008; Chuankhayan *et al.*, 2010).

Molecular properties of invertases, FTs and FEHs

FTs and VIs are characterized by an N-terminal untranslated leader sequence and a vacuolar targeting signal which are cleaved off after protein folding and final targeting (Fig. 2.8; Altenbach and Ritsema, 2007). This is why fructan synthesis and accumulation is generally believed to take place in the vacuoles (Vijin and Smeekens, 1999).

The molecular mass for the unprocessed translation product is approximately 80 kDa. After maturation the enzyme generally consists of a C-terminal domain of approximately 27 kDa and a N-terminal domain of approximately 55 kDa (Koops and Jonker, 1996). The small (C-terminal) subunit is indispensable to get active FTs but the specificity of the enzyme is encoded in the large subunit (Altenbach *et al.*, 2004).

Plant FT and VIs are also characterized by several potential glycosylation sites (Asn-Xaa-Ser/Thr), the number of which depends on the proteins (Sprenger *et al.*, 1995; Van der Meer *et al.*, 1998).

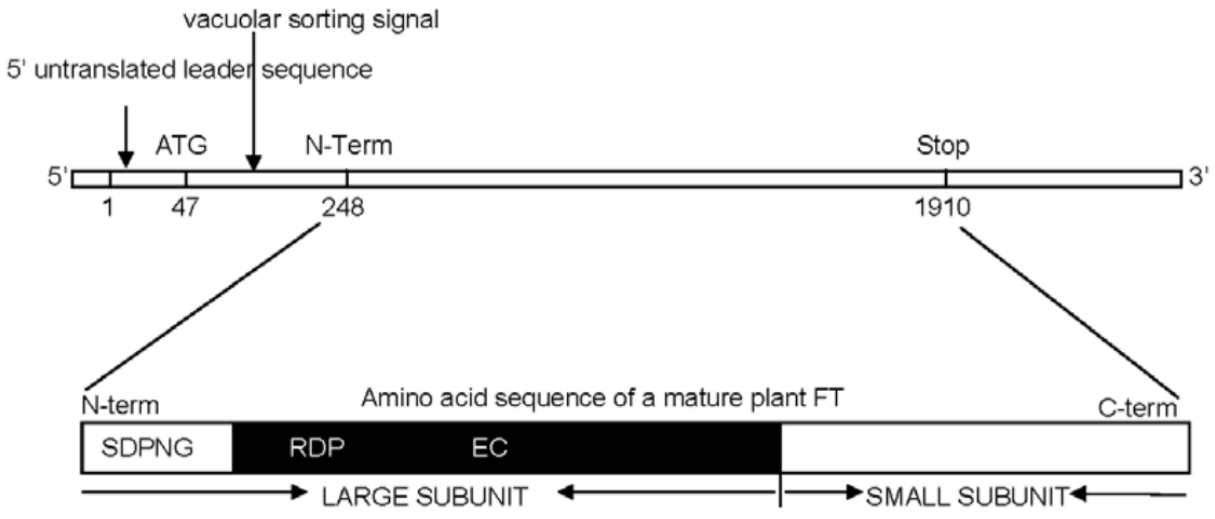

Fig. 2.8. Scheme of barley 6-SFT cDNA (from Altenbach and Ritsema, 2007)

FEHs, as FTs, are glycoproteins (Van Riet *et al.*, 2006; Van den Ende *et al.*, 2003a) with a molecular mass of approximately 70 kDa although smaller FEHs have been detected (Henson and Livingston, 1998; Van Riet *et al.*, 2006; Van den Ende *et al.*, 2003a). It is widely accepted that FEHs are located within the vacuole (Wagner and Wiemken, 1986) and, the acidic pH optimum, which characterizes these enzymes, as well as vacuolar targeting signal, which are cleaved off after final targeting, support their vacuolar localization. However for some FEHs has been suggested an apoplastic localization, as for wheat 6-FEH (Van Riet *et al.*, 2006). These FEHs might be involved in functions different from fructan degradation.

Functions of fructans

In the plant synthesizing fructans their predominant role is to be highly accessible **storage carbohydrates**, although these sugars are reserve carbohydrates less known compared with starch and Suc, even because they are produced in a limited number of plants (see *Fructans in plants* paragraph). In dicots, inulin-type fructans have been accumulated as long-term reserve carbohydrates particularly in roots and tubers (Van den Ende and Van Laere, 2007). In grasses, graminans, levans, and neoseries fructans mainly act as short-term storage compounds in stems, tiller bases, leaf sheaths, elongating leaf bases, leaf blades and roots (Van Laere and Van den Ende, 2002; Maleux and Van den Ende, 2007). For example in *Helianthus tuberosus* and *Cichorium intybus* inulins have been accumulated in the tubers or tap root over a long period (overwintering reserve). On the contrary in *Dactylis glomerata* levans have been accumulated in leaves for a short time (Maleux and Van den Ende, 2007).

Fructan mobilization in dicots is usually associated with recovery of growth (Vergauwen *et al.*, 2000). A rapid breakdown of fructans has been detected in several plants belonging to the Poaceae family, such as ryegrass (Prud'homme *et al.*, 1992), barley (Bonnett and Incoll, 1993) and wheat (Schnyder, 1993).

The concentration and degree of polymerization (DP) of the stored inulins vary between species. At the end of the growing season inulin can reach approximately 20% of fresh weight in chicory taproots (roughly 80% of the dry weight) (Vergauwen *et al.*, 2003). Fructans are also the dominant component of stem water soluble carbohydrates (WSC) in monocots (Archbold, 1940; Blacklow *et al.*, 1984). In wheat stem internodes, at the stage of maximum WSC content, they represent 85% of the WSC (Blacklow *et al.*, 1984; Turner *et al.*, 2008). Fructan are usually mobilized from stems to the grain at about mid-grain filling (Spiertz and

Sara Cimini

Ellen, 1978; Pollock and Cairns, 1991; Bonnett and Incoll, 1993; Schnyder *et al.*, 1993). Fructans mobilization is also involved in other physiological processes like regrowth in spring (Pollock and Jones, 1979) or after defoliation (Morvan-Bertrand *et al.*, 2001).

Vacuolar fructan biosynthesis is crucial in regulation of Suc concentration in the cytosol thus **preventing sugar-mediated feedback inhibition of photosynthesis** (Pollock, 1986). Indeed, Suc concentrations have to be maintained below a certain threshold to avoid photosynthesis inhibition (Morvan-Bertrand *et al.*, 2001). Correlations between Suc levels and activation of fructan synthesis under continuous illumination have been detected in cereals and in dicots (Wagner *et al.*, 1983; Vijn *et al.*, 1997; Vijn and Smeekens, 1999).

Fructans seems also to be involved in **flower opening** as suggested by Vergauwen *et al.*, (2000) in *Campanula rapunculoides*. Before flowering, petals contain high concentrations of fructans. Changes in FEHs activities during opening of the flowers are able to increase the hexoses concentration (particularly Fru) resulting in a reduction of the petal water potential and hence promoting water influx needed to permit petal expansion (Vergauwen *et al.*, 2000; Le Roy *et al.*, 2007b).

Another advantage conferred by fructan accumulation is that these polysaccharides are involved in **abiotic stresses tolerance,** particularly cold, drought and hypoxia (Hisano *et al.*, 2008; De Roover *et al.*, 2000; Volaire and Lelievre, 1997; Kawakami and Yoshida, 2002; Albrecht *et al.*, 2004; Livingston *et al.*, 2009). Since fructan biosynthesis is much less sensitive than starch biosynthesis to low temperature (Pollock, 1984), fructan-accumulating plants occur especially in temperate climate zones (Hendry and Wallace, 1993). It has been demonstrated, through several *in vitro* studies, that fructans have a direct protective effect on biological membranes, the primary target of damage by freezing and drought (Demel *et al.*, 1998; Hincha *et al.*, 2002, 2007; Vereyken *et al.*, 2003). Fructans can operate through a direct interaction with membrane lipids (Vereyken *et al.*, 2003). Depending on the 3D structure of these sugars they can preferentially interact with small-headgroup lipids rather than make a direct hydrogen bond with the phosphate groups (Valluru *et al.*, 2008). However, no experimental results have been reported in order to demonstrate that fructans directly protect membranes *in vivo* (Valluru *et al.*, 2008).

Van den Ende and Valluru (2009) also suggested that fructans, maybe together with other vacuolar compounds, might act as **scavengers of ROS**, strengthening vacuolar antioxidant mechanisms. Supporting this hypothesis, *in vitro* experiments showed that inulins have a

Sara Cimini

considerable antioxidant activity (Stoyanova *et al.*, 2011). However more data are necessary to elucidate the possible involvement of fructans in contrast ROS production.

Besides the clear advantages supplied to plants, fructans can also have positive effects on human health. In the last years, emphasis was put on the concept of functional food as an ingredient that beneficially affects one or more functions in the human body. The group of functional foods includes probiotics, prebiotics and antioxidants. Fructans, and particularly inulins and fructo-oligosaccharides (FOS), are widely accepted and used as **prebiotics**. As prebiotics, inulins and FOS are resistant to gastric acidity, to hydrolysis by mammalian gastrointestinal enzymes and to gastrointestinal absorption (Gibson and Roberfroid, 1995). Hence they reach the large intestine where they are selectively fermented by beneficial bacteria (i.e. *Lactobacilli* and *Bifidobacteria* species; Cummings and Macfarlane, 2002) which growth to the detriment of pathogenic bacteria (Gibson *et al.*, 1995; Roberfroid, 2005). During fructans fermentation, short-chain fatty acids have been produced. This production determines a reduction of the pH in the large intestine and, consequently, mineral absorption improvement, essentially of Ca^{2+} and Mg^{2+}. The improvement of Ca^{2+} and Mg^{2+} absorption may have beneficial effect on osteoporosis prevention. Lastly, several studies have focused on the potential effects of inulins and other prebiotics on reducing the risk of several diseases like cardiovascular diseases, colonic diseases, type II diabetes, hypertension, obesity and others (Van den Ende *et al.*, 2011b; Warrand, 2006; Brighenti, 2007; Tarini and Wolever, 2010).

2.2 MATERIAL AND METHODS

2.2.1 Plant Material

Plants of *Triticum durum* Desf. (cv Neolatino) were grown in experimental fields of "Consiglio per la Ricerca e la Sperimentazione in Agricoltura" in Rome in the 2010-2011 growing season. The plants were grown on 10 m^2 plots with a sowing density of up to 450 seeds m^{-2}. Irrigation, fertilization and plant protection were performed to ensure optimal plant growth. The ears were collected weekly from 7 days after anthesis (DAA) to 52 DAA (complete kernel development) and stored at -80°C. For sugar analysis, durum wheat kernels, collected from different ears for each sampling date, were peeled, grinded with pestle and mortar in liquid nitrogen, freeze dried and stored at -20°C.

2.2.2 Extraction and analysis of ascorbate and glutathione

2 g of durum wheat kernels were homogenized with eight volumes of cold 5% meta-phosphoric acid at 4°C in a porcelain mortar. The homogenate was centrifuged at 14000 g for 15 min at 4°C, and the supernatant was collected for analysis of ASC and GSH.

ASC and DHA were measured according to Kampfenkel *et al.* (1995) with minor modifications. Briefly; total ASC was determined after reduction of DHA to ASC with DTT, and the concentration of DHA was estimated from the difference between total ASC pool (ASC+DHA) and ASC pool. The reaction mixture for total ASC pool contained a 0.1 ml aliquot of the supernatant, 0.25 ml of 150 mM phosphate buffer (pH 7.4) containing 5 mM EDTA, and 0.05 ml of 10 mM DTT. After incubation for 10 min at room temperature, 0.05 ml of 0.5% N-ethylmaleimide was added to remove excess DTT. ASC was determined in a similar reaction mixture except that 0.1 ml H_2O was added rather than DTT and N-ethylmaleimide. Colour was developed in both reaction mixtures after addition of the following reagents: 0.2 ml of 10% trichloroacetic acid, 0.2 ml of 44% ortho-phosphoric acid, 0.2 ml of 4% α,α'-dipyridyl in 70% ethanol and 0.3% (w/v) $FeCl_3$. After vortexing, the mixture was incubated at 40°C for 40 min and the A_{525} was read. A standard curve was developed based on ASC in the range 0-50 μg ml^{-1}.

Sara Cimini

The total GSH pool (GSH plus GSSG) was assayed according to Zhang and Kirkham (1996) utilizing 0.4 ml aliquots of supernatant neutralized with 0.6 ml of 0.5 M phosphate buffer pH 7.5. For GSSG assay, the GSH was masked adding to the neutralized supernatant 20 µl of 2-vinylpyridine, whereas 20 µl H_2O were added in the aliquots utilized for total GSH pool assay. Tubes were mixed until an emulsion was formed. GSH content was measured in a 1 ml reaction mixture containing 0.2 mM NADPH, 100 mM phosphate buffer pH 7.5, 5 mM EDTA, 0.6 mM 5,5'-dithiobis(2-nitrobenzoic acid) and 0.1 ml of sample obtained as described above. The reaction was started by adding 3 units of glutathione reductase and was monitored by measuring the change in absorbance at 412 nm for 1 min. GSH was estimated as the difference between the amount of total GSH and that of GSSG. A standard curve in the range 0-30 µM ml^{-1} GSH was prepared.

2.2.3 Analysis of total polyphenols

A conventional solvent extraction method has been used for total polyphenol extractions from wheat kernels (Arranz and Calixto, 2010). Extractions were performed in three replicates of each sample. 50 mg ground sample were treated with 2 ml of acidic methanol (HCl) / water (50/50, v/v, pH 2). The mixture was thoroughly shaken for 1 hour at 25°C and then centrifuged at 5000 g for 10 min at 25°C and the supernatant was recovered. The residue was re-extracted with 2 ml of aceton/water (70/30, v/v), shaking and centrifugation were repeated.

The content of total polyphenols was measured using the Folin - Ciocalteu reagent according to Singleton *et al.* (1999) and slightly modified as described by Dewanto *et al.* (2002). 200 µl of the polyphenol extract were added to 425 µl deionized water and 125 µl of Folin - Ciocalteu reagent. The mixture was kept in the dark for 8 min at room temperature. Then 1.25 ml of 7% Na_2CO_3 was added together with water to adjust the final volume up to 3 ml. After 90 min of incubation at room temperature the absorbance at 760 nm was measured against water as a blank. Determinations were performed per triplicate in extracts and the results, expressed as µmol of gallic acid equivalents per g of fresh weight, were reported as mean value ± standard deviation. A standard curve was developed based on gallic acid (GA) in the range 0-50 µmol l^{-1}.

Sara Cimini

2.2.4 Total antioxidant capability

According to Merendino *et al.* (2006), 1 g of grinded kernels, stored at -80°C, was homogenized with 2 ml 50 mM sodium phosphate buffer pH 7.5 and 5 ml ethyl acetate. The homogenate was centrifuged at 4000 g for 10 min at 4°C to separate the lipophilic and the hydrophilic phase. The total antioxidant capability of both phases was determined using the Trolox Equivalent Antioxidant Capacity (TEAC) assay, based on the scavenging of the 2,2'-azino-bis-3-ethylbenzothiazo-line-6-sulfonic acid) (ABTS) radical ($ABTS^{\bullet}$) into a colourless product (Miller *et al.*, 1993; Re *at al.*, 1999). Trolox (6-hydrolxy-2,5,7,8-tetramethychroman-2-carboxylic acid) was used as an antioxidant standard. The capability of the lipophilic and the hydrophilic phases to scavenge the $ABTS^{\bullet}$ was expressed as trolox equivalent using a standard dose-response curve. Trolox stock solution (Trolox 10 mM) was prepared in ethanol or in 50 mM sodium phosphate buffer pH 7.5 to determine respectively the total antioxidant capability of the lipophilic and hydrophilic phases. ABTS was dissolved in 0.1 M phosphate buffer pH 7.4 to a 5 mM concentration. $ABTS^{\bullet}$ was produced by adding 1.76 mM potassium persulfate. The mixture was kept in the dark at room temperature for 12–16 h before use. The radical was stable in this form for more than one week when stored in the dark at room temperature. The $ABTS^{\bullet}$ working solution was freshly-made by diluting the original solution with 0.1 M phosphate buffer or ethanol to an absorbance of 0.7 (± 0.02) at 734 nm. To measure the antioxidant activity, the delta absorbance in 1 min was calculated. This was performed at least three times in triplicates.

2.2.5 Sugar extraction

Durum wheat kernel sample (50 mg) was heated at 90°C in 1 ml ethanol. 167 µl of rhamnose solution (8 mg/ml) and 5 ml deionized water (100°C) were added. Rhamnose is used as an internal standard. Extractions were performed in a shaking water bath during 60 min at 80°C. After incubation and cooling, the sample was centrifuged at 9000 g for 10 min. 50 µl of supernatant was collected twice in a test tube. One of the supernatants was diluted with 950 µl water and the sugars were analysed on a HPAEC-PAD (called watery extract from here). To identify the sugars, a calibration solution was made consisting of rhamnose, Glc, fructose, melibiose and Suc with a concentration of 5 µg/ml. The other supernatant was used for acid hydrolysis.

Sara Cimini

2.2.6 Acid hydrolysis to determine fructan content

50 µl of the watery extract was added to 1.2 M HCl-solution (2.5 µl) and incubated for 90 min at 70°C. The hydrolysis was stopped by adding 1 M H_2CO_3 (2 µl). Deionized water was added up to a final volume of 1 ml and the mixture was analysed on a HPAEC-PAD. The calculations of the fructan concentration and DP were performed as described in Verspreet *et al.* (2012).

2.2.7 Sugar measurements on HPAEC-PAD

Carbohydrates were analysed using the high performance anion exchange chromatography with pulsed amperometric detection (HPAEC-PAD) performed on a Dionex ICS 3000 chromatography system (Sunnyvale, CA, USA) equipped with a CarboPac PA -100 column (4 x 250 mm) and an ED-40 electrochemical detector. As solvents, milliQ water, 200 mM NaOH-solution and 400 mM NaAc in 100 mM NaOH-solution were used. The elution conditions used to quantify the sugars rhamnose, glucose, fructose, melibiose and Suc are according to Verspreet *et al.* (2012) and the elution conditions used to identify fructans are according to Vergauwen *et al.* (2000).

2.2.8 Enzyme extraction

50 mg of freeze-dried wheat kernel samples were crushed with mortar and pestle in 600 µl of 50 mM sodium acetate pH 5.0 also containing 1 mM β-mercaptoethanol, 10 mM sodium bisulfite, 0.1% (w/v) polyclar and 0.02% (w/v) sodium azide) and 3 µl of 200 mM phenylmethylsulfonyl fluoride dissolved in pure ethanol. The homogenate was centrifuged for 5 min at 14000 g at 4°C. An aliquot (450 µl) of the supernatant was mixed to 250 mg of solid ammoniumsulphate (80% saturation) and incubated on ice for 1 hour. The mixture was centrifuged for 5 min at 14000 g. Then the supernatant was discarded and the pellet was washed two times with 600 µl of ice-cold 80%-saturated ammoniumsulphate in 50 mM sodium acetate buffer pH 5.0. The pellet was then dissolved in 140 µl sodium acetate buffer pH 5.0 containing 0.02% sodium azide. This enzyme extract was subsequently used to analyze the activities of the enzymes involved in fructan metabolism.

Sara Cimini

2.2.9 Protein content measurement

Protein measurement was performed according to Bradford (1976) using bovine serum albumin as a standard. In particular the protein content was determined using the Bradford Bio-Rad reagent. Into a clean and dry test tube, 797.5 µL of water were mixed to 2.5 µL of each enzyme extract. Subsequently 200 µL of dye Bradford Bio-Rad reagent were added to each test tube. The tubes were strongly mixed. For the blank, 2.5 µL of sodium acetate buffer pH 5.0 were used instead of enzyme extract. Protein solutions are normally assayed in triplicate. The mixtures were incubated at room temperature for 15 minutes. The absorbance at 595 nm was measured and the protein content was expressed as mg/ml.

2.2.10 Substrates

The substrates used were 2 M Suc in sodium acetate buffer pH 5.0 with 0.02% sodium azide, 500 mM 1-Kes from Sigma Aldrich in sodium acetate buffer pH 5.0 with 0.02% azide, 500 mM n-Kes (purified from *Xanthophyllomyces dendrorhous* by Rudy Vergauwen) in sodium acetate buffer pH 5.0 with 0.02% sodium azide and 20 mM kernel substrate (KS) in sodium acetate buffer pH 5.0 with 0.02% sodium azide. KS is a carbohydrate extract from *T. aestivum* kernels without hexoses, Suc and kestoses and was previously made by Rudy Vergauwen. The substrates were stored at -20°C.

2.2.11 Enzyme activity determinations

The reaction mixtures containing 5 µL of the stock substrates and sodium acetate buffer pH 5.0 up to a final volume of 30 µL were started by adding 20 µL of enzyme extract. The substrates were used in 6 different combinations: Suc, n-Kes, 1-Kes, Suc + n-Kes, Suc + 1-Kes, n-Kes + 1-Kes and KS. The mixtures were incubated at 30°C. Aliquots were taken after 0, 30, 60, 120 min of incubation and overnight. The reaction was stopped by keeping an aliquot for 5 min at 95°C. Samples were diluted ten times with water containing 20 µM mannitol and 0.04% sodium azide and stored at -20°C until further analysis.
Samples were analysed by HPAEC-PAD on an ICS3000 chromatography system (Dionex, Sunnyvale, CA). Analysis and detection were performed at 32°C and the flow rate was 250 µL per min. 15 µL sample was injected on a Guard CarboPac PA 100 (2 x 50 mm) in series with an analytical CarboPac PA 100 (2 x 250 mm) equilibrated for 9 min with 90 mM CO_2-

free NaOH. Sugars were eluted in 90 mM NaOH, with an increasing sodium acetate gradient: from 0 to 6 min, the sodium acetate concentration increased linearly from 0 to 10 mM; from 6 to 16 min the concentration increased linearly from 10 to 100 mM; from 16 to 26 min, the concentration increased linearly from 100 to 175 mM, then the columns were regenerated with 500 mM sodium acetate for 1 min and equilibrated with 90 mM NaOH for 9 min for the next run. Data were recorded and processed with Chromeleon software.

2.2.12 Isolation of total RNA and DNase treatment

The RNA was extracted from *T. durum* kernels cv. Neolatino, collected at 7, 14, 21, 28, 35 and 52 DAA. The kernels were stored at -80°C until the RNA extraction time. Total RNA was extracted by TRIzol Reagent (Ambion 15596-018) following the instructions provided by the supplier. 100 mg of kernels were ground into power in a mortar using liquid nitrogen and 2 ml TRIzol Reagent were added. Moreover, 100 µl of Plant RNA Isolation AID (Ambion AM9690) were added in order to facilitate the removal of polysaccharides and polyphenols. Following homogenization, the sample was centrifuged at 12000 x g for 10 minutes at 4°C. 400 µl of chloroform were added to the supernatant. The supernatant was vigorously mixed by inversion and incubated at room temperature for 5 minutes. Subsequently the sample was centrifuged at 12000 x g for 15 min at 4°C. The aqueous phase and 1 ml isopropanol were mixed, kept at room temperature for 10 min, and then centrifuged at 12000 x g for 10 min at 4°C. The pellet was washed twice with 2 ml 75% ethanol and resuspended in 40 µl RNase-free water + 1 µl RNase Inhibitor by passing the solution up and down several times through a pipette tip. The sample was incubated in a heat block set at 60°C for 10 min, froze in liquid nitrogen and stored at -80°C. To verified RNA purity 260/280 and 260/230 wavelength ratios were considered. The 260/280 ratio should be approximately 2.0 and the 260/230 ratio should be around 2.0-2.2. The purified RNA was quantified by spectrophotometric assay at 260 nm.
In order to eliminate the genomic DNA, DNase treatment was performed by using TURBO DNA-free Kit (Applied Biosystems AM1907). A typical reaction of 50 µl was used for DNase treatment. 5 µl of 10X TURBO DNase Buffer and 1 µl of TURBO DNase were added to 8 µg of total RNA reaching a final volume of 45 µl. The sample was gently mixed and incubated at 37°C for 30 min. 5 µl of DNase Inactivation Reagent were added and the sample was incubated at room temperature for 5 min mixing occasionally. Finally the sample was

Sara Cimini

centrifuged at 10000 x g for 1.5 min and the supernatant was collected. The RNA content was again quantified by spectrophotometric assay at 260 nm.

2.2.13 Reverse transcription

RNA was reverse transcribed using High Capacity RNA-to-cDNA Kit (Applied Biosystems 4387406) following the instructions shown next. The sample was gently mixed and briefly centrifuged. The sample was incubated at 37°C for 60 min and subsequently a further incubation at 95°C for 5 min was carried out. The sample was stored at -20°C

	+ reverse transcriptase	+ reverse transcriptase
2X RT Buffer	10 µ	10 µ
20X RT Enzyme Mix	1 µ	-
Sample	1 µg	1 µg
Nuclease-free H_2O	Q.S.‡ to 20 µl	Q.S. to 20 µl

‡ Quantity Sufficient

2.2.14 Semi-quantitative PCR

The obtained cDNA was utilized for amplification with specific primer designed for housekeeping genes and for enzymes involved in fructan synthesis and degradation. The polymerase chain reaction (PCR) was carried out by using the Advantage-GC cDNA Polymerase Mix (Clontech 639112) according to the manufacturer's instructions. The Advantage-GC cDNA Polymerase Mix, which allow an efficient amplification of GC-rich cDNA templates, contains KlenTaq-1 DNA Polymerase as the primary polymerase and a minor amount of a 3′→5′ proofreading polymerase and TaqStart. Following conditions were utilized for amplification with specific primer: an initial denaturation for 5 min at 95°C, followed by a tested number of cycles specific for each gene. Each cycle consisted of 30 sec at 95°C, 30 sec at the specific annealing temperature (dependent on the couple of primer used) and 1 min at 72°C. The specific primer used for the PCR reactions were:

Gene Name	Accession Number	Primer Sequence	T annealling	N° of cycles	Product size
w18S	AY049040	FW 5′-GAGCCTGCGCTTAATTTGAC-3′ Rev 5′-TAGCAGGCTGCGGTCTCGTT-3′	52°C	24	174 bp
w1-FEHw3	AJ564996	FW 5′-ACTGGTGGTGACATAGATCAAA-3′ ‡ Rev 5′-CTGTAGCCGTTCAGCTCAC-3′	52°C	30	221 bp
6&1-FEH	AB089269	FW 5′-CCCAGTGATCCAACATGTCA-3′ Rev 5′-GCGTTCAATTCTAGTCCAACTCAT-3′	54°C	34	178 bp
6-SFT	AB029887	FW 5′-AGTTCCAAGGACAATTGCTCTC-3′ † Rev 5′-ACGGCAGAAGCATCAAGGT-3′ †	54°C	32	201 bp

‡ Van Riet *et al.*, 2008
† Huynh *et al.*, 2012

Sara Cimini

Primers that are not marked in the table above were manually designed and checked using the software Primer 3 available on-line http://frodo.wi.mit.edu/. The primers were synthesized by Primm.

The PCR products, together with a loading buffer (5:1), were loaded and run on a 1.5% agarose gel in TAE at constant voltage (75 V) and visualized with ethidium bromide (EtBr). Images of EtBr-stained agarose gels were acquired with a ChemiDoc™ XRS (Bio-Rad) and bands quantification was performed by Image Lab™ software (Bio-Rad). Band intensity was expressed as relative absorbance units. Normalization with respect to a positive control was calculated to normalize variations in sample concentration and as a control for reaction efficiency. Mean and standard deviation of all experiments performed were calculated after normalization.

2.2.15 Heterologous expression in *Pichia pastoris*

PCR for cloning

Ta67 cloning

The PCR conditions for cloning were as follows: 93°C for 5 min followed by 37 amplification cycles: 93°C for 30 sec, 52°C for 30 sec and 72°C for 2 min with the primers Ta67F1 (5'-GACGTGGTTAGCCCAGTGCT-3') and Ta67R1 (5'-GTAACAATGTATGATCCGTCTG-3'). A final extension at 72°C for 10 min was performed. 1 µg of a cDNAs collection obtained from *T. aestivum* kernels at late milky stage was used.

The obtained PCR product was used for a Nested-PCR performed using the following primers: Ta67F (5'-TTCCCGTGGAGCAACGCCATG-3' Tm 62.8°C) and Ta67R (5'-ATCTCGTGCAAAAAGATCTAG-3' Tm 50.2°C).

All the PCR reactions were performed using the Advantage-GC cDNA Polymerase Mix (Clontech 639112) according to the manufacturer's instructions.

Additional specific primers for Ta67 cloning were designed in order to introduce *EcoRI* and *SacII* restriction sites at the 5' and 3' ends, respectively. The primers were: Ta67PichF (5'-AATGACC**GAATT**CCCGTGGAGCAACGCCA-3' Tm 82°C) and Ta67PichR (5'-ACC**CCGCGG**ATTATCTCGTGCAAAAAG-3' Tm 74°C). In bold are indicated the *EcoRI* and *SacII* restriction sites.

Sara Cimini

Cloning and transformation of Escherichia coli

After polyA-tailing at 72°C for 20 min (Poly(A) Tailing Kit, Ambion) the amplified DNA was cloned into TOPO XL vector (TOPO XL PCR Cloning kit, Invitrogen) and transformed into *Escherichia coli* competent cells by heat-shock at 42°C for 45 sec. *E. coli* cells, containing the exogenous DNA construct, were grown on LB medium (1% tryptone, 1% NaCl, 0.5% yeast extract, 1.5% agar) added with 50 µg/ml kanamycin. The plates were incubated at 37°C overnight. The presence of the cDNA into the vector was checked by PCR using vector specific primers (M13). The plasmids from positive colonies were sequenced.

Cloning and transformation of Pichia pastoris

The TOPO XL recombinant vector (containing the cDNA of interest) and the pPicZαA vector (Invitrogen) were digested with *EcoRI* and *SacII* restriction enzymes. After extraction of the digested Ta67cDNA and digested pPicZαA vector from a 1.1% (w/v) agarose gel (E.Z.N.A. Cycle-Pure Spin Protocol, Omega, bio-tek), the latter was dephosphorylated (Alkaline Phosphatase from shrimp, Roche). Then the cDNA of interest was cloned into the vector (Rapid DNA Ligation Kit, Roche) resulting in the recombinant pPicZαA expression plasmids. These plasmids were transformed into *Escherichia coli* competent cells by heat-shock at 42°C for 45 sec. *E. coli* cells, containing the expression plasmid, were grown on YT medium (1.6% bacto tryptone, 0.5% NaCl, 1% yeast extract, 1.5% agar) added with 30 µg/ml zeocine. The presence of the cDNA of interest into the vector was checked by PCR using vector specific primers (AOX). The plasmids from positive colonies were purified using Midiprep (Quantum PrepTM Plasmid Midiprep Kit, BIO-RAD) and sequenced.

After plasmid linearization using *PmeI*, *P. pastoris* X-33 strain was transformed by electroporation and plated on YPDS medium (2% peptone, 1% yeast extract, 2% glucose, 1 M sorbitol and 1.5% agar) added with two different zeocin concentrations: 100 µg/ml and 500 µg/ml.

Expression and enzyme precipitation

Positive colonies were grown according to the EasySelect™ Pichia Expression Kit instructions.

Start phase: 3 ml YPD (2% peptone, 1% yeast extract, 2% glucose) supplemented with zeocine (100 µg/ml) was inoculate with a single positive colony and grown at 30°C overnight, shaking at 200 rpm.

Growing phase: 500 µl of start culture were transferred into 80 ml BMGY medium (2% peptone, 1% yeast extract, 100 mM potassium phosphate, pH 6.0, 1% glycerol, 1.34% YNB and 4 x 10^{-5}% biotin). The growing culture was incubated overnight at 30°C shaking at 200 rpm.

Induction phase: Pichia cells, collected by centrifugation at 1500 × g for 10 minutes at room temperature, were transferred to 20 ml of BMMY medium (2% peptone, 1% yeast extract, 100 mM potassium phosphate, pH 6.0, 0.5% methanol, 1.34% YNB and 4 x 10^{-5}% biotin). Every day 2% methanol was added to maintain the gene expression of the recombinant protein.

After 4 days of induction, the Pichia supernatant was collected by centrifugation at 1000 x g for 10 min at 4°C. 150 µl of sodium-acetate buffer (1 M, pH 5.0 with 0.02% sodium azide) and ammonium sulphate (80% final saturation) were added to Pichia supernatant (± 15 ml) containing the recombinant proteins. After 50 min incubation on ice, the supernatant was centrifuged for 25 min, at 20000 rpm, 4°C. The pellet was dissolved in 1 ml of 50 mM sodium-acetate buffer pH 5.0 with 0.02% sodium azide and centrifuged for 3 min at maximum speed, 4°C.

Enzyme activity determination

50 µl of protein extract were mixed with the selected sugar substrates in a total reaction volume of 100 µl sodium acetate buffer 50 mM, pH 5.0 with 0.02% sodium azide. Reaction mixtures were incubated at 30°C for several time points: 0, 30 min, 60 min, 180 min, 15 h, 24 h, 48 h, 90 h. The reactions were stopped at each time points by diluting 10 µl of the mixtures in 1 ml of water (with 0.02% sodium azide) and keeping the dilutions at 90°C for 5 min. Enzyme activities were determined by anion exchange chromatography associated to a pulsed amperometric detector (HPAEC-PAD).

For Ta67 enzyme activity determination protein extract was mixed with 100 mM Suc, 50 mM 1-K, 50 mM n-K and with all the possible combination made using these sugars.

For Ta68 enzyme activity determination protein extract was mixed with 100 mM Suc, 50 mM n-K and with 100 mM Suc + 50 mM n-K.

The enzyme activity determination was also carried out directly on Pichia supernatant by incubating 75 µl of supernatant with the selected sugar substrates in a total reaction volume of 100 µl sodium acetate buffer 50 mM, pH 5.0 with 0.02% sodium azide.

2.2.16 *T. aestivum* cDNA library screening and cloning of partial putative FEHs

The PCR conditions for cloning were as follows: 93°C for 5 min followed by 35 amplification cycles: 93°C for 30 sec, 52°C for 30 sec and 72°C for 1 min with the degenerate primers wFEH-F (5'-CTYWTSTACMRGAGYRARGACTT-3' Tm 54.1°C) and wFEH-R (5'-GAGTCRAAGAANGWYTTTGAWGC-3' Tm 53.3°C). A final extension at 72°C for 10 min was performed. 1 µg of a cDNAs collection obtained from *T. aestivum* kernels at late milky stage was used.

After polyA-tailing at 72°C for 20 min (Poly(A) Tailing Kit, Ambion) the amplified DNA was cloned into pCR®2.1-TOPO vector (Invitrogen) and transformed into *E. coli* competent cells by heat-shock at 42°C for 45 sec. *E. coli* cells, containing the exogenous DNA construct, were grown on LB medium (1% tryptone, 1% NaCl, 0.5% yeast extract, 1.5% agar) supplemented by 50 µg/ml kanamycin. 40 µl of 40 mg/ml X-gaL in dimethylformamide were spread on each LB plate. The plates were incubated at 37°C overnight. Blue/white colony screening was performed for easy selection of recombinants. Moreover the presence of the cDNA into the vector was checked by PCR using vector specific primers (M13). The plasmids from positive colonies were sequenced.

2.2.17 Sequence alignments and phylogenetic analysis

The search for INVs, fructosyl transferases (FTs) and fructan exohydrolases (FEHs) sequences was carried out with BLAST (Altschul S.F. *et al.*, 1990) using, as query, the sequences of AcV-INV (accession number CAA06839), Ta1-FFT (accession number BAE19751), Ta1-SST (accession number BAB82470), Ta6-SFT (accession number BAB82469), Ac6G-FFT (accession number CAA69170), Ta1-FEH (accession number CAD48199), TaCW-INV (accession number AAC96065) and ZmN-INV (accession number ACF84899), and BLOSUM62 as the scoring matrix. These sequences were taken from the RefSeq database (Pruitt, *et al.*, 2005), built and distributed by the NCBI. All sequences annotated as putative, partial, precursors or without functional data reported in the literature, were discarded.

Sara

After data collection was complete, the sequences were multiply aligned using the program ClustalW (Thompson *et al.*, 1994). Multiple alignment was refined with the editor JalView (Waterhouse *et al.*, 2009). From this multiple alignment, a phylogenetic tree was constructed using the Neighbor-joining method (Saitou and Nei, 1995). The statistical evaluation of the results was performed by bootstrap analysis. In this analysis the bootstrap replications were 1000. The program TreeView (Page, 1996) was used to display the tree.

2.2.18 Model Building

Three-dimensional structures of the proteins of interest were predicted via homology modeling. The best templates were identified using the program PHYRE (Bennett-Lovsey *et al.*, 2008). The alignment between the target and the template sequences were refined and validated using the information contained in the multiple sequence alignment previously calculated. After template identification, the construction of three-dimensional models was made by the server SWISS-MODEL, used by the interface Swiss PDB Viewer (Guex and Peitsch, 1997).

Sara Cimini

2.3 RESULTS

2.3.1 Antioxidant capacity during durum wheat kernel maturation

Kernel development was studies from 7 days after anthesis (DAA) to complete maturation (52 DAA). The antioxidant capability of *T. durum* cv. Neolatino during kernel development was estimated by measuring three different parameters: total ASC, total GSH and polyphenols. Also the total antioxidant capacity has been measured on the same samples.

Total ASC content

At the beginning of kernel maturation, the total ASC content (reduced and oxidized form) was high (1.26 µmol / g FW), and then it decreased very slowly until 21 DAA, after which the total ASC content decreased strongly reaching very low values in mature kernels (0,06 µmol / g FW at 52 DAA; Fig. 2.9).

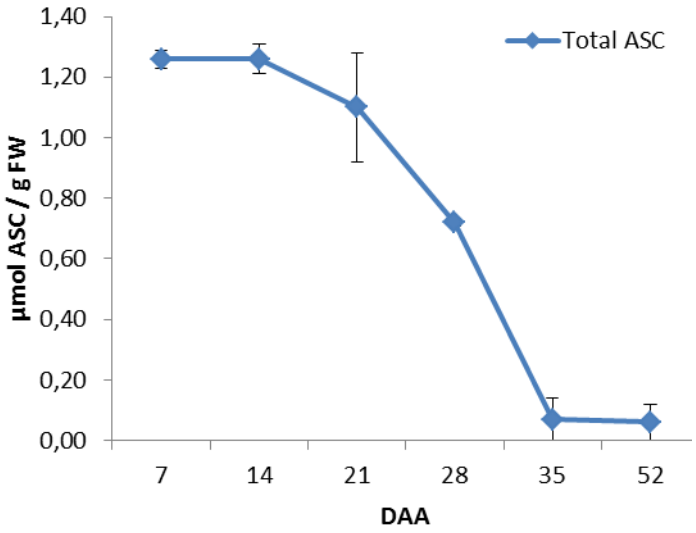

Fig. 2.9. Total ASC content (ASC + DHA) during durum wheat kernel maturation. The values, expressed as µmol/g FW, are the means of three independent experiments ± SD.

Total GSH content

During the first weeks of kernel maturation no remarkable variations in the total glutathione pool were observed in wheat kernels. In particular, up to 21 DAA, the total GSH content (reduced and oxidized form) remained constant at values around 420 nmol / g FW. After 21 DAA it decreased to 308 nmol / g FW at 28 DAA and after which it remained almost stable until the end of kernel maturation (52 DAA) (Fig. 2.10).

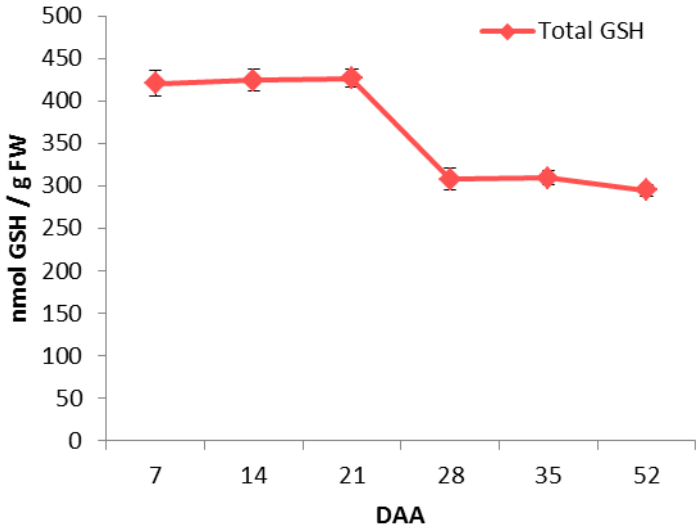

Fig. 2.10. Total GSH content (GSH + GSSG) during durum wheat kernel maturation. The reported values, expressed as nmol/g FW, are the means of three independent experiments ± SD.

Phenolic compounds content

Conventional solvent extraction is the typical analytical methodology used for total polyphenol extraction from cereal grains. Acetone and methanol are efficient solvent in extracting total phenolic compounds. Results of polyphenols analyses extracted using methanol/acetone solvent are shown in figure 2.11. A significant increase in the total polyphenol content was observed during the development of durum wheat kernels. The starting value 2.46 mg GAE / g FW at 7 DAA linearly increased until 4.03 mg GAE / g FW at 21 DAA, a slower increase in the phenolic content was also detected between 21 and 35 DAA, passing from 4.03 to 4.57mg GAE / g FW. Finally, a very rapid increase was observed during the last period of kernel developing, reaching 7.28 mg GAE / g FW at 52 DAA (Fig. 2.11).

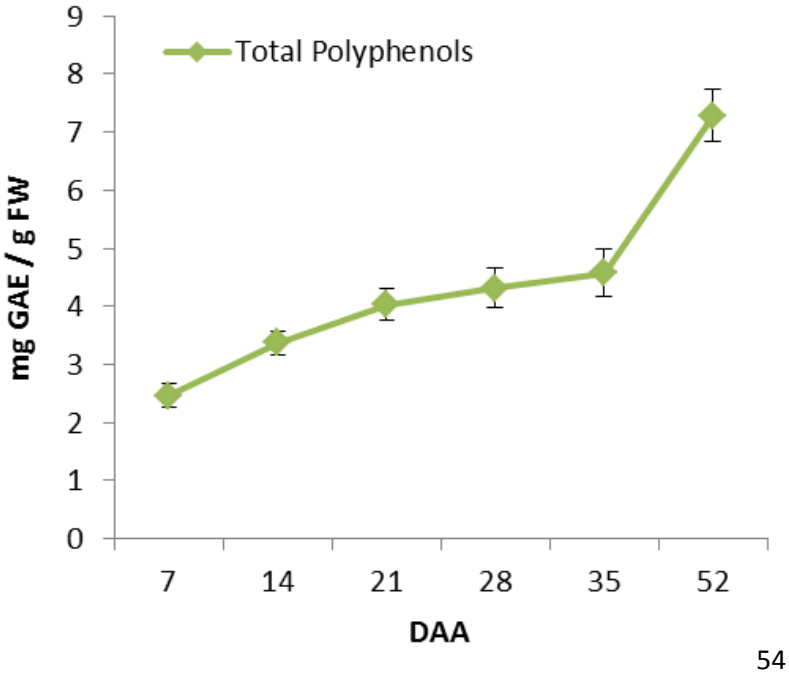

Fig. 2.11. Extractable polyphenols content in methanol/acetone extracts of durum wheat kernel during development. The reported values, expressed as mg of gallic acid equivalents / g FW, are the means of three independent experiments ± SD.

Total antioxidant capability

Since many other molecules with antioxidant properties are present in kernel tissues, in addition to ASC, GSH and phenolic compounds, the global antioxidant activity was measured. In particular, the whole lipophilic and hydrophilic antioxidant capabilities were measured by using the TAEC method, during wheat kernel development.

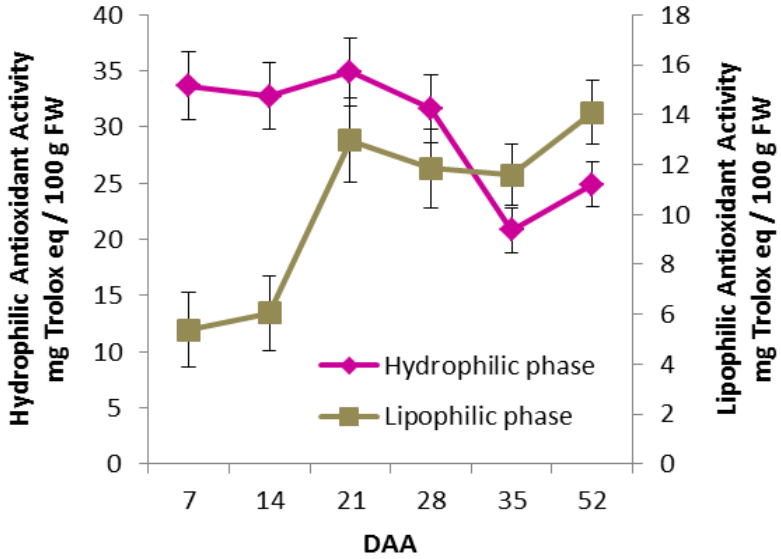

Fig. 2.12. Hydrophilic and lipophilic antioxidant activities during durum wheat kernels development. The antioxidant activity was expressed as mg of trolox equivalents / 100 g FW. The values are the means of three independent experiments ± SD.

Different trends were found in hydrophilic and lipophilic phases. The antioxidant activity due to the lipophilic metabolites increased gradually until 21 DAA after which no further statistically significant increase was observed (Fig. 2.12). On the other hand, the hydrophilic antioxidant activity did not show statistically significant variations ($p < 0.05$) up to 28 DAA but subsequently rapidly decreased during the following period of maturation (Fig. 2.12).

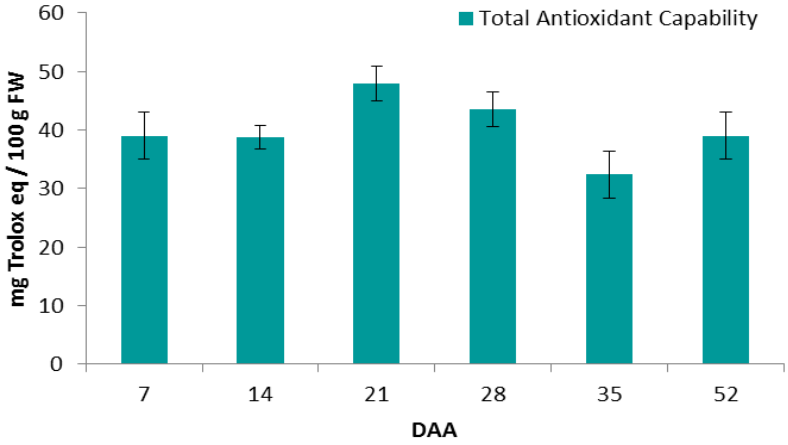

Fig. 2.13. Total antioxidant activities during durum wheat kernels development. The total antioxidant activity, calculated by the sum of lipophilic and hydrophilic antioxidant activities, was expressed as mg of trolox equivalents / 100 g FW. The values are the means of three independent experiments ± SD.

Therefore, while the hydrophilic antioxidant activity was higher in immature kernels, the lipophilic antioxidant activity was higher in mature wheat kernels and lower in immature ones. Nevertheless, the total antioxidant capacity (measured as a sum of the two components) did not significantly differ during kernels development (Fig. 2.13).

2.3.2 Sugar analysis during durum wheat kernel maturation

Fructan content

A deepened analysis on fructans and other carbohydrates has been performed during durum wheat kernel maturation of Neolatino cultivar. Fructan content was analyzed in the kernels at different maturation phases, from 7 to 52 DAA. This part of the thesis has been performed in collaboration with the Molecular Plant Physiology Laboratory (K.U. Leuven, Belgium) and the Laboratory of Food Chemistry and Biochemistry (K.U. Leuven, Belgium).

The analysis indicated that fructan content, expressed as % of dry matter (% dm), was higher at early stages of kernel development (35% dm) and that the most relevant decrease (95%) was observed between 7 and 21 DAA. Subsequently the fructan content only weakly decreased till the end of maturation (Fig. 2.14).

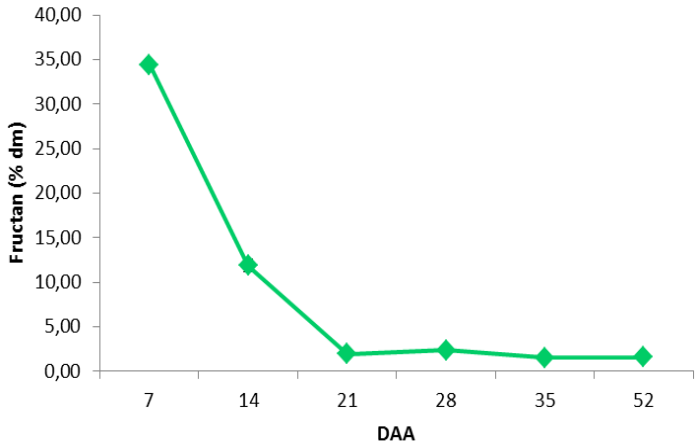

Fig. 2.14. Fructan content of durum wheat kernels at different DAA. Samples were analyzed in the lab of Prof Delcour (KU Leuven). All the values are the mean of two experiments ± SD and are expressed as % dm.

A deeper analysis of the kinds of sugars present in maturing kernels was performed by HPAEC-PAD. This analysis indicated that alterations in the content of the different types of fructans also occurred during kernel maturation, since the chromatographic profile showed

that fructans with higher DP prevailed in immature phases (7-14 DAA). Then the DP decreased with the progression of kernel maturation (2.15A).

The presence of Glc, Fru, Suc, 1-K, maltose (Mal), 6-K, n-K, 1,1-nystose (1,1-Nys; 1,1-kestotetraose), Bif and raffinose (Raf) was observed in wheat kernels during maturation (Fig. 2.15 B). Mal was the most abundant sugar found in the early phases of kernel maturation (7 DAA). Moreover, the amount of Glc, Fru, Bif and 1-K was substantially higher at 7 DAA compared to the amount of Suc, 6-K and 1,1-Nys (Fig. 2.15 B).

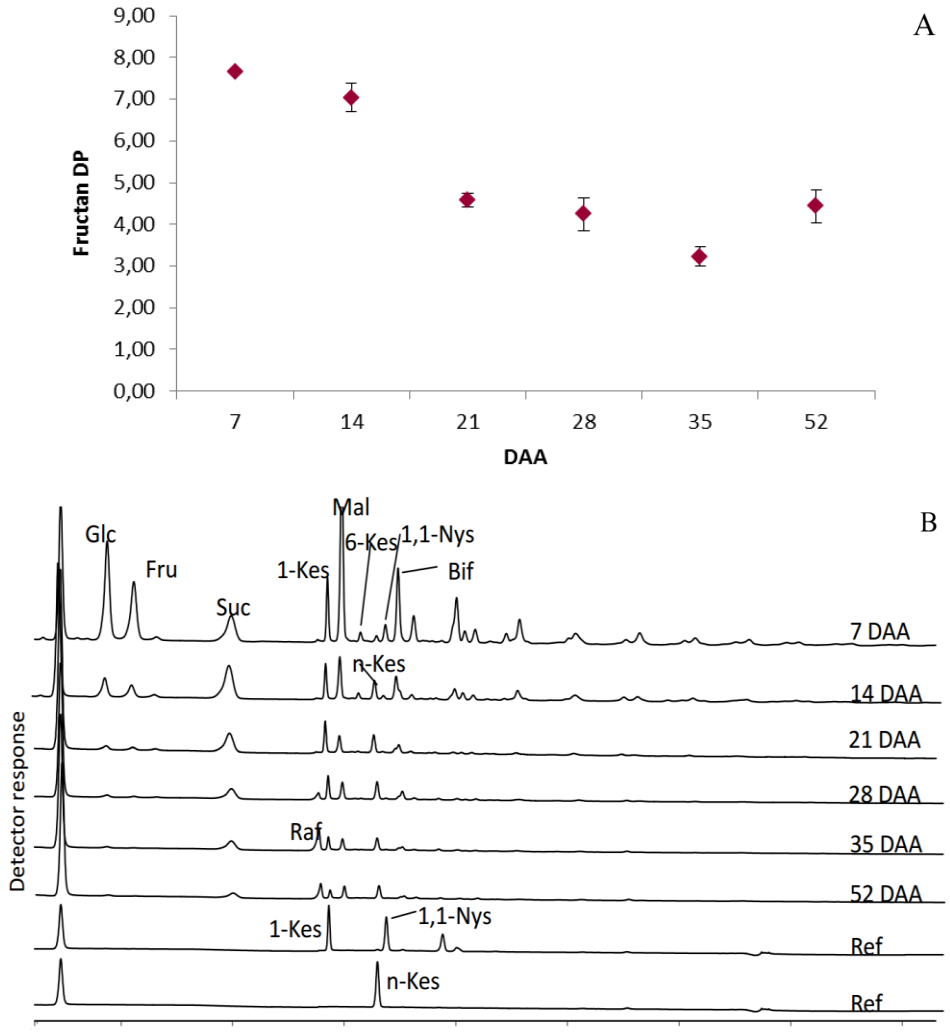

Fig. 2.15. Qualitative sugar profiles of durum wheat kernels at different DAA performed by HPAEC-PAD. Samples were analyzed in the lab of Prof Delcour (KU Leuven). **(A)** Changes on fructan DP during durum wheat kernel maturation. All the values are the mean of two experiments ± SD **(B)** Sugar profiles. Known compounds are indicated: glucose (Glc), fructose (Fru), sucrose (Suc), 1-kestose (1-Kes), maltose (Mal), 6-kestose (6-Kes), neokestose (n-Kes), 1,1-nystose (1,1-Nys), bifurcose (Bif) and raffinose (Raf).

One week later (14 DAA), the observed amount of most of the sugars was lower, except for Suc, the amount of which weakly increased and for n-K, which appeared at 14 DAA (Fig. 2.15 B). At 21 DAA, the content of all the sugars in wheat kernels further declined, except for 1-K, the amount of which remained at the same level as 1 week before.

After 4 weeks from anthesis the amount of sugars in the kernels is restricted to a small amount of Suc, 1-K, Mal, n-K and Bif. After 5 weeks from anthesis, a small amount of Raf was found. Finally, at the end of maturation, very few soluble sugars were still present and in a very small amount (fig. 2.15).

Mono-saccharides and sucrose content

A more precise quantification of monosaccharides and sucrose shows that alterations in mono-saccharides content were similar to those of fructans: a drastic decrease was observed in the first phases of kernel development, between 7 and 21 DAA. From 21 to the end of maturation the levels of free glucose and fructose were maintained at minimal values (Fig. 2.16 A).

Suc content followed a different trend compare to that of mono-saccharides and fructans. Suc content transiently increased at early stages and then progressively decreased starting from 14 DAA and reaching the minimum value at the end of kernel development (Fig. 2.16 B). The most relevant decrease (64 %) was observed between 14 and 21 DAA.

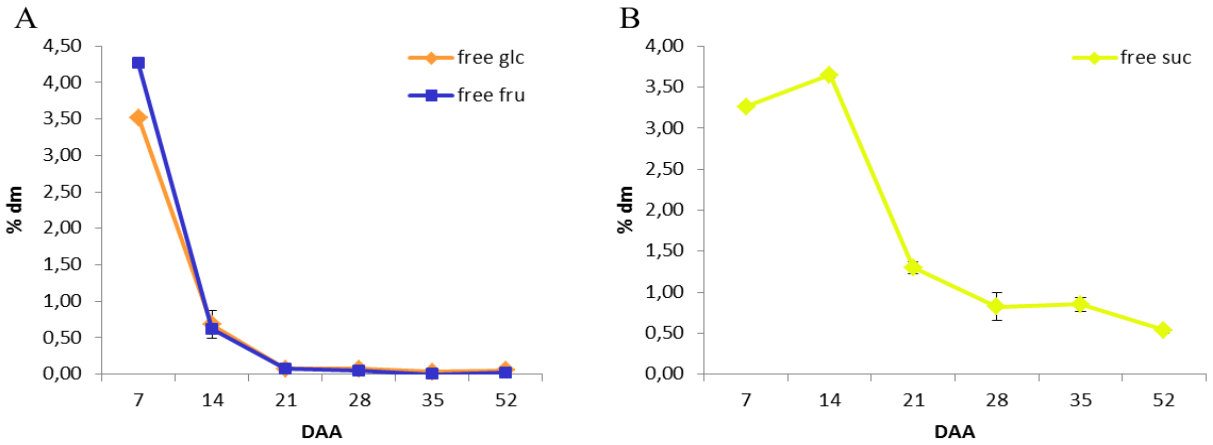

Fig. 2.16. Mono-saccharides and sucrose content in Neolatino kernels collected from 7 and 52 DAA. **(A)** Free Glc and Fru content. **(B)** Free Suc content. All the values are the mean of two experiments ± SD and are expressed as % of dry matter (% dm).

2.3.3 Water-soluble protein content during durum wheat kernel maturation

Protein content	mg / g DW ± SD
7 DAA	8.42 ± 0.08
14 DAA	5.95 ± 0.13
21 DAA	4.85 ± 0.26
28 DAA	4.11 ± 0.19
35 DAA	4.57 ± 0.06
52 DAA	1.46 ± 0.11

The determination of the water-soluble protein content of *T. durum* kernels has been performed in order to calculate the specific activity of enzymes involved in sucrose and fructan metabolisms.

While total protein content increased during kernel maturation (De Gara *et al.*, 2003a) the amount of the water-soluble proteins gradually decreased (Tab. 2.1).

Tab. 2.1. Content of soluble protein in durum wheat kernels expressed as mg/g DW ± SD .

2.3.4 Enzyme activity determinations during durum wheat kernel maturation

In order to increase knowledge about the mechanisms responsible for the observed variations in the sugar profile, the activities of the enzymes involved in fructans metabolism were measured. Particular attention has been placed on those enzymes involved in n-K and graminans metabolism. Wheat kernel protein extracts obtained from kernels collected from 7 to 52 DAA were incubated with different sugar substrates as explained in 2.2.11 paragraph. Enzyme activities were expressed as nmol/mg prot.min. The results are shown below as graphs (Fig. 2.17-2.23) and as accompanying chromatograms (Appendix A1-A7). This part of the thesis has been performed in collaboration with the Molecular Plant Physiology Laboratory (K.U. Leuven, Belgium) and the Laboratory of Food Chemistry and Biochemistry (K.U. Leuven, Belgium).

Sucrose as substrate

The biosynthetic activity was first analyzed by measuring the capability of kernel protein extract to convert Suc into fructans (A1). When kernel protein extracts were incubated with 50 mM Suc, INVs exhibited a very high activity, in particular at 7 DAA (Fig. 2.17). Indeed, a high content of Glc and Fru was observed as the results of Suc incubation with proteic extract from kernels collected at 7DAA. The release of Glc and Fru was due to invertase activity. This activity sharply decrease between 7 and 14 DAA and then it further progressively decreased until almost undetectable levels at the end of kernel maturation (Fig. 2.17). When Suc is used as the only substrate, fructan synthesis also occurs. In particular at 7 DAA the synthesis of n-K, 1-K and 6-K was observed.

In presence of Suc as exogenous substrate, the rate of 1-K synthesis was about 20 times higher than that of the 6-K and n-K. During the second week from the anthesis, fructan synthesis gradually decreased until reaching value almost undetectable at the end of maturation period (Fig. 2.17).

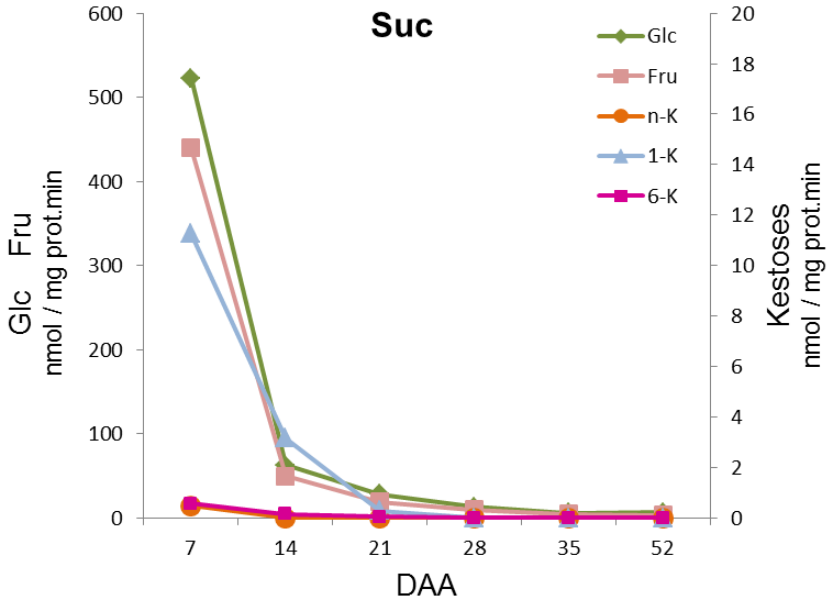

Fig. 2.17. Sugars produced after incubation of kernel enzymatic extracts with 50 mM sucrose as substrate at different stages of kernel maturation. All the values are expressed as nmol/mg prot.min.

1-kestose as substrate

When kernel protein extracts were incubated only with 50 mM 1-K, some fructan synthesis was detected (A2). In particular the synthesis of oligofructans with higher DP, such as 1,1-Nys and 1&6G-kestotetraose (6G&1-Nys) was found. The 1,1-Nys synthesis, due to 1-FFT activity, was greater and persist longer compare to the 6G&1-Nys synthesis, the latter produced by the activity of 6G-FFT (Fig. 2.18).

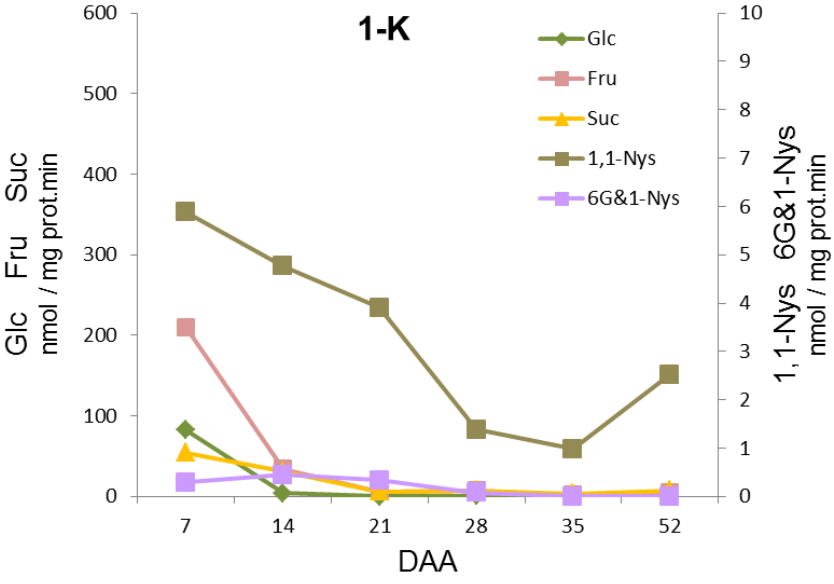

Fig. 2.18. Sugars produced after incubation of kernel enzymatic extracts with 50 mM 1-K as substrate at different stages of kernel maturation. All the values are expressed as nmol/mg prot.min.

Indeed, while 6G&1-Nys synthesis was almost undetectable at 28 DAA, 1,1-Nys synthesis still occurs at the end of kernel development when a significant increase in its synthesis, in presence of 1-K as single substrate, occurred after 35 DAA, even if the production of 1,1-Nys was lower at the end of kernel maturation than during the first DAA (Fig. 2.18).

However, fructan synthesis was significantly lower than 1-K breakdown. High 1-kestose exohydrolase (1-KEH) activities were found early in kernel maturation as confirmed by Glc, Fru and Suc production (Fig. 2.18). 1-KEH activity sharply decreased from 7 to 14 DAA and then it gradually became almost undetectable at the end of maturation (Fig 2.18).

n-kestose as substrate

When n-K was supply as single exogenous substrate no higher oligosaccharides synthesis was observed. Indeed only Glc, Fru, Suc and most probably Bla, the breakdown product of n-K, were formed (A3 and Fig. 2.19).

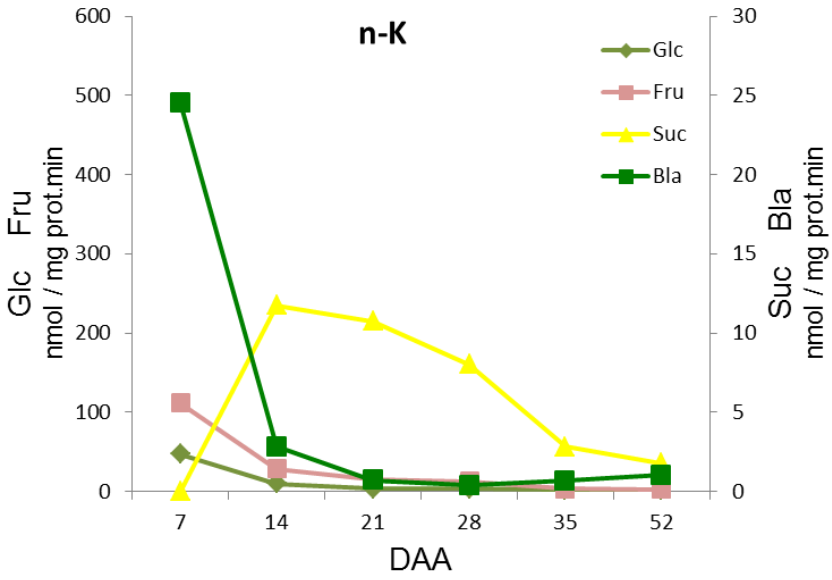

Fig. 2.19. Sugars produced after incubation of kernel enzymatic extracts with 50 mM n-K as substrate at different stages of kernel maturation. All the values are expressed as nmol/mg prot.min.

At 7 DAA, Bla amount was higher than Glc and Fru and no Suc accumulation was detected (Fig. 2.19). Suc accumulation began at 14 DAA after which it progressively decreased during the last period of kernel maturation. On the contrary, a 12-fold decrease of the Bla content was observed between 7 and 14 DAA, a further decrease occurred from 14 to 21 DAA, after which a certain production of Bla remained until the end of kernel maturation (Fig. 2.19).

1-kestose plus sucrose as substrates

When a combination of 50 mM 1-K and 50 mM Suc was used as substrates, a synthesis of Bif occurs demonstrating the presence of 6-SFT activity (A4 and Fig. 2.20). This enzyme uses Suc as donor substrate of fructosyl unit and 1-K as acceptor substrate. The amount of Bif reached a maximum pick at 14 DAA after which it strongly decreased until almost undetectable values at 28 DAA (Fig. 2.20). Moreover, a small amount of n-K, as a consequence of the activity of 6G-FFT, was observed from 7 DAA until 21 DAA, after this stage of maturation its amount was also almost undetectable (Fig. 2.20). 6G-FFT is also involved in the synthesis of 6G&1-Nys. Consistently these fructans showed a trend similar to n-K (Fig. 2.20). Finally, the presence of 1-FFT activity has been confirmed by 1,1-Nys synthesis although, a higher amount of this sugar, was found when the enzyme extracts were incubated with 1-K alone (Fig. 2.18). Surprisingly, different trends of accumulation of 1,1-Nys were detected when 1-K plus Suc or 1-K alone were used as substrate, even though the enzyme catalyzing its biosynthesis always was 1-FFT.

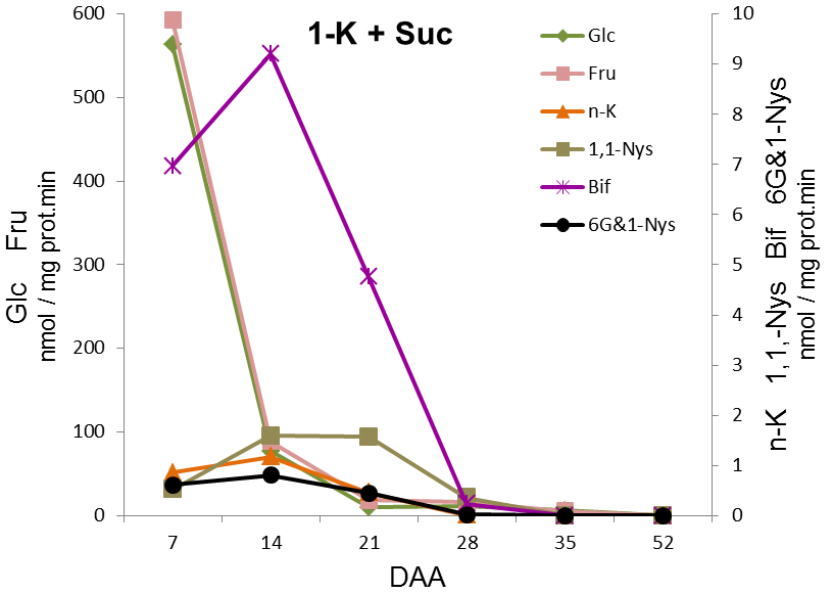

Fig. 2.20. Sugars produced after incubation of kernel enzymatic extracts with a combination of 50 mM 1-K and 50 mM Suc as substrates at different stages of kernel maturation. All the values are expressed as nmol/mg prot.min.

In fact, a maximum pick was found at 14 DAA when a combination of 1-K and Suc was used while the highest activity was detected at 7 DAA when only 1-K was used. This discrepancy could be due to the fact that the enzymes involved in fructan metabolism have been reported to be multifunctional, according to the available substrates. Moreover the same enzyme could have different affinity for different substrates, and this might also contribute to make more complex the interpretation of the obtained results.

n-kestose plus sucrose as substrates

When kernel enzymatic extracts were incubated with 50 mM n-K and 50 mM Suc, the latter acted as donor substrate of fructosyl unit while n-K as acceptor substrate. As a consequence of this reaction catalyzed by 1-SFT, the sugar 6G&1-Nys was formed (A5 and Fig. 2.21). The synthesis of 6G&1-Nys was higher in the early phases of maturation and then progressively decreased to become almost undetectable starting from 28 DAA (Fig. 2.21).

6G&1-Nys production was the only higher oligofructan synthesis observed when a combination of n-K and Suc was supply as substrates. Indeed, in addition at the synthesis of 6G&1-Nys, breakdown of Suc and n-K had also been observed. It is noteworthy that the Bla production was 12 times higher (at 7 DAA) when n-K was used as the only substrate (Fig. 2.19) while the production of Glc and Fru occurred in similar amounts.

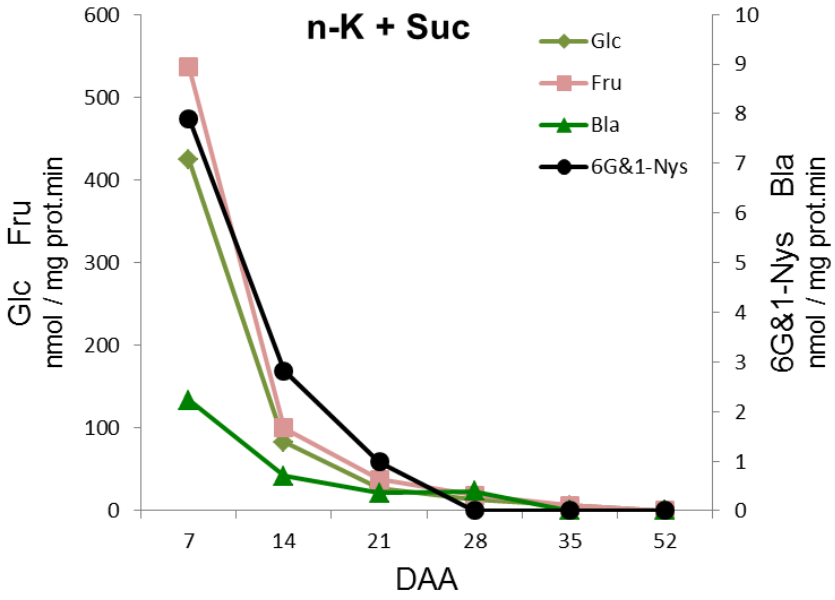

Fig. 2.21. Sugars produced after incubation of kernel enzymatic extracts with a combination of 50 mM n-K and 50 mM Suc as substrates at different stages of kernel maturation. All the values are expressed as nmol/mg prot.min.

1-kestose plus n-kestose as substrates

When a combination of 50 mM 1-K and 50 mM n-K was used as substrates, the enzyme 1-FFT catalyzed the synthesis of 6G&1-Nys using 1-K as donor substrate and n-K as acceptor substrate (A6 and Fig. 2.22). This activity rate was relatively higher at 7 DAA, it strongly declined in the following 7 days (75%), after which it slowly further decreased. At 35 DAA still some 6G&1-Nys was produced, only at 52 DAA their production was almost undetectable.

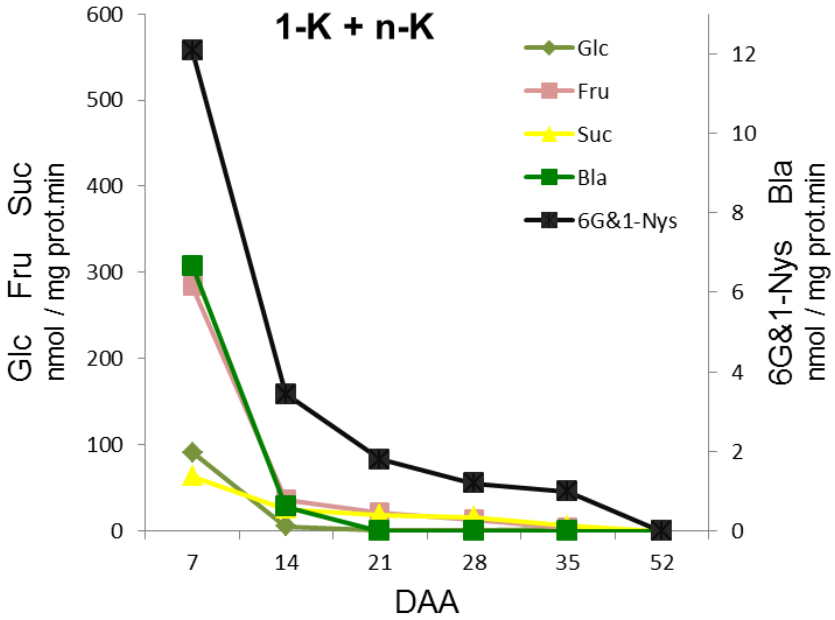

Fig. 2.22. Sugars produced after incubation of kernel enzymatic extracts with a combination of 50 mM 1-K and 50 mM n-K as substrates at different stages of kernel maturation. All the values are expressed as nmol/mg prot.min.

The 6G&1-Nys synthesis (observed using 1-K and n-K as substrate; Fig. 2.22) and 1,1-Nys synthesis (observed using only 1-K as substrate; Fig. 2.18), both catalyzed by 1-FFT, were the only higher oligofructan synthesis observed in the last period of kernel development. Finally, Bla was produced as result of n-K breakdown (Fig. 2.22). However this breakdown activity happened at lower rate (approximately 3.6 times lower) compare with n-K used as single substrate (Fig. 2.19).

Graminans and fructan neoseries as substrates

The incubation of kernel enzymatic extracts with graminans and neoseries fructan (hereafter called kernel substrate) was carried out in order to investigate FEHs activity during kernel development.

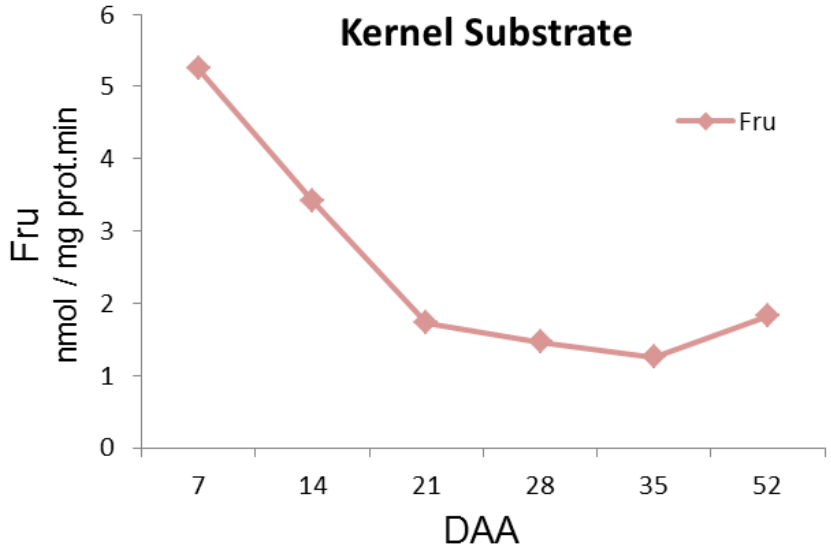

Fig. 2.23. Sugars produced after incubation of kernel enzymatic extracts with 2 mM wheat kernel graminans and neoseries fructans as substrates at different stages of kernel maturation. All the values are expressed as nmol/mg prot.min.

Graminan and neoseries fructan breakdown rate was higher at the beginning of kernel development (5.3 nmol/mg pt.min at 7 DAA) and then progressively decreased until 35 DAA. In the last period of kernel maturation a small increase in graminan and neoseries fructan degradation occurs (A7 and Fig. 2.23).

A summary of the main biosynthetic activity observed in *T. durum* kernels during maturation is shown in figure 2.24. Since each enzyme can use various substrates, herewith we show only the enzymatic activities observed in the best assay conditions. With the exception of 6-SFT, in general the enzyme activities with all the substrates tested were highest at 7 DAA after which they sharply declined. In the majority of the identify biosynthetic enzymes the activity was almost undetectable at 52 DAA (Fig. 2.24). Diversely from the other biosynthetic enzyme, 6-SFT transiently increased during the first two weeks from the anthesis and then gradually declined until almost zero starting from 35 DAA (Fig. 2.24). The 1-FFT showed the highest activity rate at 7 DAA and its activity was the most extended during kernel development. Indeed 1-FFT was the only oligofructans biosynthetic activity observed at 35 DAA (Fig. 2.24). On the contrary, the activities of 6G-FFT and 6-SST ended in the early phases of kernel development, 7 and 14 DAA respectively (Fig. 2.24).

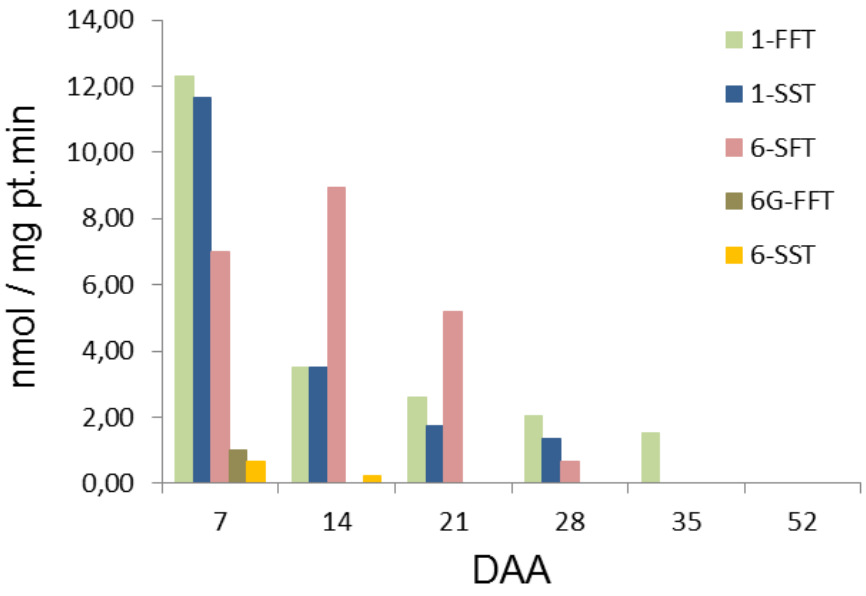

Fig. 2.24. Summary of the main biosynthetic activity observed in *T. durum* kernels during maturation. The values are expressed as nmol/mg prot.min.

2.3.5 Expression levels of fructan enzymes during durum wheat kernel maturation

In order to verify whether the observed changes in fructan biosynthetic activities were due to variations in gene expression, the transcript levels of 6-SFT, the main enzyme involved in graminans synthesis, were analyzed at three different times of kernel development: 7, 14 and 52 DAA (Fig. 2.25). The obtained results indicate that the increase in the activity of 6-SFT observed from 7 to 14 DAA was coherent with an increase in its gene expression; while, surprisingly at the end of kernel maturation (52 DAA) a certain amount of 6-SFT mRNA was still present in spite of no enzymatic activity was still detectable (Fig. 2.25 and Fig. 2.24).

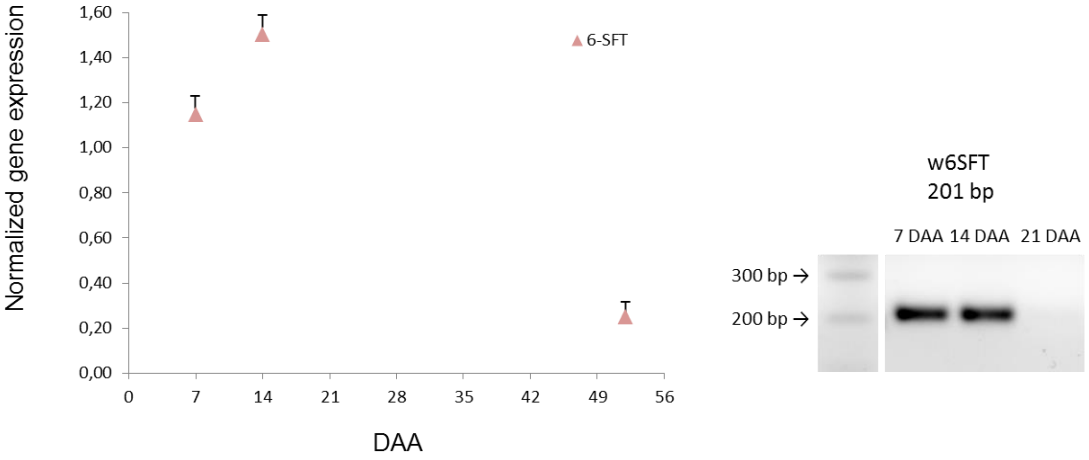

Fig. 2.25. (A) Normalized expression of 6-SFT in wheat kernels at 7, 14 and 52 DAA. Values are expressed as 6-SFT relative expression on 18S taken as housekeeping gene and are the mean of two independent experiments ± SD. **(B)** Agarose gel of PCR products.

The transcript levels of enzymes involved in fructans hydrolysis were also investigated. In particular our attention has been focus on the transcript levels of 1-FEHw3 and 6&1-FEH, which might play an important role in the degradation of branched and low DP wheat graminans such as Bif. Although graminan and neoseries fructan hydrolysis was higher at the beginning of kernel development and then progressively decreased (Fig. 2.23), the transcript levels of 1&6-FEH increased from 7 to14 DAA and at 52 DAA 1&6-FEH gene expression was maintained at the same level (Fig. 2.26).

As regard 1-FEH w3 transcript levels, they do not change between 7 and 14 DAA. At 52 DAA its expression was almost halved. Therefore, although no 1-FEH activity was observed at 52 DAA, a certain amount of 1-FEHw3 mRNA was detected (Fig. 2.26).

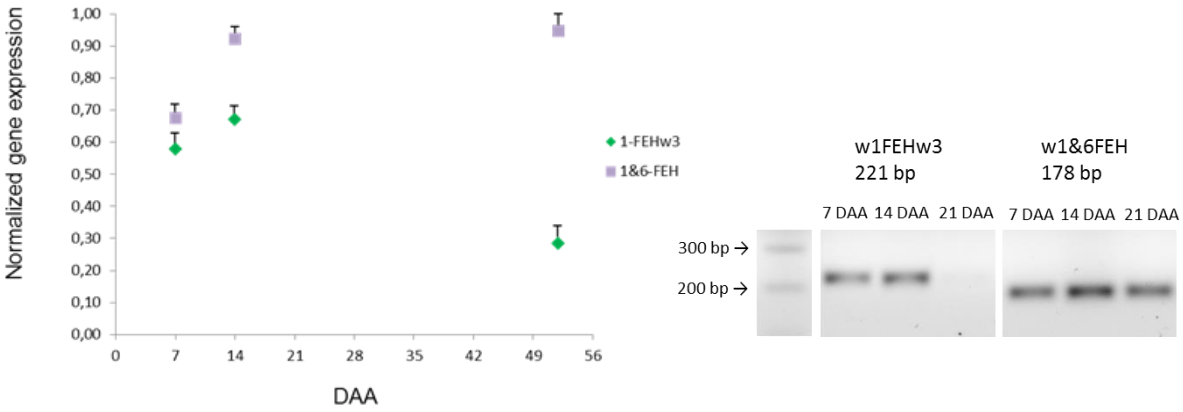

Fig. 2.26. (A) Normalized expression of 1-FEHw3 and 1&6-FEH in wheat kernels at 7, 14 and 52 DAA. Values are normalized on 18S expression and are the mean of two independent experiments ± SD. **(B)** Agarose gel of PCR products.

2.3.6 Identification of new enzymes of fructan metabolism in wheat

Another goal of this work was to find out novel FT and FEH activities not jet described in wheat. For this purpose the functional characterization of two unknown recombinant FT proteins was carried out. Moreover, a screening of *T. aestivum* cDNA library was performed in order to identify novel FEHs involved in neoserie's fructans degradation as well as new FTs not jet identified in wheat. This work has been conducted during a training period at the Molecular Plant Physiology Laboratory (K.U. Leuven, Belgium) headed by Prof. Wim Van den Ende.

Pichia pastoris as heterologous protein expression system

The cloning of the full-length cDNA encoding an unknown FT protein and its functional characterization by heterologous expression in *Pichia pastoris* was performed.

P. pastoris is methylotrophic yeast easier to genetically manipulate and cultured than mammalian cells and that can be grown to high cell densities. Moreover, since *P. pastoris* is a eukaryote, it has the numerous advantages needed to synthetize soluble recombinant proteins that have undergone all the post-translational modifications required for functionality and that are correctly folded. When methanol is present as carbon and energy source it is oxidized to formaldehyde and hydrogen peroxide by the alcohol oxidase (AOX) of *P. pastoris*. The expression of this enzyme is under control of a strong promoter and takes place only when methanol is present (Cereghino and Cregg, 2000; Daly and Hearn, 2005).

Sara Cimini

The *P. pastoris* expression vector pPicZαA contains this strong promoter AOX1 whose regulation is characterized by a repression/derepression mechanism plus an induction mechanism: growth on glucose represses transcription (even in presence of the inducer methanol); then the culture is de-repressed (growth on glycerol alone) and induced in presence of methanol (Ellis *et al.*, 1985; Koutz *et al.*, 1989; Tschopp *et al.*, 1987). Moreover this vector contains alpha-factor secretion signal which allow secretion of the heterologous proteins into the expression medium (Cregg *et al.*, 1993). For all these reasons *P. pastoris* is considered a highly reliable system for heterologous expression of several enzymes.

Cloning and functional characterization of the recombinant FT 67 protein

Cloning of T. aestivum FT 67 cDNA into the expression vector pPicZαA

A 1600-nucleotide long sequence encoding for an unknown protein from *T. aestivum* (Ta67) was amplified by RT-PCR as described in 2.2.15 paragraph. Two specific primers were designed in order to introduce *EcoRI* and *SacII* restriction sites respectively at the 5'- and 3'-ends of the Ta67 clone. The introduction of two different restriction sites allows directional cloning of the Ta67 cDNA into the pPICZαA vector. pPICZαA vector contains a multiple cloning site downstream from the AOX1 promoter and α-factor secretion signal (Fig. 2.27). Direct selection of the transfectants is permitted by the zeocin resistance gene present in the vector. Moreover the proper integration of the cDNA into the vector was checked by PCR using vector specific primers suitably constructed for this scope. Plasmids from positive colonies were purified and sequenced in order to control the accuracy of the sequence. The recombinant plasmid of pPICZαA-Ta67 was linearized by *Pme I* and transformed into Pichia X-33 by electroporation. Integration of the linearized expression vector into *P. pastoris* genome occurs via homologous recombination at the AOX1 locus.
For details on cloning protocol see 2.2.15 paragraph.

The deduced amino acid sequence of the Ta67 cDNA showed 65-75% identity with vacuolar INVs from monocotyledonous plant and 60-70% identity with FTs. In order to investigate about the activity of the cloned Ta67 cDNA, before moving on to the functional characterization of the recombinant protein by heterologous expression in *P. pastoris*, the deduced amino acid sequence of the Ta67 cDNA was analyzed by comparison with amino acid sequence of already known wheat FTs and monocotyledonous vacuolar INVs (Fig. 2.28).

Sara Cimini

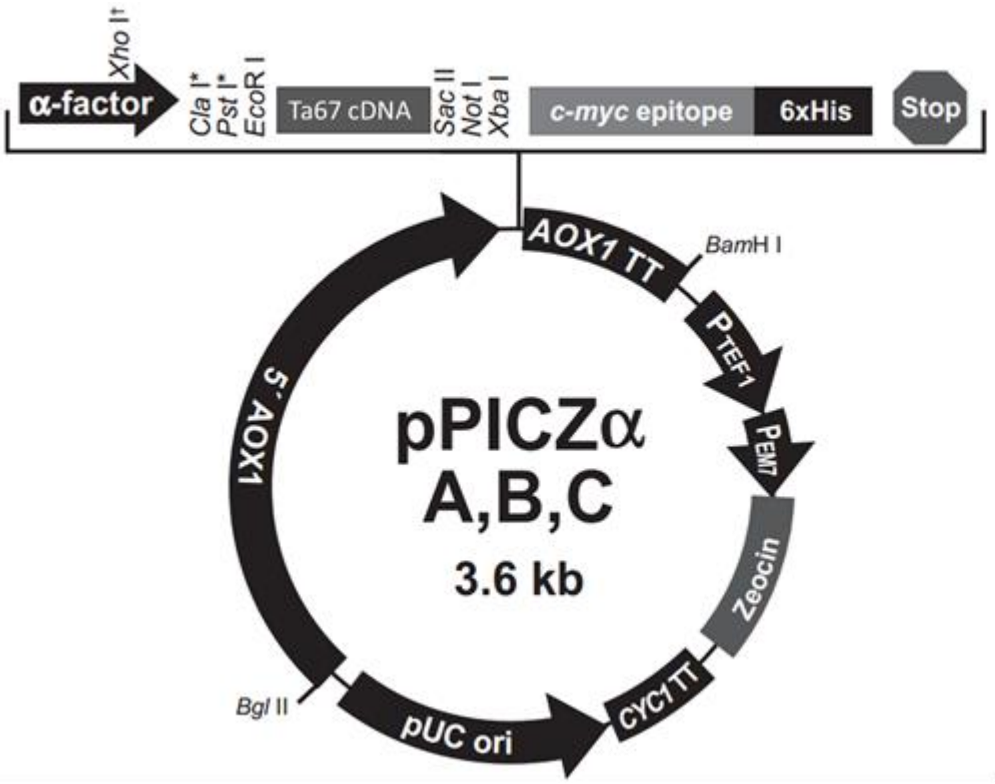

Fig. 2.28. Map of the recombinant plasmid of pPICZαA-Ta67. The Ta67 cDNA has been placed in the multiple cloning site.

INVs usually have an unchanged WMNDPNG motif, while FTs are altered in this motif and in particular Poaceae always contain a tyrosine (Y) instead of a tryptophan (W) (Schroeven *et al.*, 2008). Also the WSGSAT motif plays a critical role in the determination of acceptor substrate specificity in GH23 plant enzymes. Indeed while all the vacuolar INVs are characterized by the presence of a W in the first position of this motif (Le Roy *et al.*, 2007a), in all FTs a leucin (L) or a methionine (M) were found. Finally, with few exceptions, 1-SSTs contain an asparagine (N) in the GWAS/N motif, whereas all vacuolar INVs and 6-SFTs have a serine (S). In Ta67 cDNA a Y instead of a W was found to characterize the WMNDPNG, a L instead of a W is present in the WSGSAT motif and a N was found in the GWAS/N motif (Fig. 2.28).

```
ZmV-INV|P49175.1       ---------------------MIPAVADPTTLDGGGARRPLLPETDPRGRAAAGAEQKRP 39
TaV-INV|CAG25609.1     ------------------------MEARD--GGSAP--LPCSYAPLPE-DAEAATTVGRA 31
HvV-INV|CAF22241.1     ------------------------MPTMD--TTDR-----GSYAQLPD-DAEAGSAH--- 25
LpV-INV|AAL92880.1     ----------------------MPMEARD--GVSMP----YSYAALPE-DAEAAVVG--R 29
OsV-INV|AAF87246.1     ------------------------METRD--DVADASALPYSYSPLPAGDAASADLAAAR 34
Ta6-SFT|BAB82469.1     ------------------------MGS------HGKPPLPYAYKPLPS--------DADG 22
Ta6-SFT|ACI43225.3     ------------------------MGS------HGKPPLPYAYKPLPSG----AAVDADG 26
Ta67                   SEQUENTIETRITICUMFTCLONEMKSR-----AGTPPVLYSYASMQQ------------ 43
Ta1-FFT|BAE19751.1     ------------------------MESSRGILIPGTPPLPYAYEPLPSSSADANGQEDRR 36
Ta1-FFT|ACH73191.1     ------------------------MESSRGILIPGTPPLPYAYEPLPSSSADANGQEDRR 36
Ta1-SST|BAB82470.1     ------------------------MDSSRVILIPGTPPLPYAYEQLPSSSADAKGIEEER 36
```


Sara Cimini

```
ZmV-INV|P49175.1         PATPTVLTAVVSAVLLLVLVAVTVLASQHVDGQAGGVPAGEDAVVVEVA--------ASR 91
TaV-INV|CAG25609.1       RRTAGPLCAALMLVTAAVLLMVAALAGVRLAGQLPADGIVGVSGDQTTVDAA-MMSTSSR 90
HvV-INV|CAF22241.1       RRRTGPLCAAILLTSAALLLAVAALAGVRVAGQLPVAGVI-MSGQPTTVDVVPTTSTSSR 84
LpV-INV|AAL92880.1       GRRTGPLFAALLLTLVAALLAVAALAGVRLVGELPAGGVX-MPNHPMEVMDV----SGSR 84
OsV-INV|AAF87246.1       RSRRRPLCVALFLASAAVILAVAVLSGVRLAGRP--------ATTTMVVPGVVEMEMASR 86
Ta6-SFT|BAB82469.1       ERAGCTRWRVCAVALTASAMVVVVVGATLLAG---------------------------F 55
Ta6-SFT|ACI43225.3       ERTGWTRWRVCATVLTASAMVVVVVGATLLAG---------------------------F 59
Ta67                     RSGGGMRWRECVAVLGAAAMVVFVVTHSLLPGARVGDLGDVV--------------SPVL 89
Ta1-FFT|BAE19751.1       ITGG-VRWRAWAAVLAVG---ALVVAAAVFGASRVDRDAVASSVPAT------------- 79
Ta1-FFT|ACH73191.1       ITGG-VRWRAWAAVLAVG---ALVVAAAVFGASRVDRDAVASSVPAT------------- 79
Ta1-SST|BAB82470.1       AGGGGLRWRACAAVLAASAVVALVVAAAVFGASGAGWDAVAASVPATPATEF----PRSR 92

ZmV-INV|P49175.1         GVAEGVSEKSTAPLLG-------SGALQDFSWTNAMLAWQRTAFHFQPPKNWMNDPNGPL 144
TaV-INV|CAG25609.1       GPESGVSEKTSGAAAH-GGMLGADASGNAFPWSNAMLQWQRTGFHFQPEKNWMNDPNGPV 149
HvV-INV|CAF22241.1       GPEYGVSEKTSGAGAH-GGMLGADAG-NAFPWSNAMLQWQRTGFHFQPEKNWMNDPNGPV 142
LpV-INV|AAL92880.1       GPESGVSEKTSGAASESGGMLGADAGSNAFPWSNAMLQWQRTGFHFQPEKNWMNDPNGPV 144
OsV-INV|AAF87246.1       GPESGVSEKTSGAEEM-VRLMGGAAGGEAFPWSNAMLQWQRTGFHFQPERNWMNDPNGPV 145
Ta6-SFT|BAB82469.1       RVDQAVDEEAAG----------------GFPWSNEMLQWQRSGYHFQTAKNYMSDPNGLM 99
Ta6-SFT|ACI43225.3       RVDQAVDEEAAA----------------GFPWSNEMLQWQRSGYHFQTAKNYMSDPNGLM 103
Ta67                     RLRRARREEAAVPSSE-KTVGEIGDEADGFPWSNAMLQWQRTGYHFQPDKNYMNDPNAPM 148
Ta1-FFT|BAE19751.1       -AEHGVLEKASG----------PYSASGGFPWSNAMLQWQRTGYHFQPEKNYQNDPNGPV 128
Ta1-FFT|ACH73191.1       -AEHGVLEKASG----------PYSASGGFPWSNAMLQWQRTGYHFQPEKNYQNDPNGPV 128
Ta1-SST|BAB82470.1       GKEHGVSEKTSG----------AYSAN-AFPWSNAMLQWQRTGYHFQPDKYYQNDPNGPV 141

ZmV-INV|P49175.1         YHKGWYHLFYQWNPDSAVWGN-ITWGHAVSRDLLHWLHLPLAMVPDHPYDANGVWSGSAT 203
TaV-INV|CAG25609.1       YYKGWYHLFYQYNPDGAIWGNKIAWGHAASRDLLRWRHLPVAMSPDQWYDINGVWSGSAT 209
HvV-INV|CAF22241.1       YYKGWYHLFYQYNPDGAIWGNKIAWGHAASRDLLRWRHLPVAMSPDQWYDINGVWSGSAT 202
LpV-INV|AAL92880.1       YYKGWYHLFYQYNPEGAIWGNKIAWGHAVSRDMLRWRHLPIAMFPDQWYDINGAWSGSAT 204
OsV-INV|AAF87246.1       YYKGWYHLFYQYNPDGAVWGNKIAWGHAVSRDLVHWRHLPLAMVPDQWYDVNGVWTGSAT 205
Ta6-SFT|BAB82469.1       YYRGWYHMFFQYNPVGTDWDDGMEWGHAVSRNLVQWRTLPIAMVADQWYDILGVLSGSMT 159
Ta6-SFT|ACI43225.3       YYNGWYHMFFQYNPVGTDWDDGMEWGHAVSRNLVTWRTLPIAMVADQWYDILGVLSGSMT 163
Ta67                     YYRGWYHFFYQYNPEGVTWGN-ISWGHAVSRDMVHWHHLPLAMVPDRWYDINGVLTGSAT 207
Ta1-FFT|BAE19751.1       YYKGWYHFFYQHNPGGTGWG-NISWGHAVSRDMVHWRHLPLAMVPEHWYDIEGVLTGSIT 187
Ta1-FFT|ACH73191.1       YYKGWYHFFYQHNPGGTGWG-NISWGHAVSRDMVHWRHLPLAMVPEHWYDIEGALTGSIT 187
Ta1-SST|BAB82470.1       YYGGWYHFFYQYNPSGSVWEPQIVWGHAVSKDLIHWRHLPPALVPDQWYDIKGVLTGSIT 201

ZmV-INV|P49175.1         RLPDGRIVMLYTGSTAESSAQVQNLAEPADASDPLLREWVKSDANPVLVPPPGIGPTDFR 263
TaV-INV|CAG25609.1       VLPDGRIVMLYTGST-NASVQVQCLAFPTDPSDPLLINWTKYENNPVMYPPPGVGEKDFR 268
HvV-INV|CAF22241.1       VLPDGRIVMLYTGST-NASVQVQCLAFPTDPSDPLLINWTKYENNPVMYPPPGVGEKDFR 261
LpV-INV|AAL92880.1       VLPDGRIVMLYTGST-NASVQVQCLAFPSDPSDPLLTNWTKYEGNPVLYPPPHVGEKDFR 263
OsV-INV|AAF87246.1       TLPDGRLAMLYTGST-NASVQVQCLAVPSDPDDPLLTNWTKYHANPVLYPPRTIGDRDFR 264
Ta6-SFT|BAB82469.1       VLPNGTVIMIYTGATNASAVEVQCIATPADPTDPLLRRWTKHPANPVIWSPPGVGTKDFR 219
Ta6-SFT|ACI43225.3       VLPNGTVIMIYTGATNASAIEVQCIATPADPNDPFLRRWTKHPANPVIWSPPGIGTKDFR 223
Ta67                     ILPDGKVVLLYTGNT-DTLAQVQCVAEPADPHDPLLRTWIKHPANPVLFPPPGTYKKDFR 266
Ta1-FFT|BAE19751.1       VLPDSRVILLYTGNT-ETFAQVTCLAEAADPSDPLLREWVKHPANPVVYPPPGIGMKDYR 246
Ta1-FFT|ACH73191.1       VLPDGRVILLYTGNT-ETFAQVTCLAEAADPSDPLLREWVKHPANPVVYPPPGIGMKDYR 246
Ta1-SST|BAB82470.1       VLPDGKVILLYTGNT-ETFAQVTCLAEPADPSDPLLREWVKHPANPVVFPPPGIGMKDFR 260

ZmV-INV|P49175.1         DPTTACRTPAGNDTAWRVAIGSKDRDH---AGLALVYRTEDFVRYDPAPALMHA-VPGTG 319
TaV-INV|CAG25609.1       DPTTAWFDGS--DDTWRLVIGSKDDHH---AGMVMTYKTKDFIDYELVPGLLHR-VPGTG 322
HvV-INV|CAF22241.1       DPTTAWFDGP--DDMWRLVIGPKDDRH---AGMVMTYKTKDFMDYELVPGLLHR-VPGTG 315
LpV-INV|AAL92880.1       DPTTAWYDGS--DGMWRIVIGSKDNRR---AGMALTYKTKNFHDFELVPGVLHR-VPATG 317
OsV-INV|AAF87246.1       DPTTAWRDPS--DGDWRIVIGSKDEHH---AGIAVVYRTADFVTYDLLPGLLHR-VEATG 318
Ta6-SFT|BAB82469.1       DPMTAWYDES--DDTWRTLLGSKDDNNGHHDGIAMMYKTKDFLNYELIPGILHR-VERTG 276
Ta6-SFT|ACI43225.3       DPMTAWYDES--DDTWRTLLGSKDDHDGHHDGIAMMYKTKDFLNYELIPGILHR-VQRTG 280
Ta67                     DPMTAWFDKS--DNTWRTMIGSKDNNG--HAGIALMYKTKDFVKFELIPRPVHR-VEGTG 321
Ta1-FFT|BAE19751.1       DPTTAWFDNS--DNTWRIIIGSKNDTD--HSGIVFTYKTKDFVSYEMIPGYLYRGPAGTG 302
Ta1-FFT|ACH73191.1       DPTTAWFDNS--DNTWRIIIGSKNDTD--HSGIVFTYKTKDFVSYELIPGYLYRGPAGTG 302
Ta1-SST|BAB82470.1       DPTTAWFDES--DGTWRTIIGSKNDSD--HSGIVFSYKTKDFLSYELMPGYMYRGPKGTG 316

ZmV-INV|P49175.1         MWECVDFYPVAAGSGAAAGSGDGLETSAAPGPGVKHVLKASLDDDKHDYYAIGTYDPATD 379
TaV-INV|CAG25609.1       MWECIDLYPVGGLRGIDM-TEAVAAASNNGGGDVLHVMKESSDDDRHDYYALGRYDAAKN 381
HvV-INV|CAF22241.1       MWECIDLYPVGGVRGIDM-TDAVTAASNNGGDDVLHVMKESSDDDRHDYYALGRYDATKN 374
LpV-INV|AAL92880.1       MWECIDLYPVGGARGIDM-TEAVAAASNSGGGEVLHVMKESSDDDRHDYYALGRYDAATN 376
OsV-INV|AAF87246.1       MWECIDFYPVAGGEGVDM-TEAMYAR-NKG---VVHVMKASMDDDRHDYYALGRYDPARN 373
Ta6-SFT|BAB82469.1       EWECIDFYPVG-------------RRTSDNSSEMLHVLKASMDDERHDYYSLGTYDSAAN 323
Ta6-SFT|ACI43225.3       EWECIDFYPVG-------------HRSNDNSSEMLHVLKASMDDERHDYYSLGTYDSAAN 327
Ta67                     MWECVDFYPVR-------------GNSN-SSQEELYVLKASMDDERHDYYALGKYDAVTN 367
Ta1-FFT|BAE19751.1       MYECIDLYAVGGGR-------KASDMYNSTAKDVLYVLKESSDDDRRDYYALGRFDAAAN 355
Ta1-FFT|ACH73191.1       MYECIDLFAVGGGR-------AASDMYNSTAEDVLYVLKESSDDDRRDYYALGRFDAAAN 355
Ta1-SST|BAB82470.1       EYECIDLYAVGGGR-------KASDMYNSTAEDVLYVLKESSDDDRHDWYSLGRFDAAAN 369

ZmV-INV|P49175.1         TWTPDSAEDDVGIGLRYDYGKYYASKTFYDPVLRRRVLWGWVGETDSERADILKGWASVQ 439
TaV-INV|CAG25609.1       TWTPLDSDADVGIGLRYDWGKFYASKTFYDPSKKRRVLWGWVGETDSEHADVAKGWASLQ 441
HvV-INV|CAF22241.1       TWTPLDVDADLGIGLRYDWGKFYASKTFYDPAKKRRVLWGWVGETDSESADVAKGWASLQ 434
LpV-INV|AAL92880.1       KWTPLDADADVGIGLRYDWGKFYASKTFYDPAKKRRVLWGWVGETDSERADVAKGWASLQ 436
OsV-INV|AAF87246.1       AWTPLDAAADVGIGLRYDWGKFYASKTFYDPAKRRRVLWGWVGETDSERADVAKGWASLQ 433
Ta6-SFT|BAB82469.1       RWTPIDPELDLGIGLRYDWGKFYASTSFYDPAKKRRVLMGYVGEVDSKRADVVKGWASIQ 383
Ta6-SFT|ACI43225.3       TWTPIDPELDLGIGLRYDWGKFYASTSFYDPAKKRRVLMGYVGEVDSKRADVVKGWASIR 387
Ta67                     TWTPLDLEADVGIGLRYNWGKLFASTTFYDPAKRRRVMWAYVGETDSNRTDLAKGWANLQ 427
Ta1-FFT|BAE19751.1       TWTPIDTEQELGVALRYDYGRYDASKSFYDPVKQRRIVWGYVVETDSWSADAAKGWANLQ 415
Ta1-FFT|ACH73191.1       TWTPIDTEQELGVALRYDYGRYDASKSFYDPVKQRRIVWGYVVETDSWSADAAKGWANLQ 415
Ta1-SST|BAB82470.1       KWTPIDEELELGVGLRYDWGKYYASKSFYDPVKKRRVVWAYVGETDSERADITKGWANLQ 429
```


Sara Cimini

```
ZmV-INV|P49175.1        SIPRTVLLDTKTGSNLLQWPVVEVENLRMSGKSFDGVALDRGSVVPLDVGKATQLDIEAV 499
TaV-INV|CAG25609.1      SIPRTVVLDTKTGSNLLQWPVEEVETLRTNSTNLGGVTVEHGSVFPLSLHRATQLDIEAS 501
HvV-INV|CAF22241.1      STPRAVVLDTKTGSNLLQWPVEEVETLRTNSTDIGGVTIDRGSVFALNLHRATQLDIEAS 494
LpV-INV|AAL92880.1      SIPRTVVLDTKTGSNLIQWPVVEVETLRTNSTNLGSIIVEHGSVFPLSLHRATQLDIEAS 496
OsV-INV|AAF87246.1      -------LDTKTGSNLLQWPVEEVETLRTNSTDFGGITVDYASVFPLNLHRATQLDILAE 486
Ta6-SFT|BAB82469.1      SVPRTIALDEKTRTNLLLWPVEEIETLRLNATELSDVTLNTGSVIHIPLRQGTQLDIEAT 443
Ta6-SFT|ACI43225.3      SVPRTIALDEKTRTNLLLWPVEEIETLRLNATELSDVTLNTGSVIHIPLRQGTQLDIEAT 447
Ta67                    SIPRTVELDEKTRTNLIQWPVEEIETLRHNATDLSGITISTGSVFPLHLRQAAQLDIEAS 487
Ta1-FFT|BAE19751.1      SIPRTVELDEKTRTNLIQWPVEELDTLRINTTDFSGITVGAGSVVSLPLHQTSQLDIEAS 475
Ta1-FFT|ACH73191.1      SIPRTVELDEKTRTNLIQWPVEELDTLRINTTDLSGITVGAGSVVSLPLHQTSQLDIETS 475
Ta1-SST|BAB82470.1      SIPRTVELDEKTRTNLVQWPVEELDALRINTTDLSGITVGAGSVAFLPLHQTAQLDIEAT 489

ZmV-INV|P49175.1        FEVDASDAAGVTEADVTFNCSTSAGAAGRGLLGPFGLLVLADDD----LSEQTAVYFYLL 555
TaV-INV|CAG25609.1      FRLDPLDVAAAKEADVGYNCSTSGGTTGRGTLGPFGLLVLADARHHSGDMERTGVYFYVA 561
HvV-INV|CAF22241.1      FRLDQLDIAASNEADVGYNCSTSGGAAGRGKLGPFGLLVLADARRYGGDAERTAVYFYVA 554
LpV-INV|AAL92880.1      FRLDPLDVAAAKEADVGYNCSTSGGAAGRGALGPFGLLVLADARRHGGDTEQTAVYFYVA 556
OsV-INV|AAF87246.1      FQLDPLAVDAVLEADVGYNCSTSGGAAGRGALGPFGLLVLADKR-HRGDGEQTAVYFYVA 545
Ta6-SFT|BAB82469.1      FHLDASAVAALNEADVGYNCSSSGGAVNRGALGPFGLLVLAAGD---RRGEQTAVYFYVS 500
Ta6-SFT|ACI43225.3      FHLDASAVAALNEADVGYNCSSSGGAVNRGALGPFGLLVLAAGD---RRGEQTAVYFYVS 504
Ta67                    FRLNTSDIAAHNEADIGYNCSTSGGATNRGALGPFGLLLTNG------HSEQMAMYFYMS 541
Ta1-FFT|BAE19751.1      FRINASAIEALNEVDVGYNCTLTSGAATRGALGPFGILVLAN-V---ALTERTAVYFYVS 531
Ta1-FFT|ACH73191.1      SRINASTIEALNEVDAGYNCTMTSGAATRGALGPFGILVLAN-V---ALTEQTAVCFYVF 531
Ta1-SST|BAB82470.1      FRIDASAIEALNEADVSYNCTTSSGAATRGALGPFGLLVLAN-R---ALTEQTGVYFYVS 545

ZmV-INV|P49175.1        KGTDGSLQTFFCQDELRASKANDLVKRVYGSLVPVLDGENLSVRILVDHSIVESFAQGGR 615
TaV-INV|CAG25609.1      RGLDGGLRTHFCHDETRSSHANDIVKKVVGNIVPVLDGEEFSVRVLVDHSIVESFAMGGR 621
HvV-INV|CAF22241.1      RGLDGGLHTHFCHDEMRSSHANDIVKRVVGNTVPVLDGEELSVRVLVDHSIVESFAMGGR 614
LpV-INV|AAL92880.1      RGLDGNLRTHFCHDESRSSRANDIVKRVVGNIVPVLDGEALSVRVLVDHSIVESFAQGGR 616
OsV-INV|AAF87246.1      KGSDGGVTTHFCQDESRSSHADDIVKRVVGNVVPVLDGETFSLRVLVDHSIVESFAQGGR 605
Ta6-SFT|BAB82469.1      RGLDGGLHTSFCQDELRSSRAKDVTKRVIGSTVPVLDGEAFSMRVLVDHSIVQGFAMGGR 560
Ta6-SFT|ACI43225.3      RGLDGGLHTSFCQDELRSSRAKDVTKRVIGSTVPVLDGEAFSMRVLVDHSIVQGFAMGGR 564
Ta67                    RSLDGDLRTHFCHDESQSSLARNVVKRVVGSTVPVLNGEALSARILVDHSIVESFVMGGR 601
Ta1-FFT|BAE19751.1      KGLDGGLRTHFCHDELRSTHATDVAKEVVGSTVPVLDGEDFSVRVLVDHSIVQSFVMGGR 591
Ta1-FFT|ACH73191.1      KGLDGGLRTHFCHDELRSTHATDVAKEVVGSTVPVLDGEDLSVRVLVDHSIVQNFVMGGR 591
Ta1-SST|BAB82470.1      KGLDGGLRTHFCHDELRSSHASDVVKRVVGSTVPVLDGEDFSVRVLVDHSIVQSFAMGGR 605

ZmV-INV|P49175.1        TCITSRVYPTRAIYDSARVFLFNNATHAHVKAKSVKIWQLNSAYIRPYPATTTSL-- 670
TaV-INV|CAG25609.1      LTATSRVYPTEAIYANAGVYLFNNATSARVNVTRLVVHEMDSSYN--QAYMTSL--- 673
HvV-INV|CAF22241.1      LTATSRVYPTEAIYANAGVYLFNNATGIQVTTTRLVVHEMDSS-------------- 657
LpV-INV|AAL92880.1      SVVTSRVYPTEAIYANAGVYLFNNATGARVTATSLVVHEMDPSYNQNQAEMASL--- 670
OsV-INV|AAF87246.1      STATSRVYPTEAIYANAGVFLFNNATSARVTAKKLVVHEMDSSYN--QAYMA----- 655
Ta6-SFT|BAB82469.1      TTMTSRVYPMEAYQEAK-VYLFNNATGASVTAERLVVHEMDSAHNQLSNMDDHSYVQ 616
Ta6-SFT|ACI43225.3      TTMTSRVYPMEAYQEAK-VYLFNNATGASVMAERLVVHEMDSAHNQLSNMDDHSYVQ 620
Ta67                    LTATSRVYPTEAIYEAAGLYVFNNATGSTLIVDKLVVHEMHSTPMQLDLFARD---- 654
Ta1-FFT|BAE19751.1      MTATSRAYPTEAIYAAAGVYLFNNATGASITAEKLVVHDMDSSYNRIFTDEDLLVLD 648
Ta1-FFT|ACH73191.1      MTATSRAYPTKAIYAAAGVYLFNNATGASITAEKLVVHDMDSSYNRIFTDEDLLVLD 648
Ta1-SST|BAB82470.1      LTATSRAYPTEAIYAAAGVYMFNNATGTSVTAEKLVVHDMDSSYNHIYTDDDLVVVD 662
```

Fig. 2.28. Multiple sequence alignment of the Ta67 amino acid sequence and the amino acid sequences of FTs already known in *T. aestivum* (1-FFT – BAE19751; 1-FFT – ACH73191; 1-SST – BAB82470; 6-SFT – BAB82469; 6-SFT – ACI43225). The consensus motifs, crucial for the FT activity, are indicated in bold. The estimated start of the mature protein (deduced by comparison with other monocotyledonous FTs) is indicated in bold and italics. The ESTs encoding Ta67 clone are highlighted using different colors: EST1 (GenBank BQ240781) highlighted in green; EST2 (GenBank BQ241194) blue written and underlined; EST3 (GenBank BJ236717) highlighted in yellow; EST4 (GenBank BJ241971) highlighted in pink.

Functional characterization of the recombinant T. aestivum FT 67 protein

After ammonium sulphate precipitation of the Ta67 recombinant protein heterologously expressed in *P. pastoris*, functional analysis was carried out by incubating the recombinant protein with all possible combination made using these sugars: Suc 100 mM, 1-K 50 mM, n-K 50 mM. Since with the standard protocol (described in 2.2.15 paragraph) we were not able to detect a specific activity for this clone we tried to use reaction buffers having different pH values (from 2.5 to 8), to keep the reaction mixture at several temperatures (form 4°C to 30°C) and to use protein extraction systems alternative to ammonium sulphate precipitation

Sara Cimini

(Q Sepharose High Performance strong anion exchange columns; Mini Q columns prepacked with minibeads; Vivaspin sample concentrator with a cutoff of 30 kDa). However we are still not able to detect a specific activity for this clone.

In relation to the obtained results, we speculate that specific glycosylation pattern of this clone might be involved in the formation of dimers or multimers leading to protein inactivity. The dimer/multimer formation could be also simplified in presence of acidic pH, and considering that the optimum pH of plant FTs is 5.0 this could be a crucial point. Although *P. pastoris* is a useful expression system for heterologous proteins, glycoproteins derived from *P. pastoris* expression system are generally hyperglycosylated and contain high mannose-type N-glycans (Gong *et al.*, 2009). This feature of *P pastoris* X-33 wild type strain could probably compromise the expression of active Ta67 protein. The enzyme alpha-1,6-mannosyltransferase (och1p) plays a key role in modifying glycoproteins with high mannose-type N-glycans (Zhang *et al.*, 2011). Therefore, the use of *P. pastoris* X-33 strain with OCH1 gene deletion as a host for production of glycoproteins with smaller N-glycans could be a strategy for the heterologous expression of problematic enzymes, such as Ta67.

Functional characterization of the recombinant FT 68 protein

To date the 6G-FFT activity has not been yet described in wheat. 6G-FFT is an F-type enzyme preferring 1-K, instead of Suc, as donor substrate. This enzyme is able to create β(2,1) linkages between two fructosyl residues and, differently from 1-FFT, β(2,6) linkages between a fructosyl and a glucosyl residue.

We focused our attention on the Ta68 cDNA (Fig. 2.29), since its deduced amino acid sequence has a high identity percentage (65%) compare with 6G-FFT of *Lolium perenne* (Lp6G-FFT, *Accession Number* AAM13671) (Fig. 2.30). The nucleotide sequence of the Ta68 clone has been derived in the Molecular Plant Physiology laboratory (K.U. Leuven) through successive BLAST searching and partial overlapping of *T. asetivum* ESTs (Fig. 2.29).

Sara Cimini

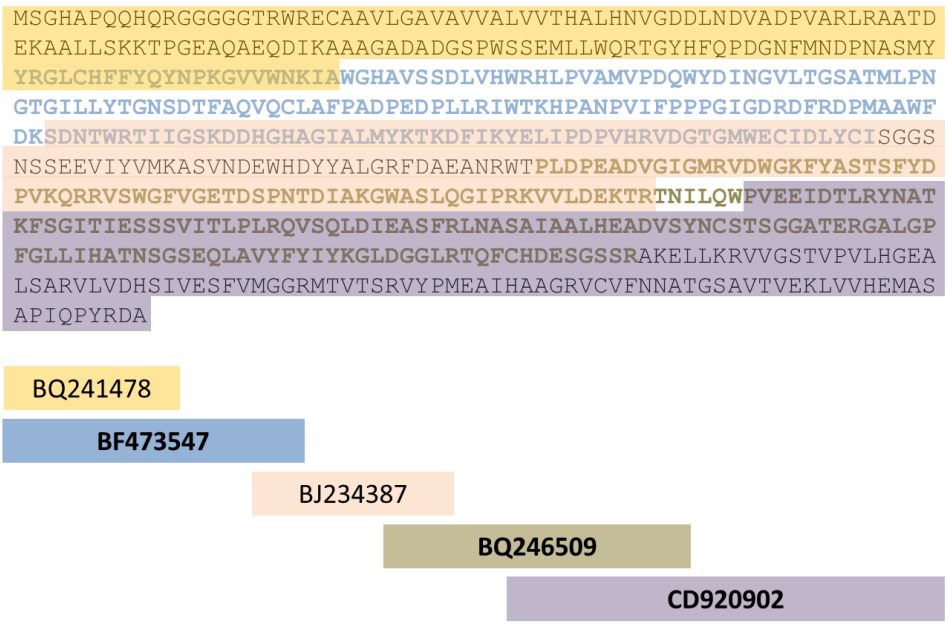

Fig. 2.29. Deduced amino acid sequence of the Ta68 protein. Colored boxes show the overlapping ESTs encoding for Ta68. The number in each boxes correspond to the GenBank ID of each EST.

As previously described for the Ta67 clone, also in the Ta68 a Y instead of a W was found in the WMNDPNG and an L instead of a W in the WSGSAT motif (Fig. 2.30). These are key features distinguishing FTs from INVs (Le Roy *et al.*, 2007a). Moreover the presence of an S before the nucleophile is a recurring feature in 6-SFT of monocotyledonous plants, while an N is generally found in 1-SST, 1-FFT and 6G-FFT (Ritsema *et al.*, 2005). In Ta68 an N was found in this position (Fig. 2.30).

Looking at the residues involved in the determination of the donor substrate specificity, they significantly differ in Ta68 compare to Lp6G-FFT, except for the presence of a histidine (H) adjacent to the arginine (R) of the D/R couple (Fig. 2.30).

Score	Expect	Method	Identities	Positives	Gaps
812 bits(2097)	0.0	Compositional matrix adjust.	404/624(65%)	482/624(77%)	20/624(3%)

```
Ta68        TPPVL-YSYASM---------QQRSGGGMRWRECVAVLGAAAMVVFVVTHSLLPGARV--   54
Lp6G-FFT    TAPLLPYAYAPLPSSADDARENQSSGGGVRWRACAA----SALVVLLVVVGFFAGGRVDL   67

Ta68        GDLGDVVSPVLRLRRARREEAAVPSSEKTVGEIGDEADGFPWSNAMLQWQRTGYHFQPDK   114
Lp6G-FFT    GQDGEVSATSSVPGSSRGKDSGV--SEKESPADG----GFPWSNAMLQWQHTGFHFQPLK   121

Ta68        NYMNDPNAPMYYRGWYHFFYQYNPEGVTWGNISWGHAVSRDMVHWHHLPLAMVPDRWYDI   174
Lp6G-FFT    HYMNDPNGPVYYGGWYHLFYQHNPYGDSWGNVSWGHAVSKDLVNWRHLPVALVPDQWYDI   181
```

```
Ta68        NGVLTGSATILPDGKVVLLYTGNTDTLAQVQCVAEPADPHDPLLRTWIKHPANPVLFPPP  234
Lp6G-FFT    NGVLTGSITVLPDGRVILLYTGNTDTFSQVQCLAVPADPSDPLLRSWIKHPANPILFPPP  241

Ta68        GTYKKDFRDPMTAWFDKSDNTWRTMIGSKDNNGHAGIALMYKTKDFVKFELIPRPVHR-V  293
Lp6G-FFT    GIGLKDFRDPLTAWFEHSDNTWRTIIGSKDDDGHAGIVLSYKTTDFVNYELMPGNMHRGP  301

Ta68        EGTGMWECVDFYPVRGNS------NSSQEELYVLKASMDDERHDYYALGKYDAVTNTWTP  347
Lp6G-FFT    DGTGMYECLDIYPVGGNSSEMLGGDSSPEVLFVLKESANDEWHDYYALGWFDAAANTWTP  361

Ta68        LDLEADVGIGLRYNWGKLFASTTFYDPAKRRRVMWAYVGETDSNRTDLAKGWANLQSIPR  407
Lp6G-FFT    QDPEADLGIGLRYDWGKYYASKSFYDPIKNRRVVWAFVGETDSEQADKAKGWASLMSIPR  421

Ta68        TVELDEKTRTNLIQWPVEEIETLRHNATDLSGITISTGSVFPLHLRQAAQLDIEASFRLN  467
Lp6G-FFT    TVELDKKTRTNLIQWPVEEIETLRRNVTDLGGITVEAGSVIHLPLQQGGQLDIEASFRLN  481

Ta68        TSDIAAHNEADIGYNCSTSGGATNRGALGPFGLLL-TNGHSEQMAMYFYMSRSLDGDLRT  526
Lp6G-FFT    SSDIDALNEADVGFNCSSSDGAAVRGALGPFGLLVFADGRHEQTAAYFYVSKGLDGSLLT  541

Ta68        HFCHDESQSSLARNVVKRVVGSTVPVLNGEALSARILVDHSIVESFVMGGRLTATSRVYP  586
Lp6G-FFT    HYCHDESRSTRAKDVVSRVVGGTVPVLDGETFSVRVLVDHSIVQSFVMGGRTTVTSRAYP  601

Ta68        TEAIYEAAGLYVFNNATGSTLIVDKLVVHEMHS  619
Lp6G-FFT    TEAIYAAAGVYLFNNATSATITAEGLVVYEMAS  634
```

Fig. 2.30. Multiple alignment of the Ta68 and Lp6G-FFT amino acid sequences. The consensus motifs are highlighted using different colors: in red the catalytic triad; in grey the estimated beginning of the mature protein; in blue critical residues for the determination of the acceptor substrate specificity; in yellow critical residues for the determination of the donor substrate specificity.

Then we proceeded with the heterologous expression of Ta68 cDNA in *P. pastoris*. The full-length Ta68 cDNA, previously cloned in pPICZαA vector in the Molecular Plant Physiology laboratory (K.U. Leuven), was transformed into Pichia X-33 by electroporation. After ammonium sulphate precipitation of the Ta68 recombinant protein heterologously expressed in *P. pastoris*, functional analysis was carried out by incubating the recombinant protein with a combination of 100 mM Suc and 50 mM 1-K. Since no enzymatic activity has been detected on protein extract we also tested the activity on the Pichia supernatant without heterologous protein purification. The incubation of the Pichia supernatant with a combination of 100 mM Suc and 50 mM 1-K was followed for 90h.

Sara Cimini

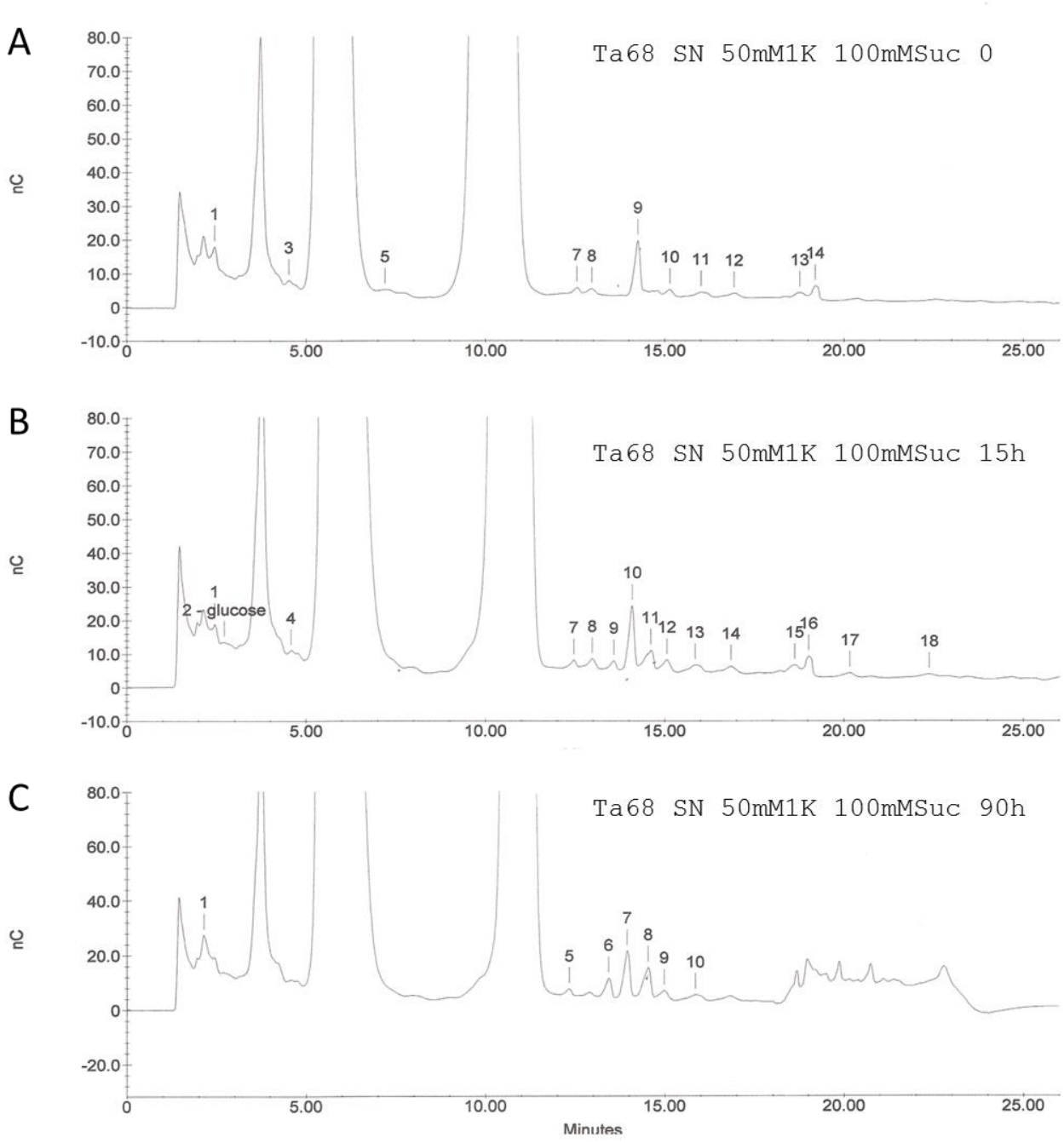

Fig. 2.31. HPAEC-PAD chromatogram showing time-dependent incubations of Pichia supernatant containing the heterologous Ta68 protein with a combination of Suc 100 mM and 1-K 50 mM for 15 **(B)** and 90 h **(C)**. A 0h sample (blank) is also presented **(A)**.

Although the chromatograms presents a very high contamination (Fig. 2.31A), due to the impossibility to conduct ammonium sulphate precipitation without activity losses, in figure 2.31B after 15 h of incubation is evident the formation of two peaks: one (peak number 9)

corresponding to the n-K and the peak number 11 that is actually a double peak corresponding to the sugars 6G&1-Nys and Bif or 1,6G-kestotetraose. The chromatogram after 90 h of incubation (Fig. 2.31C) clearly shows the two peaks corresponding to the sugars mentioned above.

No enzymatic activity was observed after incubation of the supernatant with 100 mM Suc or with 50 mM n-K alone (data not shown).

Future perspectives

Although these results should be regarded as preliminary, it seems evident that the Ta68 clone shows 6G-FFT/6G-SST activity. This activity is not jet characterized in wheat and it could be important to better understand the n-K metabolism. A n-K synthesis (Fig. 2.31B peak number 9; Fig. 2.31C peak number 6), occurring after incubation of the Pichia supernatant with a combination of Suc and 1-K, indicates the transfer of a fructosyl residue from 1-K to Suc by the 6G-FFT activity (Fig. 2.32A). The presence of 6G&1-Nys (Fig. 2.31B peak number 11; Fig. 2.31C peak number 8), as second reaction product, could be due to the transfer of a fructosyl residue from the Suc, which acts as donor substrate, to the 1-K, which acts as acceptor substrate (Fig. 2.32B). Finally a third reaction product, which could be the Bif or the 1,6G-kestotetraose (Fig. 2.31B, peak number 11; Fig. 2.31C, peak number 8), is formed.

While the 1-K or the n-K is used as donor substrate for the Bif or the 1,6G-kestotetraose synthesis respectively, Suc is used as donor substrate in both cases (Fig. 2.32C and Fig. 2.32D).

In order to have more and reliable information about the Ta68 enzymatic activity and to determine the kinetic parameters of this enzyme it is necessary develop a strategy able to guarantee the Ta68 heterologous expression and purification without activity losses.

Sara Cimini

	Donor substrate	Acceptor substrate	Products
A	G-F-F	G-F	F-G-F + G-F
B	G-F	G-F-F	F-G-F-F + G
C	G-F	G-F-F	G-F-F (F) + G
D	G-F-F	F-G-F	F-F-G-F + G-F

Fig. 2.32. Summary presenting the enzymatic reactions that may occur after incubation of the Pichia supernatant containing the heterologously expressed Ta68 with a combination of Suc 100 mM and 1-K 50 mM.

Search for novel FEHs not yet characterized in wheat

In order to find enzymatic activities involved in fructan breakdown pathway, not jet described in wheat, a screening of a cDNA library made from *T. aestivum* kernels at late milky stage was carried out. Through BLAST searches (http://blast.ncbi.nlm.nih.gov/Blast.cgi), using Ta1-FEHw2 (Q84LA1) as query, a collection of FEHs already characterized in *T. aestivum* has been obtained. After identification of conservative protein domains, degenerate primers for wheat FEHs have been constructed (Fig. 2.33).

After amplification using wFEH F and wFEH R as degenerate primers, the PCR product was cloned into pCR®2.1-TOPO (Fig. 2.34) vector and *E. coli* competent cells were transformed with the recombinant plasmid. The presence of the vector with incorporated the PCR product was checked by PCR with vector specific primers (M13 Forward and M13 Reverse). The plasmids from positive colonies were sequenced.

```
                                                wFEH F                                                  wFEH R
Accession number
BAD99104          6-KEH_2       ---NGYGAALLYKSEDFLNW 235    -DDSRLWPRIDYGNFYASKTFFDS 331
BAD99105          6-KEH_1       ---NGYGAALLYKSEDFLNW 237    -DDSRLWPRIDYGNFYASKTFFDS 333
BAE44509          6&1-FEH       ---NGIGTALLYKSEDFMSW 234    -DDNRLWTRIDYGTFYASKSFFDS 331
Q84LA1            1-FEHw2       ---NGYSAALLYKSEDFLNW 237    -DDRRLWLRIDYGTFYASKSFFDS 334
CAD92365          1-FEHw3       ---NGYSAALLYKSEDFLNW 237    -DDRRLWLRIDYGTFYASKSFFDS 334
Q84PN8            1-FEHw1       ---NGYSAALLYKSEDFLNW 238    -DDRRLWLRIDYGTFYASKSFFDS 335
Q2UXF7            6-FEH         GGPNGIASTLIYRSKDFRHW 233    ADDCRTWRRFDYGHVYASKSFFDS 339
```

Fig. 2.33. Multiple alignment of FT amino acid sequences from *T. aestivum*. The positions of the primers wFEH F and wFEH R are indicated in orange and in green, respectively.

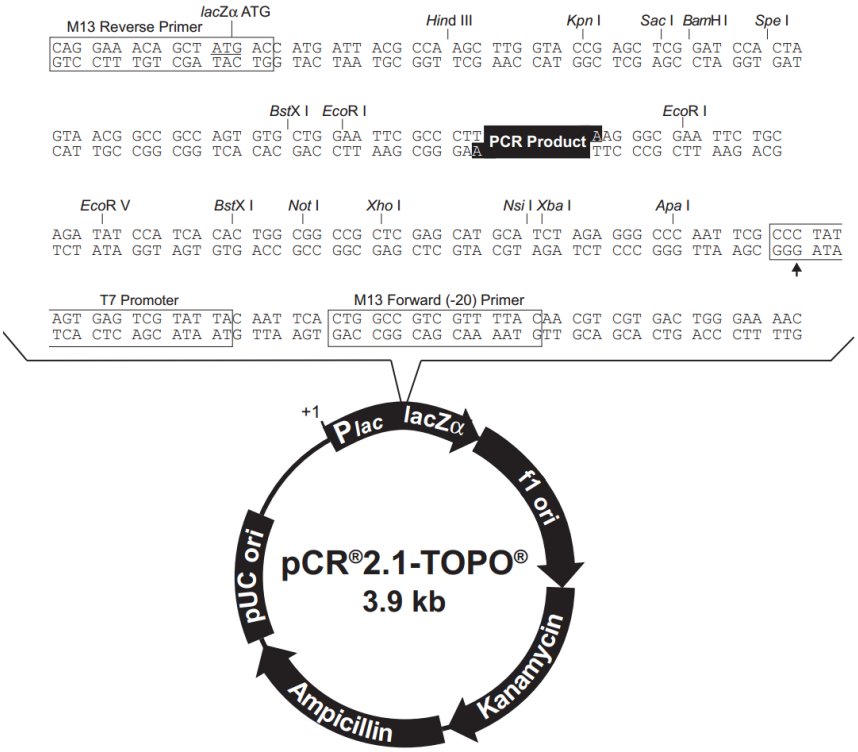

Fig. 2.34. Map of the pCR®2.1-TOPO vector. The PCR product has been placed in the multiple cloning site. The vector specific primers (M13 Forward and M13 Reverse) are shown.

Through this screening, three classes of FEHs were identified. Within the class 1 we can distinguish two different isoforms: isoform a (wFEH14) that correspond to the already described 6-KEH1 (BAD99104) and isoform b (wFEH18) that shows a very high similarity respect to the 6-KEH2 (BAD99105) (Fig. 2.35). However, in the wFEH18 cDNA a very interesting Y instead of a C was found in the EC motif that is not present in the 6-KEH (BAD99105). Within the class 3, the already characterized 1-FEHw1 (Q84PN8), 1-FEHw2 (Q84LA1) and 1-FEHw3 (CAD92365) were found (Fig. 2.35). Finally, clones having sequences not related to FEHs already described in wheat belong to the class 2 (Fig. 2.35).

Blue boxes in figure 2.35 indicate interesting residues characterizing the partial FEHs belonging to the class 2 (Fig. 2.35).

Obviously more studies will be necessary to obtain the full-lenght cDNA sequence of the selected clones and to proceed with the protein heterologous expression in *P. pastoris*. Indeed, we aim to understand if the sequences included in this class encode for enzymes whose activities are already described in wheat or not.

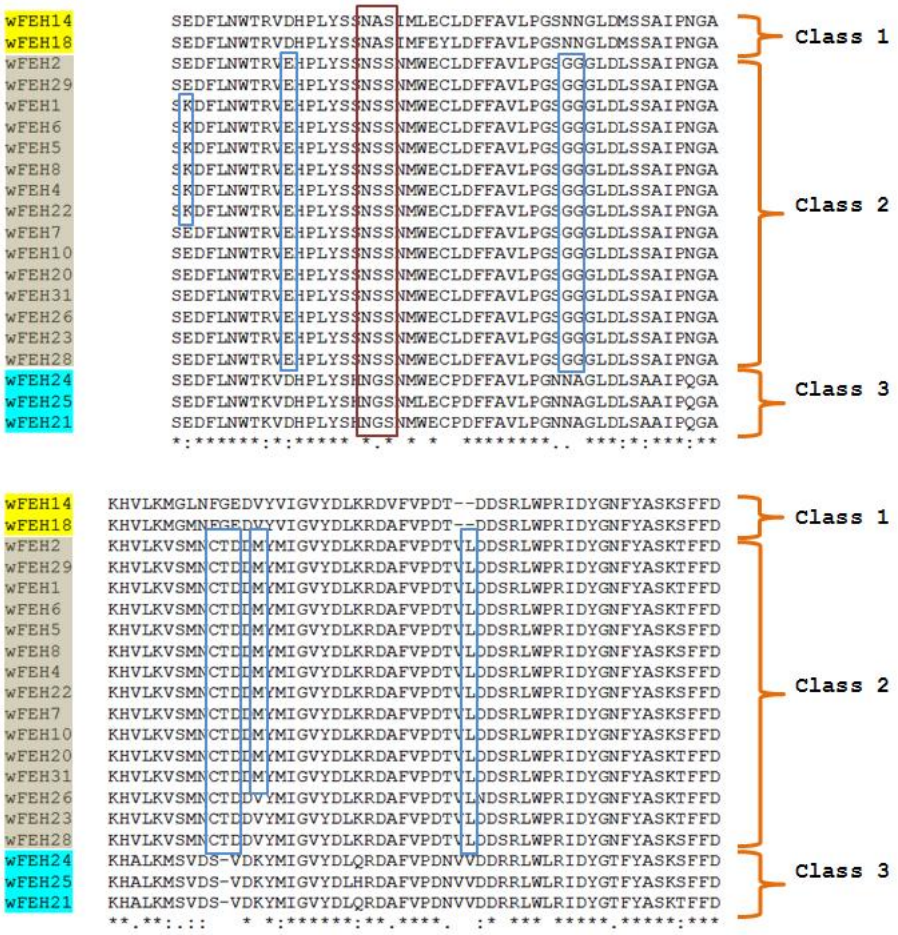

Fig. 2.35. Multiple alignment of the deduced amino acid sequences of partial FEHs cDNA obtained by amplification using wFEH F/R degenerate primers. Brown box highlights a putative glycosylation site. Blue boxes highlight interesting residues characterizing the FEH clones belonging to the class 2.

Future perspectives

Wheat accumulates a mixed type of fructan with β(2,1) and β(2,6)-linked fructosyl units, called graminan, characterized by a DP around 3 to 20 (Yoshida *et al.*, 2007). Several clones of wheat FT, able to cover the main types of fructan synthetic enzymes, have been cloned by Kawakami and Yoshida: 1-SST (Kawakami and Yoshida, 2002), 6-SFT (Kawakami and Yoshida, 2002) and 1-FFT (Kawakami and Yoshida, 2005). In relation to the enzymes responsible for fructan breakdown, several wheat FEHs have been purified and functionally characterized: 1-FEH w1 and 1-FEH w2 (Van den Ende *et al.*, 2003a), 1-FEH w3 (Van Riet *et al.*, 2008), 6-KEH1 and 6-KEH2 (Van den Ende *et al.*, 2005), 6-FEH (Van Riet *et al.*, 2006) and 6&1-FEH (Kawakami *et al.*, 2005). However, in order to improve the knowledge on fructan metabolism in wheat and to fill the gap of FEH genes encoding for enzymes that have not yet been reported yet, it is necessary a more in deep analysis of gene-expression systems. Here we presented a screening of a gene expression library made from *T. aestivum* kernels at late milky stage aimed at finding FEHs not yet described in wheat. It is known that during the milky stage an appreciable sugar increase takes place in the endosperm; while, after that phase, a decrease in the sugar content occurs. The screening of a cDNA library, made from *T. aestivum* kernels at late milky stage, has given us the opportunity to analyze the gene expression of several FEHs involved in the breakdown of fructans previously accumulated. This analysis identified an interesting class of FEHs. The cloning and the functional characterization of the clones belonging to this class (a work still in progress) will contribute to figure out if they have enzymatic activity not yet described in literature or if they are an isoform of already known enzymes.

Sara Cimini

2.3.7 Evolutionary and structural analysis of fructan metabolism enzymes

Phylogenetic analysis of invertases and of enzymes of fructan metabolism

Search for INVs, FTs and FEHs known sequences in plants found 60 sequences. The multiple sequence alignment was used to calculate an unrooted phylogenetic tree of INVs (CW-INV; V-INV; N-INV), FTs and FEHs (Fig. 2.36).

The bootstrap analysis provides indications in support of robustness of the tree generated since this analysis provides assessments of confidence for each clade of an observed tree, based on the proportion of bootstrap trees showing that same clade (Efron, 1996). Values between 700 and 1000 provide indications in support of validity of the tree.

Supporting what has been previously demonstrated by Vijin and Smeekens (1999), in this phylogenetic tree, two main groups were discerned, completely distinct and distant from each other: the first group contains CW-INVs and FEHs and the second group contains V-INVs and FTs. Moreover a third group containing only N-INVs can be identified.

This analysis also shows that the sequence identity of FEHs is higher for CW-INVs (45-52%) while it is lower with V-INVs (36-39%) and with FTs (33-36%). Similarly, FTs have a higher sequence identity with V-INVs (48-57%) and lower with CW-INVs (37-39%). Additionally, two subgroups have been further identified within each group. One subgroup, circled in green, contains sequences of monocots and the other subgroup, circled in blue, contains sequences of dicots. The ability of correctly grouping the sequences in the two classes of angiosperm further validated our analysis approach.

Fig. 2.36. Unrooted phylogenetic tree of protein sequences of some INVs, FTs and FEHs. Their respective accession numbers are: *Allium cepa* Ac.1-SST CAA06838 Ac.6G-FFT CAA69170 Ac.V-INV CAA06839; *Asparagus officinalis* Ao.V-INV AAB71136; *Aegilops tauschii* At.1-FFT ACL14897; *Campanula rapunculoides* Cr1.1-FEH CAD49079; *Chenopodium rubrum* Cr2.CW-INV CAA57389; *Cichorium intybus* Ci.1-FEH1 CAC19366 Ci.1-FEH2a CAC37922 Ci.1-FEH2b CAC37923 Ci.1-FFT AAD00558 Ci.1-SST AAB58909 Ci.V-INV CAC12104: *Cynara scolymus* Cs.1-FFT CAA04120 Cs.1-SST CAA70855; *Daucus carota* Dc.CW-INV AAA03516 Dc.V-INV CAA53098 Dc.N-INV CAA76145; *Festuca arundinacea* Fa.1-SST CAC05261; *Helianthus tuberosus* Ht.1-FFT CAA08811; *Hordeum vulgare* Hv.1-SST CAD98793 Hv.6-SFT CAA58235 Hv.CW-INV CAD58960; *Lolium perenne* Lp.1-FEH AAY81958 Lp.1-SST AAO86693 Lp6-FT AAM14603 Lp.6G-FFT BAF99808 Lp.N-INV CAM32308; *Lolium temulentum* Lt.N-INV CAA05869; *Nicotiana tabacum* Nt.CW-INV CAA57428 Nt.V-INV CAC83577; *Oryza sativa* Os.CW-INV AAT84401 OsN-INV NP_001047012; *Pisum sativum* Ps1.CW-INV AAC17166; *Poa secunda* Ps2.6-SFT AAG36767; *Solanum lycopersicum* Sl.CW-INV1 Q8LRN7 Sl.CW-INV2 CAB85896; *Solanum tuberosum* St.CW-INV Q9M4K8 St.V-INV ADM47340; *Triticum aestivum* Ta.1-FEH CAD48199 Ta.6&1-FEH BAE44509 Ta.6-FEH CAJ28591 Ta.6-KEH 1

Sara Cimini

BAD99104 Ta.6-KEH 2 BAD99105 Ta.1-FFT BAE19751 Ta.1-SST BAB82470 Ta.6-SFT BAB82469 Ta.CW-INV AAC96065 Ta.V-INV CAG25609; *Triticum monococcum* Tm.V-INV AAS88729; *Vicia faba* Vf.CW-INV1 CAA84526 Vf.CW-INV2 CAA84527 Vf.V-INV CAA89992; *Vitis vinifera* Vv.V-INV AAB47171 Vv.N-INV ABS52644; *Zea mays* Zm.CW-INV AAD02511 Zm.N-INV ACF84899. The numbers of bootstrap analysis are indicated on branches (1000 replicates).

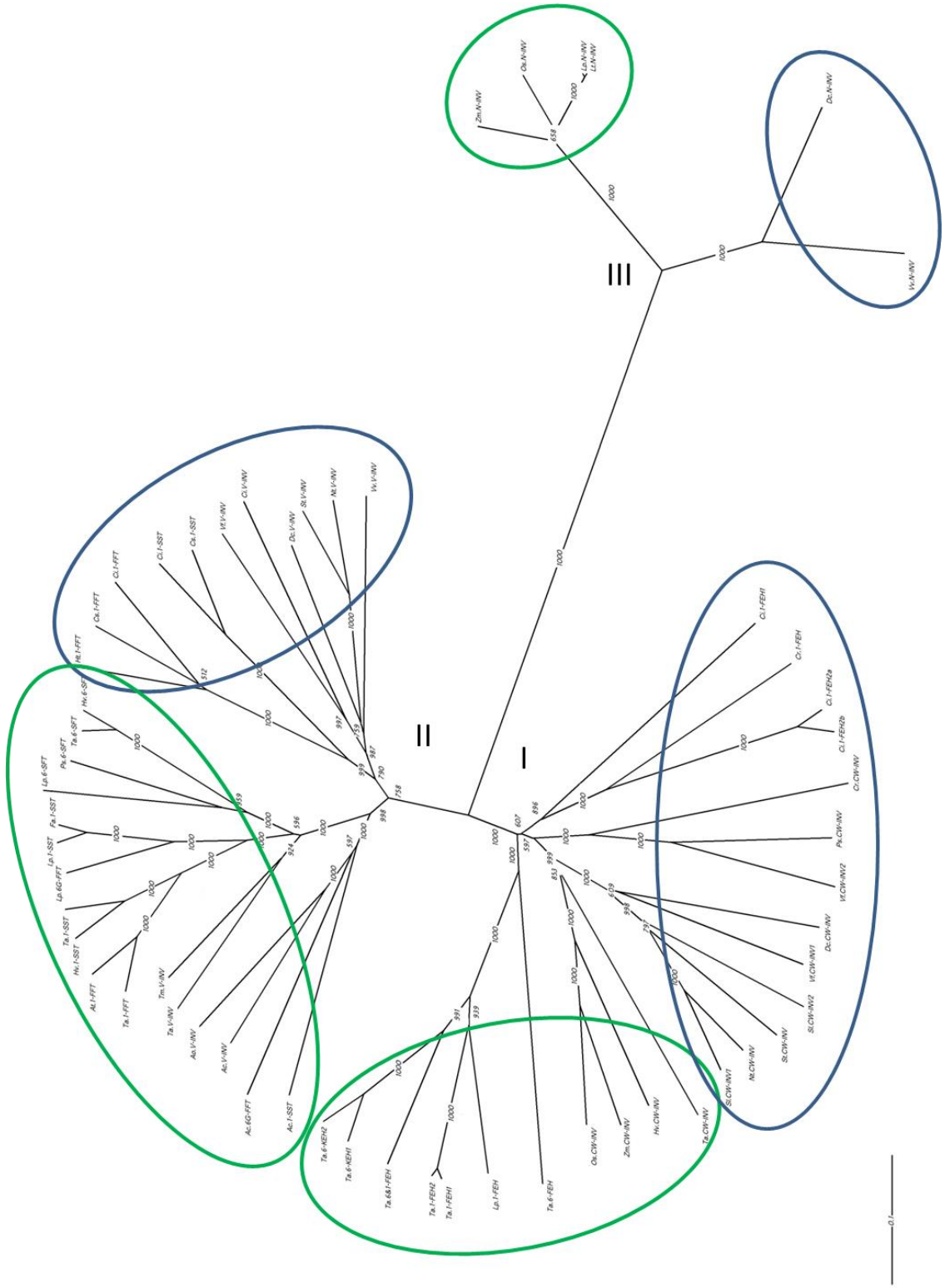

Structural analysis of fructosyltransferase

Recently, the three-dimensional protein structure of the first FT has been solved (Chuankhayan *et al.*, 2010). The solved FT is from the fungus *Aspergillus japonicus* (AjFT; 3LF7 pdb ID). This makes possible to compare this experimentally solved structure with those predicted for plant FTs having different substrate and reaction specificity. For this purpose, three-dimensional models of 1-FFT (1-FFT, accession number BAE19751) and 6-SFT (6-SFT, accession number BAB82469) from *T. aestivum* (Ta1-FFT and Ta6-SFT, respectively), chosen as model of plant FTs, were constructed. The structure of *Arabidopsis thaliana* CW-INV (AtCW-INV, accession number NP_566464) that shares a sequence identity percentage of 38% with Ta1-FFT and of 39% with Ta6-SFT, was used as template for homology modeling. FTs and CW-INVs share a sequence identity much higher than that between plant FTs and AjFT, which is of 18-20%.

```
Ta6-SFT|BAB82469.1          TASAMVVV--VVGATLLAG--------FRVDQAVDEEAAG------GFPW 71
Ta1-FFT|BAE19751.1          AVGALVVAAAVFGASRVDRDAVASSVPATAEHGVLEKASGPYSASGGFPW 100
AtCW-INV|NP_566464.1        NIGLWLLLTLLIGNYVVNL---------EASHHVYKRLTQS-----TNTK 43

Ta6-SFT|BAB82469.1          SNEMLQWQRSGYHFQTAKNYMSDPNGLMYYRGWYHMFFQYNPVGTDWDDG 121
Ta1-FFT|BAE19751.1          SNAMLQWQRTGYHFQPEKNYQNDPNGPVYYKGWYHFFYQHNPGGTGWGN- 149
AtCW-INV|NP_566464.1        SPSVNQPYRTGFHFQPPKNWMNDPNGPMIYKGIYHLFYQWNPKGAVWGN- 92

Ta6-SFT|BAB82469.1          MEWGHAVSRNLVQWRTLPIAMVADQWYDILGVLSGSMTVLPNGTVIMIYT 171
Ta1-FFT|BAE19751.1          ISWGHAVSRDMVHWRHLPLAMVPEHWYDIEGVLTGSITVLPDSRVILLYT 199
AtCW-INV|NP_566464.1        IVWAHSTSTDLINWDPHPPAIFPSAPFDINGCWSGSATILPNGKPVILYT 142

Ta6-SFT|BAB82469.1          GATNASAVEVQCIATPADPTDPLLRRWTKHPANPVIWS--PPGVGTKDFR 219
Ta1-FFT|BAE19751.1          GNT-ETFAQVTCLAEAADPSDPLLREWVKHPANPVVYP--PPGIGMKDYR 246
AtCW-INV|NP_566464.1        GID-PKNQQVQNIAEPKNLSDPYLREWKKSPLNPLMAPDAVNGINASSFR 191

Ta6-SFT|BAB82469.1          DPMTAWYDESDDTWRTLLGSKDDNNGHHDGIAMMYKTKDFLNYELIPGIL 269
Ta1-FFT|BAE19751.1          DPTTAWFDNSDNTWRIIIGSKNDTD--HSGIVFTYKTKDFVSYEMIPGYL 294
AtCW-INV|NP_566464.1        DPTTAWLGQ-DKKWRVIIGSKIHRR----GLAITYTSKDFLKWEKSPEPL 236

Ta6-SFT|BAB82469.1          HR-VERTGEWECIDFYPVG-----RRTSDNSS----EMLHVLKASMDDER 309
Ta1-FFT|BAE19751.1          YRGPAGTGMYECIDLYAVGGG---RKASDMYNSTAKDVLYVLKESSDDDR 341
AtCW-INV|NP_566464.1        HY-DDGSGMWECPDFFPVTRFGSNGVETSSFGEPNEILKHVLKISLDDTK 285

Ta6-SFT|BAB82469.1          HDYYSLGTYDSAANRWTPIDPELDLGIGLRYDWGKFYASTSFYDPAKKRR 359
Ta1-FFT|BAE19751.1          RDYYALGRFDAAANTWTPIDTEQELGVALRYDYGRYYASKSFYDPVKQRR 391
AtCW-INV|NP_566464.1        HDYYTIGTYDRVKDKFVPDNGFKMDGTAPRYDYGKYYASKTFFDSAKNRR 335

Ta6-SFT|BAB82469.1          VLMGYVGEVDSKRADVVKGWASIQSVPRTIALDEKTRTNLLLWPVEEIET 409
Ta1-FFT|BAE19751.1          IVWGYVVETDSWSADAAKGWANLQSIPRTVELDEKTRTNLIQWPVEELDT 441
AtCW-INV|NP_566464.1        ILWGWTNESSSVEDDVEKGWSGIQTIPRKIWLDRSGKQ-LIQWPVREVER 384
```

Fig. 2.37. Multiple sequence aligment of the AtCW-INV sequence (NP_566464) and of the two *T. aestivum* FTs sequences whose three-dimensional structure has been predicted (Ta1-FFT, BAE19751; Ta6-SFT, BAB82469). The alleged beginning of the mature FTs is indicated in blue. In yellow are indicated the conserved motifs containing the catalytic triad residues (displayed in bold). In green are displays other conserved motifs containing residues (displayed in bold) that can create an appropriate environment for the binding of the substrate at -1 and +1 subsites.

Sara Cimini

In figure 2.37 is shown the multiple sequence alignment between the AtCW-INV sequence and the sequences of the two plant FTs whose three-dimensional structure has been predicted. The plant FTs mature protein was estimated to start at the FPWSNEM motif (Fig. 2.37; Balk and Boer, 1999). The residues upstream of the FPWSNAM motif are considered more susceptible to evolutionary change since they are not part of the mature protein.

Fig. 2.38. Ribbon model of the predicted three-dimensional structure of 1-FFT protein from *T. aestivum*.

The three-dimensional protein models, built by SWISS-MODEL, were analyzed and compared to the structure of AjFT by the molecular graphics program PyMOL (http://pymolsourceforge.net). As for all enzymes belonging to clan GH-J, both in the structure of AjFT and in three-dimensional models of plant FTs, the presence of two domains is clearly identifiable: a larger domain, corresponding to the β-propeller domain, characterized by five repeated structural units radially arranged around a central axis; a smaller domain, corresponding to the β-sandwich domain, located at the C-terminal side (Fig. 2.38). The active site is located within the β-propeller domain. According to the -n to +n subsite nomenclature proposed by Davies *et al.* (1997) the hydrolysis of substrate takes place between the -1 and +1 subsite.
As shown in figure 2.39, the -1 subsite is highly conserved between fungi and plant FTs.

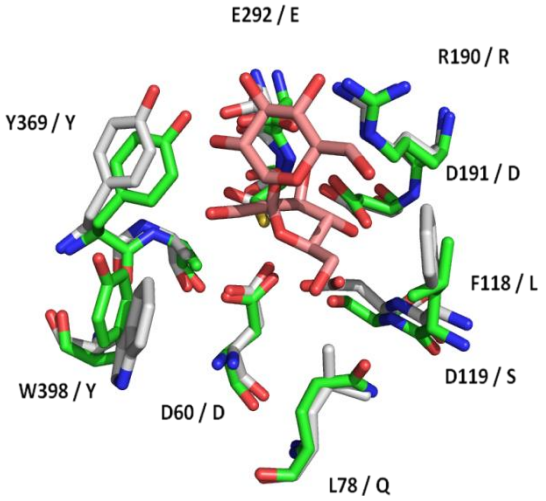

Fig. 2.39. A close view of the superposition of the -1 subsite in the active site of plant and fungal FTs. AjFT is displayed in white, while Ta6-SFT is displayed in green. Ta1-FFT is not shown for simplicity. A sucrose molecule (pink) is shown at the substrate binding pocket. The figure was prepared using PYMOL (http://pymolsourceforge.net). Labels indicate residues involved in the interaction and stabilization of the substrate at -1 subsite.

In AjFT, Asp191, Asp60 and Glu292 are the residues involved in the interaction and stabilization of the substrate at -1 subsite. These residues are conserved both in Ta 6-SFT and in Ta 1-FFT (Fig. 2.37 and Fig 2.39). Additional residues in AjFT that can help to create the appropriate environment for the binding of substrate at this subsite are Asp119, Phe118, Leu78, Trp398, Tyr369 and Arg190 (Chuankhayan *et al.*, 2010). As previously mentioned, these residues appeared to be conserved both in Ta6-SFT and in Ta1-FFT, except in the case of the Trp mutated in Tyr, the other observed mutations are conservative mutations.

Much relevant differences were observed at the +1 subsite. In AjFT structure, the residues involved in the interaction with the substrate at the +1 subsite, were located in two extended loops placed in the blade II and IV of the β-propeller. In plant FTs, the corresponding loops had smaller size than in AjFT. As shown in figure 2.40, the comparison of the molecular surface of AjFT and plant FTs has indicated an important difference in the shape and size of the substrate binding pocket determined by the different extensions of these loops. The differences of the shape and size of these loops made the active-site pocket of AjFT much deeper and narrower than that of plant FTs.

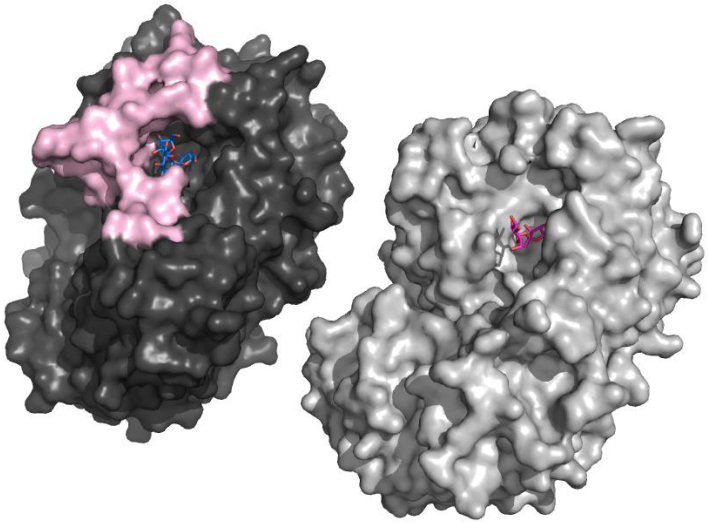

Fig. 2.40. Molecular surface of AjFT (dark grey) and of Ta6-SFT (light grey). In AjFT structure, the two loops placed in the blade II and IV of the β-propeller were colored in pink. Both enzymes are represented in complex with sucrose. The figure was prepared using PYMOL (http://pymolsourceforge.net).

For this reason, in order to define the residues constituting the +1 subsite in plant FTs, a comparative analysis with the known structure of AtCW-INV was carried out. In AtCW-INV structure, the residues involved in the interaction and stabilization of the substrate at the +1 subsite, are Asp240, Arg148, Trp82, Trp47 and Lys242 (Fig. 2.41).

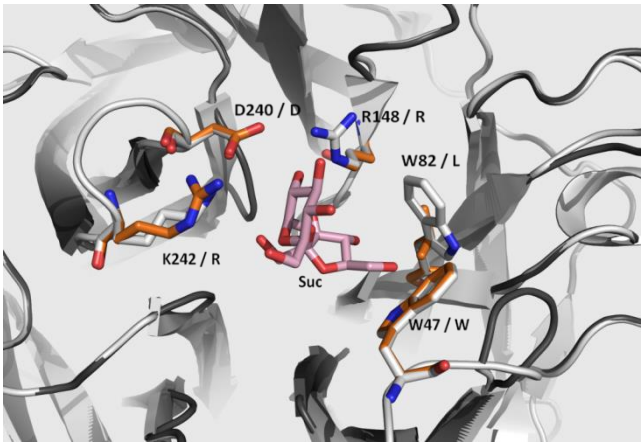

Fig. 2.41 A close view of the superposition of the +1 subsites in the active site of plant FT and of AtCW-INV. AtCW-INV side chains are displayed in white; Ta6-SFT side chains are in orange. A sucrose molecule (pink) is shown at the substrate binding pocket. The figure was prepared using PYMOL (http://pymolsourceforge.net). Labels indicate the residues involved in the interaction and stabilization of the substrate at the +1 subsite in AtCW-INV.

In the two protein model analyzed, these residues are highly conserved with the exception of Trp82 that is mutated to Leu in both the enzymes (Fig. 2.37 and Fig. 2.41). This Trp residue is always present in INV but it is mutated in the FTs analyzed.

A comparative analysis of 3D models of Ta1-FFT and Ta6-SFT was conducted in order to identify structural features potentially responsible for the different reaction specificity of these enzymes. This analysis revealed a marked sequence and structure similarity between the two FTs analyzed. A significantly different region possibly related to the reaction specificity is represented by a loop connecting the second and the third β strand of blade I (Fig. 2.42A). This loop has different amino acid composition and different size in Ta1-FFT and in Ta6-SFT. In particular, this loop in Ta1-FFT is shorter, less negatively charged and more flexible than in Ta6-SFT, which is longer, characterized by a higher content of negatively charged residues and fewer content of Gly. The characteristics of this loop, observed in Ta1-FFT and Ta6-SFT, recur in any other plant 1-FFT and 6-SFT analyzed (Fig. 2.42B).

The importance of this loop in determining reaction specificity is suggested by its position in the tridimensional structure. Indeed, in both analyzed plant FTs, it is positioned in the region flanking the cleft at the interface between the two domains near the pocket-shaped active site of the propeller domain (Fig. 2.43).

Sara Cimini

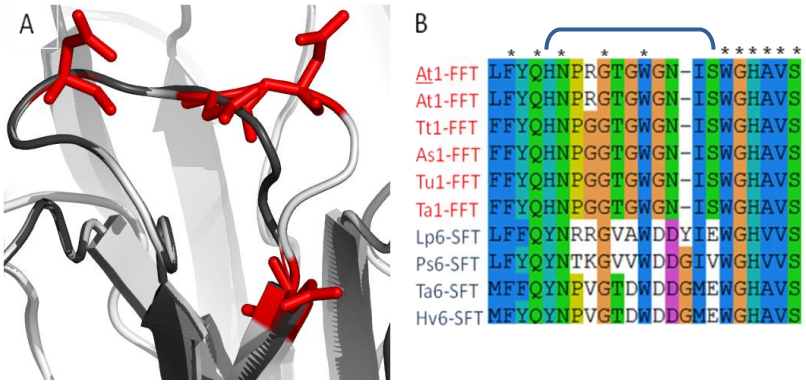

Fig. 2.42. (A) Details of the loop connecting the second and the third β strand of blade I. Ta6-SFT is displayed in white, while Ta1-FFT in gray. The negatively charged amino acids are in red. The figure was prepared using PYMOL (http://pymolsourceforge.net).
(B) Portion of the multiple alignment of a selection of plant 1-FFT and 6-SFT sequences. The residues encompassing the loop connecting the second and third β strand of blade I, are indicated with the parenthesis. At, *Arabidopsis thaliana*; At, *Aegilops tauschii*; Tt *Triticum turgidum*; As, *Aegilops saersii*; Tu, *Triticum urartu*; Ta, *Triticum aestivum*; Lp, *Lolium perenne*; Ps, *Poa secunda*; Hv, *Hordeum vulgare*.

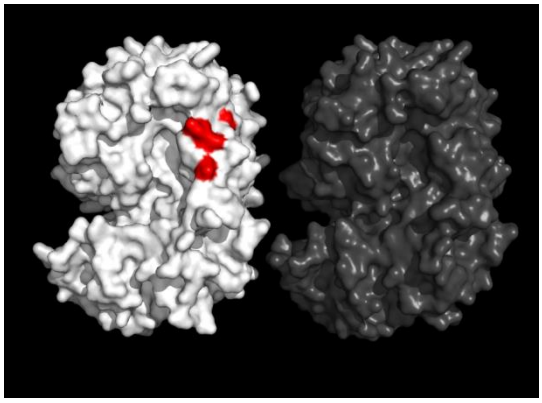

Fig. 2.43. The comparison of the molecular surface of 6-SFT (white) and 1-FFT (gray) of *T. aestivum*. The negatively charged residues are colored in red. The figure was prepared using PYMOL (http://pymolsourceforge.net).

2.4 DISCUSSION

2.4.1 Characterization of the antioxidant capacity during durum wheat kernel maturation

The early phases of kernel development, during which embryos are formed and the storage of carbohydrates, proteins and lipids takes place, are typically characterized by high metabolic activities. During these phases a central role is played by ROS-regulating systems aimed to maintain cellular ROS homeostasis. The relevance of these systems decreases during the following dehydration phase which usually start from 21 DAA (De Gara *et al.*, 2003a). It is known that APX and CAT are very active in immature wheat kernels; whereas, maure dehydrated kernels do not contain APX even if they maintain a certain CAT activity (De Gara *et al.*, 2003a). Besides APX and CAT, the activities of other enzymes involved in ASC and GSH recycle, like AFRR, DHAR and GR, are regulated during kernel development and germination (De Gara *et al.*, 2003a; Ishibashi *et al.*, 2008). The antioxidant metabolites ASC and GSH, the most abundant water-soluble antioxidants, play multiple functions in plant growth and development as well as in cellular defence mechanisms (Foyer and Noctor, 2009). They serve not only for regulating the lifetime of ROS but also to participate in a wide range of other redox signaling and regulatory functions. *Arabidopsis* mutants, characterized by low ASC levels, present slow growth and late flowering phenotypes (Dowdle *et al.*, 2007). Changes in the ASC and GSH metabolism also occur in seed development and germination processes (Tommasi *et al.*, 2001; De Gara *et al.*, 2003a). During kernel development, ASC and GSH levels are tightly regulated: these redox metabolites are very important especially in the growth processes occurring early in kernel development. Moreover, while mature wheat kernels retain GSH, they are depleted in ASC as already reported in literature (De Gara *et al.*, 2003a; Merendino *et al.*, 2006). Consistently, we observed higher levels of ASC and GSH at the beginning of kernel maturation (until 21 DAA) and then the ASC levels drastically declined until almost zero at the end of kernel maturation while the GSH levels only decreased by 35% from 7 to 52 DAA. The observed changes in the ASC and GSH levels have been proposed to be necessary for the transition into the different developmental phases of seed development as well as activation of programmed cell death in the endosperm (Arrigoni *et al.*, 1992; De Gara *et al.*, 2003a; Paradiso *et al.*, 2012).

Sara Cimini

Other molecules accumulated in wheat kernels and known to be involved in the regulation of seed and embryo developmental processes by promoting cell division, expansion and starch synthesis are soluble sugars, especially Glc Fru and Suc (Gibson, 2005). Consistently, the expression of a significant number of plant genes is altered in response to sugar levels. Many of the genes that are under sugar control are involved in defense responses against several stresses, like chilling, herbicide injury or pathogen attack during which changes in redox balance occurs. High level of atrazine tolerance to *Arabidopsis* seedlings is associated with sucrose and glucose treatment (Sulmon *et al.*, 2004). Tolerance to anoxia in *Arabidopsis* seedling is found following treatment with sucrose (Loreti *et al.*, 2005). Thus soluble sugars can act directly affecting gene expression through sugar-specific signaling pathways and indirectly playing a regulation in association with redox, ROS, light and stress signals (Gibson, 2005; Couée *et al.*, 2006; Nagao *et al.*, 2006). The analysis of mono- and di-saccharides content performed in our experimental conditions revealed that their concentration was higher in the first two weeks from anthesis, after this stage a very low content of mono- and di-saccharides has been detected. Interestingly, the behavior of mono- and di-saccharides mirrors that of ASC content. This is consistent with the role of soluble sugars in plants and with the metabolic activities usually characterising cell division and grain filling phases of kernel development. Contrary to what we observed for Glc and Fru, Suc was still present in dry kernels. The presence of Suc could be probably related with the induction of desiccation tolerance occurring during seed maturation and starting from 21 DAA in wheat kernels since this processes has been reported to involve carbohydrates in particular oligosaccharides (Buitink *et al.*, 2000, Black *et al.*, 1999).

In addition, other important water-soluble carbohydrates derived from sucrose, called fructans, are recognized not only as source of carbon and energy, but also as compounds involved in several regulatory functions at both the cellular and whole-organism level by controlling cellular metabolism, plant growth and development as well as resistance against different stresses (Valluru and Van den Ende, 2008).

At this purpose, the variation in fructan content has been studied during durum wheat kernel maturation.

As already reported (De Gara *et al.*, 2003a; Merendino *et al.*, 2006; Paradiso *et al.*, 2008), total fructan content was at highest levels at early stage of maturation and then declined with the progression of the state of maturation of durum wheat kernels. In our experimental

Sara Cimini

condition at 21 DAA a very small amount of fructans was detectable. With the progression of kernel development, a decrease of fructan content could be correlated with the synthesis of starch. Moreover, since other metabolites are stored in kernel tissues after 21DAA it is probable that the carbonyl units of fructans are used in several biosynthetic pathways. It is also possible that fructan hydrolysis, occurring at milky stage (14 DAA), can contribute to the reduction of the water potential, favoring cell expansion.

Recent *in vitro* studies suggest that fructans have antioxidant properties (Stoyanova *et al.*, 2011). Accordingly, fructans may contribute to the determination of the hydrophilic antioxidant activity with ASC and GSH. Consistently, hydrophilic antioxidant activity, as well as ASC and GSH levels, started to decline from 21 DAA.

Although hydrophilic antioxidant activity decreased during kernel maturation, total antioxidant activity did not significantly change. This was due to an increase in the lipophilic antioxidant activity found between 14 and 21 DAA.

Recently it was suggested that polyphenols are the biggest contributor to the antioxidant properties of wheat (Zuchowski *et al.*, 2011). These molecules can contribute to the overall mechanism of cellular ROS homeostasis influencing the lipophilic antioxidant activity. Indeed, polyphenol content, as well as lipophilic antioxidant activity, increased with the progression of kernel maturation, contrary to what found for hydrophilic antioxidant activity.

2.4.2 Characterization of fructan metabolism during durum wheat kernel maturation

High resolution HPAEC-PAD 'fingerprint' of fructans contained in durum wheat kernels revealed that total fructan content is not the only interesting parameter describing fructan metabolism during kernel maturation. Different types of fructans have been detected at different stages, revealing the presence of different FTs and FEHs activities.

Graminans-type fructans are typical of most plants belonging to the *Poaceae* family, such as wheat (Bancal *et al.*, 1992; Yoshida *et al.*, 2007). However, the structure of fructans in wheat is still unknown. A relative high amount of Bif was found at 7 DAA. Then Bif significantly decreased with the progression of kernel development until a very low level at 35 DAA. Early in the maturation (7 DAA), the presence also of 1-K, 6-K, 1,1-Nys and other unknown fructans with higher DP were detected. 1-K levels, although decrease during maturation, were

Sara Cimini

found to remain at relative higher levels compare to the other fructans till the end of kernel maturation. While the other fructans abovementioned had maximum concentrations at 7 DAA, n-K had highest level at 14 DAA and it maintained this level until 28 DAA and slightly decreased afterwards. The trisaccharides 1-K and n-K had still detectable levels in completely dry kernel.

This analysis suggested that fructan that have been synthetized during kernel maturation are continuously rearranged . In general, fructans with higher DP (such as Bif and 1,1-Nys) were found mainly in the first two weeks of kernels development and then fructans with lower DP were typically detected. It has been proposed that the partial degradation of longer DP fructans increases the number of molecules (fructose, sucrose, and lower DP fructans) having scavenging capacities and facing the increased oxidative stress under stress conditions (Van den Ende and Valluru, 2008).

Experiments performed on wheat kernels during maturation surprisingly shows that kernels are not only the site for fructan storage but also a site for their active synthesis, in particular at early maturation phases, when tissues are still photosynthetically active.

Fructan synthesis

Using different combinations of donor and acceptor substrates, a screening of fructan synthesis and degradation reactions occurring during kernel maturation was performed. Accordingly with fructan content, we observed a higher FT and FEH activity at 7 DAA and then they progressively declined. The synthesis of the three kestoses, 1-K, 6-K and n-K, took place after incubation of the kernel protein extracts with Suc as single substrate. The synthesis of 1-K, the level of which was relative higher in comparison with the other oligofructans, was probably catalysed by the enzyme 1-SST (Kawakami and Yoshida, 2002). A much smaller amount of 6-K was formed compare to 1-K. This trisaccharides was probably produced by 6-SFT that transfer the fructosyl unit preferentially to a fructan molecule, but in its absence, it can also use Suc (Sprenger *et al.*, 1995). Alternatively, 6-K can be produced by sucrose:sucrose 6-fructosyltransferase (6-SST). Finally also n-K was detected at 7 DAA using Suc as single substrate. In these conditions, n-K can be produced by the enzyme 6G-FFT/1-FFT as reported by Lasseur *et al.* (2006). This enzyme activity is not yet described in wheat. A much higher level of n-K was produced by the same enzyme when the kernel protein extracts were incubated with a combination of Suc and 1-K, indicating that this enzyme

Sara Cimini

preferentially use 1-K as acceptor substrate. From total fructan analysis was evident that the maximum concentration of n-K, differently from the other fructans, was at 14 DAA instead of 7 DAA. A possible explanation, considering the activities found *in vitro*, is that n-K in wheat kernels is mainly produced by degradation of 6G&1-Nys by 1-FEH activity.

Using 1-K as single substrate the synthesis of higher oligofructans was observed, in particular 1,1-Nys and 6G&1-Nys. The 1,1-Nys was probably formed as an elongation of 1-K by the enzyme 1-FFT. The production of 1,1-Nys was much lower when Suc was included in the reaction mixture probably due to the inhibitory effect of Suc on 1-FFT activity (Van den Ende *et al.*, 1996).

Bif, the main sugar found in durum wheat kernel at 7 DAA, was formed after incubation of kernel protein extracts with a combination of 1-K and Suc. The maximum of Bif production was found at 14 DAA although the maximum Bif concentration occurred already after the first week from anthesis. It is possible that Bif accumulation occur later in time compare to the maximum activity at 7 DAA. The enzyme responsible for Bif synthesis is 6-SFT which use Suc as donor and 1-K as acceptor substrate by β(2,6) linkage formation.

The synthesis of 6G&1-Nys was observed after incubation of kernel protein extracts with 1-K as single substrate by the 6G-FFT enzyme activity. About the same 6G&1-Nys levels were produced, by the same enzyme, after incubation using both 1-K (donor substrate) and Suc (acceptor substrate). Higher 6G&1-Nys levels were obtained using combinations of n-K and 1-K or n-K together with Suc. In both cases, n-K is used as acceptor substrate. Enzyme purification will be needed to better elucidate the enzyme activity involved in the synthesis of 6G&1-Nys in durum wheat kernels.

The behaviour of the FT activities during kernel maturation revealed that with the exception of 6-SFT, a significant decrease was observed between 7 and 14 DAA. On the contrary, the maximum activity of 6-SFT, the principal enzyme involved in graminan synthesis, was at 14 DAA. This activity, seems regulated at transcriptional level during kernel maturation.

It is noteworthy that since invertase activity is very high early in kernel maturation it is not easy distinguish the activity of FTs from a side activity of INVs.

Sara Cimini

Fructan breakdown

The observed breakdown of 1-K into Suc and Fru, theoretically catalysed by 1-KEH activity, could be actually due to the invertase activity that is very high at the beginning of kernel maturation. Probably the same occur in the case of n-K breakdown into Bla. Consistently, as for FTs, the high invertase activity found at 7 DAA make very difficult distinguish between genuine FEH from invertase side activity. However, invertase activity strongly decreased starting from 7 DAA, while FEH activity declined slower maintaining relative higher levels at 14 DAA. Accordingly, the breakdown activity found later in kernel development was probably mainly correlated with FEHs instead of INVs.

The transcript levels of 1-FEH, one of the main enzymes involved in fructan breakdown, remained at relative higher levels during the first two weeks after anthesis and then they progressively declined until low but still detectable levels. The transcript levels of 6G&1-FEH, an important enzyme for branched and low DP graminan breakdown, transiently increased and then remained unchanged till the end of kernel maturation. In both cases, although no fructan degradation was found anymore in dry kernels, at 52 DAA transcripts coding for 1-FEH and 1&6-FEH were found. These observation suggest that these enzymes play an important role also in the period in which fructans are mainly synthesized and that, in this phase, a strict correlation exist between their enzyme activity and .gene expression. After this period we have observed a remarkable decrease in the activity of the enzymes that it is not correlated with a decrease in their gene expression, since their mRNA amount seem to be almost constant until the end of maturation period, thus suggesting that these enzymes are not regulated at transcriptional levels.

The high FEH activity observed when also fructan concentration and the FT activity is at maximum levels, could be explained considering the involvement of FEH enzyme in the 'elongation-trimming' pathway that implies the contribution of FEHs in fructan synthesis (Bancal *et al.*, 1992; Van den Ende *et al.*, 2003a).
This pathway has been proposed by Bancal *et al.* (1992) in order to explain the transition from β(2-1)-linked oligomers to those enriched in β(2-6)-linkages. They suggest that this transition could occur as result of selective trimming of β(2-1)-linked terminal fructosyl units from highly branched oligomers catalysed by FEHs.

Sara Cimini

2.4.3 Evolutionary and structural analysis of fructan metabolism enzymes

An evolutionary study centered on INVs, FTs and FEHs was conducted based on 60 sequences from different organisms. A phylogenetic bootstrap tree representing all INVs isoenzymes and all enzymes involved in fructan metabolism was built in order to highlight the evolutionary relationships between these enzymes. Consistently with the literature the phylogenetic analysis of INVs, FTs and FEHs showed that FTs are closely related to VIs whereas FEHs are closely related to CWIs. INVs with neutral pH are distant from these enzymes and constitute a separate group. Moreover, the evolution of FTs and of FEHs occurred after separation of monocots and dicots as already reported in literature (Wei and Chatterton, 2001; Ritsema et al., 2006; Altenbach et al., 2009).

After this phylogenetic study, a structural analysis of FTs was carried out. Several crystal structures of enzymes belonging to GH32 family have been resolved up to now (as reviewed by Lammens *et al.*, 2009). As regards plant GH32 crystal structures, only one INV and one FEH structures have been characterized in *Arabidopsis thaliana* and *Cicorium intybus* respectively (Verhaest *et al.*, 2005; Lammens *et al.*, 2008). The first FT structure has been recently obtained from the fungus *Aspergillus japonicas*. The availability of the structure of AjFT has shown the way forward to new and interesting studies concerning not only fungi, but also plant FTs. The sequence identity between plant and fungi FTs is low (18-20% sequence identity). For this reason a comparative analysis between the known structure of AjFT and the predicted structure of two plant FTs, which have different substrates and reaction specificity, was made for the first time. This analysis showed that fungi and plant FTs have significant structural differences although they belong to GH-J clan. These differences do not affect the -1 subsite, which is involved in the binding of donor substrate since it is well conserved between fungi and plants. On the other hand, clear differences are observed at the +1 subsite, since the residues involved in the definition of this subsite lie in completely different positions on the structure of the FTs analyzed. As a matter of fact, indeed, the AjFT is characterized by the presence of two loops much longer than those of plant FTs. In AjFT the residues of +1 subsite are positioned precisely at the level of these two loops. These loops are responsible for the shape of the sucrose binding pocket. The definition of the +1 subsite in the three-dimensional models was made by comparing the plant FTs with the structure of AtCW-INV. These proteins have a sequence identity (38-39%) higher than that between FTs and AjFT (18-20%). At this subsite the residues involved in the interaction with the substrate are highly conserved, except in the case of Trp82, which is always present

Sara Cimini

in INVs but is always mutated in FTs. Finally, from the comparison of the Ta1-FFT and Ta6-SFT models, it is possible to suggest that the differences in size and the amino acid composition of the loop connecting the second and the third β strand of blade I, are involved in the definition of the reaction specificity. In 6-SFT the size and the amino acid composition of this loop might favor the acceptor substrate orientation thus allowing the formation of β(2-6) linkage. On the contrary, in the case of 1-FFT, the acceptor substrate orientation favors the formation of β(2-1) linkage. Recently the 6-SST/6-SFT crystal structure, purified from *Pachysandra terminalis,* have been determined (Lammens *et al.*, 2012). This enzyme is responsible for the unexpected presence of graminan and levan-type fructans in the eudicot *P. terminalis* (Van den Ende *et al.*, 2011c). The availability of a plant FT structure will provide the possibility to better analyze differences between plant and fungal FT. Moreover it will facilitate the prediction of reliable 3D models of other plant FTs in order to further investigate about specific amino acids probably involved in the determination of the enzyme reaction specificity.

Sara

Chapter 3

Biotic stress and metabolic pathways triggered by Ophiobolin A

3.1 INTRODUCTION

3.1.1 Reactive oxygen species during biotic stress

A broad range of diseases caused by bacteria, viruses, fungi, invertebrates and even other plants occurs throughout the regions where Triticeae crops are produced. Every region is characterized by its own array of organisms specialized to utilize the host plant in that particular environment. Plants have evolved sophisticated resistance mechanisms carried on in order to defend themselves against pathogens attacks, among which physical barriers and several biochemical strategies are included. These mechanisms are such elaborated that only a small number of pathogens are able to provoke diseases in a single plant species (compatible response). On the contrary, the majority of phytopathogens are blocked by plant defenses (incompatible response) (De Gara *et al.*, 2003b). ROS signaling and impairment in the ROS-dependent pathways activated by plant pathogen cross-talk, seems to be pivotal in defining plant responses and, as a consequence, plant resistance against a certain pathogen attack. During incompatible response, ROS production occurs in a biphasic manner. A transient, very rapid and biologically non-specific ROS production usually takes place within minutes of the interaction with the pathogen. This is followed by a second, massive and prolonged burst of ROS production that occurs hours after pathogen attack and that is generally correlated with the onset of the defenses and hypersensitive response (HR) (Torres, 2010). The HR is aimed to potentially limit the spread of pathogens from the infection point, since it ends with a localized plant cell death, thus determining an inhospitable environment surrounding the invading pathogens. On the other hand, during compatible response only the first pick of ROS production takes place and the pathogen is able to penetrate and provoke plant disease (Baker and Orlandi, 1995). ROS production during plant-pathogen interactions is mainly apoplastic (Levine *et al.*, 1994) and NADPH oxidases as well as cell wall peroxidases are the main involved enzymatic mechanisms.

Plant NADPH oxidase, located in plasma membrane, is the main enzyme responsible for apoplastic oxidative burst and successful recognition of the pathogen (Torres *et al.*, 2006; Kobayashi *et al.*, 2006). This enzyme is analogous, but not identical, to that found in mammalian phagocytes (Bollwell *et al.*, 2002; De Gara *et al.*, 2003b; Kar, 2011) and it has been described in many plant species (Torres and Dangl, 2005). NADPH oxidase transfers reducing equivalents from cytosolic NADPH to extracellular oxygen, producing $O_2^{\bullet -}$. This

molecule is rapidly dismutated to H_2O_2 by the action of apoplastic SOD isoenzymes. Recently, the involvement of cell wall peroxidase to the apoplastic oxidative burst has been reported to occur in many plant-pathogen interactions (Bindschedler *et al.*, 2006; Choi *et al.*, 2007) but also other apoplastic copper amine oxidase, flavin polyamine oxidase, oxalate oxidase and lipoxygenase may be involved (De Gara *et al.*, 2003b). After pathogen recognition, ROS are produced not only in the apoplast. Chloroplasts, peroxisomes and mitochondria can be a source of ROS inside plant cell.

Alterations in ROS scavenging enzymes occur under biotic stress conditions as well as during abiotic stresses (Mittler, 2002; Gill and Tuteja, 2010; Torres, 2010). During plant-pathogen interactions, an increase of ROS production and a down-regulation of scavenging/antioxidant systems may contribute to cell response to virulent pathogen attack, resulting in ROS accumulation (Fig. 3.1; Mittler *et al.*, 2004; Pitzschke *et al.*, 2006). SOD, CAT, APX, and mitochondrial alternative oxidase as well as antioxidants like ASC and GSH contrast ROS accumulation. Literature data report that the regulation of these enzymes may occur at different levels: for example, CAT down-regulation is essentially carried out at transcriptional level (Dorey *et al.*, 1998), while APX regulation seems to involve both transcriptional and translational processes (Shigeoka *et al.*, 2002).
Therefore, as response to many pathogen infections, a down-regulation of ROS scavenging systems and alterations in the ASC-GSH redox state seem to play a central role in order to favor ROS accumulation (Klessig *et al.*, 2000; De Gara *et al.*, 2003b; Torres, 2010).

ROS can directly kill phytopathogens, particularly H_2O_2, $O_2^{\bullet -}$ and $OH^{\bullet}$. ROS could also counteract phytopathogens penetration and proliferation by surrounding them with an oxidative environment. Moreover, H_2O_2 hinder phytopathogenic penetration because it facilitates peroxidase reactions catalyzing intra- and inter-molecular cross-links between structural components of cell wall and lignin polymerization (Ros Barcelò, 1997; De Gara *et al.*, 2003b) delaying pathogen penetration. Lastly, due to the diffusible nature of H_2O_2, it can also acts as intracellular signal activating defense genes (Dynowski *et al.*, 2008) or interacting with other signal components like phosphorylation cascades (Kovtun *et al.*, 2000). ROS interact with other signaling molecules, especially salicylic acid (SA) and nitric oxide (NO), in order to activate plant responses to pathogen attack. It is known that SA concentration is correlated with the activation of systemic acquired resistance (SAR) and enhanced resistance

to pathogens (Yalpani *et al.*, 1991). Beside all the above, ROS have been recognized to orchestrate the HR as well as programmed cell death in several plants and model systems (Levine *et al.*, 1994; Mur *et al.*, 2008).

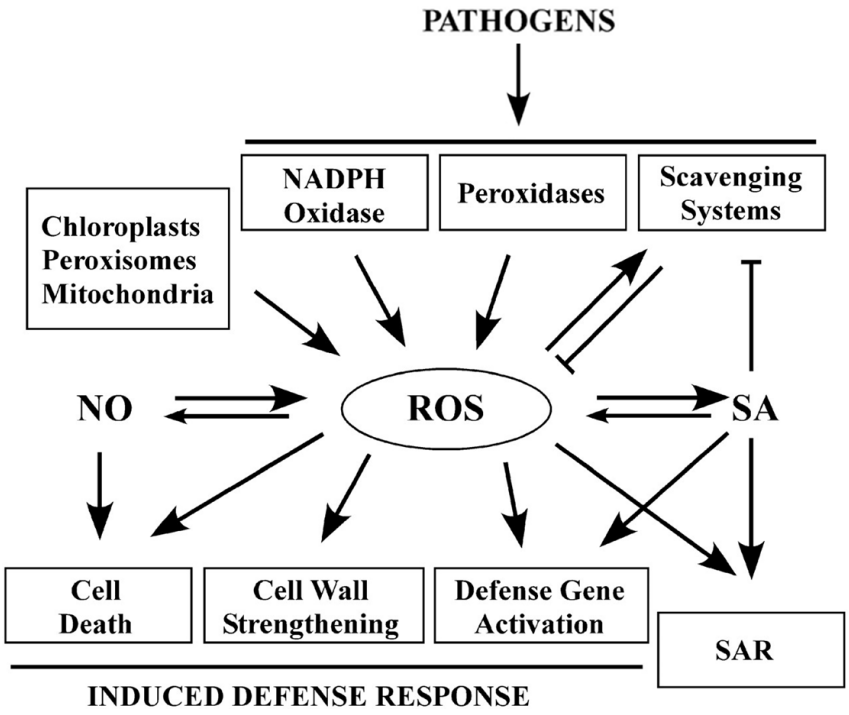

Fig 3.1. ROS production during plant-pathogen interactions. (From Torres *et al.*, 2006)

3.1.2 Ophiobolins

Diseases caused by fungal infections affect, every year, cereal crops productivity in many regions of the world. Phytopathogenic fungi, mainly of the genus *Bipolaris* as *Bipolaris oryzae*, *Bipolaris maydis* and *Bipolaris sorghicola*, are able to attack several crops, such as rice, maize and sorghum, by causing brown spot lesions on the leaves. These symptoms may be attributed to toxin secretion by the pathogen and diffusion in host tissues (Gayed, 1962). The phytotoxins produced by these fungiare secondary metabolites named ophiobolins and belonging to the family of sesterterpenoid compounds. Ophiobolin-

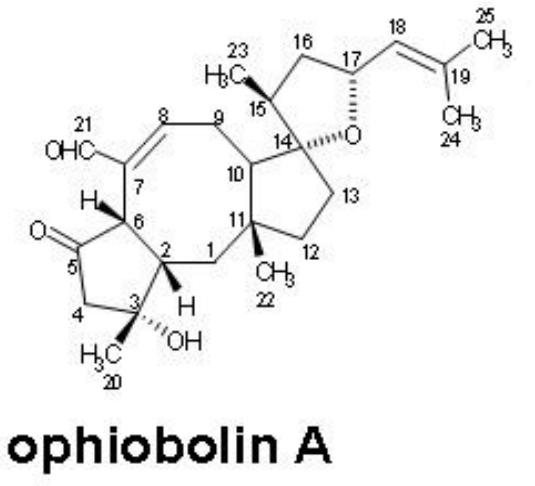

Fig. 3.2. Ophiobolin A structure.

producing terrestrial fungi mainly attack monocotyledons, but they can also attack various herbaceous dicotyledons species, although grass weeds have been proved to be more sensitive to the phytotoxins (Evidente *et al.*, 2006). The interest in *Bipolaris* ssp. and their bioactive metabolites derives from their previous implication in two devastating plant disease epidemics: the Bengal rice famine in India in 1943 and the Southern corn leaf blight epidemic in the USA in 1972 (Au *et al.*, 2000a).

The discovery of the sesterterpenoid ophiobolins (C25)filled the gap between diterpenes (C20), which have four isoprene units, and triterpenes (C30), which have six isoprene units (Au *et al.*, 2000a). Ophiobolin A (Fig. 3.2) was the first member of the group to be isolated and characterized in the mid-1960s (Canonica *et al.*, 1966a; Nozoe *et al.*, 1965). Currently, 25 biogenic analogs of ophiobolins have been identified and their structure determined. These include ophiobolin B from *B. oryzae* (Canonica *et al.*, 1966b), ophiobolin C from *B. zizaniae* (Nozoe *et al.*, 1966), ophiobolin D from *Cephalosporium caerulens* (Itai *et al.*, 1967; Nozoe *et al.*, 1967), and ophiobolin F from *B. maydis* (Nozoe *et al.*, 1968). Ophiobolins are not confined to the *Bipolaris* pathogenic fungi group, but in 1984 ophiobolins G and H were isolated from *Aspergillus ustus* (Culter *et al.*, 1984). Moreover marine-derived fungal ophiobolins were recently identified and demonstrated to inhibit the biofilm formation of *Mycobacterium* species (Arai *et al.*, 2012).

From a biosynthetic point of view, ophiobolins are characterized by a skeleton which is derived from a head-to-tail linkage of five isoprene units (Au *et al.*, 2000a). The 5-8-5 ring system skeleton gets up from cyclization of geranylfarnesyl pyrophosphate as confirmed by the $^{3}H/^{14}C$ ratio of ophiobolins and their derivatives (Au *et al.*, 2000a).

Ophiobolins are phytotoxins because they are thought to be involved in the development of the characteristic brown spot lesions on leaves and the physiological changes in infected plants induced by the application of drops of toxins on the plants (Sugawara *et al.*, 1987; Chattopadhyay and Sammaddar, 1980).

Ophiobolins can lead to plant death through multiple mechanisms of action, including inhibition of root and coleoptile growth in wheat and rice seedlings, inhibition of seed germination, changes in cell membrane permeability, stimulation of β-cyanin leakage, releases of electrolytes and glucose from the roots, and decreases in photosynthetic CO_2-fixation, the latter causing respiratory changes and enhancing stomatal opening (Au *et al.*, 2000a). Ophiobolin A seems also to inhibit protein and nucleic acid synthesis or to act as an inhibitor

Sara Cimini

of β-1,3-glucan synthetase in plant cells (Au *et al.*, 2000a). However, the mode of action of ophiobolins leading to this disease syndrome still remains to be better elucidated.
According to Gianani *et al.* (1979) ophiobolin B might act as an inhibitor of proton extrusion, which, in turn, would impair other transport processes. Regarding ophiobolin A, it has been found that proton extrusion inhibition is due to an effect on the permeability of the plasma membrane to potassium (Cocucci *et al.*, 1983). The phytotoxin action of ophiobolin A may also be due to the disruption of the synthesis of the primary cell wall which involves the formation of the β-1,3 glucosyl linkage (Fukushima *et al.*, 1993).

An extensive area of research relating to the understanding of the pathogenic mechanisms of action of ophiobolin A concerns its interaction with calmodulin. Leung *et al.* (1984) demonstrated an interaction between ophiobolin and maize calmodulin *in vitro* and proposed that calmodulin was the target for the toxin in plant cells. Au *et al.*, (Au and Leung, 1998; Au *et al.*, 2000b) used directed mutagenesis to map the ophiobolin A inhibitory site in the bovine brain calmodulin: they found that lysine 75 is the inhibitory site, while lysines 77 and 148, which are both involved in binding calmodulin, are ineffective in interacting with ophiobolin A. In maize roots, the phytotoxic effects of ophiobolin A are well correlated with calmodulin inhibition: both effects are time dependent and irreversible, and the patterns of inhibition and phytotoxicity are the same for several analogues of ophiobolin A (Leung *et al.*, 1985). In addition, when maize roots are treated with ophiobolin A, a smaller amount of active calmodulin is present in the root extract, indicating a possible *in vivo* inhibition of calmodulin biosynthesis or increased turnover by ophiobolin A (Leung *et al.*, 1985).

The current work aims to characterize ophiobolin A-mediated effects on cell proliferation versus death features in plant cells. Tobacco Bright Yellow – 2 cells have been utilized, as model cell line, because its facilities of being used both in molecular/biochemical and cytological studies.

Sara

3.2 MATERIAL AND METHODS

3.2.1 Production, extraction, purification and physicochemical stability measurements for Ophiobolin A

In the laboratory of Prof. Evidente, Ophiobolin A production and extraction were done as well as physicochemical stability measurements. Ophiobolin A was isolated from the strain of *Drechslera gigantea* as described in Evidente *et al.* (2006). Ophiobolin A purity (> 95%) was determined by RP-HPLC-UV. Ophiobolin A stability in methanol and in the cell culture medium was investigated after incubation for 7 days at 37°C (Bury *et al.*, 2013).

For this work the Ophiobolin A dilutions were prepared dissolving Ophiobolin A in pure ethanol. The dilution was then added to the cell suspension using 0.45 µm sterile filters. The amount of ethanol never overcame 0.2% of the total volume.

3.2.2 Growth and cell culture

The suspension of tobacco (*Nicotiana tabacum* L. cv Bright-Yellow 2) cells, hereafter referred to as TBY-2 cells, was routinely propagated and cultured according to Nagata *et al.* (1992; 4,302g/l MS Basalt Salt (ICN Flow), 30g/l Sucrose, 0.1g/l Myo-inositol, 0.2g/l KH_2PO_4, 1mg/l Thiamine-HCl, 2mg/l 2,4-D, pH 5.8). The cells were subcultured to fresh medium every week and were incubated on a rotary shaker at 130 rpm, at 27°C, in darkness.
For the experiments, a stationary culture (cells at the end of the normal 7 days growth period) was diluted 4/100 (v/v) in fresh culture medium and cultured for 3 days.
Aliquots of control versus Ophiobolin A-treated cells were sub-cultured into fresh Ophiobolin A-free medium after 24h from the treatment in order to test the reversibility of Ophiobolin A-induced effects on TBY-2 cells. Aliquots of control and treated cells were washed three times with fresh medium by centrifugation at 250xg for 5 min at room temperature. The obtained pellets were re-suspended up to 4ml using fresh medium, added to 100ml of fresh medium and cultured as mentioned above.

At the indicated times, aliquots of cells were collected by vacuum filtration on Whatman 3MM paper for analyses.

Sara

3.2.3 Package Cell Volume and Optical Density

The Package Cell Volume (PCV), which corresponds to the ratio between the cell volume and the total suspension volume, was measured by collecting 2 ml aliquots of cell suspension and centrifuging them at 250xg for 6 min at room temperature without brake (Locato *et al.*, 2006).

Cell growth was also followed by measuring Optical Density (OD) at 600 nm (Pellny *et al.*, 2009). For high concentrations, cells were diluted 1 in 4 in phosphate-buffered saline buffer.

3.2.4 Nuclear Morphology and Mitotic Index

To observe nuclear morphology TBY-2 cells were stained by Hoechst 33258 dye, as reported in Houot *et al.* (2001), and visualized using a fluorescence microscope (Leica, Wetzlar, Germany) with an excitation filter of 340 to 380 nm and a barrier filter of 410 nm.

The mitotic index is calculated as the percentage of the ratio between dividing cells and the number of cells scored. For each analysed time at least three hundred cells were observed. The number of dividing cells is determined by Hoechst 33258 staining.

3.2.5 Glutathione and ascorbate extraction

The cells were homogenized with two volumes of cold 5% meta-phosphoric acid at 4°C in a porcelain mortar. The homogenate was centrifuged at 20,000 g for 15 min at 4°C, and the supernatant was collected for analysis of ascorbate and glutathione content. The glutathione pool was assayed according to Zhang and Kirkham (1996) as previously described (2.2.2 paragraph). ASC and DHA were measured according to Kampfenkel *et al.* (1995) with minor modifications as previously described (2.2.2 paragraph).

3.2.6 Confocal microscopy and fluorescence analyses

To analyse the distribution of GSH between the intracellular compartments, TBY-2 cells were stained with 5μM CellTracker Green 5-chloromethylfluorescein diacetate (CMFDA molecular probe; specificity 95%) as previously described by Markovic *et al.* (2007). CMFDA is not a fluorescent probe but it is enzymatically converted to fluorescent 5-chloromethylfluorescein (Tauskela *et al.*, 2000). A 20 μl of CMFDA-cell suspension mixture

Sara Cimini

was transferred to a microscopic slide and visualized using a fluorescence microscope (Leica, Wetzlar, Germany) and by using an inverted confocal microscope (DMIRE2, Leica Microsystems, Wetzlar, Germany). The excitation wavelength for CMFDA was 488 nm. The emission wavelength was 510-540 nm. For the confocal microscope, images were obtained using a ×40 oil immersion objective (NA 1.4) equipped with a mode-locked Titanium-Sapphire laser (Chamaleon, Coherent, Santa Clara, CA) for CMFDA excitation at 488 nm nm. Internal photon multiplier tubes collected eight bit unsigned images at a 400 Hz scan speed. Image background values (defined as intensities below 7% of the maximum intensity) were set to zero and colored black.

3.2.7 Nuclei semi-purification

Protoplast preparations have been performed in order to carry out semi-purification of nuclei from TBY-2 cell suspension. 1 g (FW) of control and ophiobolin A-treated cells was re-suspended in 4 ml protoplast extraction buffer (0.4 M mannitol, 25 mM TRIS-MES, pH 5.5 with HCl with 0.25 % (w/v) cellulose (Sigma, C1794), 0.05 % (w/v) pectolyase (Sigma, P5936), 0.1 % (v/v) pectinase (Sigma, P4716) added on the day). The cells were incubated in the dark with gentle agitation for about 90 minutes to obtain protoplasts. Progress was monitored by observing sub-samples of the cells under the light microscope. Protoplasts were recovered by centrifugation at 300xg for 5 minutes at room temperature without brake. The pellet was washed twice with the protoplast washing buffer (0.4 M mannitol, 25 mM TRIS-MES, pH 6.5 with HCl) in the same centrifugation conditions. After the second washing step, protoplasts have been re-suspended in 2 ml NIBA (Nuclear Isolation Buffer with 1% (v/v) Protease Inhibitor Cocktail and 1mM DTT). From this step every operation was performed on ice. Protoplasts have been disrupted using a Dounce homogenizer, with 6 strokes with the loose followed by 9 strokes with the tight fitting pestle. Progress was monitored using the light microscope. Aliquots of the lysate have been put through a vacuum filtration on 4 layers of Miracloth paper. 2 ml of the filtrate were washed twice with TBS (20mM TRIS, 137mM NaCl, pH 7,6) by centrifugation at 1500xg for 10 minutes at 4°C without brake. After the second washing step the pellet has been re-suspended in 600 µL of TBS in order to obtain semi-purified suspension of nuclei.

Sara Cimini

3.2.8 Flow cytometry

1 ml of semi-purified nuclei was labeled with 2 µl of propidium iodide. DNA profiles were examined using a flow cytometry station (MACSQuant Analyzer, Miltenyi). Histogram or density plots were arranged using the MACSQuant Digital software. For each sample, a minimum of 5,000 and a maximum of 15,000 particles were examined. Analyses were performed on five replicates for each sample. The percentage of the nuclei containing 2C and 4C DNA was calculated.

3.2.9 Nuclear protein extraction and PARP activity determination

The nuclear suspension was shaken at medium-high speed for 30 minutes at 4°C in a vortex with tube attachment. It was then centrifuged (10 min; 4°C; 12000 g,), the supernatant was recovered, frozen in liquid nitrogen and stored at -80°C.

The activity of PARP on nuclear protein extract has been measured by the immuno-detection of the poly(ADP)ribose chain as described by De Block *et al.* (2004). The total concentration of the extracted nuclear proteins was determined using a standard Bradford assay and the samples were normalised to a concentration of 0.5 mg protein in a volume of 15 µl using 1xTBS buffer. These samples were spotted on a Hybond C membrane, which was pre-wetted with TBS buffer, and air-dried. The membrane was the moistened by floating on TBS buffer until evenly wet followed by submergence. It was then followed by a minimum of one hour blocking in TBS with 5% (w/v) dried skimmed milk and 0.1% (v/v) Tween 20 with gentle agitation. The anti-PAR primary antibody was diluted 1:2500 in TBS with 1% (w/v) dried skimmed milk and 0.1% (v/v) Tween 20 and the membrane was incubated in this for 1 hour at room temperature with gentle agitation. The membrane was then washed 5 times for 5 minutes in TBS with 1% (w/v) dried skimmed milk and 0.1% (v/v) Tween 20 followed by incubation with the anti-rabbit IgG alkaline phosphatase conjugate (diluted 1:5000 in 1% blocking solution) for 1 hour at room temperature with gentle agitation. After washing 5 times for 5 minutes in TBS with 0.1% (v/v) Tween 20, followed by two rinses with TBS, the membrane was developed by incubation in BCIP-NBT for 10-30 minutes until a clear signal was obtained. The reaction was stopped by washing the membrane repeatedly with ddH_2O. The image has been captured as a TIFF document, using a desktop scanner, and spot intensities analysed with the UN-SCAN-IT software.

Sara Cimini

3.2.10 Cell viability

Cell viability was calculated as the percentage of cells which did not stain with trypan blue (de Pinto *et al.*, 1999). A 0.05 ml aliquot of cell suspension was transfer in a test tube with 0.05 ml of 4% trypan blue solution (v/v). After 5 min, a 20 µl of trypan blue-cell suspension mixture was transferred to a microscopic slide and the viable (unstained) and non-viable (blue-stained) cells were counted. For each sample 1,000 cells were scored.

3.2.11 DNA laddering

Cells at 48h from ophiobolin A treatment (1 g) were collected and homogenized in liquid N_2. DNA was extracted using the CTAB method according to Murray and Thompson (1980). The lysis buffer (Tris-HCl 0.1 M pH 7.5, NaCl 0.5 M, EDTA 50 mM, containing 1:7 (v/v) of 10% SDS), was added to the obtained fine powder in a rate of 1:5 (w/v) with cellular material. The homogenates were transferred in centrifuge tubes and incubated with 0.3 M sodium acetate, in ice for 10 minutes. Then they were centrifugated at 12000 g, for 5 minutes at 4°C and their supernatants recovered. These supernatants were added with 100% isopropanol in a rate 1:1 (v/v) and kept in ice for 1 minute. The treated samples were centrifugated at 12000 g for 5 minutes at 4°C and their pellet recovered. Each pellet was solubilised in 500 µL di CTAB and 500 µL of extraction buffer (Tris-HCl 10 mM pH 8, EDTA 1 mM) and incubated at 65°C for 15 minutes. At this point a volume of chloroform was added to the samples and they were centrifugated at 10000 g for 10 minutes at 4°C. The aqueous phase was recovered and a volume of 100 % ethanol was added. DNA precipitation was induced by incubating the tubes at – 20°C for 90 minutes and then the samples were centrifugated at 15000 g for 10 minutes at 4°C and the supernatants eliminated. DNA samples were re-suspended in extraction buffer and digested with 100 µg ml^{-1} DNase-free RNase for 1 h at 37 °C. The concentration and purity of DNA were determined by using a spectrophotometer (NanoDrop® ND-1000, Wilmington, DE, USA).

Then they were electrophoresed on a 1.5% (w/v) agarose gel containing 1x TAE (40 mM TRIS-acetate, and 1 mM EDTA pH 8.0), and stained with ethidium bromide.

Sara Cimini

3.2.12 Extracellular generation of H_2O_2

The extracellular release of H_2O_2 in control and ophiobolin A treated cells was determined by measuring the absorbance at 560 nm of the Fe^{3+}–xylenol orange complex according to de Pinto *et al.* (2006).

3.2.13 Intracellular generation of H_2O_2

The dihydrorhodamine (DHR) 123 is used for detecting intracellular generation of H_2O_2 in control and ophiobolin A treated cells. A stock solution of 2 mM was prepared in dimethylsulfoxide and it was stored in the dark at -20°C. 50 µl cells were mixed with 5 µl of 50 µM DHR 123. The fluorescence of single cells was observed by a fluorescence microscope (Leica, Wetzlar, Germany) with an excitation filter of 450–490 nm and a barrier filter of 510 nm.

3.2.14 Enzyme assays of APX

Aliquots (0.3 g) from each analysed cell suspension (control and ophiobolin A-treated cells) were homogenized in liquid N_2 with a mortar and pestle. Two volumes of a buffer containing 50 mM TRIS–HCl (pH 7.5), 0.05% (w/v) cysteine, and 0.1% (w/v) BSA, were added just as the last trace of liquid N_2 disappeared. The thawed mixture was then ground and centrifuged at 20000 *g* for 15 min. The supernatant was used for spectrophotometric analysis.
APX activity was determined following the H_2O_2-dependent oxidation of ASC at 290nm in a reaction mixture composed of 350µM ASC, 170µM H_2O_2, 50–100µg proteins and 0.1M Tris-Acetate buffer, pH 6.4. The activity of APX was corrected by subtracting the non-enzymatic H_2O_2-dependent ASC oxidation and the H_2O_2-not dependent ASC oxidation. An extinction coefficient of 2,7$mM^{-1}cm^{-1}$ was used.

Sara Cimini

3.3 RESULTS

3.3.1 Ophiobolin A phytotoxic effects in *planta*

Figure 3.3 illustrates typical phytotoxic activity of a pathogenic fungus (*Drechslera gigantea Heald & Wolf*) extract containing ~10^{-4} M Ophiobolin A to *Lolium multiflora* plants. *Lolium*, as all monocots, is quite sensitive to ophiobolin producing fungi as well as to toxin itself. As it is well seen, ophiobolin A has dramatic effect on plant vigor, having a strong necrotic effect.

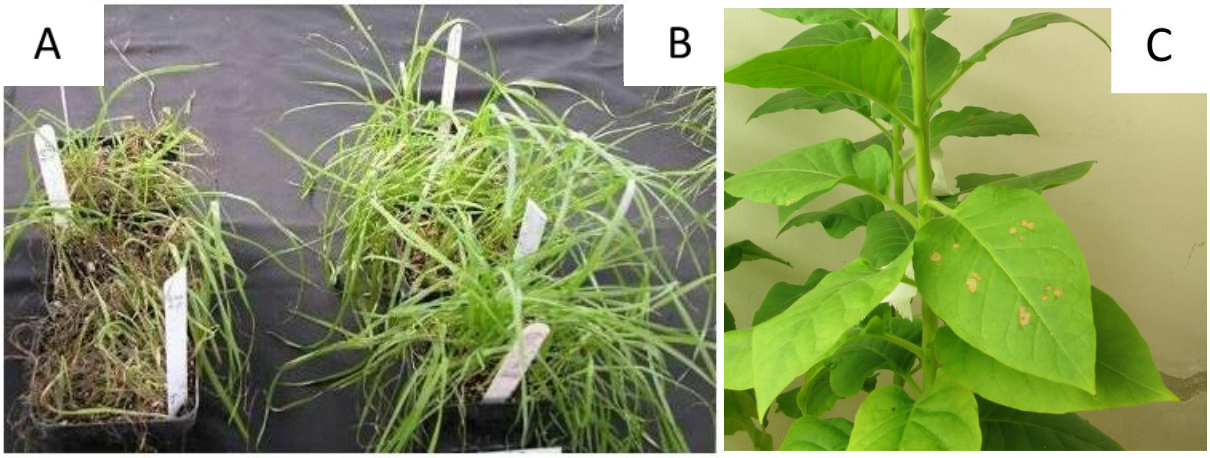

Fig. 3.3. Ophiobolin A phytotoxic effects. Illustration of the necrotic effects caused by a pathogenic fungus (*Drechslera gigantea Heald & Wolf*) extract containing ~10^{-4} M Ophiobolin A to *Lolium multiflora* plants **(A)**, with control condition on the right **(B)**. Effect of 100 μM ophiobolin infiltration in tobacco leaves **(C)**.

Ofiobolin A also induced typical HR spots when it was infiltrated at 100 μM concentration in tobacco leaves (Fig. 3.3C)

3.3.2 Characterization of ophiobolin A stability

The physicochemical stability of ophiobolin A was analyzed in TBY-2 cell culture media in order to establish whether the effects observed in plant cells after treatment with ophiobolin A were due to the compound itself or to its degradation derivate(s) produced in the culture media used for cell growth.

The analysis performed on the degradation of ophiobolin A in TBY-2 plant cell culture media show that after 4 days of incubation, nearly 40% of the ophiobolin A was degraded to 3-anhydro-6-epi-ophiobolin A, the main known degradation product of ophiobolin A (Table 1).

Sara Cimini

Ophiobolin A degradation was much lower within the third day of incubation. In particular, starting from 5 µM ophiobolin solution, the degradation was nearly 6% after 1 day of incubation and 22% and 27% after 2 and 3 days of incubation, respectively (Table 1). Similar results were obtained starting from 10 µM ophiobolin solution (Table 1). No other detectable degradation products were identified in the TBY-2 culturing medium during the four days of analysis.

Time (days)	Starting solution Oph. A 5 µM		Starting solution Oph. A 10 µM	
	Ophiobolin A	3-anhydro-6-*epi*-ophi A	Ophiobolin A	3-anhydro-6-*epi*-ophi-A
1	94±1	6±1	92±1	8 ±2
2	78±2	22±1	76±1	24±1
3	73±1	27±1	71±2	29±2
4	59±2	41±2	58±1	42±1

Table 1. Ophiobolin A stability in TBY-2 plant cell culture media over time. The production of 3-anhydro-6-epi-ophiobolin A by ophiobolin A degradation was measured over time by incubating ophiobolin A at two different concentrations in TBY-2 culture media and in the same cell growth conditions (at 27°C in the dark on a rotary shaker at 130 rpm). The amounts of ophiobolin A and 3-anhydro-6-epi-ophiobolin A were assayed over time as described in the 3.2.1 paragraph. The results are expressed as the percentage of ophiobolin A present at time 0 and are the mean values ± SD of three different experiments.

3.3.3 Ophiobolin A triggered diverse responses in TBY-2 cells depending on the applied dose

Ophiobolin A triggered diverse responses in TBY-2 cells depending on the applied dose since it induced an alteration in cell proliferation or cell viability according to the used concentration.

3.3.3.1 Ophiobolin A effect on TBY-2 cell viability

The effects of ophiobolin A and its degradation product 3-anhydro-6-epi-ophiobolin A on TBY-2 plant cell viability were analyzed using trypan blue assay, a dye selectively entering

dead or dying cells. The data from this analysis revealed that 5 µM ophiobolin A did not induce any decrease in cell viability until 72 h after the treatment, while higher ophiobolin A concentrations induced TBY-2 cell death. The observed cell death was dose-dependent in the first 20 – 24 hours of treatment, after which almost 100% mortality was found in cells treated with 10 µM or higher toxin concentrations (Fig. 3.4A).

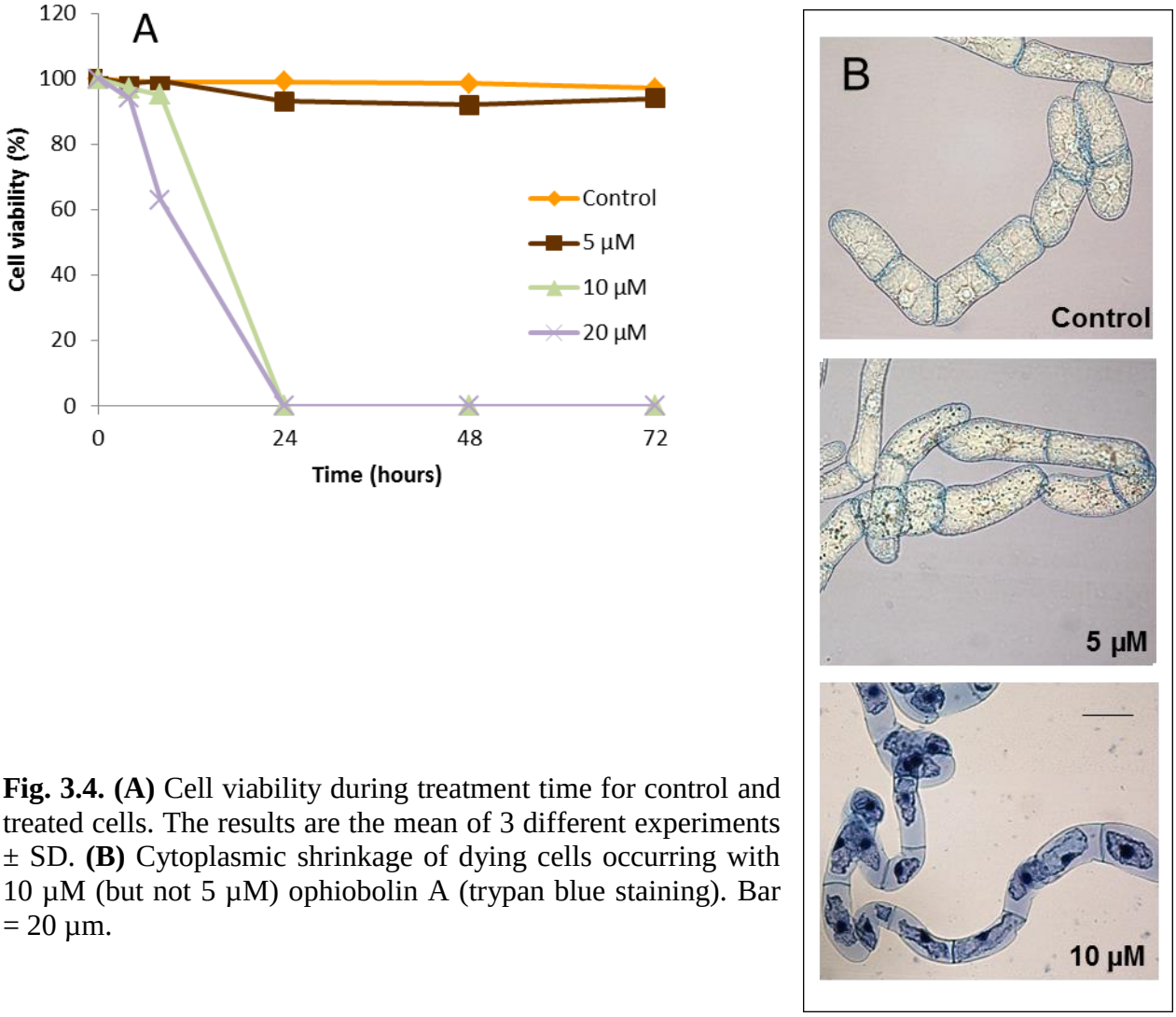

Fig. 3.4. (A) Cell viability during treatment time for control and treated cells. The results are the mean of 3 different experiments ± SD. **(B)** Cytoplasmic shrinkage of dying cells occurring with 10 µM (but not 5 µM) ophiobolin A (trypan blue staining). Bar = 20 µm.

Since a certain amount of ophiobolin A was degraded to 3-anhydro-6-epi-ophiobolin in TBY-2 culture medium, the effect of this molecule was also tested. 3-anhydro-6-epi-ophiobolin had no effect on the TBY-2 cells; neither the growth nor the viability of the cells were altered, even after 72 h of treatment at concentrations up to 10 µM of 3-anhydro-6-epi-ophiobolin (data not shown).

PCD hallmarks in ophiobolin A - treated cells

Cytoplasm shrinkage has been recognized as a useful hallmark to distinguish programmed cell death (PCD) from the necrotic processes in plant cell cultures (de Pinto *et al.*, 2012). Fig. 3.4B shows that treatment with 10 µM ophiobolin A induced cytoplasm shrinkage in nearly all trypan blue-positive cells, suggesting that the compound induced PCD in TBY-2 plant cells. No cellular shrinkage was detected in the control cells or in cells treated with 5 µM ophiobolin A (Fig. 3.4B).

The analysis of the nuclear morphology further supports the activation of PCD by 10 µM ophiobolin A since micronuclei formation, that typically occurs in plant cell undergoing PCD (Houot *et al.*, 2001), was observed in TBY-2 cells (Fig. 3.5A). In contrast, nuclei from TBY-2 cells treated with 5 µM ophiobolin A had the same morphology as those from the control cells (data not shown). DNA laddering, another PCD hallmark determined by the activation of endonucleases during the PCD process, was also evident in TBY-2 cells treated with 10 µM ophiobolin A, while no DNA laddering was present in either cells subjected to 5 µM ophiobolin treatment (data not shown) or in control cells (Fig. 3.5B).

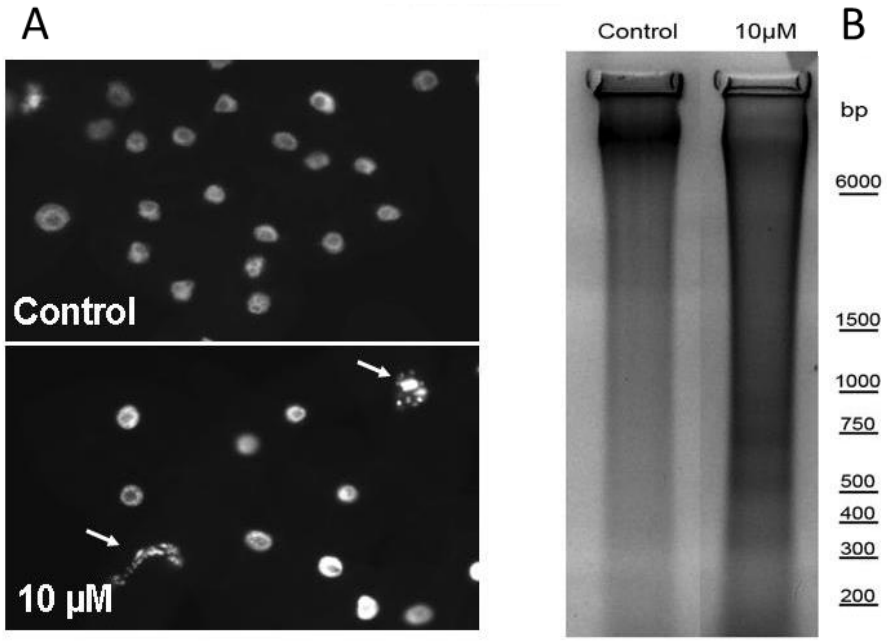

Fig. 3.5. (A) Nuclear morphology of control and ophiobolin A-treated cells. Cells were dyed by Hoechst 33258 to visualize nuclear morphology under fluorescence microscopy (bar = 20 µm). Pictures show cell nuclei at 24 h after treatment with 10 µM ophiobolin A. **(B)** Analyses of DNA laddering in control and ophiobolin A-treated cells. Cells were collected after 72 h of treatment. The picture shows a representative electrophoretic run with 100 µg of DNA that was loaded in each line.

ROS production during ophiobolin A-triggered PCD

It is well known that early H_2O_2 production acts as a signal to activate PCD-dependent defense mechanisms in plant cells (de Pinto *et al.*, 2012). Under ophiobolin A treatment, no precocious H_2O_2 production occured, while an increasing amount of this ROS was evident starting from 8 hours after treatment, when a certain number of cells already showed death symptoms (Table 2). The analysis of H_2O_2 production, by specific fluorescent probe, confirms that H_2O_2 accumulation was observed only in cells positive to trypan blue staining (data not shown) and showing cytoplasmic shrinkage. Therefore H_2O_2 production was only evident in cells in advanced stage of PCD (Fig. 3.6). As expected, H_2O_2 production was not detectable in either control cells or cells treated with 5 µM ophiobolin A over all the analyzed period (Fig. 3.6).

Time after treatment (hours)	Cell viability (%)	H_2O_2 (µM)
0	100 ± 0,1	n.d.
4	98 ± 2	n.d.
8	92 ± 3	0,33 ± 0,2
15	42 ± 10	8,62 ± 1,9

Table 2. The extracellular release of H_2O_2 by TBY-2 cells after 10 µM ophiobolin A treatment. The production of H_2O_2 by tobacco cells was detectable only as cultured cells started dying (see also Fig. 3.6). n.d. = not detectable

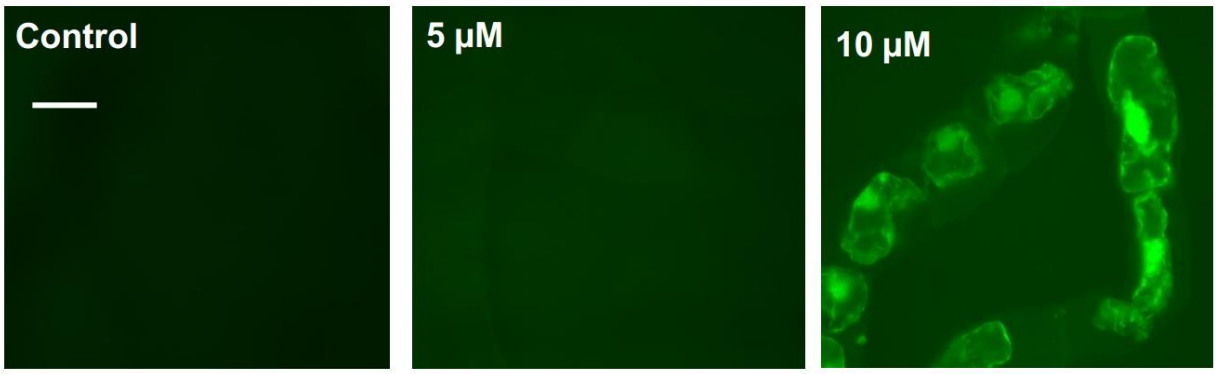

Fig. 3.6. Intracellular production of H_2O_2 in TBY-2 cells under all the analyzed experimental conditions. The TBY-2 cells were stained with DHR 123 and visualized under fluorescence microscopy. The pictures show the control cells and the ophiobolin A-treated cells 24 h after treatment. Bar = 20 µm.

Changes in the intracellular ascorbate and glutathione pools and in APX activity during ophiobolin A-triggered PCD

Since levels and redox state of ASC and GSH are tightly related to the responses of plants to a wide range of biotic and abiotic stresses, analyses of the cellular ASC and GSH pools were carried out for control and 10 µM ophiobolin A treated cells. Moreover, several evidences suggest that alteration in the levels and redox state of ASC and GSH as well as in the activity of APX isoenzymes occurs in TBY-2 cells in route to PCD (de Pinto *et al.*, 2002, 2006; Vacca *et al.*, 2004; Locato *et al.*, 2008, 2009), even if different metabolic pathways can be activate in their course to death by cells undergoing PCD caused by different stimuli (Vannini *et al.*, 2012).

It has been previously described that during the growth curve, ASC content of TBY-2 cells increased for the first 3 days, after which it progressively decreased to the initial values mimicking the mitotic index changes (de Pinto *et al.*, 1999). In our experimental conditions, alterations in the total ASC pool in control cells have a similar trend to that found in the literature data for the same cell line (de Pinto *et al.*, 1999), since the total ASC pool increased in the first days of growth, reaching its maximum level between 72 – 80 hours of growth from cell inoculum in the new culture medium, after which it gradually declined (data not shown). On the other hand, after 10 µM ophiobolin A treatment, the total ASC pool progressively decreases starting from 4 h from treatment (Fig. 3.7). The ASC redox state after ophiobolin A treatment inducing PCD does not change during the time (Table 3).

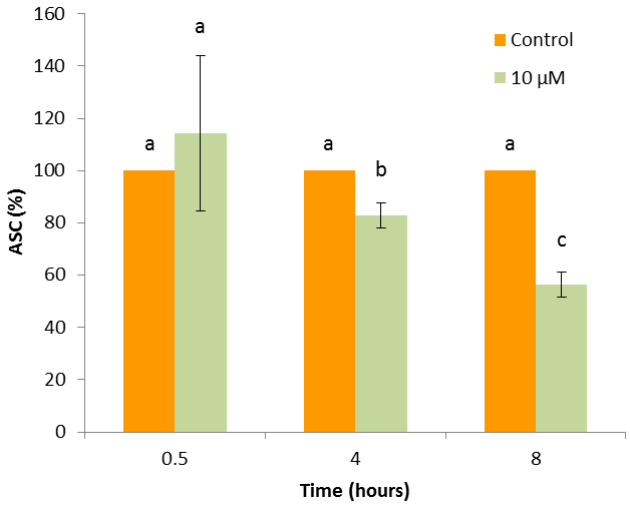

Fig. 3.7. Changes in ASC content induced by ophiobolin A treatment. Cells from a three-day culture were treated with 10 µM ophiobolin A and collected at different times from the treatment. The total ASC content (reduced plus oxidized forms) was determined as expressed as % compare to control. Values represent means (± SD) of two different experiments. Superscript letters indicate statistical significance ($p < 0.05$). Values with the same letter are not statistically different.

		ASC Tot µmol / g FW	ASC red µmol / g FW	DHA µmol / g FW	Redox state
Control	0.5 h	0.70 ± 0.16	0.58 ± 0.04	0.12 ± 0.04	0.83 ± 0.03
	4 h	0.66 ± 0.18	0.59 ± 0.03	0.07 ± 0.03	0.89 ± 0.02
	8 h	0.86 ± 0.16	0.80 ± 0.02	0.06 ± 0.02	0.93 ± 0.01
10 µM	0.5 h	0.86 ± 0.40	0.61 ± 0.11	0.24 ± 0.04	0.71 ± 0.06
	4 h	0.54 ± 0.12	0.48 ± 0.01	0.05 ± 0.03	0.90 ± 0.02
	8 h	0.49 ± 0.13	0.39 ± 0.04	0.10 ± 0.02	0.80 ± 0.03

Table 3. ASC and DHA content in TBY-2 cells treated with 10 µM ophiobolin A. The values reported in table are expressed as µmol / g FW. Redox state is calculated as ratio between reduced form of ASC and the total ASC pool. Values represent means of two different experiments.

Similarly to what occurred for ASC pool, in 10 µM ophiobolin A treated cells the total GSH pool remained constant immediately after the treatment, and then progressively decreased (Fig. 3.8). While in control cells about 90% of the extracted glutathione was in the reduced form at all the analyzed times, in ophiobolin A treated cells the GSH redox state slightly decreases (Table 4).

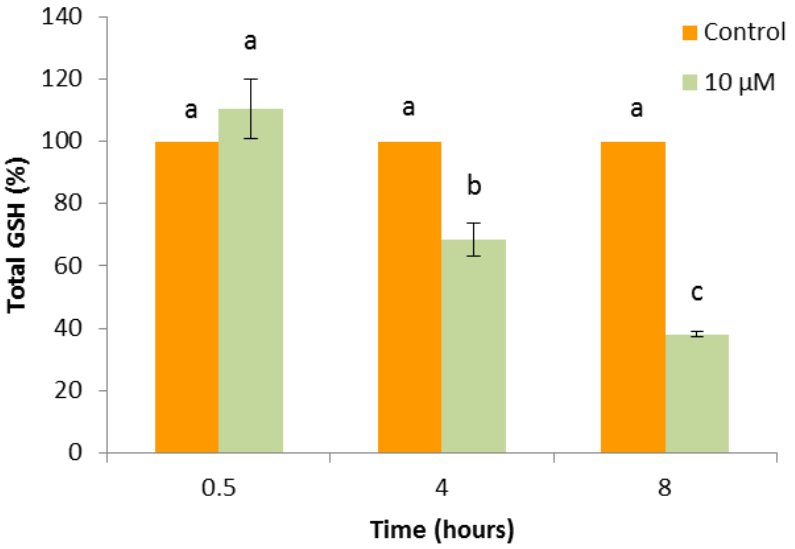

Fig. 3.8. Changes in GSH content induced by ophiobolin A treatment express as % compare to control. Control and 10 µM treated cells were collected at the times indicated and used for the determination of the total GSH pools (reduced plus oxidized forms). Values represent means (± SD) of two different experiments. Superscript letters indicate statistical significance ($p < 0.05$). Values with the same letter are not statistically different.

		GSH Tot µmol / g FW	GSH red µmol / g FW	GSSG µmol / g FW	Redox state
Control	0.5 h	5.18 ± 1.08	4.80 ± 0.91	0.19 ± 0.17	0.93 ± 0.02
	4 h	4.39 ± 1.24	4.08 ± 1.12	0.16 ± 0.12	0.93 ± 0.01
	8 h	5.33 ± 1.36	4.97 ± 1.26	0.18 ± 0.10	0.93 ± 0.01
10 µM	0.5 h	5.92 ± 1.75	5.53	0.19 ± 0.19	0.94 ± 0.01
	4 h	2.68 ± 0.50	2.35	0.17 ± 0.12	0.87 ± 0.02
	8 h	1.60 ± 0.38	1.24	0.18 ± 0.13	0.77 ± 0.03

Table 4. GSH content and redox state in TBY-2 cells treated with 10 µM ophiobolin A. The values reported in table are expressed as µmol / g FW. Redox state is calculated as ratio between reduced form of GSH and the total GSH pool. Values represent means (± SD) of two different experiments.

Among the components of the cellular antioxidant system that mostly contribute to the alteration of ROS level during PCD activation, APX has been reported to plays a crucial role, since an immediate decrease in the activities of all the isoenzymes present in TBY-2 cells occur after PCD activation by heat shock (Locato *et al.*, 2009). A special role for the cytosolic isoenzyme of APX in determining the redox unbalance occurring during PCD activate by ROS, NO and heat shock has been suggested (de Pinto *et al.*, 2002; Vacca *et al.*, 2004, de Pinto *et al.*, 2006, Locato *et al.*, 2008). Therefore, cytosolic APX behavior was analyzed in TBY-2 cells treated with ophiobolin A inducing cell death.

Cytosolic APX activity remained unchanged at least for the first 8 hours after ophiobolin A treatment (Fig. 3.9): a statistically significant decrease in its activity only occurred after 15 hours, when the cell viability was already compromised.

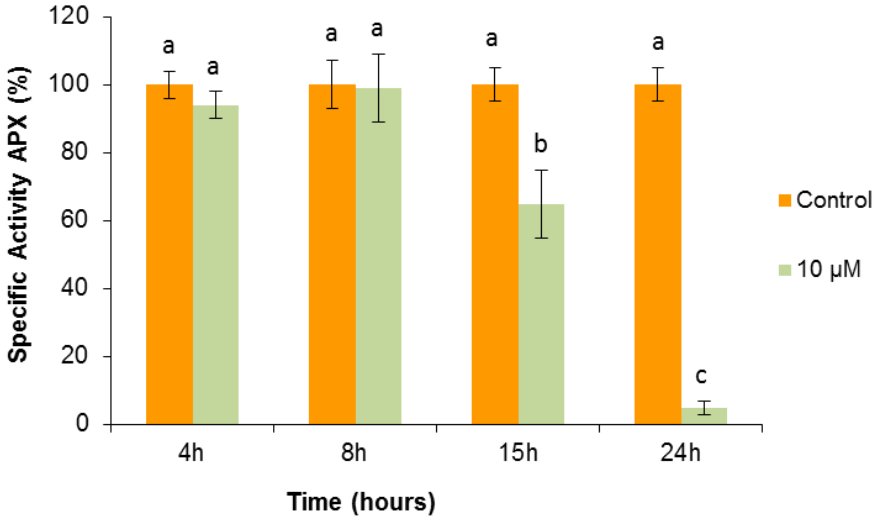

Fig. 3.9. Effects of 10 µM ophiobolin A treatment on ascorbate peroxidase (APX) activity. Specific activity of APX was measured in control and treated cells at different times from the treatment. Values are expressed as percentage of the control mean at 4h. Values represent means (± SD) of three different experiments. Superscript letters indicate statistical significance ($p < 0.05$). Values with the same letter are not statistically different.

After 24 hours of treatment, cytosolic APX activity was near to undetectable levels, probably due to the fact that mostly of the cells were in an advanced state of PCD (Fig. 3.9).

3.3.3.2 Ophiobolin A effect on TBY-2 cell cycle

TBY-2 cells were insensitive to treatments with 1 or 2.5 µM ophiobolin A, since no variations in cell growth, measured as PCD or OD density, were evident under these conditions. On the

other hand, ophiobolin A at 5 μM or higher concentrations induced a block in culture growth during time (Fig. 3.10A and 3.10B).

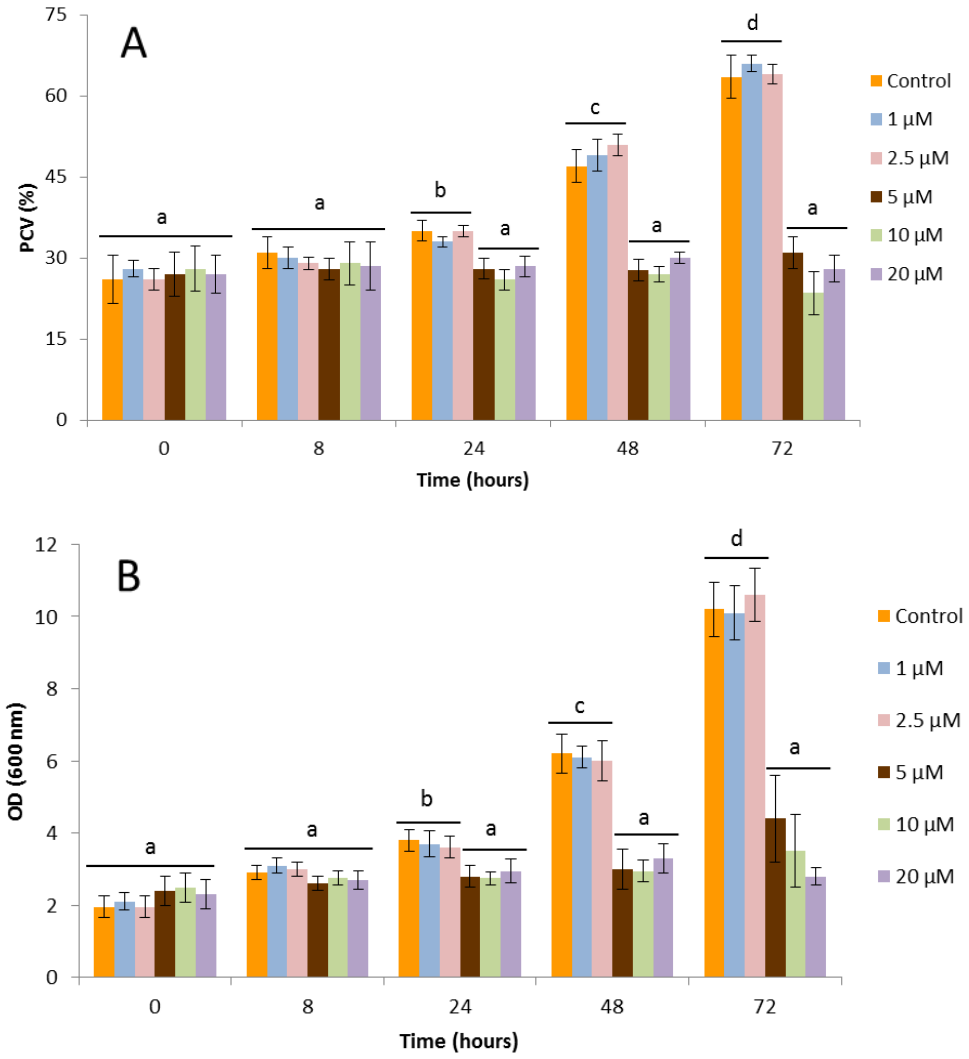

Fig. 3.10. The effects of ophiobolin A on TBY-2 cell growth. TBY-2 cells in exponential phase were incubated with different concentrations of ophiobolin A. **(A)** PCV, an indicator of the increase in cell number and volume was measured for TBY-2 control and ophiobolin-treated cells (1, 2.5, 5, 10, 20 μM) over treatment time. **(B)** Optical density, OD, an indicator of cell density evaluated by measuring the absorbance at 600 nm. All the results are the mean of 3 independent experiments ± SD. Superscript letters indicate statistical significance ($p < 0.05$). Values with the same letter are not statistically different.

The capability of ophiobolin A to block cell proliferation was also evident by measuring the relative growth ratio over time, i.e. the increase in PCV occurring in a unit of time during the growth curve (Fig. 3.11). As previously mentioned 5 μM ophiobolin did not affect cell viability.

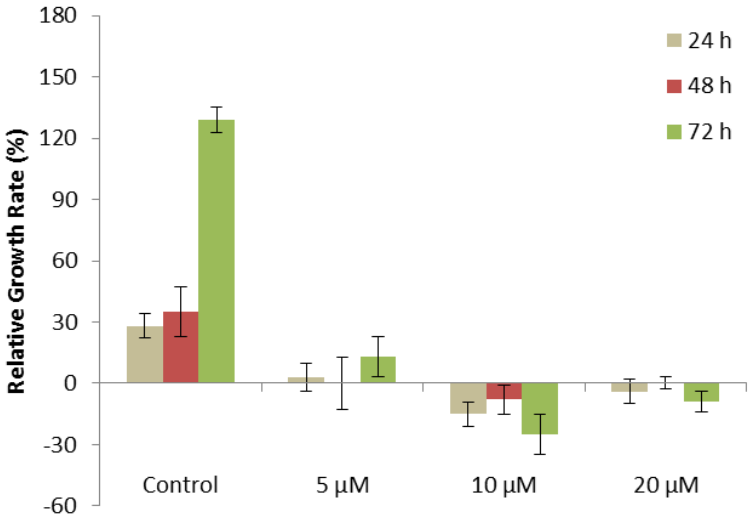

Fig. 3.11. The relative growth rate of control and ophiobolin A-treated cells. Relative growth rate was calculated as PCV increase with regard to the initial PCV. The results are the mean of 3 different experiments ± SD.

TBY-2 cells treated with 5 µM ophiobolin A for 24 hours, restored their proliferative ability when they were washed and cultured in ophiobolin A-free media, even if a weak but nevertheless statistically significant delay in reaching the exponential phase was observed (Fig. 3.12).

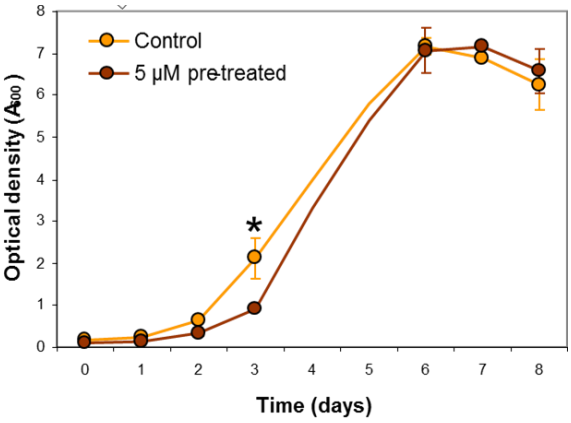

Fig. 3.12. Time course of the growth rate of TBY-2 control cells and the ophiobolin A-treated cells. The latter were washed and re-cultured in fresh ophiobolin A-free media after 24 hours from the treatment with 5 µM ophiobolin A. These values are the mean of three independent experiments ± SD. Statistically significant differences between control and treated cells are indicated as * (at day three) with $p < 0.05$ (Student's t-test).

In order to obtain further information on the mechanism by which sub-lethal ophiobolin A concentrations stop cell growth, the effect of toxin on mitotic index was analysed. According to literature data, a peak of the mitotic index occurred at day three of growing curve of TBY-2 cells, at the beginning of the exponential phase (Fig. 3.13. de Pinto *et al.*, 1999). In TBY-2 cell, treated at day 3 of the growing curve with 5 µM ophiobolin A, the number of cell undergoing mitosis decreased by 69 ± 5% at 24 h post-treatment (Fig. 3.13), thus supporting that sub-lethal concentration of ophyobolin A affected cell cycle inducing its block in a phase different from mitosis.

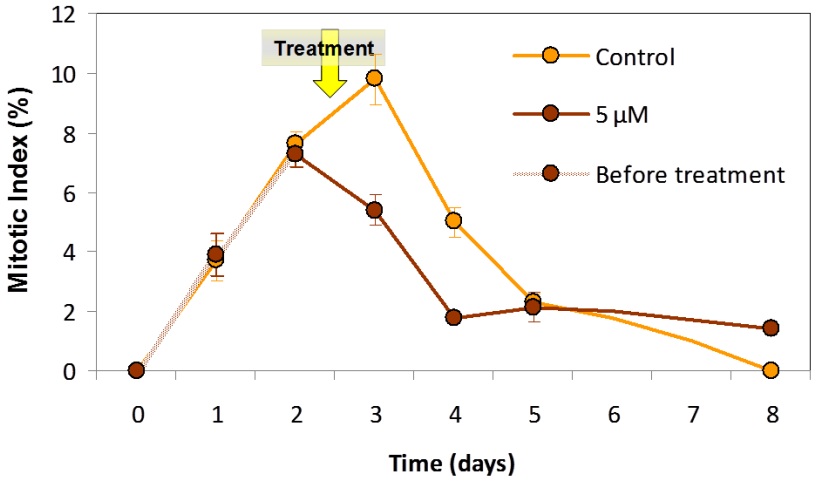

Fig. 3.13. Mitotic index for control and 5 µM treated cells. The mitotic index is calculated as the percentage of the ratio between dividing cells and the number of cells scored. The number of dividing cells is determined by Hoechst 33258 staining. The results are the mean of 3 different experiments ± SD.

The identification of the cell distribution during the various phases of the cell cycle was performed by propidium iodide staining and cytofluorimetric analysis for control and treated cells at 24 h from the treatment with 5 µM Ophiobolin A. In control and treated cells, the fraction of cells in G1 was the highest. However, a statistically significant enrichment of the S/G2 phase fraction was evident in ophiobolin A treated cells (Fig. 3.14). In particular, the treatment induces an increase of nearly 30% of S/G2 phase nuclei.

	Nuclei G1 (%)	Nuclei S + G2 (%)
Control	65 ± 6.1	35 ± 6.1
5 µM	54 ± 6.6	46 ± 6.6

Fig. 3.14. Analysis of cell distribution during the various phases of cell cycle. A semi-purified nuclear fraction from control and treated cells (5 µM ophiobolin A) at 24h from the treatment were analyzed for cell cycle by propidium iodide staining and flow cytometry. The results are the mean of 3 different experiments.

Recently it has been reported that GSH is required for the progression of cell cycle in plants as in animals (Diaz-Vivancos *et al.*, 2010). In order to verify if ophiobloin A altered the metabolism of this redox pair, changes in the intracellular GSH pool during the exponential growth phase (corresponding to 0, 24 h, 48 h and 120 h from the start of the treatment) of control and treated cells were assessed. According to the literature data, GSH content was at the highest levels at the beginning of the exponential phase (de Pinto *et al.*, 1999). From the time of the treatment it started to decrease from a value of about 1000 nmol/g FW until 143,5 nmol/g FW at 120 h. At this time, TBY-2 cells grown under standard conditions ended the exponential phase and began the stationary phase (Fig. 3.15). In treated cells GSH decrease

was delayed compared to what occurs in control cells. In particular, no statistically significant differences have been detected between time 0 and after 24 h from the treatment (Fig. 3.15).

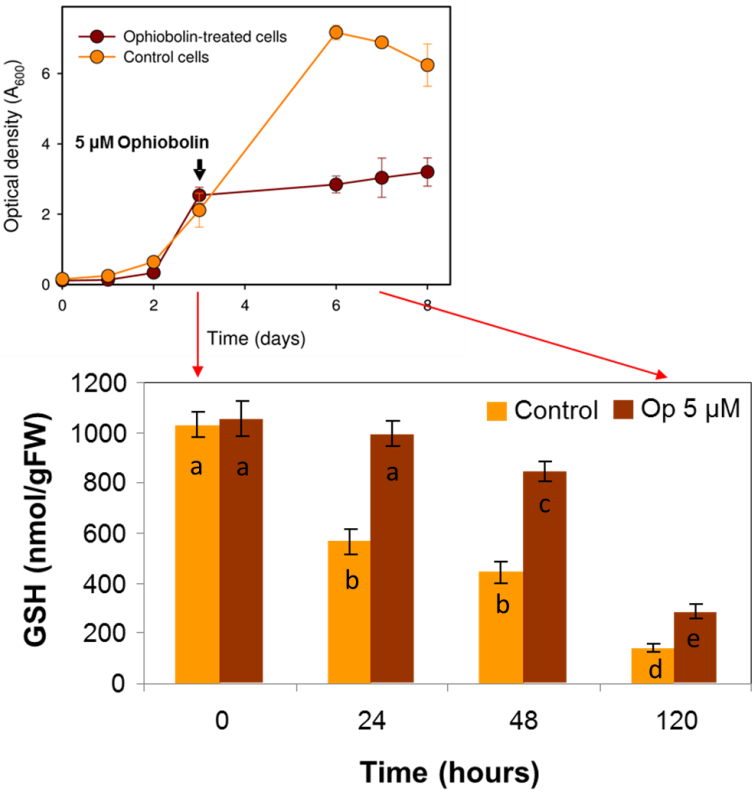

Fig. 3.15. Total glutathione (GSH + GSSG) content during the exponential growth phase of TBY-2 cells (control and 5 µM ophiobolin A treated cells). The results are the mean of 3 different experiments ± SD. Different letters indicate values that are statistically different ($p < 001$)

Under our experimental conditions, the redox state, expressed as ratio of reduced glutathione (GSH) to total GSH content (GSH + GSSG), of control cells was constant throughout the growth cycle, with values close to 1.

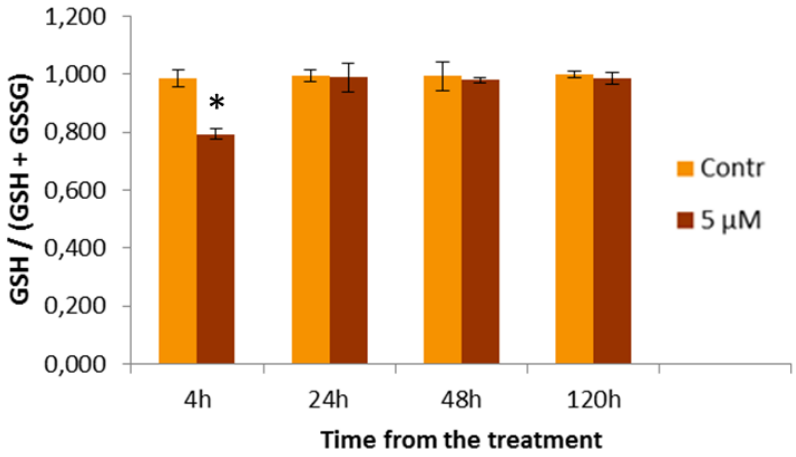

Fig. 3.16. Redox state of GSH (reduced GSH / total GSH) for control and 5 µM ophiobolin A treated cells. The results are the mean of 3 different experiments ± SD. Statistically significant difference is indicated as * with $p < 0.01$ (Student's t-test).

On the contrary, in the 5 µM ophiobolin A-treated cells a statistically significant decrease ($p < 0.05$) of the redox state was evident at 4 h from the treatment, even if this alteration was only

transient, since in the following analyzed times the GSH redox states in the treated cells were comparable with those of the control cells (Fig. 3.16).

Changes in cellular GSH distribution between cytoplasm and nucleus at different times of the cellular growth period have also been investigated, by using a probe that specifically emits fluorescence after interaction with reduced GSH. In figure 3.17, GSH localization in untreated TBY-2 cells has been analyzed by confocal microscopy during culture growth.

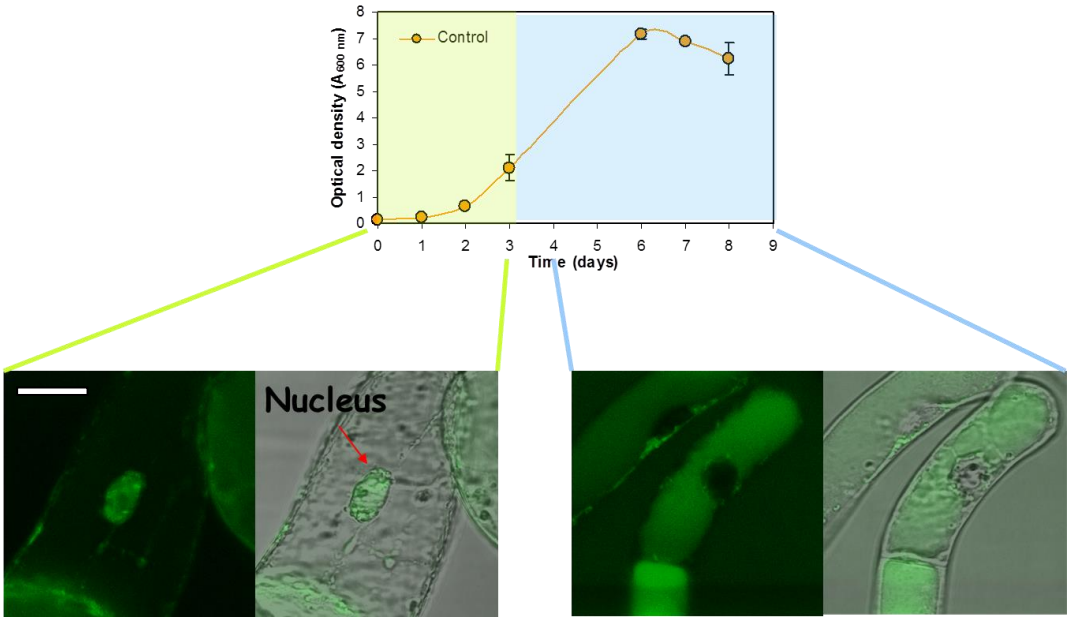

Fig. 3.17. GSH localization in untreated TBY-2 cells during cell proliferation by confocal analysis. GSH distribution is typically nuclear during the first three days from cell inoculum in the new culture medium and cytoplasmic from the fourth days till the stationary phase. TBY-2 cells were stained with CMFDA staining-green fluorescence. Bar = 40 µm.

As highlighted from confocal analysis using CMFDA staining-green fluorescence, under standard conditions (control) GSH is recruited in the nucleus in early phases of cell proliferation (the first 3 days from the inoculation time). On the other hand, starting from the fourth day till the stationary phase of the culture period, most of the total cellular GSH pool was localized in the cytoplasm (Fig. 3.17)

Similar results were obtained by fluorescence microscopy (Fig. 3.18A and 3.18B).

Interestingly, both confocal (data not shown) and fluorescence microscopy analysis (Fig. 3.18C and D) indicate that a different partitioning was observed in 5 µM ophiobolin A-treated cells. Indeed in treated cells GSH seems to be mostly maintained in the nuclei during the whole culture period (Fig. 3.18C and D).

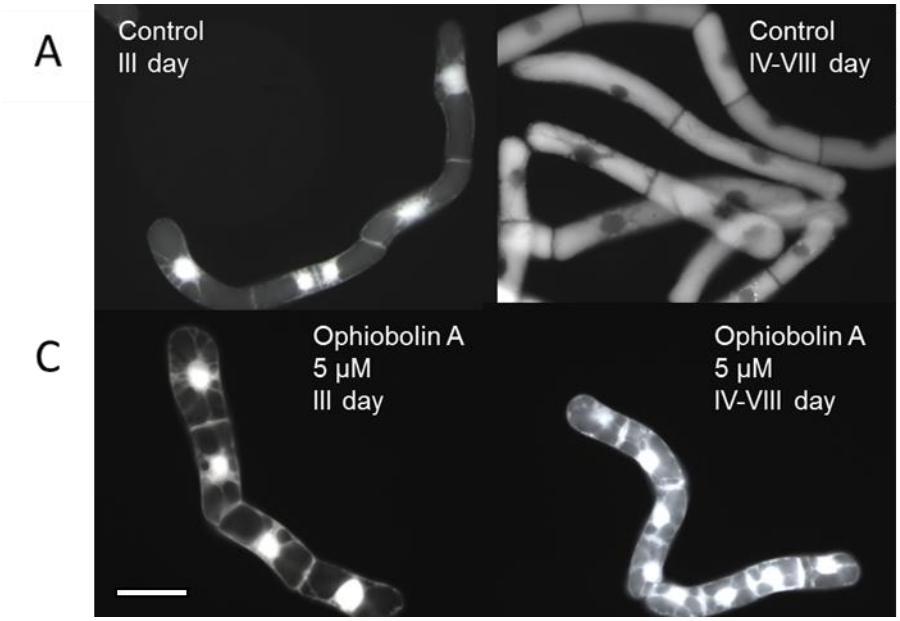

Fig. 3.18. GSH intracellular partitioning in TBY-2 cells under all the analyzed experimental conditions. TBY-2 cells were stained with Hoechst 33258 and visualized under fluorescence microscopy. The pictures show the control cells (**3.18A** and **B**) and the 5 µM ophiobolin A-treated cells (**3.18C** and **D**). Bar = 20 µm.

Among the nuclear metabolic pathways involved in cell division a pivotal role is played by Poly (ADP-ribose) polymerases (PARPs).

PARPs are nuclear enzyme involved in DNA metabolic transitions, the activity of which normally increases during the phase of active cell proliferation in plant tissues or cell culture (Pellny *et al.*, 2009). PARPs are also involved in the responses of plants to abiotic stress (De Block *et al.*, 2005; Vanderauwera *et al.*, 2007) as well as to biotic stress (Adams-Phillips *et al.*, 2010). On these bases, analyses of changes in PARP activities were performed during the exponential growth phase of control and 5 µM ophiobolin A treated cells.

In control cells nuclear PARP activity varied during the different phases of culture: it increased from day 1 to day 4 of the culture period (data not shown), after which it progressively declined (Fig. 3.19), thus mirroring the behavior of mitotic index (see fig. 3.13).

In 5 µM ophiobolin A-treated cells no statistically significant differences in PARP activities have been observed during the whole analyzed period (Fig 3.19).

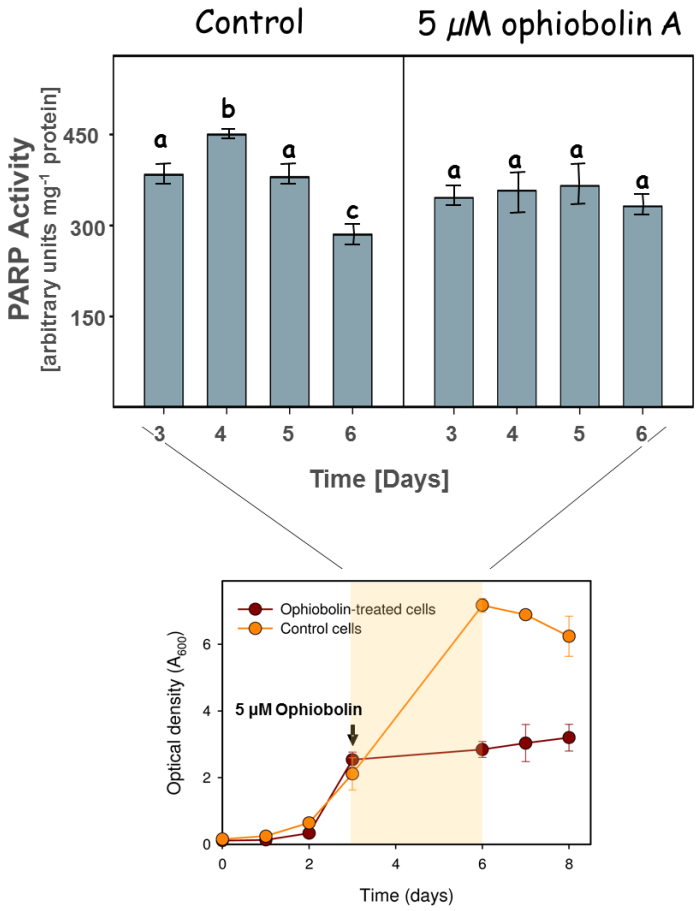

Fig. 3.19. Calculated PARP activity by immuno-detection of the poly (ADP-ribose) chains, as describe by De Block *et al.*, 2005, in control and treated cells during the exponential growth phase.

3.4 DISCUSSION

The great majority of the data available in literature about phytotoxic properties of ophiobolin A, have been performed on monocot plants due to the catastrophic losses of cereal yield caused by ophiobolin producing fungi. In order to better elucidate the mechanisms activated by plants against ophiobolin A, a cellular model system has been used. The *in vitro* study presented here, showed that also non-cytotoxic ophiobolin A concentrations are able to induce severe alterations in cellular metabolism. At concentrations higher than a threshold value (≥ 10 µM), ophiobolin A induces cell death that displays characteristic PCD hallmarks, like cytoplasm shrinkage, micronuclei formation and DNA laddering, suggesting that the toxin is able to activate an apoptosis-like process. It is known that PCD is part of the HR, activated in order to face the spread of pathogens by surrounding them with a barrier of dead tissue (Mur *et al.*, 2008). The activation of PCD in tobacco cells by ophiobolin A suggests the ability to activate defense responses against ophiobolin-producing fungi, which is consistent with the fact that dicot plants have been reported to be more resistant than monocots to *Bipolaris spp.* infection (Evidente *et al.*, 2006). During the establishment of defense responses and HR, a rapid production of ROS, indicated as an oxidative burst, is a hallmark of successful recognition of plant pathogens and activation of defense strategy (Torres, 2010). This ROS production is typically apoplastic and occurs mainly via the activation of a plasma membrane NADPH oxidase and/or cell wall enzymes. The apoplastic H_2O_2 accumulation alone may be insufficient to activate PCD (Mur *et al.*, 2005). Indeed, ROS produced in mitochondria, chloroplasts and peroxisomes have been associated with HR cell death (Maxwell *et al.*, 2002; Foyer and Noctor, 2005; Mur *et al.*, 2008). ROS accumulation is used to promote pathogen killing, to strengthen the cell wall by means of peroxidative crosslinking reactions, and to induce the PCD signaling pathway (de Pinto *et al.*, 2012). Although O_2^- is the proximal product generated by NADPH oxidase, H_2O_2 has been reported as the pivotal signal molecule because of its ability to cross cell membranes and its long half-life relative to those of the radical ROS (Gechev and Hille, 2005). Moreover it is spontaneously or enzymatically generated by O_2^- dismutation. Consistently, a biphasic production of H_2O_2 characterizes HR, with a first unspecific and transitory peak occurring within minutes after infection, before any morphological symptoms of cell death are evident (Levine *et al.*, 1994). A biphasic production of H_2O_2 has also been observed in TBY-2 cells undergoing PCD by different

Sara Cimini

elicitors (Vacca *et al.*, 2004; de Pinto *et al.*, 2006). Surprisingly, the ophiobolin A-dependent PCD was not preceded by any increase in the H_2O_2. Only a tardive (8-15 h from the ophiobolin A treatment) H_2O_2 accumulation was detected, when the death process was already well evident (58 % cell mortality at 15 h). As we observed for apoplastic H_2O_2 production, an H_2O_2 accumulation inside the cells was found only several hours after the ophiobolin A treatment thus supporting that ophiobolin A induces a ROS-independent PCD pathways.

The fact that ophiobolin dependent PCD is activated by a signaling pathway independent by ROS is also supported by APX behavior. In contrast with evidences previously reported that indicate a decrease in APX as a precocious event in the ROS – dependent PCD (Vacca *et al.*, 2004; de Pinto *et al.*, 2006) APX is not affected by ophiobolin A treatment inducing PCD, since in ophiobolin dependent PCD, a decrease in the cytosolic APX activity was detected only when cell viability was already strongly compromised.

Consistently, in cells undergoing ophiobolin –dependent PCD, ASC and GSH decrease their level without any change in their redox state, while a significant decrement in their redox state characterizes the ROS-dependent PCD (de Pinto *et al.*, 2006; Locato *et al.*, 2008).

Our data support the hypothesis that ophiobolin-dependent PCD does not occur with the same signaling pathways as previously described (Vacca *et al.*, 2004; de Pinto *et al.*, 2006) at least regarding ROS-related systems. Interestingly, an uncommon model of PCD has been demonstrated to be induced by fumonisin B1 and AAL toxin, which are mycotoxins produced by phytopathogenic fungi. In this case, it has been demonstrated that PCD activation was not dependent on H_2O_2 production (Lachaud *et al.*, 2011). As these molecules are not chemically related to ophiobolin A and because they are both produced by phytopathogenic fungi, our data suggest that H_2O_2-independent PCD could be a plant response to pathogens that occurs with a certain frequency. Further studies are required to identify the signaling pathway leading to this H_2O_2-independent PCD.

In relation to the mechanisms by which sub-lethal concentrations of ophiobolin A (5 µM in TBY-2 cells) inhibit cell proliferation without affecting cell viability, our analyses suggest that this toxin arrests cell proliferation blocking cell cycle in a phase different from mitosis. Indeed, while in control TBY-2 cells a peak of the mitotic index was observed at the beginning of the exponential phase, in treated cells the percentage of cells undergoing mitosis

Sara Cimini

was strongly reduced. An inhibitory effect of ophiobolin A on cell division is consistent with the inhibitory effect of ophiobolin A on coleoptile growth and seed germination reported in monocot-susceptible plants (Au *et al.*, 2000a).

Moreover, flow cytometry analysis indicates that the anti-proliferative action of ophiobolin A was exerted before mitosis since the percentage of cells in S-G2 phase is higher and a significant decrease of the percentage of cells in G1 phase was observed in treated cells in comparison with control ones.

In eukaryotes, cell cycle progression is driven by an intrinsic redox cycle characterized by transient oxidative processes. Specifically, in the eukaryotic cell cycle it is possible to identify an oxidative phase, starting with cell division and G1 phase, and a reductive phase, during which DNA synthesis and mitosis occur (Chiu and Dawes, 2012). Thus, fluctuations of cellular oxidative state influences cell cycle progression. In animals, a moderate oxidative environment occurring in G1 phase is able to activate a signaling pathway leading to cell proliferation (Menon *et al.*, 2003; Menon and Goswami, 2007). At higher ROS concentrations, similar to those characterizing stressing conditions, cell division is blocked and, after prolonged block of the cell cycle, cells activate PCD program. Hence, cell division is highly regulated by cellular redox environment and loss of redox control can result in alteration of cell cycle progression (Chiu and Dawes, 2012).

The redox regulation of the cell cycle has been much more intensively studied in animals than in plants. However in plants, a strong correlation between cellular redox state and cell cycle block of root quiescent center has been observed (Jiang and Feldman, 2005; Jiang *et al.*, 2006; Dinneny *et al.*, 2008). It is known that GSH plays a critical role in the antioxidant network of plant and animal cells, participating in redox signaling network able to influence growth and development (Foyer and Noctor, 2005; Noctor *et al.*, 2012). Many cell cycle regulators, such as cyclin D, and several transcription factors directly involved in mitogenic cyclin activation are found to have reactive cysteine residues undergoing to redox processes (Chiu and Dawes, 2012). Variation in the cellular redox balance occurring during physiological conditions of cell cycle progression or under oxidative stress conditions can strongly affect these redox processes, thus controlling the progression of specific phase of the cell cycle (Alic *et al.*, 2004).

Consistently, the highest GSH levels were observed in TBY-2 control cells, as well as in *Arabidopsis thaliana* cells, when the mitotic activity is at the highest values (de Pinto *et al.*, 1999; Pellny *et al.*, 2009). Interestingly, not only the level of GSH affects cell proliferation

Sara Cimini

but its flux between nucleus and cytoplasm seems to be pivotal for the normal progression of cell cycle in animal and plant cells (Diaz-Vivancos *et al.*, 2010). GSH fluxes between nucleus and cytoplasm have been observed in our experimental conditions. In control cells, when the proliferating activity is at the highest values, a nuclear recruitment of GSH was found; GSH translocates to the nucleus before exponential growth phase. Subsequently, starting from day four of culture period when cells stop dividing and the cell cycle is mainly block in G1/G0 phase, GSH was largely localized in the cytosol. Similar changes in GSH partitioning have been also reported in 3T3 fibroblast cell line (Markovic *et al.*, 2007) and in *Arabidopsis* cells suspension (Pellny *et al.*, 2009; Diaz-Vivancos *et al.*, 2010). In the nucleus GSH may act as regulator of several nuclear proteins, including transcription factors that require a reduced environment to bind DNA. The mechanisms involved in GSH transport and sequestration is still unclear but they are probably activated and deactivated in response to cell cycle checkpoints (Pallardó *et al.*, 2009).

In ophiobolin A treated cells, mainly blocked in S/G2 phase, GSH remained recruited into the nucleus. This probably avoids its utilization in metabolic pathways occurring in other cellular compartment even because ophyobolin A treatment also causes a decrease in total GSH level during time. Ophiobolin A treatment blocks GSH fluxes between nucleus and cytoplasm probably altering the redox state of both nucleus and cytoplasm and thus unbalancing the signaling network needed for cell cycle control. Since ophiobolin A is a calmodulin antagonist (Au *et al.*, 2000b) it is also possible that alterations in Ca^{2+} fluxes may alter the permeability of nuclear pores, facilitating GSH sequestration into the nucleus and that the sequestration of GSH into the nucleus blocks cell cycle proliferation.

An impairment of nuclear metabolism caused by sub-lethal concentration of ophiobolin A is also supported by alterations in the activity of PARPs, enzymes transferring ADP-ribose groups from NAD to nuclear protein and involved in DNA repair and protein de-acetylation (Liang *et al.*, 2013; Robu *et al.*, 2013). In control TBY-2 cells, as well as in *Arabidopsis* cells, the activity of PARPs strongly increases in the exponential phase of cellular grown curve (Pellny et al 2009); while, under treatment with sub-lethal concentration of ophiobolin A no increase in PARP activity occurs during the exponential phase.

Our data do not allow to understand whether the impairment of GSH fluxes between nuclei and cytoplasm is related to the alteration in PARP activity. However, it is interesting to note that PARPs are strictly affected by availability of pyridine nucleotide, another key actor in

Sara Cimini

cellular redox processes. Therefore, alteration of GSH fluxed and PARP could be part of a general redox impairment. It is also possible that an altered availability of GSH in nuclei could affect nuclear metabolism by altering the level of protein glutathionylation. Emerging evidences suggest that this post transductional modification can modulate enzyme activity as well as protein – protein or protein-nucleic acid interaction.

Further study are in progress in order to better characterize the cross-talk between GSH and other events controlling cell cycle progression.

References

Adams-Phillips L., Briggs A.G. and Bent A.F. (2010) Disruption of poly(ADP-ribosyl)ation mechanisms alters responses of Arabidopsis to biotic stress. *Plant Physiol.* **152:** 267–280;

Adom K.K. and Liu R.H. (2002) Antioxidant activity of grains. *J Agric Food Chem.* **50:** 6182-6187;

Ainsworth E.A., Rogers A. and Leakey A.D.B. (2008) Targets for crop biotechnology in a future high-CO_2 and high-O_3 world. *Plant Physiol.* **147:** 13–19;

Al Ghamdi A.A. (2009) Evaluation of oxidative stress tolerance in two wheat (*Triticum aestivum*) cultivars in response to drought. *Int J Agric Biol.* **1:** 7-12;

Albrecht G., Mustroph A. and Fox T.C. (2004) Sugar and fructan accumulation during metabolic adjustment between respiration and fermentation under low oxygen conditions in wheat roots. *Physiol Plant.* **120:** 93-105;

Alic N., Felder T., Temple M.D., Gloeckner C., Higgins V.J., Briza P. and Dawes I.W. (2004) Genome-wide transcriptional responses to a lipid hydroperoxide: adaptation occurs without induction of oxidant defenses. *Free Radic Biol Med.* **37:** 23-35;

Altenbach D. and Ritsema T. (2007) Structure-function relations and evolution of fructosyltransferases. In N Shiomi, N Benkeblia, S Onodera, eds, Recent Advances in Fructooligosaccharides Research. Research Signpost, Kerala, India. 135–156;

Altenbach D., Nüesch E., Meyer A.D., Boller T. and Wiemken A. (2004) The large subunit determines catalytic specificity of barley sucrose:fructan 6-fructosyltransferase and fescue sucrose:sucrose 1-fructosyltransferase. *FEBS Lett.* **567:** 214-218;

Altenbach D., Rudiño-Pinera R., Olvera C., Boller T., Wiemken A. and Ritsema T. (2009) An acceptor-substrate binding site determining glycosyl transfer emerges from mutant analysis of a plant vacuolar invertase and a fructosyltransferase. *Plant Mol Biol.* **69:** 47-56;

Altschul S.F., Gish W., Miller W., Myers E.W. and Lipman D.J. (1990) Basic local alignment search tool. *J Mol Biol.* 215: 403-410.

Apel K. and Hirt H. (2004) Reactive oxygen species: metabolism, oxidative stress, and signal transduction. *Annu Rev Plant Biol.* **55:** 373–399;

Arai M., Niikawa H. and Kobayashi M. (2012) Marine-derived sesterterpenes, ophiobolins, inhibit biofilm formation of *Mycobacterium* species. *J Nat Med.* in press;

Archbold H.K. (1940) Fructosans in the monocotyledons. A review. *New Phytol.* **39:** 185-219;

Arora A., Sairam R.K. and Srivastava G.C. (2002) Oxidative stress and antioxidative system in plants. *Curr Sci.* **82:** 1227-1238;

Arranz S. and Calixto F.S. (2010) Analysis of polyphenols in cereals may be improved performing acidic hydrolysis: A study in wheat flour and wheat bran and cereals of the diet. *J Cereal Sci.* **51:** 313-318;

Arrigoni O., De Gara L., Tommasi F. and Lico R. (1992) Changes in ascorbate system during seed development of Vicia faba. *Plant Physiol.* **99:** 235-238;

Asada K. (2006) Production and scavenging of reactive oxygen species in chloroplasts and their functions. *Plant Physiol.* **141:** 391–396;

Sara Cimini

Au T.K. and Leung P.C. (1998) Identification of the binding and inhibition sites in the calmodulin molecule for ophiobolinA by site-directed mutagenesis. *Plant Physiol.* **118:** 965-973;

Au T.K., Chick W.S.H. and Leung P.C. (2000b) Initial kinetics of the inactivation of calmodulin by the fungal toxin ophiobolin A. *Int J Biochem Cell Biol.* **32:** 1173-1182;

Au T.K., Chick, W.S.H. and Leung P.C. (2000a) The biology of ophiobolins. *Life Sci*. **67:** 733-742;

Baier M. and Dietz K.J. (1996) Primary structure and expression of plant homologues of animal and fungal thioredoxin-dependent peroxide reductases and bacterial alkyl hydroperoxide reductases. *Plant Mol Biol.* **31:** 553-564;

Baker C.J. and Orlandi E.W. (1995) Active Oxygen in Plant Pathogenesis. *Annu Rev Phytopathol.* **33:** 299-321;

Bancal P., Carpita N.C. and Gaudillere J.P. (1992) Differences in fructan accumulated in induced and field-grown wheat plants: an elongation-trimming pathway for their synthesis. *New Phytol.* **120:** 313-321;

Barrero J.M., Millar A.A., Griffiths J., Czechowski T., Scheible W.R., Udvardi M., Reid J.B., Ross J.J., Jacobsen J.V. and Gubler F. (2010) Gene expression profiling identifies two regulatory genes controlling dormancy and ABA sensitivity in Arabidopsis seeds. *Plant J.* **61:** 611-622;

Beard J.L. (2008) Why iron deficiency is important in infant development. *J Nutr*. **138:** 2534–2536;

Benech-Arnold R.L., Gualano N., Leymarie J., Côme D. and Corbineau F. (2006) Hypoxia interferes with ABA metabolism and increases ABA sensitivity in embryos of dormant barley grains. *J Exp Bot.* **57:** 1423-1430;

Bennett-Lovsey R.M., Herbert A.D., Sternberg M.J. and Kelley L.A. (2008) Exploring the extremes of sequence/structure space with ensemble fold recognition in the program Phyre. *Proteins*. **70:** 611-625;

Bewley J.D. (1997) Seed Germination and Dormancy. *Plant Cell.* **9:** 1055-1066;

Bhatt I. and Tripathi B.N. (2011) Plant peroxiredoxins: catalytic mechanisms, functional significance and future perspectives. *Biotechnol Adv.* **29:** 850-859;

Bhatti H.N., Asgher M., Abbas A., Nawaz R. and Sheikh M.A. (2006) Studies on kinetics and thermostability of a novel acid invertase from *Fusarium solani*. *J Agric Food Chem.* **54:** 4617-4623;

Bhutta Z.A. (2008) Micronutrient needs of malnourished children. *Curr Opin Clin Nutr Metab Care*. **11:** 309–314;

Bindschedler L.V., Dewdney J., Blee K.A., Stone J.M., Asai T., Plotnikov J., Denoux C., Hayes T., Gerrish C., Davies D.R., Ausubel F.M. and Bolwell G.P. (2006) Peroxidase-dependent apoplastic oxidative burst in Arabidopsis required for pathogen resistance. *Plant J.* **47:** 851-863;

Black M., Corbineau F., Gee H., Gee H. and Côme D. **(1999)** Water content, raffinose, and dehydrins in the induction of desiccation tolerance in immature wheat embryos. *Plant Physiol.* **120:** 463-471;

Sara Cimini

Blacklow W.M., Darbyshire B. and Pheloung P. (1984) Fructans polymerized and depolymerized in internodes of winter wheat as grain-filling progressed. *Plant Sci Lett*. **36:** 213–218;

Blasbalg T.L., Wispelwey B. and Deckelbaum R.J. (2011) Econutrition and utilization of food-based approaches for nutritional health. *Food Nutr Bull*. **32:** S4-S13;

Blokhina O., Virolainen E. and Fagerstedt K.V. (2003) Antioxidants, oxidative damage and oxygen deprivation stress: a review. *Ann Bot.* **91:** 179-194;

Bohnert H.J. and Jensen R.G. (1996) Strategies for engineering water stress tolerance in plants. *Trends in Biotechnol.* **14:** 89-97;

Bollwell G.P., Bindschedler L.V., Blee K.A., Butt V.S., Davies D.R., Gardner S.L., Gerrish C. and Minibayeva F. (2002) The apoplastic oxidative burst in response to biotic stress in plants: a three-component system. *J Exp Bot.* **53:** 1367–1376;

Bonnett G.D. and Incoll L.D. (1993) Effects on the stem of winter barley of manipulating the source and sink during grain-filling. I. Changes in accumulation and loss of mass from internodes. *J Exp Bot.* **44:** 75-82;

Bonnett G.D. and Simpson R.J. (1995) Fructan exohydrolase activities from *Lolium rigidum* that hydrolyze β-2,1- and β-2,6-glycosidic linkages at different rates. *New Phytol.* **131:** 199-209;

Bonnett G.D., Sims I.M., Simpson R.J. and Cairns A.J. (1997) Structural diversity of fructan in relation to the taxonomy of the Poaceae. *New Phytol.* **136:** 11-17;

Borisjuk L., Rolletschek H., Radchuk R., Weschke W., Wobus U. and Weber H. (2004) Seed development and differentiation: a role for metabolic regulation. *Plant Biol (Stuttg).* **6:** 375-386;

Borraccino G., Mastropasqua L., De Leonardis S. and Dipierro S. (1994) The role of the ascorbic acid system in delaying the senescence of oat (*Avena saliva L.*) leaf segments. *J Plant Physiol.* **144:** 161-166;

Bowler C., VanMontagu M. and Inzé D. (1992) Superoxide dismutase and stress tolerance. *Annu Rev Plant Physiol Plant Mol Biol.* **43:** 83–116;

Bradford M.M. (1976) A rapid and sensitive method for the quantifi¬cation of microgram quantities of protein utilizing the principle of protein-dye binding. *Anal. Biochem.* **72:** 248-254;

Branca F. and Ferrari M. (2002) Impact of micronutrient deficiencies on growth: the stunting syndrome. *Ann Nutr Metab.* **46:** 8-17;

Brandolini A., Hidalgo A., Plizzaria L. and Erba D. (2011) Impact of genetic and environmental factors on einkorn wheat (*Triticum monococcum L. subsp. monococcum*) polysaccharides. *J Cereal Sci.* **53:** 65–72;

Brighenti F. (2007) Dietary fructans and serum triacylglycerols: a meta-analysis of randomized controlled trials. *J Nutr*. **137:** 2552S-2556S;

Bueno P., Varela J., Gimeenez-Gallego G. and del Rio L.A. (1995) Peroxisomal copper, zinc superoxide dismutase: characterization of the isoenzyme from watermelon cotyledons. *Plant Physiol.* **108:** 1151–1160;

Sara Cimini

Buitink J., Hemminga M.A. and Hoekstra F.A. (2000) Is there a role for oligosaccharides in seed longevity? An assessment of intracellular glass stability. *Plant Physiol.* **122:** 1217-1224;

Burchi F., Fanzo J. and Frison E. (2011) The Role of Food and Nutrition System Approaches in Tackling Hidden Hunger. *Int J Environ Res Public Health.* **8:** 358-373;

Bury M., Novo-Uzal E., Andolfi A., Cimini S., Wauthoz N., Heffeter P., Lallemand B., Avolio F., Delporte C., Cimmino A., Van Antwerpen P., Zonno M.C., Vurro M., Poumay Y., Berger W., Evidente A., De Gara L., Kiss R. and Locato V. (2012) Ophiobolin A, a fungal sesterpenoid phytotoxin, displays high *in vitro* growth-inhibitory effects in mammalian than in plant cells and it also display *in vivo* antitumor activity. *Int J Oncol.* (Submitted);

Cairns A.J. (2003) Fructan biosynthesis in transgenic plants. *J Exp Bot.* **54:** 549-567;

Canonica L., Fiecchi A., Galli Kienle M. and Scala A. (1966b) Isolation and constitution of cochliobolin B. *Tetrahedron Lett.* **13:** 1329-1333;

Canonica L., Fiecchi A., Kienle M.G. and Scala A. (1966a) The constitution of cochliobolin. *Tetrahedron Lett.* **11:** 1211-1218;

Cereghino J.L. and Cregg J.M. (2000) Heterologous protein expression in the methylotrophic yeast *Pichia pastoris*. *FEMS Microbiol Rev.* **24:** 45-66;

Chalmers J., Lidgett A., Cummings N., Cao Y., Forster J. and Spangenberg G. (2005) Molecular genetics of fructan metabolism in perennial ryegrass. *Plant Biotechnol J.* **3:** 459-374;

Charmet G. (2011) Wheat domestication: lessons for the future. *C R Biol.* **334:** 212-220;

Chatterton N.J., Harrison P.A. (1997) Fructan oligomers in *Poa ampla*. *New Phytol.* **136:** 3-10;

Chatterton N.J., Harrison P.A., Thornley W.R. and Bennett J.H. (1993) Structures of Fructan Oligomers in Orchardgrass (*Dactylis glomerata L.*). *J Plant Physiol.* **142:** 552–556;

Chattopadhyay A.K. And Samaddar K.R. (1980) Effects of Helminthosporium oryzae Infection and Ophiobolin on the Phenol Metabolism of Host Tissues. *J Phytopath.* **98:** 193–202;

Chen J.Q. and Black C.C. (1992) Biochemical and immunological properties of alkaline invertase isolated from sprouting soybean hypocotyls. *Archives of Biochemistry and Biophysics*. **295:** 61–69;

Chen K. and Arora R. (2011). Dynamics of the antioxidant system during seed osmopriming, post-priming germination and seedling establishment in Spinach (*Spinacia oleracea*). *Plant Sci.* **180:** 212-220;

Chinnusamy V., Schumaker K. and Zhu J.K. (2004) Molecular genetic perspectives on cross-talk and specificity in abiotic stress signalling in plants. *J Exp Bot.* **55:** 225-236;

Chiu J. and Dawes I.W. (2012) Redox control of cell proliferation. *Trends Cell Biol.* **22:** 592-601;

Choi H.W., Kim Y.J., Lee S.C., Hong J.K. and Hwang B.K. (2007) Hydrogen peroxide generation by the pepper extracellular peroxidase CaPO2 activates local and systemic cell death and defense response to bacterial pathogens. *Plant Physiol.* **145:** 890-904;

Sara Cimini

Chono M., Honda I., Shinoda S., Kushiro T., Kamiya Y., Nambara E., Kawakami N., Kaneko S. and Watanabe Y. (2006) Field studies on the regulation of abscisic acid content and germinability during grain development of barley: molecular and chemical analysis of pre-harvest sprouting. *J Exp Bot.* **57:** 2421-2434;

Chrispeels M.J. (2000) Biotechnology and the poor. *Plant Physiol.* **124:** 3-6;

Chuankhayan P., Hsieh C.Y., Huang Y.C., Hsieh Y.Y., Guan H.H., Hsieh Y.C., Tien Y.C., Chen C.D., Chiang C.M. and Chen C.J. (2010) Crystal structures of Aspergillus japonicus fructosyltransferase complex with donor/acceptor substrates reveal complete subsites in the active site for catalysis. *J Biol Chem.* **285:** 23251-23264;

Coccuci S.M., Morgutti S., Coccuci M. and Gianani L. (1983) Effects of ophiobolin A on potassium permeability, transmembrane electrical potential and proton extrusion in maize roots. *Plant Sci Lett.* **32:** 9-16;

Couée I., Sulmon C., Gouesbet G. and El Amrani A. (2006) Involvement of soluble sugars in reactive oxygen species balance and responses to oxidative stress in plants. *J Exp Bot.* **57:** 449–459;

Cregg J.M., Vedvick T.S. and Raschke W.C. (1993) Recent advances in the expression of foreign genes in *Pichia pastoris*. *Bio/Technology*. **11**: 905-910;

Cummings J.H. and Macfarlane G.T. (2002) Gastrointestinal effects of prebiotics. *Br J Nutr.* **87:** S145-151;

Cutler H.G., Crumley F.G., Cox R.H., Springer J.P., Arrendale R.F., Cole R.J. and Cole P.D. (1984) Ophiobolins G and H: new metabolites from a novel source, *Aspergillus ustus*. *J Agric Food Chem.* **32:** 778-782;

Dalton T.P., Shertzer H.G. and Puga A. (1999) Regulation of gene expression by reactive oxygen. *Annu. Rev. Pharmacol. Toxicol.* **39:** 67–101;

Daly R. and Hearn M.T. (2005) Expression of heterologous proteins in *Pichia pastoris*: a useful experimental tool in protein engineering and production. *J Mol Recognit.* **18**:119-138;

D'Arcy-Lameta A., Ferrari-Iliou R., Contour-Ansel D., Pham-Thi A.T. amd Zuily-Fodil Y. (2006) Isolation and characterization of four ascorbate peroxidase cDNAs responsive to water deficit in cowpea leaves. *Ann Bot.* **97:** 133-140;

Davies G.J., Wilson K.S. and Henrissat B. (1997) Nomenclature for sugar-binding subsites in glycosyl hydrolases. *Biochem J.* **321:** 557–559;

De Block M., Verduyn C., De Brouwer D. and Cornelissen M. (2004) Generating stress tolerant crops by economizing energy consumption. *Pflanzenschutz-Nachrichten Bayer.* **57:** 105-110;

De Block M., Verduyn C., De Brouwer D., Cornelissen M. (2005) Poly(ADP-ribose) polymerase in plants affects energy homeostasis, cell death and stress tolerance. *The Plant J.* **41:** 95–106;

De Coninck B., Le Roy K., Francis I., Clerens S., Vergauwen R., Halliday A.M., Smith S.M., Van Laere A. and Van den Ende W. (2005) Arabidopsis AtcwINV3 and 6 are not invertases but are fructan exohydrolases (FEHs) with different substrate specificities. *Plant Cell Environ.* **28:** 432-443;

Sara Cimini

De Gara L. (2004) Ascorbate metabolism and plant growth – from germination to cell death. In H Asard, J May, N Smirnoff, eds, Vitamin C: its function and biochemistry in animals and plants. BIOS Scientific Publishers Ltd, Oxford, 83-95;

De Gara L., de Pinto M.C. and Tommasi F. (2003b) The antioxidant systems vis-à-vis reactive oxygen species during plant–pathogen interaction. *Plant Physiol Biochem.* **41:** 863–870;

De Gara L., de Pinto M.C., Moliterni V.M. and D'Egidio M.G. (2003a) Redox regulation and storage processes during maturation in kernels of Triticum durum. *J Exp Bot.* **54:** 249-258;

De Gara L., Locato V., Dipierro S. and de Pinto M.C. (2010) Redox homeostasis in plants. The challenge of living with endogenous oxygen production. *Respir Physiol Neurobiol.* **173:** S13-9;

de Pinto M.C., Francis D. and De Gara L. (1999) The redox state of the ascorbate-dehydroascorbate pair as a specific sensor of cell division in tobacco BY-2 cells. *Protoplasma.* **209:** 90-97;

de Pinto M.C., Locato V., De Gara L. (2012) Redox regulation in plant programmed cell death. *Plant Cell Environ.* **35:** 234-244;

de Pinto M.C., Paradiso A., Leonetti P., De Gara L. (2006) Hydrogen peroxide, nitric oxide and cytosolic ascorbate peroxidase at the crossroad between defence and cell death. *The Plant J.* **48:** 784-795;

de Pinto M.C., Tommasi F., De Gara L. (2002) Changes in the antioxidant systems as part of the signalling pathway responsible for the programmed cell death activated by nitric oxide and reactive oxygen species in tobacco BY-2 cells. *Plant Physio.* **130:** 698-708;

de Pinto M.C., Tommasi, F. and De Gara L. (2000) Enzymes of the ascorbate biosynthesis and ascorbate-glutathione cycle in cultured cells of tobacco Bright Yellow 2. *Plant Physiol and Biochem.* **38:** 541-550;

De Roover J., Vandenbranden K., Van Laere A. and Van den Ende W. (2000) Drought induces fructan synthesis and 1-SST (sucrose:sucrose fructosyltransferase) in roots and leaves of chicory seedlings (*Cichorium intybus L.*). *Planta.* **210:** 808-814;

DeClerck F.A.J., Fanzo J., Palm C. and Remans R. (2011) Ecological approaches to human nutrition. *Food Nutrition Bull.* **32:** S41-S50;

Demel R.A., Dorrepaal E., Ebskamp M.J., Smeekens J.C. and de Kruijff B. (1998) Fructans interact strongly with model membranes. *Biochim Biophys Acta.* **1375:** 36-42;

Desikan R., A-H-Mackerness S., Hancock J.T. and Neill S.J. (2001) Regulation of the Arabidopsis transcriptome by oxidative stress. *Plant Physiol.* **127:** 159-172;

Dewanto V., Wu X., Adom K.K. and Liu R.H. (2002) Thermal processing enhances the nutritional value of tomatoes by increasing total antioxidant activity. *J Agric Food Chem.* **50:** 3010-3014;

Diaz Vivancos P., Wolff T., Markovic J., Pallardó F.V. and Foyer C.H. (2010) A nuclear glutathione cycle within the cell cycle. Biochem J. 431: 169-178;

Dietz K.J. (2011) Peroxiredoxins in plants and cyanobacteria. *Antioxid Redox Signal.* **15:** 1129-1159;

Sara Cimini

Dietz K.J., Horling F., König J. and Baier M. (2002) The function of the chloroplast 2-cysteine peroxiredoxin in peroxide detoxification and its regulation. *J Exp Bot.* **53:** 1321-1329;

Dinneny J.R., Long T.A., Wang J.Y., Jung J.W., Mace D., Pointer S., Barron C., Brady S.M., Schiefelbein J. and Benfey P.N. (2008) Cell identity mediates the response of Arabidopsis roots to abiotic stress. *Science.* **320:** 942-945;

Dolferus R., Ji X. and Richards R.A. (2011) Abiotic stress and control of grain number in cereals. *Plant Sci.* **181:** 331-341;

Dorey S., Bailleul F., Saindrenan P., Fritig B. and Kauffmann S. (1998) Tobacco class I and II catalases are differentially expressed during elicitor-induced hypersensitive cell death and localized acquired resistance. *Mol Plant Microb Int.* **11:** 1102-1109;

Dowdle J., Ishikawa T., Gatzek S., Rolinski S. and Smirnoff N. (2007) Two genes in *Arabidopsis thaliana* encoding GDP-L-galactose phosphorylase are required for ascorbate biosynthesis and seedling viability. *Plant J.* **52:** 673-689;

Dubcovsky J. and Dvorak J. (2007) Genome plasticity a key factor in the success of polyploidy wheat under domestication. *Science.* **316:** 1862–1866;

Duchateau N., Bortlik K., Simmen U., Wiemken A. and Bancal P. (1995) Sucrose:Fructan 6-Fructosyltransferase, a key enzyme for diverting carbon from sucrose to fructan in barley leaves. *Plant Physiol.* **107:** 1249–1255;

Dynowski M., Schaaf G., Loque D., Moran O. and Ludewig U. (2008) Plant plasma membrane water channels conduct the signalling molecule H_2O_2. *Biochem J.* **414:** 53-61;

Edelman J. and Jefford T.G. (1968) The mechanism of fructosan metabolism in higher plants as exemplified in *Helianthus tuberosus*. *New Phytol.* **67:** 517–531;

Efron B., Halloran E. and Holmes S. (1996) Bootstrap confidence levels for phylogenetic trees. *Proc Natl Acad Sci USA.* **93:** 7085-7090;

Ellis C., Turner J.G. and Devoto A. (2002) Protein complexes mediate signalling in plant responses to hormones, light, sucrose and pathogens. *Plant Mol Biol.* **50:** 971-980;

Ellis S.B., Brust P.F., Koutz P.J., Waters A.F., Harpold M.M. and Gingeras T.R. (1985) Isolation of Alcohol Oxidase and Two other Methanol Regulatable Genes from the Yeast, *Pichia pastoris*. *Mol. Cell. Biol.* **5**: 1111-1121;

Elstner E.F. (1991) Mechanisms of oxygen activation in different compartments of plant cells. In Active Oxygen/Oxidative Stress in Plant Metabolis, eds. EJ Pelland, KL Steffen. Rockville, MD: Am. Soc. Plant Physiol. 13–25;

Evers T. and Millar S. (2002) Cereal grain structure and development: some implications for quality. *J Cereal Sci.* **36:** 261–284;

Evidente A., Andolfi A., Cimmino A., Vurro M., Fracchiolla M. and Charudattan R. (2006) Herbicidal potential of ophiobolins produced by *Drechslera gigantea*. *J Agric Food Chem.* **54:** 1779-1783;

FAO (1996) Rome Declaration on World Food Security and World Food Summit Plan of Action;

FAO (2005) 31st Session of the Committee on World Food Security. Special Event on Impact of Climate Change, Pests and Disease on Food Security and Poverty Reduction;

Sara Cimini

FAO (2009) The state of food insecurity in the world;

FAO (2012) Crop prospects and food situation (June 2012);

FAOSTAT (2011) http://faostat.fao.org/site/567/default.aspx#ancor (accessed, March 2011);

Fardet A. (2010) New hypotheses for the health-protective mechanisms of whole-grain cereals: what is beyond fibre? *Nutr Res Rev.* **23:** 65-134;

Feldman M. (1995) Wheats. In: Smartt J, Simmonds NW, eds. Evolution of crop plants. Harlow, UK: Longman Scientific and Technical, 185–192;

Feldman M. (2001) Origin of cultivated wheat. In: Bonjean AP, Angus WJ, eds. The world wheat book: a history of wheat breeding. Paris, France: Lavoisier Publishing, 3–56;

Feurtado J.A. and Kermode A.R. (2007) A merging of paths: abscisic acid and hormonal cross-talk in the control of seed dormancy maintenance and alleviation. In: Bradford KJ, Nonogaki H, eds. Seed development, dormancy and germination. Oxford: Blackwell Publishing. 176–223;

Foley J.A., Ramankutty N., Brauman K.A., Cassidy E.S., Gerber J.S., Johnston M., Mueller N.D., O'Connell C., Ray D.K., West P.C., Balzer C., Bennett E.M., Carpenter S.R., Hill J., Monfreda C., Polasky S., Rockström J., Sheehan J., Siebert S., Tilman D. and Zaks D.P.M. (2011) Solutions for a cultivated planet. *Nature.* **478:** 337-342;

Foyer C.H. and Harbinson J.C. (1994) Oxygen metabolism and the regulation of photosynthetic electron transport. In Causes of Photooxidative Stress and Amelioration of Defense Systems in Plant, eds. CH Foyer, PM Mullineaux. 1–42;

Foyer C.H. and Noctor G. (2005) Redox homeostasis and antioxidant signaling: a metabolic interface between stress perception and physiological responses. *Plant Cell.* **17:** 1866-1875;

Foyer C.H. and Noctor G. (2009) Redox regulation in photosynthetic organisms: signaling, acclimation, and practical implications. *Antioxid Redox Signal.* **11:** 861-905;

Foyer C.H., Souriau N., Perret S., Lelandais M., Kunert K.J., Pruvost C. and Jouanin L. (1995) Overexpression of glutathione reductase but not glutathione synthetase leads to increases in antioxidant capacity and resistance to photoinhibition in poplar trees. *Plant Physiol.* **109:** 1047–1057;

Foyer C.H., Theodoulou F.L. and Delrot S. (2001) The functions of inter- and intracellular glutathione transport systems in plants. *Trends Plant Sci.* **6:** 486-492;

Fujishima M., Sakai H., Ueno K., Takahashi N., Onodera S., Benkeblia N. and Shiomi N. (2005) Purification and characterization of a fructosyltransferase from onion bulbs and its key role in the synthesis of fructo-oligosaccharides *in vivo*. *New Phytol.* **165:** 513-524;

Fukushima Y., Sakagami Y. and Marumo S. (1993) β-Glucan biosynthesis inhibitors isolated from fungi as hyphal malformation inducer. *Bioorg Med Chem Lett*. **3:** 1219-1222;

Galinski E.A. (1993) Compatible solutes of halophilic eubacteria: molecular principles, water-solute interaction, stress protection. *Experientia.* **49:** 487-496;

Gawlik-Dziki U., Świeca M. and Dziki D. (2012) Comparison of phenolic acids profile and antioxidant potential of six varieties of spelt (*Triticum spelta L.*). *J Agric Food Chem.* **60:** 4603-4612;

Sara Cimini

Gayed S.K. (1962) The pathogenicity of six strains of Helminthosporium sativum to three cereals with special reference to barley. *Mycopathol Mycol Appl.* **18:** 271-279;

Gechev T.S. and Hille J. (2005) Hydrogen peroxide as a signal controlling plant programmed cell death. *J Cell Biol.* **168:** 17-20;

Gianani L., Cocucci S., Pardi D. And Randazzo G. (1979) Effects of ophiobolin B on cell enlargement and H^+/K^+ exchange in maize coleoptile tissues. *Planta.* **146:** 271-274;

Gibson G.R, Beatty E.R, Wang X, Cummings J.H. (1995) Selective stimulation of bifidobacteria in the human colon by oligofructose and inulin. *Gastroenterology.* **108:** 975-982;

Gibson G.R. and Roberfroid M.B. (1995) Dietary modulation of the human colonic microbiota: introducing the concept of prebiotics. *J Nutr.* **125:** 1401-1412;

Gibson S.I. (2005) Control of plant development and gene expression by sugar signaling. *Curr Opin Plant Biol.* **8:** 93-102;

Gill S.S. and Tuteja N. (2010) Reactive oxygen species and antioxidant machinery in abiotic stress tolerance in crop plants. *Plant Physiol Biochem.* **48:** 909-930;

Girotti A.W. (2001) Photosensitized oxidation of membrane lipids: reaction pathways, cytotoxic effects and cytoprotective mechanisms. *J Photochem Photobiol.* **63:** 103–13;

Golden M.H.N. (1991) The nature of nutritional deficiency in relation to growth failure and poverty. *Acta Paediatr Scand Suppl.* **374:** 95-110;

Gong B., Cukan M., Fisher R., Li H., Stadheim T.A. and Gerngross T. **(2009)** Characterization of N-linked glycosylation on recombinant glycoproteins produced in *Pichia pastoris* using ESI-MS and MALDI-TOF. *Methods Mol Biol.* 534: 213-223;

Goosen C., Yuan X.L., van Munster J.M., Ram A.F., van der Maarel M.J. and Dijkhuizen L. (2007) Molecular and biochemical characterization of a novel intracellular invertase from *Aspergillus niger* with transfructosylating activity. *Eukaryot Cell.* **6:** 674-681;

Gornall J., Betts R., Burke E., Clark R., Camp J., Willett K. and Wiltshire A. (2010) Implications of climate change for agricultural productivity in the early twenty-first century. *Phil Trans R Soc B.* **365:** 2973–2989;

Graham R.D., Welch R.M., Saunders D.A., Ortiz-Monasterio I., Bouis H.E., Bonierbale M., de Haan S., Burgos G., Thiele G., Liria R., Meisner C.A., Beebe S.E., Potts M.J., Kadian M., Hobbs P.R., Gupta R.K. and Twomlow S. (2007) Nutritious subsistence food systems. *Adv Agron.* **92:** 1-74;

Grantham-McGregor S.M. and Ani C.C. (1999) The role of micronutrients in psychomotor sad cognitive development. *Br Med Bull.* **55:** 511-527;

Guex N. and Peitsch M.C. (1997) SWISS MODEL and the Swiss-Pdb Viewer: An environment for comparative protein modeling. *Electrophoresis*. **18:** 2714-2723;

Hafner S. (2003) Trends in maize, rice and wheat yields for 188 nations over the past 40 years: a prevalence of linear growth. *Agric Ecosyst Environ.* **97:** 275-283;

Halliwell B. (2006) Reactive species and antioxidants. Redox biology is a fundamental theme of aerobic life. *Plant Physiol.* **141:** 312-322;

Sara Cimini

Hendry G.A.F. (1993) Evolutionary origins and natural functions of fructans – a climatological, biogeographic and mechanistic appraisal. *New Phytol.* **123:** 3-14;

Hendry G.A.F. and Wallace R.K. (1993) The origin, distribution and evolutionary significance of fructans. In M. Suzuki, N.J. Chatterton, Sci. and Technol. of Fructans. CRC Press, Boca Raton, FL. 119-139;

Henson C.A. and Livingston D.P.3rd (1998) Characterization of a fructan exohydrolase purified from barley stems that hydrolyzes multiple fructofuranosidic linkages. *Plant Physiol Biochem.* **36:** 715-720;

Herbette S., Lenne C., Leblanc N., Julien J.L., Drevet J.R. and Roeckel-Drevet P. (2002) Two GPX-like proteins from *Lycopersicon esculentum* and *Helianthus annuus* are antioxidant enzymes with phospholipid hydroperoxide glutathione peroxidase and thioredoxin peroxidase activities. *Eur J Biochem.* **269:** 2414-2420;

Heun M., Schäfer-Pregl R., Klawan D., Castagna R., Accerbi M., Borghi B. and Salamini F. (1997) Site of einkorn wheat domestication identified by DNA fingerprinting. *Science*. **278:** 1312–1314;

Hincha D.K., Livingston D.P.3rd, Premakumar R., Zuther E., Obel N., Cacela C. and Heyer A.G. (2007) Fructans from oat and rye: composition and effects on membrane stability during drying. *Biochim Biophys Acta.* **1768:** 1611-1619;

Hincha D.K., Zuther E., Hellwege E.M. and Heyer A.G. (2002) Specific effects of fructo- and gluco-oligosaccharides in the preservation of liposomes during drying. *Glycobiology.* **12:** 103-110;

Hisano H., Kanazawa A., Yoshida M., Humphreys M.O., Iizuka M., Kitamura K. and Yamada T. (2008) Coordinated expression of functionally diverse fructosyltransferase genes is associated with fructan accumulation in response to low temperature in perennial ryegrass. *New Phytol.* **178:** 766-780;

Houot V., Etienne P., Petitot A.S., Barbier S., Blein J.P. and Suty L. (2001) Hydrogen peroxide induces programmed cell death features in cultured tobacco BY-2 cells in a dose-dependent manner. *J Exp Bot.* **52:** 1721-1730;

Hull M.R., Long S.P. and Jahnke L.S. (1997) Instantaneous and developmental effects of low temperature on the catalytic properties of antioxidant enzymes in two Zea species. *Austral J Plant Physiol.* **24:** 337-343;

Huynh B.L., Mather D.E., Schreiber A.W., Toubia J., Baumann U., Shoaei Z., Stein N., Ariyadasa R., Stangoulis J.C., Edwards J., Shirley N., Langridge P. and Fleury D. (2012) Clusters of genes encoding fructan biosynthesizing enzymes in wheat and barley. *Plant Mol Biol.* **80:** 299-314;

Huynh B.L., Wallwork H., Stangoulis J.C., Graham R.D., Willsmore K.L., Olson S. and Mather D.E. (2008) Quantitative trait loci for grain fructan concentration in wheat (*Triticum aestivum L.*). *Theor. Appl. Genet.* **117:** 701–709;

Ishibashi Y., Yamamoto K., Tawaratsumida T., Yuasa T. and Iwaya‐Inoue M. (2008) Hydrogen peroxide scavenging regulates germination ability during wheat (*Triticum aestivum L.*) seed maturation. *Plant Signal Behav.* **3:** 183-188;

Isla M.I., Salerno G., Pontis H., Vattuone M.A. and Sampietro A.R. (1995) Purification and properties of soluble acid invertase from *Oryza sativa*. *Phytochemistry*. **38:** 321-325;

Sara Cimini

Itai A., Nozoe S., Tsuda K. and Okuda S. (1967) The structure of cephalonic acid, a pentaprenyl terpenoid. *Tetrahedron Lett.* **42:** 4111-4112;

Jacobsen J.V., Pearce D.W., Poole A.T., Pharis R.P. and Mander L.N. (2002) Abscisic acid, phaseic acid and gibberellin contents associated with dormancy and germination in barley. *Physiol Plant.* **115:** 428-441;

Jaggard K.W., Qi A. and Ober E.S. (2010) Possible changes to arable crop yields by 2050. *Phil Trans R Soc B.* **365:** 2835-2851;

Jahnke L.S., Hull M.R. and Long S.P. (1991) Chilling stress and oxygen metabolizing enzymes in *Zea mays* and *Zea diploperennis*. *Plant Cell Environ.*. **14:** 97-104;

Jain N.K. and Roy I. (2010) Trehalose and protein stability. *Curr Protoc Protein Sci.* Chapter 4: Unit 4.9;

Jaleel C.A., Riadh K., Gopi R., Manivannan P., Inès J., Al-Juburi H.J., Chang-Xing Z., Hong-Bo S. and Panneerselvam R. (2009) Antioxidant defense responses: physiological plasticity in higher plants under abiotic constraints. *Acta Physiol Plant.* **31:** 427-436;

Jaspers P. and Kangasjärvi J. (2010) Reactive oxygen species in abiotic stress signaling. *Physiol Plant.* **138:** 405-413;

Jiang K. and Feldman L.J. (2005). Regulation of root apical meristem development. *Annu Rev Cell Dev Biol.* **21:** 485–509;

Jiang K., Ballinger T., Li D., Zhang S. and Feldman L. (2006). A role for mitochondria in the establishment and maintenance of the maize root quiescent center. *Plant Physiol.* **140:** 1118–1125;

Jovanović N., Bouchard A., Hofland G.W., Witkamp G.J., Crommelin D.J. and Jiskoot W. (2006) Distinct effects of sucrose and trehalose on protein stability during supercritical fluid drying and freeze-drying. *Eur J Pharm Sci.* **27:** 336-345;

Jung B.G., Lee K.O., Lee S.S., Chi Y.H., Jang H.H., Kang S.S., Lee K., Lim D., Yoon S.C., Yun D.J., Inoue Y., Cho M.J. and Lee S.Y. (2002) A Chinese cabbage cDNA with high sequence identity to phospholipid hydroperoxide glutathione peroxidases encodes a novel isoform of thioredoxin-dependent peroxidase. *J Biol Chem.* **277:** 12572-12578;

Kampfenkel K., Van Montagu M. and Inzé D. (1995) Effects of iron excess on *Nicotiana plumbaginifolia* plants. *Plant Physiol.* **107:** 725-735;

Kar R.K. (2011) Plant responses to water stress: role of reactive oxygen species. *Plant Signal Behav.* **6:** 1741-1745;

Kawakami A. and Yoshida M. (2002) Molecular characterization of sucrose:sucrose 1-fructosyltransferase and sucrose:fructan 6-fructosyltransferase associated with fructan accumulation in winter wheat during cold hardening. *Biosci Biotechnol Biochem.* **66:** 2297-305;

Kawakami A. and Yoshida M. (2005) Fructan:fructan 1-fructosyltransferase, a key enzyme for biosynthesis of graminan oligomers in hardened wheat. *Planta.* **223:** 90-104;

Kawakami A., Yoshida M. and Van den Ende W. (2005) Molecular cloning and functional analysis of a novel 6&1-FEH from wheat (*Triticum aestivum L.*) preferentially degrading small graminans like bifurcose. *Gene.* **358:** 93-101;

Sara Cimini

Kennedy G., Pedro M.R., Seghieri C., Nantel G. and Brouwer I. (2007) Dietary diversity score is a useful indicator of micronutrient intake in non breast-feeding Filipino children. *J Nutr.* **137:** 1-6;

Kern M. (2002) Food, Feed, Fibre, Fuel and industrial products of the future: challenges and opportunities. Understanding the strategies potential of plant genetic engineering. *J Agron Crop Sci.* **188:** 291-305;

Kishor P., Hong Z., Miao G.H., Hu C. and Verma D. (1995) Overexpression of [delta]-Pyrroline-5-Carboxylate Synthetase Increases Proline Production and Confers Osmotolerance in Transgenic Plants. *Plant Physiol.* **108:** 1387-1394;

Klessig D.F., Durner J., Noad R., Navarre D.A., Wendehenne D., Kumar D., Zhou J.M., Shah J., Zhang S., Kachroo P., Trifa Y., Pontier D., Lam E. and Silva H. (2000) Nitric oxide and salicylic acid signaling in plant defense. *Proc Natl Acad Sci.* **97:** 8849-8855;

Kliebenstein D.L., Monde R.-A. and Last R.L. (1998) Superoxide dismutase in Arabidopsis: An eclectic enzyme family with dispartate regulation and protein localozation. *Plant Physiol.* **118:** 637-650;

Knudsen K.E.B. (1997) Carbohydrate and lignin contents of plant materials used in animal feeding. *Anim Feed Sci Technol.* **67:** 319-338;

Kobayashi M., Kawakita K., Maeshima M., Doke N. and Yoshioka H. (2006) Subcellular localization of Strboh proteins and NADPH-dependent O_2^--generating activity in potato tuber tissues. *J Exp Bot.* **57:** 1373-1379;

Konno Y., Vedvick T., Fitzmaurice L. and Mirkov T.E. (1993) Purification, characterization, and subcellular localization of soluble invertase from tomato fruit. *J Plant Physiol*. **141:** 385-392;

Koops A.J. and Jonker H.H. (1996) Purification and characterization of the enzymes of fructan biosynthesis in tubers of *Helianthus tuberosus* Colombia (II. Purification of sucrose:sucrose 1-fructosyltransferase and reconstitution of fructan synthesis *in vitro* with purified sucrose:sucrose 1-fructosyltransferase and fructan:fructan 1-fructosyltransferase). *Plant Physiol.* **110:** 1167–1175;

Koutz P.J., Davis G.R., Stillman C, Barringer K., Cregg J.M. and Thill G. (1989) Structural Comparison of the *Pichia pastoris* Alcohol Oxidase Genes. *Yeast.* **5:** 167-177;

Kovtun Y., Chiu W.L., Tena G. and Sheen J. (2000) Functional analysis of oxidative stress-activated mitogen-activated protein kinase cascade in plants. *Proc Natl Acad Sci USA.* **97:** 2940-2945;

Kvaratskhelia M., Winkel C. and Thorneley R.N. (1997) Purification and characterization of a novel class III peroxidase isoenzyme from tea leaves. *Plant Physiol.* **114:** 1237-1245;

Lachaud C., Da Silva D., Amelot N., Béziat C., Brière C., Cotelle V., Graziana A., Grat S., Mazars C. and Thuleau P. (2011) Dihydrosphingosine-induced programmed cell death in tobacco BY-2 cells is independent of H_2O_2 production. *Mol Plant.* **4:** 310-318;

Lammens W., Le Roy K., Schroeven L., Van Laere A., Rabijns A. and Van den Ende W. (2009) Structural insights into glycoside hydrolase family 32 and 68 enzymes: functional implications. *J Exp Bot.* **60:** 727-740;

Lammens W., Le Roy K., Van Laere A., Rabijns A. and Van den Ende W. (2008) Crystal structures of *Arabidopsis thaliana* cell-wall invertase mutants in complex with sucrose. *J Mol Biol.* **377:** 378-385;

Lammens W., Le Roy K., Yuan S., Vergauwen R., Rabijns A., Van Laere A., Strelkov S.V. and Van den Ende W. (2012) Crystal structure of 6-SST/6-SFT from *Pachysandra terminalis*, a plant fructan biosynthesizing enzyme in complex with its acceptor substrate 6-kestose. Plant J. **70:** 205-219;

Langridge P., Paltridge N. and Fincher G. (2006) Functional genomics of abiotic stress tolerance in cereals. *Brief Funct Genomic Proteomic.* **4:** 343-354;

Lasseur B., Lothier J., Djoumad A., De Coninck B., Smeekens S., Van Laere A., Morvan-Bertrand A., Van den Ende W. and Prud'homme M.P. (2006) Molecular and functional characterization of a cDNA encoding fructan:fructan 6G-fructosyltransferase (6G-FFT)/fructan:fructan 1-fructosyltransferase (1-FFT) from perennial ryegrass (Lolium perenne L.). *J Exp Bot.* **57:** 2719-2734;

Le Roy K., Lammens W., Van Laere A. and Van den Ende W. (2008) Influencing the binding configuration of sucrose in the active sites of chicory fructan 1-exohydrolase and sugar beet fructan 6-exohydrolase. *New Phytol.* **178:** 572-580;

Le Roy K., Lammens W., Verhaest M., De Coninck B., Rabijns A., Van Laere A. and Van den Ende W. (2007a) Unraveling the difference between invertases and fructan exohydrolases: a single amino acid (Asp-239) substitution transforms Arabidopsis cell wall invertase1 into a fructan 1-exohydrolase. *Plant Physiol.* **145:** 616-625;

Le Roy K., Vergauwen R., Cammaer V., Yoshida M., Kawakami A., Van Laere A. and Van den Ende W. (2007b) Fructan 1-exohydrolase is associated with flower opening in *Campanula rapunculoides. Funct Plant Biol.* **34:** 972–983;

Leakey A.D.B. (2009) Rising atmospheric carbon dioxide concentration and the future of C4 crops for food and fuel. *Proc Biol Sci.* **276:** 2333–2343;

Lee H.S. and Sturm A. (1996) Purification and characterization of neutral and alkaline invertase from carrot. *Plant Physiol.* **112:** 1513–1522;

Lee S.H., Ahsan N., Lee K.W., Kim D.H., Lee D.G., Kwak S.S., Kwon S.Y., Kim T.H. and Lee B.H. (2007) Simultaneous overexpression of both CuZn superoxide dismutase and ascorbate peroxidase in transgenic tall fescue plants confers increased tolerance to a wide range of abiotic stresses. *J Plant Physiol.* **164:** 1626-1638;

Léon P. and Sheen J. (2003) Sugar and hormone connections. *Trends Plant Sci.* **8:** 110-116;

Leung P.C., Taylor W.A., Wang J.H. and Tipton C.L. (1984) Ophiobolin A. A natural product inhibitor of calmodulin. *J Biol Chem.* **259:** 2742-2747;

Leung P.C., Taylor W.A., Wang J.H. and Tipton C.L. (1985) Role of calmodulin inhibition in the mode of action of ophiobolin A. *Plant Physiol.* **77:** 303 -308;

Levine A., Tenhaken R., Dixon R. and Lamb C. (1994) H_2O_2 from the oxidative burst orchestrates the plant hypersensitive disease resistance response. *Cell.* **79:** 583-593;

Lewis D.H. (1984) Occurrence and distribution of storage carbohydrates in vascular plants. In: Storage Carbohydrates in Vascular Plants (Ed. By D.H. Lewis). 1-52;

Sara Cimini

Lewis D.H. (1993) Nomenclature and diagrammatic representation of oligomeric fructans - a paper of discussion. *New Phytol.* **124:** 583-594;

Liang Y.C., Hsu C.Y., Yao Y.L. and Yang W.M. (2013) PARP-2 regulates cell cycle-related genes through histone deacetylation and methylation independently of poly(ADP-ribosyl)ation. *Biochem Biophys Res Commun;*

Livingston D.P. 3rd, Hincha D.K. and Heyer A.G. (2009) Fructan and its relationship to abiotic stress tolerance in plants. *Cell Mol Life Sci.* **66:** 2007–2023;

Livingston D.P.3rd and Henson C.A. (1998) Apoplastic sugars, fructans, fructanexohydrolase, and invertase in winter oat: responses to second-phase cold hardening. *Plant Physiol.* **116:** 403-408;

Livingston D.P.3rd, Chatterton N.J. and Harrison P.A. (1993) Structure and quantity of fructan oligomers in oat (*Avena* spp.). *New Phytol.* **123:** 725-734;

Livingston D.P.3rd, Hincha D.K. and Heyer A.G. (2009) Fructan and its relationship to abiotic stress tolerance in plants. *Cell Mol Life Sci.* **66:** 2007–2023;

Locato V., Balestrazzi A., De Gara L. and Carbonera D. (2006) Reduced expression of top1beta gene induces programmed cell death and alters ascorbate metabolism in *Daucus carota* cultured cells. *J Exp Bot.* **57:** 1667-1676;

Locato V., de Pinto M.C. and De Gara L. (2009) Different involvement of the mitochondrial, plastidial and cytosolic ascorbate-glutathione redox enzymes in heat shock responses. *Physiol Plant.* **135:** 296-306;

Locato V., Gadaleta C., De Gara L. and de Pinto M.C. (2008) Production of reactive species and modulation of antioxidant network in response to heat shock: a critical balance for cell fate. *Plant Cell Environ.* **31:** 1606-1619;

Loreti E., Poggi A., Novi G., Alpi A. and Perata P. (2005) A genome-wide analysis of the effects of sucrose on gene expression in Arabidopsis seedlings under anoxia. *Plant Physiol.* **137:** 1130-1138;

Maleux K. and Van den Ende W. (2007) Levans in excised leaves of *Dactylis glomerata*: effects of light, sugars, temperature and senescence. *J Plant Biology.* **50:** 671-680;

Manach C., Scalbert A., Morand C., Rémésy C. and Jiménez L. (2004) Polyphenols: food sources and bioavailability. *Am J Clin Nutr.* **79:** 727-747;

Markovic J., Borrás C., Ortega A., Sastre J., Viña J. and Pallardó F.V. (2007) Glutathione is recruited into the nucleus in early phases of cell proliferation. *J. Biol. Chem.* **282:** 20416–20424;

Markovic J., Mora N.J., Broseta A.M., Gimeno A., de-la-Concepción N., Viña J. and Pallardó F.V. (2009) Nuclear GSH depletion impairs cell proliferation in 3T3 fibroblasts. *PLoS ONE.* **29:** e6413;

Marx S.P., Nosberger J. and Frehner M. (1997) Hydrolysis of fructan in grasses: a beta-(2-6)-linkage specific fructan-beta-fructosidase from stubble of Lolium perenne. *New Phytol.* **135:** 279-290;

Maughan S.C., Pasternak M., Cairns N., Kiddle G., Brach T., Jarvis R., Haas F., Nieuwland J., Lim B., Müller C., Salcedo-Sora E., Kruse C., Orsel M., Hell R., Miller A.J., Bray P., Foyer C.H., Murray J.A., Meyer A.J. and Cobbett C.S. (2010) Plant homologs of the

Sara Cimini

Plasmodium falciparum chloroquine-resistance transporter, PfCRT, are required for glutathione homeostasis and stress responses. *Proc Natl Acad Sci U S A.* **107:** 2331-2336;

Maxwell D.P., Nickels R. and McIntosh L. (2002) Evidence of mitochondrial involvement in the transduction of signals required for the induction of genes associated with pathogen attack and senescence. *Plant J.* **29:** 269-279;

McMichael A.J. (2001) Impact of climatic and other environmental changes on food production and population health in the coming decades. *Proc Nutr Soc.* **60:** 195-201;

Menon S.G. and Goswami P.C. (2007) A redox cycle within the cell cycle: ring in the old with the new. *Oncogene.* **26:** 1101-1109;

Menon S.G., Sarsour E.H., Spitz D.R., Higashikubo R., Sturm M., Zhang H. and Goswami P.C. (2003) Redox regulation of the G1 to S phase transition in the mouse embryo fibroblast cell cycle. *Cancer Res.* **63:** 2109-2117;

Merendino N., D'Aquino M., Molinari R., De Gara L., D'Egidio M.G., Paradiso A., Cecchini C., Corradini C. and Tomassi G. (2006) Chemical characterization and biological effects of immature durum wheat in rats. *J Cereal Sci.* **43:** 129-136;

Millar A.A., Jacobsen J.V., Ross J.J., Helliwell C.A., Poole A.T., Scofield G., Reid J.B. and Gubler F. (2006) Seed dormancy and ABA metabolism in Arabidopsis and barley: the role of ABA 8'-hydroxylase. *Plant J.* **45:** 942-954;

Miller G., Shulaev V. and Mittler R. (2008) Reactive oxygen signaling and abiotic stress. *Physiol Plant*. **133:** 481–489;

Miller N.J., Rice-Evans C.A., Davies M.J., Gopinathan V. and Milner A. (1993) A novel method for measuring antioxidant capacity and its application to monitoring the antioxidant status in premature neonates. *Clin Sci (Lond).* **84:** 407-412;

Mittler R. (2002) Oxidative stress, antioxidants and stress tolerance. *Trends Plant Sci.* **7:** 405-410;

Mittler R., Vanderauwera S., Gollery M. and Van Breusegem F. (2004) Reactive oxygen gene network of plants. *Trends Plant Sci.* **9:** 490-498;

Morley-Smith E.R., Pike M.J., Findlay K., Köckenberger W., Hill L.M., Smith A.M. and Rawsthorne S. **(2008)** The transport of sugars to developing embryos is not via the bulk endosperm in oilseed rape seeds. *Plant Physiol.* **147:** 2121-2130;

Morvan-Bertrand A., Boucaud J., Le Saos J. and Prud'homme M.P. (2001) Roles of the fructans from the leaf sheaths and from the elongating leaf bases in the regrowth following defoliation of *Lolium perenne L. Planta.* **213:** 109-120;

Mpofu A., Sapirstein H.D. and Beta T. (2006) Genotype and environmental variation in phenolic content, phenolic acid composition, and antioxidant activity of hard spring wheat. *J Agric Food Chem.* **54:** 1265-1270;

Mur L.A., Kenton P. and Draper J. (2005). In planta measurements of oxidative bursts elicted by avirulent and virulent bacterial pathogens suggests that H2O2 is insufficient to elicit cell death in tobacco. *Plant Cell Environ.* **28:** 548–561;

Mur L.A.J., Kenton P., Lloyd A.J., Ougham H. and Prats E. (2008) The hypersensitive response; the centenary is upon us but how much do we know? *J Exp Bot.* **59:** 501–520;

Sara Cimini

Murgia I., Arosio P., Tarantino D. and Soave C. (2012) Biofortification for combating 'hidden hunger' for iron. *Trends Plant Sci.* **17:** 47-55;

Murray C.J.L. and Loped A.D. (1996) The global burden of disease. A comprehensive assessment of mortality and disability from disease, injuries and risk factors in 1990 and projected to 2020. Boston, MA: Harvard University Press;

Mutlu S., Atici O. and Nalbantoglu B. (2009) Effects of salicylic acid and salinity on apoplastic antioxidant enzymes in two wheat cultivars differing in salt tolerance. *Biologia Plantarum*. **53:** 334–338;

Nagao M., Oku K., Minami A., Mizuno K., Sakurai M., Arakawa K., Fujikawa S. and Takezawa D. (2006) Accumulation of theanderose in association with development of freezing tolerance in the moss *Physcomitrella patens*. *Phytochemistry*. **67:** 702-709;

Nagata T., Nemoto Y. and Hasezawa S. (1992) Tabacco BY-2 cell line as the "HeLa" cell biology of higher plants. *Int Rev Cytol.* **132:** 1-30;

Navrot N., Collin V., Gualberto J., Gelhaye E., Hirasawa M., Rey P., Knaff D.B., Issakidis E., Jacquot J.P. and Rouhier N. (2006) Plant glutathione peroxidases are functional peroxiredoxins distributed in several subcellular compartments and regulated during biotic and abiotic stresses. *Plant Physiol.* **142:** 1364-1379;

Nesbitt M. (1998) Where was einkorn wheat domesticated? *Trends Plant Sci.* **3:** 1360–1385;

Noctor G., Mhamdi A., Chaouch S., Han Y., Neukermans J., Marquez-Garcia B., Queval G. and Foyer C.H. (2012) Glutathione in plants: an integrated overview. *Plant Cell Environ.* **35:** 454-484;

Nomura M., Ishitani M., Takabe T., Rai A.K. and Takabe T. (1995) Synechococcus sp. PCC7942 transformed with *Escherichia coli* bet genes produces glycine betaine from choline and acquires resistance to salt stress. *Plant Physiol.* **107:** 703-708;

Nozoe S., Hirai K. and Tsuda, (1966) The structure of zizanin-A and -B, C_{25} terpenoids isolated from *Helminthosporium zizaniae*. *Tetrahedron Lett.* **20:** 2211-2226;

Nozoe S., Itai A., Tsuda K. and Okuda S. (1967) The chemical transformation of cephalonic acid. *Tetrahedron Lett.* **42:** 4113-4117;

Nozoe S., Morisaki M., Fukushima K. and Okuda S. (1968) The isolation of an acyclic C25-isoprenoid alcohol, geranylnerolidol, and a new ophiobolin. *Tetrahedron Lett.* **42:** 4457-4458;

Nozoe S., Morisaki M., Tsuda K., Iitaka Y., Takahashi N., Tamura S., Ishibashi K. and Shirasaka M. (1965) The structure of ophiobolin, a C_{25} terpenoid having a novel skeleton. *J Am Chem Soc*. **87:** 4968-4970;

op den Camp R.G., Przybyla D., Ochsenbein C., Laloi C., Kim C, Danon A, Wagner D., Hideg É., Göbel C., Feussner I., Natera M. and Apel K. (2003) Rapid induction of distinct stress responses following the release of singlet oxygen in *Arabidopsis thaliana*. *Plant Cell*. **15:** 2320–2332;

Page R.D. (1996) TreeView: an application to display phylogenetic trees on personal computers. *Comput Appl Biosci.* **12:** 357-358;

Pallardó F.V., Markovic J., García J.L. and Viña J. (2009) Role of nuclear glutathione as a key regulator of cell proliferation. *Mol. Aspects Med.* **30:** 77–85;

Sara Cimini

Paradiso A., Cecchini C., Greco E., D'Egidio M.G. and De Gara L. (2008) Variation in fructooligosaccharide contents during plant development and in different cultivars of durum wheat. *Plant Biosystems*. **142:** 656–660;

Paradiso A., de Pinto M.C., Locato V. and De Gara L. (2012) Galactone-γ-lactone-dependent ascorbate biosynthesis alters wheat kernel maturation. *Plant Biol (Stuttg).* **14:** 652-658;

Pastori G.M. and Trippi V.S. (1993) Cross resistance between water and oxidative stresses in wheat leaves. *J Agric Sci.* **120:** 289-294;

Paul M.J. and Pellny T.K. (2003) Carbon metabolite feedback regulation of leaf photosynthesis and development. *J Exp Bot.* **54:** 539-547;

Pellny T.K., Locato V., Vivancos P.D., Markovic J., De Gara L., Pallardó F.V. and Foyer C.H. (2009) Pyridine nucleotide cycling and control of intracellular redox state in relation to poly (ADP-ribose) polymerase activity and nuclear localization of glutathione during exponential growth of *Arabidopsis* cells in culture. *Mol Plant.* **2:** 442-456;

Pilon-Smits E.A.H., Ebskamp M.J.M., Paul M.J., Jeuken M.J.W., Weisbeek P.J. and Smeekens S.C.M. (1995) Improved performance of transgenic fructan-accumulating tobacco under drought stress. *Plant Physiol.* **107:** 125-130;

Pitzschke A., Forzani C. and Hirt H. (2006) Reactive oxygen species signaling in plants. *Antioxid Redox Signal.* **8:** 1757-1764;

Pollock C.J. (1984) Sucrose accumulation and the initiation of fructan biosynthesis in *Lolium temultentum L*. *New Phytol.* **96:** 527–534;

Pollock C.J. (1986) Fructans and the metabolism of sucrose in vascular plants. *New Phytol.* **104:** 1-24;

Pollock C.J. and Cairns A.J. (1991) Fructan metabolism in grasses and cereals. *Ann Rev Plant Physiol. Plant Mol. Biology.* **42:** 77-101;

Pollock C.J. and Jones T. (1979) Seasonal patterns of fructan metabolism in forage grasses. *New Phytol.* **83:** 9-15;

Pons T., Naumoff D.G., Martínez-Fleites C. and Hernández L. (2004) Three acidic residues are at the active site of a beta-propeller architecture in glycoside hydrolase families 32, 43, 62, and 68. *Proteins.* **54:** 424-432;

Potters G., De Gara L., Asard H. and Horemans N. (2002). Ascorbate and glutathione: guardians of the cell cycle, partners in crime? *Plant Physiol Biochem.* **40:** 537–548;

Potters G., Horemans N., Bellone S., Caubergs R.J., Trost P., Guisez Y. and Asard, H. (2004). Dehydroascorbate influences the plant cell cycle through a glutathione-independent reduction mechanism. *Plant Physiol.* **134:** 1479–1487;

Prasad T.K., Anderson M.D., Martin B.A. and Stewart C.R. (1994) Evidence for chilling-induced oxidative stress in maize seedlings and a regulatory role for hydrogen peroxide. *Plant Cell.* **6:** 65–74;

Prashanth S.R., Sadhasivam V. and Parida A. (2008) Over expression of cytosolic copper/zinc superoxide dismutase from a mangrove plant *Avicennia marina* in indica rice var Pusa Basmati-1 confers abiotic stress tolerance. *Transgenic Res.* **17:** 281-291;

Sara Cimini

Prentice A.M., Gershwin M.E., Schaible U.E., Keusch G.T., Victora C.G. and Gordon J.I. (2008) New challenges in studying nutrition-disease interactions in the developing world. *J Clin Invest.* **118:** 1322–1329;

Prud'homme M.P., Gonzalez B., Billard J.P. and Boucaud J. (1992) Carbohydrate content, fructan and sucrose enzyme activities in roots, stubble and leaves of ryegrass (*Lolium perenne L.*) as affected by source/sink modification after cutting. *J Plant Physiol.* **40:** 282-291;

Pruitt K.D., Tatusova T. and Maglott D.R. (2005) NCBI Reference Sequence (RefSeq): a curated non-redundant sequence database of genomes, transcripts and proteins. *Nucleic Acids Res.* **33:** D501-4;

Ramakrishnan U., Manjrekar R., Rivera J., Gonzales-Cossio T. and Martorell R. (1999) Micronutrients and pregnancy outcome: a review of the literature. *Nutr Res.* **19:** 103-159;

Re R., Pellegrini N., Proteggente A., Pannala A., Yang M. and Rice-Evans C. (1999) Antioxidant activity applying an improved ABTS radical cation decolorization assay. *Free Radic Biol Med*. **26:** 1231-1237;

Reddy A. and Maley F. (1996) Studies on identifying the catalytic role of Glu-204 in the active site of yeast invertase. *J Biol Chem.* **271:** 13953-13957;

Richards R.A. (2000) Selectable traits to increase crop photosynthesis and yield of grain crops. *J Exp Bot.* **51:** 447-458;

Ritsema T. and Smeekens S. (2003) Fructans: beneficial for plants and humans. *Curr Opin Plant Biol.* **6:** 223-230;

Ritsema T., Hernández L., Verhaar A., Altenbach D., Boller T., Wiemken A. and Smeekens S. (2006) Developing fructan-synthesizing capability in a plant invertase via mutations in the sucrose-binding box. *Plant J.* **48:** 228-237;

Ritsema T., Verhaar A., Vijn I. and Smeekens S. (2005) Using natural variation to investigate the function of individual amino acids in the sucrose-binding box of fructan:fructan 6G-fructosyltransferase (6G-FFT) in product formation. *Plant Mol Biol.* **58:** 597-607;

Roberfroid M.B. (2005) Introducing inulin-type fructans. *Br J Nutr.* **93:** S13-25;

Robu M., Shah R.G., Petitclerc N., Brind'amour J., Kandan-Kulangara F. and Shah G.M. (2013) Role of poly(ADP-ribose) polymerase-1 in the removal of UV-induced DNA lesions by nucleotide excision repair. *Proc Natl Acad Sci USA.*;

Roitsch T. and González M.C. (2004) Function and regulation of plant invertases: sweet sensations. *Trends Plant Sci.* **9:** 606-613;

Romero C., Bellés J.M., Vayá J.L., Serrano R. and Culiáñez-Macià F.A. (1997) Expression of the yeast trehalose-6-phosphate synthase gene in transgenic tobacco plants: pleiotropic phenotypes include drought tolerance. *Planta.* **201:** 293-297;

Ros Barceló A. (1997) Lignification in plant cell walls. *Int Rev Citol.* **176:** 87–132;

Ross H.A., McRae D. and Davies H.V. (1996) Sucrolytic enzyme activities in cotyledons of the faba bean. *Plant Physiol.* **111:** 329–338;

Rouhier N. and Jacquot J.P. (2002) Plant peroxiredoxins: alternative hydroperoxide scavenging enzymes. *Photosynth Res.* **74:** 259-268;

Sara Cimini

Saitou N. and Nei M. (1995) The neighbor-joining method: a new method for reconstructing phylogenetic trees. *Mol Biol Evol.* **4:** 406-425;

Sambrook J., Fritsch E.F. and Maniatis T. (1989) Molecular Cloning. A Laboratory Manual. Cold Spring Harbor Laboratory Press, Cold Spring Harbor, NY;

Scheibe R., Backhausen J.E., Emmerlich V. and Holtgrefe S. (2005) Strategies to maintain redox homeostasis during photosynthesis under changing conditions. *J Exp Bot.* **56:** 1481-1489;

Schnyder H. (1993) The role of carbohydrate storage and redistribution in the source-sink relations of wheat and barley during grain filling — a review. *New Phytol.* **123:** 233–245;

Schnyder H., Gillenberg C. and Hinz J. (1993) Fructan contents and dry matter deposition in different tissues of the wheat grain during development. *Plant Cell Environ.* **16:** 179–187;

Schroeven L., Lammens W., Van Laere A. and Van den Ende W. (2008) Transforming wheat vacuolar invertase into a high affinity sucrose:sucrose 1-fructosyltransferase. *New Phytol.* **180:** 822–831;

Seo M., Hanada A., Kuwahara A., Endo A., Okamoto M., Yamauchi Y., North H., Marion-Poll A., Sun T.P., Koshiba T., Kamiya Y., Yamaguchi S. and Nambara E. (2006) Regulation of hormone metabolism in Arabidopsis seeds: phytochrome regulation of abscisic acid regulation and gibberellin metabolism. *Plant J.* **48:** 354-366;

Shen B., Jensen R.G. and Bohnert H.J. (1997) Increased resistance to oxidative stress in transgenic plants by targeting mannitol biosynthesis to chloroplasts. *PlantPhysiol.* **113:** 1177–1183;

Shewry P.R. (2009) Wheat. *J Exp Bot.* **60:** 1537-1553;

Shigeoka S., Ishikawa T., Tamoi M., Miyagawa Y., Takeda T., Yabuta Y. and Yoshimura K. (2002) Regulation and function of ascorbate peroxidase isoenzymes. *J Exp Bot.* **53:** 1305-1319;

Shimbata T., Inokuma T., Sunohara A., Vrinten P., Saito M., Takiya T. and Nakamura T. (2011) High levels of sugars and fructan in mature seeds of sweet wheat lacking GBSSI and SSIIa enzymes. *J. Agric. Food Chem.* **59:** 4794–4800;

Shiomi N. (1989) Properties of fructosyltransferases involved in the synthesis of fructan in liliaceous plants. *J Plant Physiol.* **134:** 151–155;

Shiomi N. (1993) Structure of fructopolysaccharide. (asparagosin) from roots of asparagus (*Asparagus officinalis L.*). *New Phytol.* **123:** 263–270;

Simpson R.J., Walker R.P. and Pollock C.J. (1991) Fructan exohydrolase activity in leaves of *Lolium temulentum L*. *New Phytol.* **119:** 499-507;

Singleton V.L., Orthofer R. and Lamuela-Raventos R.M. (1999) Analysis of total phenols and other oxidation substrates and antioxidants by means of folin-ciocalteu reagent. *Meth Enzymol.* **299:** 152–178;

Smil V. (2005) Do we need higher farm yields during the first half of the 21st century? In Yields of farmed species (eds R. Sylvester-Bradley & J. Wiseman), pp. 1 – 14. Nottingham, UK: Nottingham University Press;

Sara Cimini

Spiertz J.H.J. and Ellen J. (1978) Effects of nitrogen on crop development and grain growth of winter wheat in relation to assimilation and utilization of assimilates and nutrients. *Neth J Agric Sci.* **26:** 210–231;

Sprenger N., Bortlik K., Brandt A., Boller T. and Wiemken A. (1995) Purification, cloning, and functional expression of sucrose:fructan 6-fructosyltransferase, a key enzyme of fructan synthesis in barley. *Proc Natl Acad Sci USA.* **92:** 11652-11656;

Stacy R.A., Munthe E., Steinum T., Sharma B. and Aalen R.B. (1996) A peroxiredoxin antioxidant is encoded by a dormancy-related gene, Per1, expressed during late development in the aleurone and embryo of barley grains. *Plant Mol Biol.* **31:** 1205-1216;

Stewart C.P., Dewey K.G. and Ashorn P. (2010) The undernutrition epidemic: an urgent health priority. *Lancet.* **375:** 282;

Stoyanova S., Geuns J., Hideg E. and Van Den Ende W. (2011) The food additives inulin and stevioside counteract oxidative stress. *Int J Food Sci Nutr.* **62:** 207-214;

Streller S. and Wingsle G. (1994) *Pinus sylvestris L.* needles contain extracellular CuZn superoxide dismutase. *Planta.* **192:** 195-201;

Sugawara F., Strobel G., Strange R.N., Siedow J.N., Van Duyne G.D. and Clardy J. (1987) Phytotoxins from the pathogenic fungi Drechslera maydis and Drechslera sorghicola. *Proc Natl Acad Sci U S A.* **84:** 3081-3085;

Sulmon C., Gouesbet G., Couée I. and El Amrani A. (2004) Sugar-induced tolerance to atrazine in Arabidopsis seedlings: interacting effects of atrazine and soluble sugars on psbA mRNA and D1 protein levels. *Plant Science.* **167:** 913-923;

Suzuki N., Koussevitzky S., Mittler R. and Miller G. (2012) ROS and redox signalling in the response of plants to abiotic stress. *Plant Cell Environ.* **35:** 259-270;

Tanaka T., Izawa S. and Inoue Y. (2005) GPX2, encoding a phospholipid hydroperoxide glutathione peroxidase homologue, codes for an atypical 2-Cys peroxiredoxin in Saccharomyces cerevisiae. *J Biol Chem.* **280:** 42078-42087;

Tanga G.Q., Lüscherb M. and Sturma A. (1999) Antisense repression of vacuolar and cell wall invertase in transgenic carrot alters early plant development and sucrose partitioning. *The Plant Cell.* **11:** 177-189;

Tarczynski M.C., Jensen R.G. and Bohnert H.J. (1993) Stress protection of transgenic tobacco by production of the osmolyte mannitol. *Science.* **259:** 508-510;

Tarini J. and Wolever T.M. (2010) The fermentable fibre inulin increases postprandial serum short-chain fatty acids and reduces free-fatty acids and ghrelin in healthy subjects. *Appl Physiol Nutr Metab.* **35:** 9-16;

Tauskela J.S., Hewitt K., Kang L.P., Comas T., Gendron T., Hakim A., Hogan M., Durkin J. and Morley P. (2000) Evaluation of glutathione-sensitive fluorescent dyes in cortical culture. *Glia.* **30:** 329-341;

Thompson J.D., Higgins D.G. and Gibson T.J. (1994) CLUSTAL W: improving the sensitivity of progressive multiple sequence alignment through sequence weighting, position-specific gap penalties and weight matrix choice. *Nucleic Acids Res.* **22:** 4673-4680;

Tolmay V.L. (2001) Resistance to biotic and abiotic stress in the Triticeae. *Hereditas.* **135:** 239-242;

Sara Cimini

Tommasi F., Paciolla C., de Pinto M.C. and De Gara L. (2001) A comparative study of glutathione and ascorbate metabolism during germination of *Pinus pinea L.* seeds. *J. Exp. Bot.* **52:** 1647–1654;

Torres M.A. (2010) ROS in biotic interactions. *Physiola Plant.* **138:** 414–429;

Torres M.A. and Dangl J.L. (2005) Functions of the respiratory burst oxidase in biotic interactions, abiotic stress and development. *Curr Opin Plant Biol.* **8:** 397-403;

Torres M.A., Jones J.D.G. and Dangl J.L. (2006) Reactive oxygen species signaling in response to pathogens. *Plant Physiol.* **141:** 373-378;

Tschopp J.F., Brust P.F., Cregg J.M., Stillman C. and Gingeras T.R. (1987) Expression of the lacZ Gene from Two Methanol Regulated Promoters in *Pichia pastoris*. *Nucleic Acids Res.* **15**: 3859-3876;

Turner L.B., Cairns A.J., Armstead I.P., Thomas H., Humphreys M.W. and Humphreys M.O. (2008) Does fructan have a functional role in physiological traits? Investigation by quantitative trait locus mapping. *New Phytol.* **179:** 765-775;

United Nations Standing Committee on Nutrition (SCN). (2004) Fifth report on the world nutrition situation: nutrition for improved development outcomes;

Vacca R.A., de Pinto M.C., Valenti D., Passerella S., Marra E., De Gara L. (2004) Reactive oxygen species production, impairment of glucose oxidation and cytosolic ascorbate peroxidase are early events in heat-shock induced programmed cell death in tobacco BY-2 cells. *Plant Physiol.* **134:** 1100-1112;

Valluru R. and Van den Ende W. (2008) Plant fructans in stress environments: emerging concepts and future prospects. *J Exp Bot.* **59:** 2905–2916;

Valluru R., Lammens W., Claupein W. and Van den Ende W. (2008) Freezing tolerance by vesicle-mediated fructan transport. *Trends Plant Sci.* **13:** 409-414;

Van den Ende W. and Valluru R. (2009) Sucrose, sucrosyl oligosaccahrides, and oxidative stress: scavenging and salvaging? *J Exp Bot.* **60:** 9-18;

Van den Ende W. and Van Laere A. (1995) Purification and properties of a neutral invertase from the roots of *Cichorium intybus L*. *Physiol. Plant.* **93:** 241–248;

Van den Ende W. and Van Laere A. (2007) Fructans in dicotyledonous plants: Occurrence and metabolism. Shiomi N, Benkeblia N, Onodera S, editors. Recent Advances in Fructooligosaccharides Research. Research Signpost, Kerala, India. 1–14;

Van den Ende W., Clerens S., Vergauwen R., Van Riet L., Van Laere A., Yoshida M. and Kawakami A. (2003a). Fructan 1-exohydrolase: β(2,1) trimmers during graminan biosynthesis in stems of wheat (*Triticum aestivum* L.): purification, characterization, mass mapping and cloning of two 1-FEH isoforms. *Plant Physiology.* **131:** 621–631;

Van den Ende W., Coopman M., Clerens S., Vergauwen R., Le Roy K., Lammens W. and Van Laere A. (2011a) Unexpected presence of graminan- and levan-type fructans in the evergreen frost-hardy eudicot Pachysandra terminalis (Buxaceae): purification, cloning, and functional analysis of a 6-SST/6-SFT enzyme. *Plant Physiol.* **155:** 603-614;

Van den Ende W., Coopman M., Clerens S., Vergauwen R., Le Roy K., Lammens W. and Van Laere A. (2011c) Unexpected presence of graminan- and levan-type fructans in the

Sara Cimini

evergreen frost-hardy eudicot *Pachysandra terminalis* (Buxaceae): purification, cloning, and functional analysis of a 6-SST/6-SFT enzyme. *Plant Physiol.* **155:** 603-614;

Van den Ende W., De Coninck B. and Van Laere A. (2004) Plant fructan exohydrolases: a role in signaling and defense? *Trends Plant Sci.* **9:** 523-528;

Van den Ende W., De Coninck B., Clerens S., Vergauwen R. and Van Laere A. (2003) Unexpected presence of fructan 6-exohydrolases (6-FEHs) in non-fructan plants: characterization, cloning, mass mapping and functional analysis of a novel "cell-wall invertase-like" specific 6-FEH from sugar beet (*Beta vulgaris L.*). *Plant J.* **36:** 697-710;

Van den Ende W., De Roover J. and Van Laere A. (1996) In vitro synthesis of fractofuranosyl-only oligosaccharides from inulin and fructose by purified chicory root fructan:fructan fructosyl transferase. *Physiol Plantarum.* **97:** 346–352;

Van den Ende W., Lammens W., Van Laere A., Schroeven L. and Le Roy K. (2009) Donor and acceptor substrate selectivity among plant glycoside hydrolase family 32 enzymes. *FEBS Journal.* **276:** 5788–5798;

Van den Ende W., Michiels A., De Roover J. and Van Laere A. (2002) Fructan biosynthetic and breakdown enzymes in dicots evolved from different invertases. Expression of fructan genes throughout chicory development. *The Scientific World J.* **2:** 1281–1295;

Van den Ende W., Michiels A., Van Wonterghem D., Vergauwen R. and Van Laere A. (2000) Cloning, developmental, and tissue-specific expression of sucrose:sucrose 1-fructosyl transferase from *Taraxacum officinale*. Fructan localization in roots. *Plant Physiol.* **123:** 71-80;

Van den Ende W., Peshev D., De Gara L. (2011b) Disease prevention by natural antioxidants and prebiotics acting as ROS scavengers in the gastrointestinal tract. *Trends Food Sc. & Techn.* **22:** 689-697;

Van den Ende W., Yoshida M., Clerens S., Vergauwen R. and Kawakami A. (2005) Cloning, characterization and functional analysis of novel 6-kestose exohydrolases (6-KEHs) from wheat (Triticum aestivum). *New Phytol.* **166:** 917-932;

van der Meer I.M., Koops A.J., Hakkert J.C. and van Tunen A.J. (1998) Cloning of the fructan biosynthesis pathway of Jerusalem artichoke. *Plant J.* **15:** 489-500;

Van Laere A. and Van den Ende W. (2002) Inulin metabolism in dicots: chicory as a model system. *Plant Cell Environ.* **25:** 803–815;

Van Riet L., Altenbach D., Vergauwen R., Clerens S., Kawakami A., Yoshida M., Van den Ende W., Wiemken A. and Van Laere A. (2008) Purification, cloning and functional differences of a third fructan 1-exohydrolase (1-FEHw3) from wheat (*Triticum aestivum*). *Physiol Plant.* **133:** 242-53;

Van Riet L., Nagaraj V., Van den Ende W., Clerens S., Wiemken A. and Van Laere A. (2006) Purification, cloning and functional characterization of a fructan 6-exohydrolase from wheat (*Triticum aestivum L.*). *J Exp Bot.* **57:** 213-223;

Vanderauwera S., De Block M., Van de Steene N., van de Cotte B., Metzlaff M. and Van Breusegem F. (2007) Silencing of poly(ADP-ribose) polymerase in plants alters abiotic stress signal transduction. *Proc Natl Acad Sci U S A.* **104:** 15150-15155;

Vanderauwera S., Zimmermann P., Rombauts S., Vandenabeele S., Langebartels C., Gruissem W., Inzé D. and Van Breusegem F. (2005) Genome-wide analysis of hydrogen

Sara Cimini

peroxide-regulated gene expression in Arabidopsis reveals a high light-induced transcriptional cluster involved in anthocyanin biosynthesis. *Plant Physiol.* **139:** 806-821;

Vannini C., Marsoni M., Cantara C., De Pinto M.C., Locato V., De Gara L. and Bracale M. (2012) The soluble proteome of tobacco Bright Yellow-2 cells undergoing H_2O_2-induced programmed cell death. *J Exp Bot.* **63:** 3137-3155;

Varga B., Janda T., László E. and Veisz O. (2012) Influence of abiotic stresses on the antioxidant enzyme activity of cereals. *Acta Physiol Plant.* **34:** 849-858;

Vereyken I.J., Chupin V., Islamov A., Kuklin A., Hincha D.K. and de Kruijff B. (2003) The effect of fructan on the phospholipid organization in the dry state. *Biophys J.* 85: 3058-3065;

Vergauwen R., Van den Ende W. and Van Laere A. (2000) The role of fructan in flowering of *Campanula rapunculoides*. *J Exp Bot.* **51:** 1261-1266;

Vergauwen R., Van Laere A. and Van den Ende W. (2003) Properties of fructan:fructan 1-fructosyltransferases from chicory and globe thistle, two Asteracean plants storing greatly different types of inulin. *Plant Physiol.* **133:** 391-401;

Verhaest M., Lammens W., Le Roy K., De Ranter CJ., Van Laere A., Rabijns A. and Van den Ende W. (2007) Insights into the fine architecture of the active site of chicory fructan 1-exohydrolase: 1-kestose as substrate vs sucrose as inhibitor. *New Phytol.* **174:** 90-100;

Verhaest M., Van den Ende W., Le Roy K., De Ranter C.J., Van Laere A. and Rabijns A. (2005) X-ray diffraction structure of a plant glycosyl hydrolase family 32 protein: fructan 1-exohydrolase IIa of Cichorium intybus. *Plant J.* **41:** 400-411;

Vernoux T., Wilson R.C., Seeley K.A., Reichheld J.P., Muroy S., Brown S., Maughan S.C., Cobbett C.S., Van Montagu M., Inzé D., May M.J. and Sung Z.R. (2000). The ROOT MERISTEMLESS1 / CADMIUM SENSITIVE2 gene defines a glutathione-dependent pathway involved in initiation and maintenance of cell division during postembryonic root development. *Plant Cell.* **12:** 97–110;

Verspreet J., Pollet A., Cuyvers S., Vergauwen R., Van den Ende W., Delcour J.A. and Courtin C.M. (2012) A simple and accurate method for determining wheat grain fructan content and average degree of polymerization. *J Agric Food Chem.* **60:** 2102-2107;

Vicente-Carbajosa J. and Carbonero P. (2005) Seed maturation: developing an intrusive phase to accomplish a quiescent state. *Int. J. Dev. Biol.* **49:** 645-651;

Vijn I. and Smeekens S. (1999) Fructan: More Than a Reserve Carbohydrate? *Plant Physiol.* **120:** 351-360;

Vijn I., van Dijken A., Sprenger N., van Dun K., Weisbeek P., Wiemken A. and Smeekens S (1997) Fructan of the inulin neoseries is synthesized in transgenic chicory plants (*Cichorium intybus L.*) harbouring onion (*Allium cepa L.*) fructan:fructan 6G-fructosyltransferase. *Plant J.* **11:** 387–398;

Voehringer D.W., McConkey D.J., McDonnell T.J., Brisbay S. and Meyn R.E. (1998) Bcl-2 expression causes redistribution of glutathione to the nucleus. *Proc Natl Acad Sci U S A.* **95:** 2956-2960;

Volaire F. and Lelièvre F. (1997) Production, persistence, and water-soluble carbohydrate accumulation in 21 contrasting populations of *Dactylis glomerata L.* subjected to severe drought in the south of France. *Aust J Agr Res.* **48:** 933-944;

Sara Cimini

Wagner W. and Wiemken A. (1986) Properties and subcellular localization of fructan hydrolase in the leaves of barley (*Hordeum vulgare L. cv Gerbel*). *J Plant Physiol.* **123:** 429–439;

Wagner W., Keller F. and Wiemken A. (1983) Fructan metabolism in cereals: Induction in leaves and compartmentation in protoplasts and vacuoles. *Z. Pfanzenphysiol.* **112:** 359-372;

Walker R.P., Winters A.L. and Pollock C.J. (1997) Purification and characterization of invertases from leaves of Lolium temulentum. *New Phytol.* **135:** 259–266;

Warrand J. (2006) Healthy polysaccharides, the next chapter in food products. *Food Technol. Biotechnol.* **44:** 355-370;

Waterhouse A.L. and Chatterton N.J. (1993) Glossary of fructan terms. In Science and Technology of Fructans, M. Suzuki and N. J. Chatterton, Eds. CRC Press, Boca Raton, Fla, USA. 1–7;

Waterhouse A.M., Procter J.B., Martin D.M., Clamp M. and Barton G.J. (2009) Jalview Version 2--a multiple sequence alignment editor and analysis workbench. *Bioinformatics.* **25:** 1189-1191;

Wei J.Z. and Chatterton N.J. (2001) Fructan biosynthesis and fructosyltranferase evolution: the expression of the 6-SFT (sucrose:fructan 6-fructosyltransferase) gene in crested wheatgrass (*Agropyrum cristatum*). *J Plant Physiol.* **158:** 1203-1213;

Willekens H., Langebartels C., Tiré C., van Montagu M., Inzé D. and Van Camp W. (1994) Differential expression of catalase genes in *Nicotiana plumbaginifolia* (L.). *Proc Natl Acad Sci USA.* **91:** 10450-10454;

Woodson J.D. and Chory J. (2008) Coordination of gene expression between organellar and nuclear genomes. *Nat Rev Genet.* **9:** 383-395;

World Grain Statistics. (2008) International Grain Council. http://www.igc.int/en/Default.aspx;

Yalpani N., Silverman P., Wilson T.M.A., Kleier D.A. and Raskin I. (1991) Salicylic acid is a systemic signal and an inducer of pathogenesis-related proteins in virus infected tobacco. *Plant Cell.* **3:** 809-818;

Yoshida M., Abe J., Moriyama M. and Kuwabara T. (1998) Carbohydrate levels among winter wheat cultivars varying in freezing tolerance and snow mold resistance during autumn and winter. *Physiol Plant.* **103:** 8–16;

Yoshida M., Kawakami A. and Van den Ende W. (2007) Graminan metabolism in cereals: wheat as a model system. In: Shiomi N., Benkeblia N. and Onodera S. (eds) Recent Advances in Fructooligosaccharides Research. Research Signpost, Trivandrum. 201-212;

Zhang D., Xu Y., Xin X., Zhu R. and Jin J. (2011) Pichia pastoris X-33 with OCH1 gene deletion and its expression of glycoprotein GM-CSF. *Wei Sheng Wu Xue Bao.* **51:** 622-629;

Zhang J.X. and Kirkham M.B. (1996) Antioxidant responses to drought in sunflower and sorghum seedlings. *New Phytol.* **132:** 361–373;

Ziska L.H., Bunce J.A., Shimono H, Gealy D.R., Baker J.T., Newton P.C.D., Reynolds M.P., Jagadish K.S.V., Zhu C., Howden M. and Wilson L.T. (2012) Food security and climate change: on the potential to adapt global crop production by active selection to rising atmospheric carbon dioxide. *Proc Biol Sci.* **279:** 4097-4105;

Sara Cimini

Zohary D. and Feldman M. (1962) Hybridization between amphidiploids and the evolution of polyploids in the wheat (Ægilops-Triticum) group. *Evolution*. **16:** 44-61;

Zuchowski J., Jonczyk K., Pecio L. and Oleszek W. (2011) Phenolic acid concentrations in organically and conventionally cultivated spring and winter wheat. *J Sci Food Agric*. **91:** 1089-1095;

Appendix

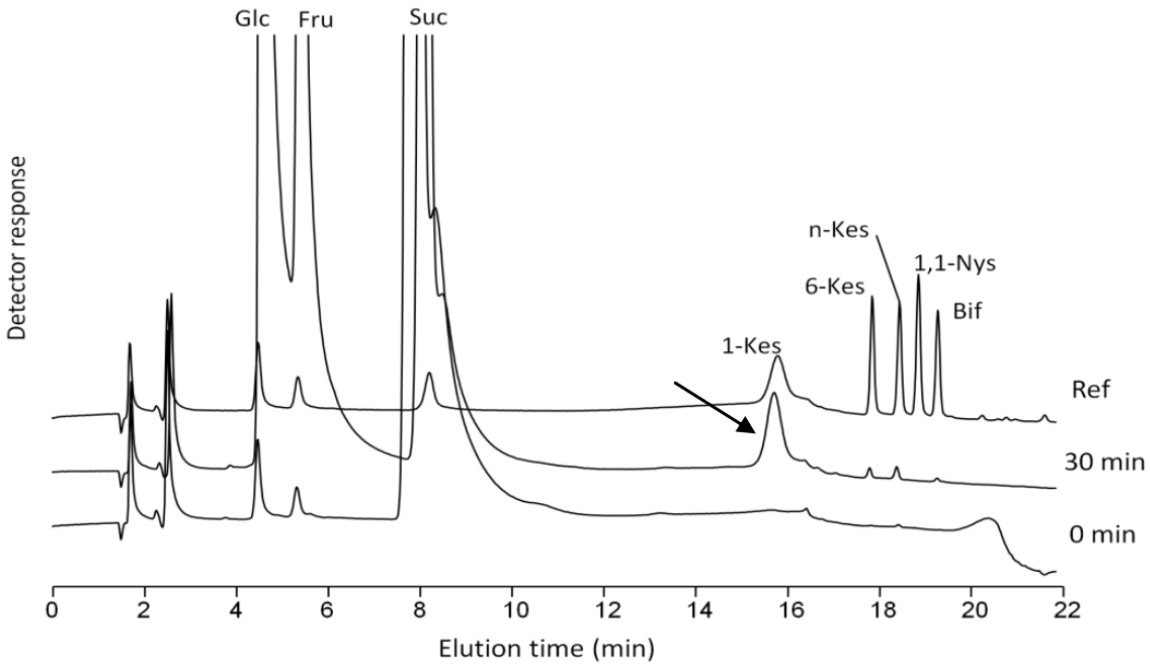

A1: Chromatogram showing sugars formed after 30 min incubation of 50 mM sucrose with a wheat kernel protein extract at 7 DAA. The arrow is indicating the 1-K peak which is formed after 30 min of incubation. Known standards are indicated as Ref: Glc (glucose), Fru (fructose), Suc (sucrose), 1-Kes (1-kestose), n-Kes (neokestose), 1,1-Nys (1,1-Nystose), Bif (bifurcose or 1&6-Nystose).

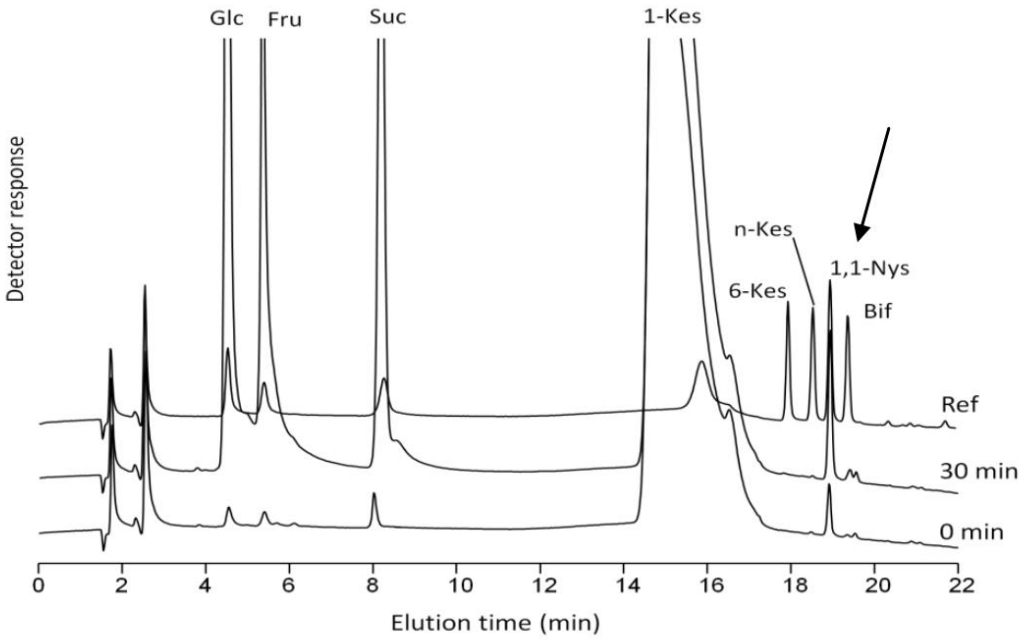

A2: Chromatogram showing sugars formed after 30 min incubation of 50 mM 1-Kes with a wheat kernel protein extract at 7 DAA. The arrow is indicating the formation of 1,1-Nys after 30 min of incubation.

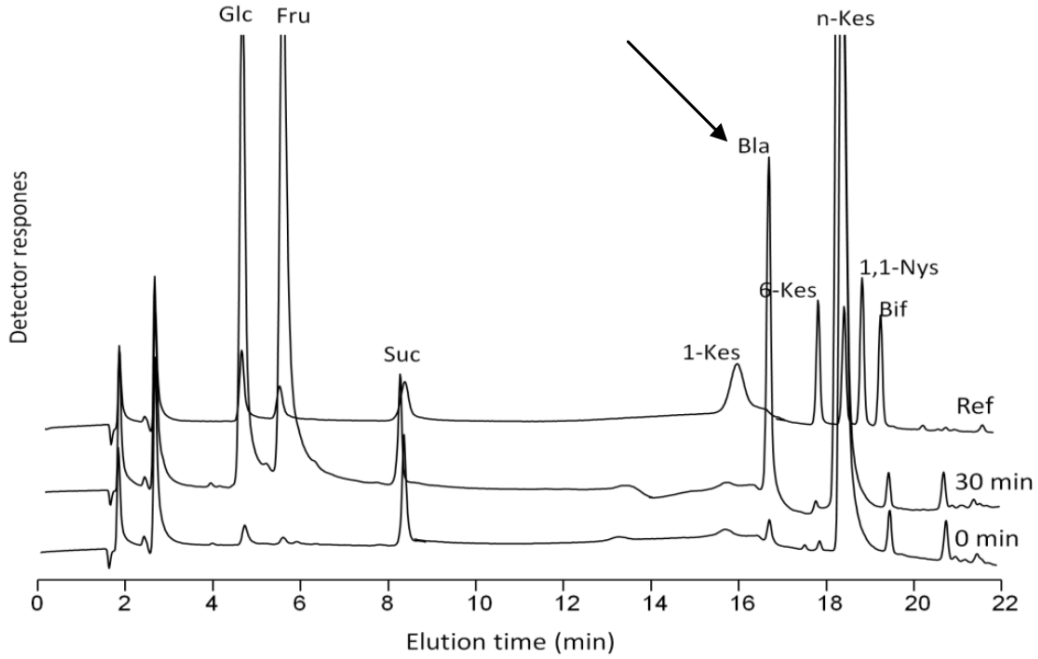

A3: Chromatogram showing sugars formed after 30 min incubation of 50 mM n-Kes with a wheat kernel protein extract at 7 DAA. The arrow is pointing the synthesis of an unknown compound which is probably the blastose (Bla).

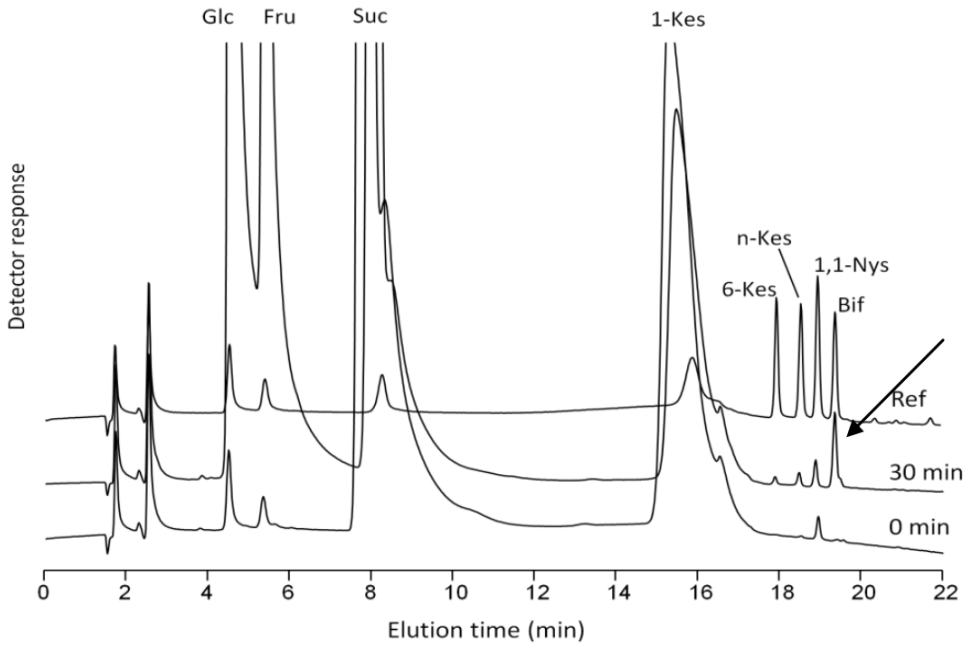

A4: Chromatogram showing sugars formed after 30 min incubation of a combination of 50 mM sucrose and 50 mM 1-kes with a wheat kernel protein extract at 7 DAA. The arrow is pointing the Bif peak that is formed after 30 min of incubation.

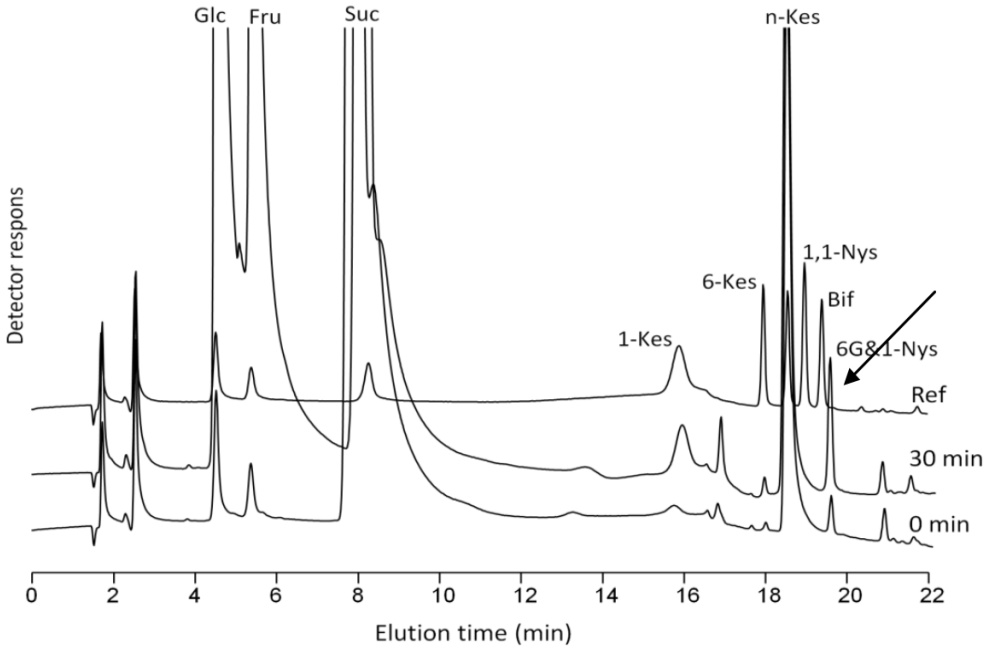

A5: Chromatogram showing sugars formed after 30 min incubation of a combination of 50 mM sucrose and 50 mM n-kes with a wheat kernel protein extract at 7 DAA. The arrow is

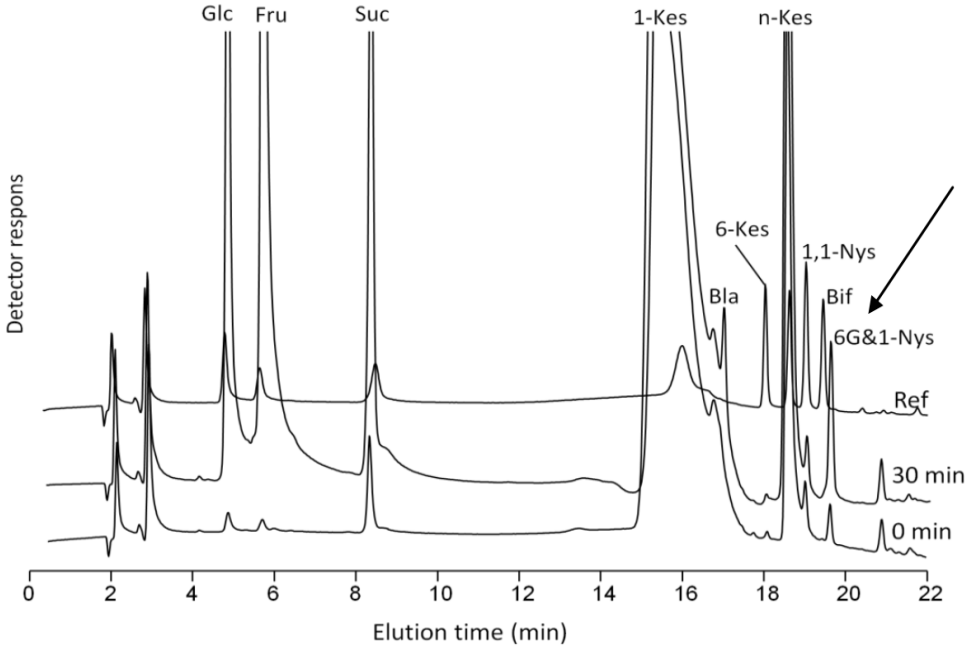

pointing the formation of 1&6G-kestotetraose (6G&1-Nys) after 30 min of incubation.

A6: Chromatogram showing sugars formed after 30 min incubation of a combination of 50 mM 1-kes and 50 mM n-kes with a wheat kernel protein extract at 7 DAA. The arrow is pointing the 6G&1-Nys peak that appears after 30 min of incubation.

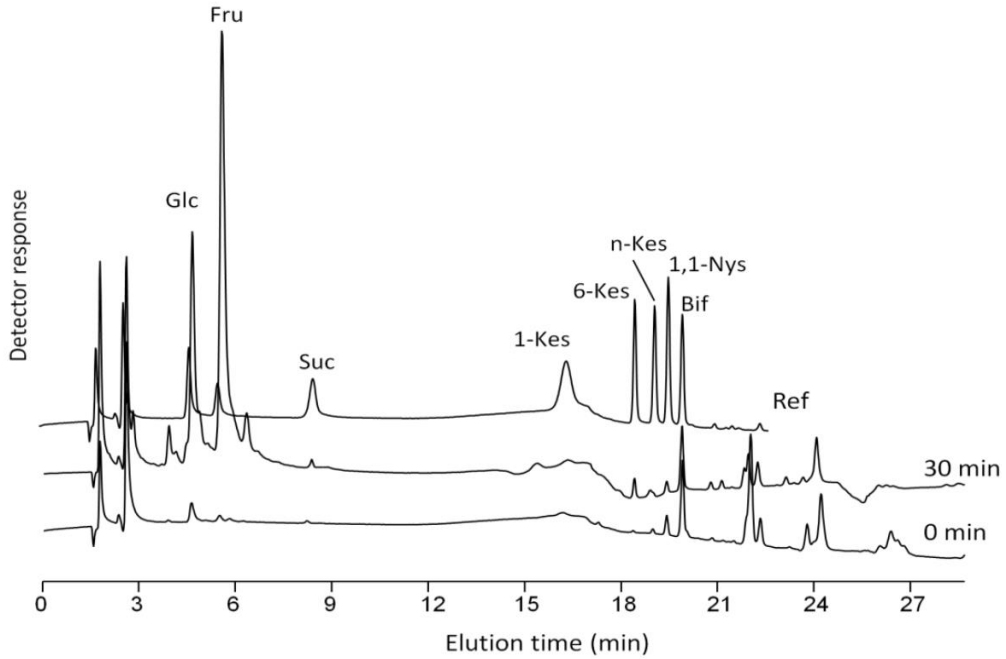

A7: Chromatogram showing sugars formed after 30 min incubation of 2 mM graminans and fructan neoseries extracted from wheat kernels with a wheat kernel protein extract at 7 DAA. The chromatogram shows the sugars formed after 30 min of incubation.

Abbreviation List

1,1-Nys	1,1-nystose
1-FEH	Fructan 1-exohydrolases
1-FFT	Fructan:Fructan 1-Fructosyltransferase
1-K	1-kestose
1-KEH	1-Kestose Exohydrolase
1-SST	Sucrose:Sucrose 1-Fructosyltransferase
6&1-FEH	Fructan 6&1-exohydrolase
6-FEH	Fructan 6-exohydrolases
6-FFT	Fructan:Fructan 6-Fructosyltransferase
6G&1-Nys	1&6G-kestotetraose
6G-FFT	Fructan:Fructan 6G-Fructosyltransferase
6-K	6-kestose
6-KEH	6-kestose exohydrolase
6-SFT	Sucrose:Fructan 6-Fructosyltransferase
6-SST	Sucrose:Sucrose 6-Fructosyltransferase
ABA	Abscissic Acid
AEZ	Agro-Ecological Zones
APX	Ascorbate Peroxidase
ASC	Ascorbate
Bif	Bifurcose (1&6-kestotetraose)
CAT	Catalase
CW-INV	Cell Wall Invertase
DAA	Days After Anthesis
DHA	Dehydroascorbate
DHAR	DHA-Reductase
DHR	Dihydrorhodamine

Sara

DP	Degree of Polymerization
DW	Dry Weight
FAO	Food and Agriculture Organization
FEH	Fructan Exohydrolase
FOS	Fructo-Oligosaccharides
Fru	Fructose
FT	Fructosyltransferases
FW	Fresh Weight
GAE	Gallic Acid Equivalents
GH32	Glycoside Hydrolase Family 32
GH68	Glycoside Hydrolase Family 68
Glc	Glucose
GPX	Glutathione Peroxidase
GR	Glutathione Reductase
GSH	Glutathione
GSSG	Glutathione Disulphide
HPAEC-PAD	high performance anion exchange chromatography with pulsed amperometric detection
HR	Hypersensitive Response
ID	Iron deficiency
IIASA	International Institute of Applied Systems Analysis
KS	Kernel Substrate
Mal	Maltose
MDHA	Monodehydroascorbate
MDHAR	MDHA-Reductase
N-INV	Neutral/Slightly Alkaline Invertases
n-K	neokestose (6G-kestose)
NO	Nitric Oxide
OD	Optical Density
PARP	Poly(ADP-Ribose) Polymerase
PCD	Programmed Cell Death
PCV	Package Cell Volume
POD	Class III Peroxidases

Sara Cimini

Raf	Raffinose
ROS	Reactive Oxygen Species
SA	Salicylic Acid
SAR	Systemic Acquired Resistance
Suc	Sucrose
TBY-2	Tobacco Bright Yellow 2
TEAC	Trolox Equivalent Antioxidant Capacity
V-INV	Vacuolar Invertase

Sara

Abstracts and Pubblications

1. Cimini S., Locato V., Paradiso A., Pasqualetti V., D'Egidio M.G., Van den Ende W., De Gara L. The good-nature of fructans: prebiotic and antioxidant effects on human health. FISV, Roma, 24 - 27 Settembre 2012.
2. Locato V., Novo-Uzal E., Cimini S., Levi M., Evidente A., De Gara L. Ophiobolin A effect on cell cycle is mediated by alteration in GSH fluxes among cell compartments. 12° Convegno FISV, Roma, 24 - 27 Settembre 2012.
3. Cimini S., Locato V., Novo-Uzal E., Andolfi A., Evidente A., De Gara L. The micotoxin ophiobolin A effects on cell proliferation and cell viability in Tobacco Bright Yellow-2 cells. Plant Biology Congress, Freiburg, 29 Luglio - 3 Agosto 2012.
4. Cimini S., Vandenpoel L., Vergauwen R., Paradiso A., Verspreet J., Locato V., Le Roy K., Cecchini C., Peshev D., Courtin C., D'Egidio M.G., Van den Ende W., De Gara L. Metabolic changes during durum wheat kernel maturation. 7th International Fructan Symposium, Saint-Jean-Le-Thomas, France, 2 - 6 Luglio 2012.
5. Cimini S., Paradiso A., Vandenpoel L., Locato V., D'Egidio M.G., Van den Ende W., De Gara L. Fructan metabolism during maturation of kernels from durum wheat. 5th International Dietary Fibre Conference, Roma, 7 - 9 Maggio 2012. ISBN 978-3-9503336-0-2
6. Locato V., Cimini S., Novo Uzal E., Levi M., Micera A., Balzamino B.O., Evidente A., De Gara L. Ophiobolin A activates different defence responses depending on the applied dose in TBY-2 cells. Joint Meeting AGI-SIBV-SIGA, Assisi, 19 - 22 Settembre 2011.
7. Locato V., Cimini S., Novo Uzal E., Levi M., De Gara L. Ophiobolin A blocks cell cycle or induces PCD in a dose-dependent manner. Riunione annuale del Gruppo di Lavoro Biologia Cellulare e Molecolare della Società Botanica Italiana, Roma, 15 - 17 Giugno 2011.
8. Novo-Uzal E., Locato V., Cimini S., Avolio F., Evidente A., De Gara L. Cytostatic and cytotoxic effects of ophiobolin A on TBY-2 cells. Annual meeting of the Society of Experimental Biology, Praga, 30 Giugno - 3 Luglio 2010.
9. Locato V., Novo-Uzal E., Cimini S., Avolio F., de Pinto M.C., Evidente A., De Gara L. A fungal toxin induces an oxidative burst-independent Programmed Cell Death. II congresso della SIBV, Roma, 12 - 14 Luglio 2010.
10. Locato V., Cimini S., Novo Uzal E., de Pinto M.C., Foyer C.H., L. De Gara. Poly ADP-ribose polymerase involvement in programmed cell death of tobacco BY-2 cells. FESPB annual meeting, Valencia, 4 - 8 Luglio 2010.
11. Locato V., Cimini S., de Pinto M.C., Foyer C.H., and De Gara L. Poly ADP-Ribose Polymerase involvement in the Programmed Cell Death of the Tobacco BY-2. SIBV, Verona, 30 Giugno - 2 Luglio 2009.
12. Bury M., Novo-Uzal E., Andolfi A., Cimini S., Wauthoz N., Heffeter P., Lallemand B., Avolio F., Delporte C., Cimmino A., Van Antwerpen P., Zonno M.C., Vurro M., Poumay Y., Berger W., Evidente A., De Gara L., Kiss R., Locato V.. Ophiobolin A, a Fungal Sesterpenoid Phytotoxin, Displays High In Vitro Growth-Inhibitory Effetcs in Mammalian than in Plant Cells and It also Display In Vivo Antitumor Activity. Cell Biology and Toxicology. (2012) (Submitted).

Sara Cimini

Index

Sara Cimini

Sara Cimini